University of Alberta

Assembly, function and structure of Tom40, the pore-forming component of the TOM complex in *Neurospora crassa*.

by

Rebecca Delyth Taylor

A thesis submitted to the Faculty of Graduate Studies and Research in partial fulfillment of the

requirements for the degree of Doctor of Philosophy

in

Molecular Biology and Genetics

Department of Biological Sciences

Edmonton, Alberta

Spring 2004

Your file Votre référence
ISBN: 0-612-96326-8
Our file Notre référence
ISBN: 0-612-96326-8

ABSTRACT:

Mitochondria are found in almost all eukaryotic organisms and are the site of many biological functions. The majority of mitochondrial proteins are encoded by nuclear genes and synthesized on cytosolic ribosomes. The TOM complex (**T**ranslocase of the **O**uter **M**embrane) is responsible for initial recognition and translocation of mitochondrial precursor proteins across the outer membrane. Tom40, the major component of the TOM complex, forms a pore through which preproteins traverse the mitochondrial outer membrane.

Little is known about the domains of Tom40 that are required for its assembly and function within the TOM complex. The initial goals of this study were to create a *tom40* null nucleus in a heterokaryotic strain of *Neurospora crassa* and to examine and characterize the effects of Tom40 depletion. These studies revealed that Tom40 is an essential gene in *N. crassa.* When the nucleus bearing the *tom40* mutation is forced to predominate, the heterokaryotic strain Tom40 levels are reduced and import of mitochondrial preproteins is affected. Mitochondria with reduced amounts of Tom40 are smaller than wildtype mitochondria and have no cristae.

The heterokaryotic strain was used to study the function and assembly of the TOM complex. A conserved region in the N- terminus of Tom40, spanning amino acids 40-60, was found to play a role in assembling the protein into the TOM complex, but not in targeting of Tom40 to mitochondria. This region also plays a role in the stability of the TOM complex and import of mitochondrial preproteins. A conserved region in the C-terminus of Tom40 (residues 321-323) appears to be part of a membrane spanning β-sheet. Deletion of these residues fails to rescue the *tom40* null nucleus, while

replacement of these amino acids with alanine results in a strain that grows slowly, has a fragile TOM complex, and shows deficiencies in the import of mitochondrial preproteins.

Studies of the Tom40 assembly pathway using variant Tom40 molecules have given us new insights into this pathway. Finally, the membrane topology of Tom40 was studied using substituted-cysteine accessibility mapping and two membrane-spanning β-strands were identified in the C-terminus of the protein.

ACKNOWLEDGEMENTS:

I want to thank the many people over the years that have provided me with invaluable technical support. These people include past and present members of the Nargang laboratory, Bonnie Crowther, Cheryl Nargang, Nancy Go and Allison Kennedy. In addition, I would like to thank the members of the molecular biology services unit at the University of Alberta for their excellent help.

Thanks go out to Dr. Doron Rapaport at the University of Munich for discussions about the nature of the Tom40 assembly intermediates, as well as providing Fig. 17A for this thesis. In addition, I would like to thank Dr. Walter Neupert, and members of his laboratory for providing protocols and reagents for this work.

I had the opportunity to work in a wonderful laboratory and I would like to thank all the past and present members for their support, help, and discussions.

I would like to thank the members of my supervisory committee for their support and guidance over the years. Thanks to Drs. R. Wozniack, J. Atchison, and J. Bell.

I must also acknowledge the support of the Alberta Heritage Foundation for Medical Research, the Natural Sciences and Engineering Research Council, the Faculty of Graduate Studies and Research at the University of Alberta, and the Department of Biological Sciences for scholarship support for the last five years. I also have to acknowledge the support of the Canadian Institutes of Health Research without whose support this work could not be accomplished.

I would like to thank my supervisor, Dr. Frank Nargang, for taking me on as a graduate student and giving me the wonderful opportunity to explore the world of science. It hasn't been an easy time, but he has been constantly supportive and encouraging throughout my degree. AND although I hate to admit it, he is right about things more often than he is wrong.

Thanks to my friends and family for continued support over the years.

Finally, thank you to Mr. Peter Moir and Dr. Pliny Hayes for inspiring me to pursue a career in science.

Table of contents

5. BIBLIOGRAPHY

List of Tables

List of Figures

List of Abbreviations:

AAC	ADP/ATP carrier
A	adenine
Å	Angstroms
ADP	adenosine diphosphate
AIF	apoptosis inducing factor
ala	alanine
ALDIII	alcohol dehydrogenase III
ALDH	alcohol dehydrogenase
ATP	adenosine triphosphate
Bcl2	B-cell lymphoma protein 2
biotin maleimide	N^{α}-(3-maleimydylpropionyl) biocytin
BSA	bovine serum albumin
BN	blue native
BNG	blue native gel
BNGE	blue native gel electrophoresis
bp	base pair
C	cytosine
Ca^{2+}	calcium ion
CCHL	cytochrome *c* heme lyase
cDNA	complimentary deoxyribonucleic acid
CoQ_{10}	ubiquinone
COXIV	cytochrome *c* oxidase subunit IV
cys	cysteine
Δ	deletion
$\Delta\psi$	membrane potential
DIG	digitonin
DDM	dodecylmaltoside
DHFR	dihydrofolate reductase
Dnm1p	dynamin related protein 1

DPP	human deafness dystonia protein
ECL	enzyme catalyzed light generation
EM	electron microscopy
EST	expressed sequence tag
ETC	electron transport chain
Hg^{2+}	mercury ion
$FADH_2$	flavin adenine dinucleotide, reduced form
$F_1\beta$	β-subunit of the F_1 ATP synthase
Fe-S	iron sulfer
Fis1p	fission protein 1
Fts	filamentation temperature sensitive
Fzo1p	fuzzy onions 1 protein
g	gravity
G	guanine
gDNA	genomic DNA
GIP	general insertion pore
hr	hour
Hsp	heat shock protein
IMF	intermediate fraction vesicles
IMS	intermembrane space
IP	immunoprecipitate
kb	kilobase
kDa	kilodaltons
KSS	Kearns-Sayre syndrome
kV	kilovolts
L	litre
leu	leucine
lys	lysine
µg	microgram
µl	microlitre
µm	micrometer

M	molar
Mas	mitochondrial assembly protein
MCC	mitochondrial inner membrane conductance channel
Mdv1p	mitochondrial division protein 1
Mdv2p	mitochondrial division protein 2
Mft52	mitochondrial fusion protein targeting factor
mg	milligrams
MGE	mitochondrial GrpE
Mgm1p	mitochondrial genome maintenance 1 protein
min	minute
MIP	mitochondrial intermediate peptidase
ml	millilitre
mM	millimolar
MMM1	maintenance of mitochodrial morphology 1
MomX	mitochondrial outer membrane protein, X kDa
MPP	matrix processing peptidase
mRNA	messenger RNA
ms	millisecond
MSF	matrix stimulation factor
mt	mitochondrial
NADH	nicotinamide adenine dinucleotide, reduced form
NMR	nuclear magnetic resonance imaging
Ω	ohms
OMV	outer membrane vesicles
Oxa1	oxidase assembly protein 1
PAG	polyacrylamide gel
PAGE	polyacrylamide gel electrophoresis
PBS	phosphate buffered saline
PBSS	phosphate buffered saline, sucrose
PBSSP	phosphate buffered saline, sucrose, PMSF
PCR	polymerase chain reaction

PiC	inorganic phosphate carrier
PK	proteinase K
PMSF	phenylmethylsulfonyl fluoride
pN	pico Newton
PTP	permeability transition pore
RIP	repeat induced point mutation
RNA	ribonucleic acid
rRNA	ribosomal RNA
ROS	reactive oxygen species
rpm	revolutions per minute
rTom20	rat Tom20
SCAM	substituted cysteine accessibility mutagenesis
SDS	sodium dodecyl sulfate
SEM	sucrose, EDTA, MOPS
SEMP	sucrose, EDTA, MOPS, PMSF
Su9	subunit 9 of the F_0 ATP synthase
T	thymine
TIM	translocase of the inner mitochondrial membrane complex
TIMM8	translocase of the inner mitochondrial membrane 8 kDa, human nomenclature
TimX	translocase of the inner mitochondrial membrane X kDa
TOM	translocase of the outer mitochondrial membrane complex
TomX	translocase of the outer mitochondrial membrane X kDa
TPR	tetratricopeptide repeat
tRNA	transfer RNA
Ugo1p	ugo = Japanese for fusion
VDAC	voltage dependent anion conducting channel or porin
vol	volume
WD repeat	tryptophan-aspartate repeat
yTom20	yeast Tom20

1. INTRODUCTION

1.1 Mitochondria

Mitochondria are double membrane bound structures that are best known for their role in the production of cellular energy in eukaryotic cells. They consist of four subcompartments: the outer membrane, the intermembrane space, the inner membrane, and the matrix (reviewed in Attardi and Schatz, 1988; Neupert, 1997). Mitochondria contain a genome whose content is species specific, but generally encodes tRNAs, rRNAs, and a subset of the proteins involved in oxidative phosporylation (Attardi and Schatz, 1988). In addition to their role in energy production mitochondria have other important functions in the cell such as cellular Ca^{2+} homeostasis, β-oxidation, and maturation of iron-sulfur (Fe-S) clusters (Eaton, 1996; Berridge, 2000; Lill and Kispal, 2000; Rutter, 2000; Bootman, 2001). The importance of mitochondria is perhaps best exemplified by their involvement in human health. Mitochondrial dysfunction has been associated with a number of diseases and mitochondria have been shown to have roles in processes such as aging and apoptosis (Morgan-Hughes and Hanna, 1999; Schapira, 1999a,b; Tatton and Olanow, 1999; Wallace, 1999; Wallace *et al.*, 1999; Wallace and Murdock, 1999; Schon *et al.*, 2000; Shoubridge, 2000, 2001)

1.1.1 Origin of mitochondria

Mitochondria are nearly ubiquitous in eukaryotic cells. In fact, recent evidence suggests that most or all of the known amitochondriate eukaryotes (called Archezoa) were descendents of cells that once contained mitochondria but lost the organelles over time (Gray, 1989,1999; Gray *et al.*, 1999, 2001; Lang *et al.*, 1999; Martin *et al.*, 2001). It has been suggested that the acquisition of mitochondria may have been the single most important event in the evolution of eukaryotic cells and occurred simultaneously with the origin of the eukaryotic lineage (Gray *et al.*, 1999; Martin *et al.*, 2001).

The origin of mitochondria and chloroplasts has been a much-debated issue since the suggestion that some organelles may have been derived from free-living cells was put forward in 1883 (Schimper, 1883). During the 1970s, with the discovery of mitochondrial and chloroplast DNA, the endosymbiont model of organellar origin

became favored to explain the origins of both mitochondria and chloroplasts (Sagan, 1967, 1993). In brief, the endosymbiont model suggests that an amitochondriate anaerobic eukaryotic progenitor cell served as a host cell for the ancestor of mitochondria, probably a relative of α-proteobacteria (Margulis, 1975, 1976; Margulis and Tzertzinis, 1987; Gray, 1999; Gray *et al.*, 1999, 2001; Lang *et al.*, 1999; Dolan *et al.*, 2000; Martin *et al.*, 2001). In the case of chloroplasts, an aerobic non-photosynthetic progenitor cell became the host for a photosynthetic cyanobacteria ancestor. Once the host engulfed these bacteria, they remained intact within the cells. Over a period of time genes from these bacteria were transferred to the host nucleus and both types of symbionts became dependent on the host cell for existence, eventually leading to modern mitochondria and chloroplasts (Sagan, 1967, 1993; Race *et al.*, 1999; Blanchard and Lynch, 2000).

1.1.2 The cellular roles of mitochondria

Mitochondria have an important role in energy production, and are the major producers of ATP in eukaryotic cells (Attardi and Schatz, 1988; Saraste, 1999; Capaldi, 2000). Energy production in mitochondria mainly occurs through oxidative phosphorylation. This is a process whereby electrons are passed along a pathway of carrier complexes (the electron transport chain (ETC)) to the terminal electron acceptor in the pathway, molecular oxygen (Saraste, 1999). There are four large enzyme complexes in the ETC and these components are located in the mitochondrial inner membrane (Morgan-Hughes and Hanna, 1999; Saraste, 1999). Complex I, NADH-ubiquinone (CoQ_{10}) oxidoreductase, is the largest complex of the ETC and transfers electrons from NADH to ubiquinone. Complex II is succinate dehydrogenase - CoQ_{10} oxidoreductase and is a direct link between the Krebs cycle and the respiratory chain. Succinate dehydrogenase converts succinate to fumarate in the Krebs cycle, producing $FADH_2$ from which electrons are transferred to ubiquinone. Complex III, CoQ_{10} – cytochrome *c* oxidoreductase, transfers electrons from ubiquinone to cytochrome *c* and complex IV, cytochrome *c* oxidase, transfers electrons from cytochrome *c* to molecular oxygen. The energy of the transferred electrons is harnessed by complexes I, III and IV to actively transport hydrogen ions (protons) across the mitochondrial inner membrane, to the

intermembrane space. Proton transport results in the generation of a proton motive force, which is used to convert ADP to ATP by complex V, the F_1F_O ATP synthase. This enzyme converts the energy contained in the proton motive force to ATP by coupling ATP synthesis with the transport of protons down their concentration gradient.

Mitochondria have also been implicated indirectly in cellular Ca^{2+} homeostasis (Berridge, 2000; Rutter, 2000; Bootman, 2001). This is important as Ca^{2+} is a powerful intracellular second messenger and has been shown to control processes such as cellular proliferation, development, learning and memory, contraction of muscle cells, secretion of proteins and fertilization in deuterostomes. In addition, high cellular concentrations of Ca^{2+} can induce both apoptosis and necrosis depending on cell type. Intracellular Ca^{2+} is primarily stored in the endoplasmic reticulum and the Golgi apparatus. Preliminary evidence for mitochondrial involvement in Ca^{2+} homeostasis was seen using confocal microscopy and electron microscopic tomography (Mannella *et al.*, 1998; Rizzuto *et al.*, 1998). In these studies it was shown that parts of mitochondria and the endoplasmic reticulum are located in close proximity to one another in mammalian cells. This study shows that at least based on the spatial localization of mitochondria, interactions between the endoplasmic reticulum and mitochondria are possible. As a complement to this study, it has also been shown that the release of Ca^{2+} ions from the endoplasmic reticulum results in stimulation of ATP synthesis in mitochondria (Robb-Gaspers *et al.*, 1998a,b). Although these results do not conclusively demonstrate a direct link between Ca^{2+} homeostasis and mitochondria, they do raise the possibility that mitochondria may have a role in this process.

Mitochondria have also been shown to be a site of β-oxidation of fatty acids in eukaryotic cells (Eaton, 1996). β-oxidation is the process where fatty acids are oxidized and is the major source of energy for the heart and skeletal muscles. β-oxidation also provides ketone bodies for peripheral circulation, which are a major source of fuel for organs such as the brain when glucose levels are low. The enzymes responsible for mitochondrial β-oxidation are found within the mitochondrial matrix, and are closely associated with ETC complexes (Halestrap and Dunlop, 1986; Eaton *et al.*, 1996a, b; Eaton, 1996).

In addition, most known Fe-S proteins are located in mitochondria and are members of the respiratory complexes (Lill and Kispal, 2000). However, other Fe-S proteins exist in both the cytosol and nucleus and are important for processes such as intracellular iron uptake and storage, or are metabolic enzymes important for the synthesis of amino acids. The assembly of these Fe-S clusters occurs in the mitochondrial matrix (Craig *et al.*, 1999; Lill *et al.*, 1999). The importance of this process is best illustrated by the fact that generation of Fe-S clusters is one of the only processes performed by mitochondria that is vital to the survival of *Saccharomyces cerevisiae* (Lill and Kispal, 2000).

Initially, it was thought that mitochondria only caused cellular death through ATP depletion and Ca^{2+} dysregulation (Di Lisa and Bernardi, 1998). It has now been shown that mitochondria are major regulators of apoptosis, a process of cell death that results in cell shrinkage, plasma membrane blebbing, and DNA fragmentation (Tatton and Olanow, 1999; Bernardi *et al.*, 2001). As an example of their importance in this process, a number of proteins that either induce or inhibit apoptosis are selectively targeted to mitochondria. These proteins include members of the Bcl2 family, which contain both pro- and anti-apoptotic members and are mitochondrial outer membrane proteins; cytochrome *c*, which along with its role in oxidative phosphorylation has been shown to be an inducer of apoptosis; and the apoptosis inducing factor (AIF), located within the mitochondrial intermembrane space (Liu *et al.*, 1996; Gross *et al.*, 1999; Lorenzo *et al.*, 1999; Tsujimoto, 2002). Mitochondria regulate apoptosis through regulation of the permeability transition pore (PTP). The components of the PTP identified to date include the voltage dependent anion conduction channel (VDAC or porin) in the mitochondrial outer membrane, and the ADP/ATP carrier (AAC), located in the mitochondrial inner membrane (Marzo *et al.*, 1998; Bernardi, 1999; Harris *et al.*, 2000; McStay and Halestrap, 2002). PTP opening increases the permeability of the inner membrane to ions and solutes and causes a rapid dissipation of membrane potential, swelling of mitochondria, and bursting of the mitochondrial outer membrane. This results in release of cytochrome *c*, AIF and other pro-apoptotic proteins to the cytosol, and initiation of apoptosis.

Aging is a process of general deterioration, and cellular aging is thought to arise from somatic mutations and other defects that are incompletely repaired (Cortopassi and Wong, 1999; Brunk and Terman, 2002; de Grey, 2002a; de Grey, 2002b). Mitochondria, as the major producers of reactive oxygen species (ROS) in eukaryotic cells, have been implicated in aging, as ROS may damage many cellular components (Martindale and Holbrook, 2002; Wei and Lee, 2002). It is not clear if the deterioration of mitochondria themselves is a cause or an effect of aging, but mitochondrial deterioration has been associated with increased production of ROS in cells. Several lines of evidence support the view that mitochondria, and mitochondrial components deteriorate over time (Cortopassi and Wong, 1999). First, mtDNA accumulates spontaneous deletions and rearrangements that expand during a lifetime, and have the potential to become pathogenic. This is especially apparent in post-mitotic tissues that are actively oxidative such as neurons in the brain and all types of muscle cells (Arnheim and Cortopassi, 1992; Cortopassi *et al.*, 1992). Skeletal muscle cells have also been shown to experience age related fiber loss, atrophy, and cytochrome oxidase deficiency (reviewed in (Cortopassi and Wong, 1999)). Finally, mitochondria from aged individuals show a decrease in membrane potential compared to mitochondria isolated from young individuals (Hagen *et al.*, 1997).

As mitochondria have many important roles in the cell, there are a variety of disorders associated with mitochondrial impairment (Morgan-Hughes and Hanna, 1999; Schapira, 1999a,b; Wallace, 1999; Wallace *et al.*, 1999; Wallace and Murdock, 1999; Schon *et al.*, 2000; Munnich and Rustin, 2001; Shoubridge, 2001; Turnbull *et al.*, 2001). These diseases show a number of different clinical presentations and represent a highly diverse group of disorders. Symptoms of mitochondrial diseases include deafness, progressive vision loss, epileptic seizures, cardiomyopathies, muscle atrophy, and neurodegenerative disorders. These diseases can be caused by inherited or sporadic mutations in mtDNA or nuclear genes encoding mitochondrial proteins. Mutations in mtDNA show maternal inheritance patterns while nuclear mutations show autosomal recessive inheritance patterns.

A major reason for the diversity of these disorders and their symptoms can be attributed to the fact that mutations in mtDNA may exist or arise in a population of wild

type mtDNA and their rates may vary in different cells and tissues due to random segregation events during mitosis. In this case, the proportion of mutant DNAs within the population of mitochondria as well as the distribution of mutant mtDNA within organelles, cells, tissues, and specific organs will affect the presence or severity of the mitochondrial disorder. The nuclear genetic background of an individual also seems to determine the severity of mitochondrial disorders. In addition, mitochondrial diseases tend to be progressive in nature, with the ratio of mtDNA mutations shifting throughout a patient's lifespan. Thus, these diseases either present or increase in severity as a person ages. An example of a mutation affecting mitochondrial DNA is Kearns-Sayre Syndrome (KSS) which is a fatal multisystemic disorder (Moraes *et al.*, 1989; Nakase *et al.*, 1990; Shanske *et al.*, 1990). KSS results from a number of mitochondrial DNA defects including large-scale DNA deletions and rearrangements. An example of a disease that results from a nuclear mutation is human deafness dystonia syndrome (Koehler *et al.*, 1999a). This disorder results from a mutation in the gene *TIMM8* that encodes a protein involved in the import of proteins into mitochondria.

1.1.3 Mitochondrial morphology, maintenance and inheritance

In general, mitochondria can be visualized as tubular structures with a single outer membrane covering a highly convoluted and invaginated inner membrane. Mitochondria have a relatively large matrix volume with the inner membrane boundary closely apposed to outer membrane (Frey and Mannella, 2000). While mitochondria can vary dramatically in length, their diameters generally fall between 0.5 to 1.0 μm (Griparic and van der Bliek, 2001). Contact sites between the inner and outer mitochondrial membrane were first defined by Hackenbrock (1966) by observing electron micrographs of mitochondria exposed to osmotic shock or changes in metabolic state (Hackenbrock, 1966; Hackenbrock, 1968; Hackenbrock and Caplan, 1969; Hackenbrock *et al.*, 1971). During osmotic shock the inner membrane was observed to pull away from the outer membrane, except at discrete loci.

Mitochondria have an elaborate morphology and can be seen to form complex interconnected reticula with contacts to the cytoskeleton, plasma membrane, and endoplasmic reticulum (reviewed (Frey and Mannella, 2000; Jensen *et al.*, 2000; Griparic

and van der Bliek, 2001)). The morphology of the mitochondrial outer membrane is simple, as it is a single membrane covering the mitochondrial inner membrane with no folds or invaginations. The structure of the inner membrane is more complex and contains many folds and invaginations. Initially, two models were proposed to describe the structure of the mitochondrial inner membrane based on conventional two-dimensional transmission electron microscopy (EM). Palade in 1952 named the projections of the inner membrane *cristae mitochondriales*, and described them as "baffle-like" projections that result from large folds in the inner membrane (Palade, 1952). This remains the most popular model of mitochondrial structure and implies the existence of broad openings in the cristae to the intermembrane space. The second model, proposed by Sjöstrand in 1956, suggested that the inner membrane forms septa that divide the matrix into many compartments (Sjöstrand, 1956).

Recent evidence based on the process of EM tomography challenges both of these models (Mannella *et al.*, 1994; Perkins *et al.*, 1997). EM tomography is a three-dimensional imaging technology that allows visualization of sample sections between 0.25 to 1.5μm in width (McEwen and Frank, 2001) as opposed to conventional microscopy, which can only visualize sample sections from 50 to 100nm in width. In the process of EM tomography, over 100 projections of a sample are taken at a series of different angles, and a computer program aligns the projections to form a three dimensional image of the section in question. Using this technique with rat liver mitochondria Mannella *et al.* (1994) showed that cristae are pleiomorphic in structure. Most of the cristae observed were tubular extensions of the inner membrane with diameters ranging from 30 to 40nm, and extending hundreds of nanometers into the matrix space. Perkins *et al.* (1997) used the same approach to visualize mitochondria from chick cerebellum. They discovered that the cristae – inner membrane junctions were approximately 28nm in diameter, again refuting the idea that cristae have broad openings that are exposed to the intermembrane space.

Mitochondrial morphology, distribution, and structure are highly tissue specific due to their diverse roles in cells (Jensen *et al.*, 2000). For example, muscle cells contain many mitochondria (mitochondria make up as much as 30% of their internal volume) in tubular arrays. These arrays are found between the actin and myosin bundles and are

thought to allow for efficient distribution of energy in the form of ATP, as well as ADP uptake. Fibroblasts, on the other hand contain few mitochondria that are scattered throughout the cell. Mitochondrial morphology and number vary over the course of the cell cycle, and are highly dependent on environmental conditions. An example of this process has been documented in *S. cerevisiae.* When *S. cerevisiae* is grown under anaerobic conditions, mitochondria form small organelles called protomitochondria, while under conditions of aerobic growth, mitochondria become large and elongated (Criddel, 1969; Plattner, 1969; Hoffmann and Avers, 1973; Stevens, 1977). In aerobic conditions mitochondria are positioned at the cell periphery, probably to aid in oxygen uptake, using the elongated structure of these mitochondria to distribute ATP through the cell. These elongated mitochondria are termed a tubular reticulum, and this is a typical structure for mitochondria found in many different eukaryotes (Jensen *et al.*, 2000). Mitochondrial number also varies in a growth dependent manner (Hoffmann and Avers, 1973; Stevens, 1977). During logarithmic growth there are between one to ten elongated mitochondria in a yeast cell, while in stationary phase, the tubular mitochondrial reticulum fragments into many small mitochondria.

Maintenance of mitochondria and mitochondrial morphology requires an on going process of mitochondrial fission and fusion events (Frey and Mannella, 2000; Jensen *et al.*, 2000; Osteryoung, 2000; van der Bliek, 2000; Griparic and van der Bliek, 2001; Osteryoung, 2001; Shaw and Nunnari, 2002). These fission and fusion events are closely regulated in cells by an unknown mechanism. In brief, division of the mitochondrial outer membrane is accomplished by at least three proteins in *S. cerevisiae.* Dmn1p, a dynamin related protein; Mdv1p, a WD repeat protein that binds Dmn1p and localizes to mitochondria; and Fis1p/Mvd2p, a protein that is evenly distributed on the outer surface of mitochondria are all required for fission of mitochondria (Otsuga *et al.*, 1998; Bleazard *et al.*, 1999; Mozdy *et al.*, 2000; Tieu and Nunnari, 2000; Tieu *et al.*, 2002). Mutations in any of these genes block mitochondrial fission and result in cells with a network of highly connected mitochondria. It has been suggested that Dmn1p controls the final stage of mitochondrial division, while Fis1p/Mdv2 may be required for assembly of the mitochondrial division apparatus but is not itself part of this complex (Tieu *et al.*, 2002). *In vivo* the inner and outer mitochondrial membranes divide simultaneously, but the inner

membrane is capable of independent division. Thus it has been suggested that the inner membrane possesses a separate division apparatus (reviewed in Griparic and van der Bliek, 2001). This apparatus is probably related to the bacterial division protein *FtsZ*.

Mitochondrial fusion requires the proteins Fzo1p and Mgm1p, and mutations in these genes lead to increased fragmentation of mitochondria and loss of mitochondrial DNA (Hermann and Shaw, 1998; Hermann *et al.*, 1998; Rapaport *et al.*, 1998a; Wong *et al.*, 2000; Fritz *et al.*, 2001). Fzo1p is found in an 800 kDa complex that connects the inner and outer membranes (Rapaport *et al.*, 1998a). The composition of this complex is unknown.

Mitochondria are essential organelles that cannot form *de novo*, but result from division of pre-existing mitochondria (Attardi and Schatz, 1988; Catlett and Weisman, 2000; Jensen *et al.*, 2000; Griparic and van der Bliek, 2001). As a result, the appropriate segregation of mitochondria to daughter cells is an important process in cell division. While it is possible that mitochondrial partitioning is a stochastic process whereby the organelles are randomly inherited by both mother and daughter cells, it seems more likely that mitochondrial partitioning is an ordered process. An increasing body of evidence suggests that attachment of mitochondria to the cytoskeleton is important for the process of mitochondrial inheritance (Catlett and Weisman, 2000). Mitochondria have been shown to be associated with actin, microtubules, and intermediate filaments, with specific associations dependent on cell type (Catlett and Weisman, 2000; Jensen *et al.*, 2000). As an example, in *S. cerevisiae* the actin cytoskeleton is important for mitochondrial inheritance, while inheritance of mitochondria in *Neurospora crassa* is dependent on microtubules (Drubin *et al.*, 1993; Hermann *et al.*, 1997; Prokisch *et al.*, 2000; Fuchs *et al.*, 2002).

1.2 Mitochondrial protein import

Although mitochondria contain their own DNA, this only encodes a small number of the proteins required for mitochondrial function and biogenesis (Attardi and Schatz, 1988). Over 98% of the proteins found in mitochondria are encoded in the nucleus, translated in the cytosol and imported into mitochondria (reviewed in Pfanner and Neupert, 1990; Bauer *et al.*, 1999b; Koehler *et al.*, 1999b; Tokatlidis and Schatz, 1999;

Voos *et al.*, 1999; Bauer *et al.*, 2000; Herrmann and Neupert, 2000; Bauer and Neupert, 2001; Paschen and Neupert, 2001; Pfanner and Geissler, 2001; Rehling *et al.*, 2001; Chacinska *et al.*, 2002; Pfanner and Wiedemann, 2002). There are four protein complexes required for import, sorting and assembly of mitochondrial precursor proteins into the four mitochondrial sub-compartments (Fig. 1). The TOM complex (**T**ranslocase of the **O**uter mitochondrial **M**embrane) is responsible for initial recognition and translocation of mitochondrial preproteins across or into the mitochondrial outer membrane. There are three translocase complexes in the mitochondrial inner membrane. The TIM23 complex (**T**ranslocase of the **I**nner mitochondrial **M**embrane) is responsible for import of matrix targeted precursors across the inner membrane, as well as a few proteins of the mitochondrial inner membrane or intermembrane space that follow a stop/transfer pathway. The TIM22 complex is required for assembly of a subset of proteins with internal targeting signals such as the carrier family of proteins, which includes AAC, into the inner membrane (Fig. 1). The OXA1 translocase inserts some nuclear encoded proteins, and most, if not all, mitochondrial encoded proteins from the matrix into the mitochondrial inner membrane (reviewed in Stuart, 2002).

The processes involved in the import of nuclear encoded proteins into mitochondria have been most well studied in the organisms *S. cerevisiae* and *N. crassa*. They serve as good models for this process as they are genetically tractable and have established methods for growth and handling. In addition, homologs of the proteins used in these processes have been identified in mammals and are fairly well conserved between diverse species (Iwahashi *et al.*, 1994; Bömer *et al.*, 1996; Komiya *et al.*, 1996; Iwahashi *et al.*, 1997; Bauer *et al.*, 1999a,b; Jin *et al.*, 1999; Koehler *et al.*, 1999a; Saeki *et al.*, 2000; Suzuki *et al.*, 2000; Yano *et al.*, 2000; Hoogenraad *et al.*, 2002)

1.2.1 Import of mitochondrial preproteins is primarily a post-translational event

Nuclear-encoded mitochondrial precursor proteins are first translated completely in the cytosol, before being targeted to and imported into mitochondria (reviewed in Pfanner and Neupert, 1990; Bauer *et al.*, 1999b, 2000; Koehler *et al.*, 1999b; Tokatlidis and Schatz, 1999; Voos *et al.*, 1999; Herrmann and Neupert, 2000; Bauer and Neupert, 2001; Paschen and Neupert, 2001; Pfanner and Geissler, 2001; Rehling *et al.*, 2001;

Chacinska *et al.*, 2002; Pfanner and Wiedemann, 2002). This process is in contrast to the targeting and translocation of proteins into the endoplasmic reticulum which are transported across the membrane in a co-translational process (reviewed in Johnson and Haigh, 2000). Evidence for post-translational import of mitochondrial precursors was first described by Harmey *et al.* (1977) and Hallermayer *et al.* (1977). Harmey *et al.* (1977) followed the synthesis and transport of mitochondrial proteins in a cell-free homogenate of *N. crassa.* Their studies showed that the mitochondrial precursor translation products were first released from ribosomes into the cytosol, before being imported and assembled into mitochondria. Hallermayer *et al.* (1977) studied the process of mitochondrial protein import in intact *N. crassa* cells. They used pulse-chase experiments to show that mitochondrial precursor proteins accumulated in the cytosol before these labeled proteins were detectable in mitochondria. They also determined that cycloheximide, an inhibitor of cytosolic translation, does not affect import of mitochondrial preproteins. Reid and Schatz (1982) reached a similar conclusion using pulse-chase experiments in *S. cerevisiae*.

More recent evidence in the literature suggests that some mitochondrial precursor proteins may be imported in a co-translational fashion. Fujiki and Verner (1991) studied the process of co-translational import using an *in vitro S. cerevisiae* system, and observed that for import of an artificial precursor protein (the N-terminus of cytochrome oxidase subunit IV fused to mouse dihydrofolate reductase (COXIV-DHFR)), efficient import was only observed in the presence of ribosomes, suggesting that translation and import are coupled. In 1993, using pulse-chase assays, and protein synthesis inhibitors, Fujiki and Verner showed that no pool of extra-mitochondrial COXIV-DHFR could be detected in yeast and import of this precursor only occurred efficiently in the absence of translation inhibitors (Fujiki and Verner, 1993) further supporting the co-translational import models. Finally, Knox *et al.* (1998) reported that the fumarase protein in *S. cerevisiae* was imported into mitochondria in a strictly co-translational process due to the fast folding kinetics of the protein. In the absence of co-translational import, folding would occur before fumarase had reached the TOM complex. As a result, the protein would not be imported properly.

1.2.2 Precursor targeting

The most well studied mitochondrial targeting sequence is the N-terminal, cleavable presequence (reviewed in Pfanner and Neupert, 1990; Neupert, 1997; Pfanner *et al.*, 1997; Voos *et al.*, 1999; Pfanner and Geissler, 2001; Chacinska *et al.*, 2002; Pfanner and Wiedemann, 2002). The majority of proteins targeted to mitochondria are synthesized with a 20 to 80 N-terminal extension that is not present in the mature protein. The presence of this presequence is necessary and sufficient for the correct recognition and import of precursors by mitochondria (Gillespie *et al.*, 1985; Horwich *et al.*, 1985; Horwich *et al.*, 1986). Mitochondrial presequences lack a common primary structure but are enriched in hydroxylated and positively charged amino acids and are deficient in negatively charged residues (von Heijne, 1986). Structural studies of these mitochondrial presequences suggest that they form amphipathic α-helices that have one positively charged face hydrophyllic face, and one neutrally charged hydrophobic face (von Heijne, 1986; Claros and Vincens, 1996). Formation of this α-helix seems to be important for precursor targeting and import as the overall charge of the presequence (Hammen *et al.*, 1996a; Hammen *et al.*, 1996b). Hammen *et al.* (1996a,b) made point mutations in the presequence of rat liver aldehyde dehydrogenase (ALDH) to assay the importance of positive charges in precursor targeting. They found that the charges in ALDH could be made neutral as long as the presequence was still capable of forming an α-helix near the N-terminus of the protein. Only a small number of the amino acids in an N-terminal presequence may contain mitochondrial targeting information. Deletion experiments were also performed with alcohol dehydrogenase III (ALDIII) (Pilgrim and Young, 1987). They found that only amino acids 17-28 of the presequence were required for targeting of ALDIII to mitochondria. Loss of the initial amino acids in the 1-17 region of the targeting sequence only reduced the efficiency of import and processing of ALDIII. The remainder of a presequence may be required to maintain appropriate secondary structure. Surprisingly, a C-terminal targeting sequence was identified in the last 36 amino acids of the DNA helicase Hmi1p of *S. cerevisiae* (Lee *et al.*, 1999). This presequence has similar properties to classical N-terminal targeting signals and is imported into mitochondria in the C- to N-terminal direction.

The remainder of mitochondrial proteins are targeted to mitochondria via internal targeting sequences (reviewed in Pfanner and Neupert, 1990; Koehler *et al.*, 1999b; Tokatlidis and Schatz, 1999; Voos *et al.*, 1999; Herrmann and Neupert, 2000; Paschen and Neupert, 2001; Pfanner and Geissler, 2001; Rehling *et al.*, 2001; Chacinska *et al.*, 2002; Pfanner and Wiedemann, 2002). Proteins with internal targeting sequences include members of the TOM and TIM complexes, other proteins found in the outer and inner mitochondrial membranes, and some proteins located in the intermembrane space. Some mitochondrial outer membrane proteins contain a short presequences-like segment near their N-terminus followed by a membrane anchor or "stop-transfer" sequence. An example of this type of protein is Tom70 (Hurt *et al.*, 1985; McBride *et al.*, 1992). Insertion of the outer membrane protein Tom22 depends on an internal segment of the protein that resembles a classical N-terminal targeting signal (Rodriguez-Cousino *et al.*, 1998). Another class of outer membrane proteins carries targeting information in a C-terminal hydrophobic region. Members of this group include the anti-apoptic protein Bcl-2 (Mitoma and Ito, 1992; Nguyen *et al.*, 1993; Shore *et al.*, 1995). A final class of outer membrane proteins are the β-barrel proteins whose targeting information is poorly defined and may require structural elements. Metabolite carrier class proteins of the inner membrane contain targeting information in internal positively charged segments called carrier sequence motifs (Smagula and Douglas, 1988; Sirrenberg *et al.*, 1998). Finally, an internal motif has been identified that functions to target proteins into the intermembrane space (Diekert *et al.*, 1999). This motif was first identified in the protein cytochrome *c* heme lyase.

1.2.3 Requirements for cytosolic ATP, Hsp70, and other chaperones

A requirement for cytosolic ATP was identified early in the study of mitochondrial protein import (Eilers *et al.*, 1987; Pfanner *et al.*, 1987). Pfanner *et al.* (1987) studied the role of ATP in the import of the ADP/ATP carrier protein (AAC), the F_1-ATPase subunit β ($F_1\beta$), the F_0-ATPase subunit 9 (Su9), and a fusion protein between the presequence of Su9 and dihydrofolate reductase (Su9-DHFR). They found that initial interactions of the preproteins with mitochondria and translocation of precursors into the matrix required the presence of ATP and that the amount of ATP required for efficient

import was precursor dependent. In addition to the ATP requirements for import, precursor proteins were more sensitive to treatment with exogenous proteases in the presence of ATP. Taken together, this suggested that ATP was involved in maintaining mitochondrial preproteins in an unfolded or "import competent" state. Eilers *et al.* (1987) studied the energy requirements for mitochondrial protein import in isolated yeast mitochondria. They found that import of preproteins was dependent on ATP and also reconfirmed an earlier observation that import of preproteins required membrane potential (Gasser *et al.*, 1982; Schleyer and Neupert, 1982). In 1988, two groups showed that Hsp70, a cytosolic heat shock protein, was required for import of mitochondrial preproteins (Deshaies *et al.*, 1988a,b; Murakami *et al.*, 1988). Hsp70 most likely binds mitochondrial preproteins following protein synthesis to keep the precursor proteins in an unfolded state. Further study revealed that the requirements of ATP for import could be bypassed if an importing preprotein was unfolded in 8M urea before import (Eilers and Schatz, 1988; Pfanner *et al.*, 1988, 1990; Sheffield *et al.*, 1990; Jascur *et al.*, 1992)). A recent paper has suggested that in mammals, the cytosolic chaperones Hsp90 and Hsp70 dock onto a specialized TPR domain in the import receptor Tom70 at the outer mitochondrial membrane and that this interaction is required for import of carrier class precursors (Young *et al.*, 2003). In yeast, it appears that only the chaperone Hsp70 is required for delivery of carrier class precursors to Tom70.

There has been much debate over the role that additional cytosolic chaperones play in the process of mitochondrial protein import. In one example, a protein of unknown function was purified from rabbit reticulocytes and rat liver cells that seemed to stimulate import of mitochondrial preproteins (Ono and Tuboi, 1988, 1990; Murakami and Mori, 1990; Murakami *et al.*, 1992; Hachiya *et al.*, 1993, 1994; Komiya *et al.*, 1994). This factor, named MSF (for **M**itochondrial import **S**timulation **F**actor), was found to stimulate unfolding and import of preproteins in an ATP dependent manner. Another potential cytosolic chaperone was identified by Cartwright *et al.* (1997). This factor, named Mft52, was identified in the cytosol of yeast and was found to contain a receptor-like "acid bristle" domain that bound positively charged presequences. Mutations in the Mft52 gene were shown to severely inhibit protein import *in vivo*. In contrast to these findings, Becker *et al.* (1992) isolated chemically pure mitochondrial preproteins, and

imported these into mitochondria in an *in vitro* system. They found that efficient import of their chemically pure precursor did not require recognition factors or cytosolic chaperones. It is possible that only a subset of mitochondrial preproteins may be dependent on cytosolic factors for efficient import.

1.2.4 An overview of the TOM complex

Initial recognition and translocation of mitochondrial precursors across the outer mitochondrial membrane is accomplished by the TOM complex (Fig. 2) (reviewed in Pfanner and Neupert, 1990; Koehler *et al.*, 1999b; Tokatlidis and Schatz, 1999; Voos *et al.*, 1999; Herrmann and Neupert, 2000; Paschen and Neupert, 2001; Pfanner and Geissler, 2001; Rehling *et al.*, 2001; Chacinska *et al.*, 2002; Pfanner and Wiedemann, 2002). This complex consists of receptors that serve to recognize mitochondrial presequences and membrane embedded components that comprise the mitochondrial general import pore (GIP) through which preproteins traverse the mitochondrial outer membrane. The TOM complex is also responsible for the insertion of proteins into the mitochondrial outer membrane.

The receptors of the TOM complex are Tom70 (TOM complex component, 70 kDa), Tom22, and Tom20 (Fig. 2) (Kiebler *et al.*, 1990; Künkele *et al.*, 1998b). In *S. cerevisiae*, two additional TOM complex receptors have been identified called Tom71 and Tom37 (Bömer *et al.*, 1996; Schlossmann *et al.*, 1996). Tom71 is a yeast homolog of Tom70. Recent evidence does not support a role for Tom37 in recognition of mitochondrial preproteins (Ryan *et al.*, 1999), but the protein has now been shown to form part of a separate protein complex required for the assembly of β-barrel proteins into the mitochondrial outer membrane (Wiedemann, 2003). Tom70 and Tom71 are receptors for proteins with internal targeting signals such as the mitochondrial metabolite carrier proteins (Hines *et al.*, 1990; Söllner *et al.*, 1990; Ryan *et al.*, 1999). The receptors, Tom20 and Tom22 function together to deliver precursor proteins to Tom40 and the GIP (Kiebler *et al.*, 1993b; Mayer *et al.*, 1995b). It is interesting to note that import of mitochondrial precursors can occur in the absence of mitochondrial surface receptors but at low efficiency and has been termed "bypass-import" (Pfaller *et al.*, 1989). The GIP has been shown to consist of the protein Tom40, Tom22, and the small

TOM components, Tom5, Tom6, and Tom7 (Künkele *et al.*, 1998a,b; Ahting *et al.*, 2001) (S. Nussberger and W. Neupert personal communication). Tom40 has been shown to be the major component of the pore through which preproteins traverse the mitochondrial outer membrane, while the small TOM components are thought to affect precursor delivery to the protein import pore as well as the stability of the TOM complex (Hill *et al.*, 1998; Künkele *et al.*, 1998a,b).

An additional protein, termed Mom30, was once thought to be a membrane embedded component of the TOM complex (Moczko *et al.*, 1992; Söllner *et al.*, 1992; Kiebler *et al.*, 1993b). However, this protein is not mentioned in recent literature and it is likely that it was erroneously considered to be a TOM complex component due to contamination of TOM complex preparations with the highly abundant 30 kDa outer membrane protein, porin. Two additional potential TOM components, called metaxin and Tom34, have been identified in humans (Armstrong *et al.*, 1997, 1999; Nuttall *et al.*, 1997; Hoogenraad *et al.*, 2002). Subsequent work has shown that these proteins are not bonafide members of the TOM complex but may be chaperones that play roles in the import of precursor proteins in mammalian cells (Abdul *et al.*, 2000; Mukhopadhyay *et al.*, 2002; Yang and Weiner, 2002).

Two different versions of the TOM complex have been identified based on purification in the presence of different detergents (Dekker *et al.*, 1998; Künkele *et al.*, 1998a,b; Ahting *et al.*, 1999; Meisinger *et al.*, 2001). The TOM holo complex can be isolated from mitochondria by solubilization of mitochondria in the mild non-ionic detergent digitonin. The holo complex is 550-600 kDa in size and contains the components Tom70, Tom22, Tom20, Tom40, Tom7, Tom6, and Tom5 (Künkele *et al.*, 1998a,b) (W. Neupert and S. Nussberger, personal communication). In *N. crassa*, the stoichiometry of Tom70, Tom40, Tom22, and Tom20 in the holo TOM complex was suggested to be 1.5:8:3.1:2. The stoichiometry of Tom5, Tom6 and Tom7 in this complex has not been determined to date.

The core complex consists of those members of the TOM complex that are strongly associated with one another. The core complex can be isolated from mitochondria solubilized in either dodecylmaltoside, or tritonX-100 and results in the dissociation of Tom20 and Tom70 from the complex (Dekker *et al.*, 1998; Ahting *et al.*,

1999; Meisinger *et al.*, 2001). The resulting complex is 400 kDa in size and is composed of Tom40, Tom22, Tom7, Tom6, and Tom5. The stochiometry of Tom40, Tom22, Tom7 and Tom6 in the core complex was determined to be 8:4:2:2, respectively. Both the TOM core and TOM holo complexes have been shown to recognize and bind mitochondrial preproteins in the absence of chaperones and lipids (Stan *et al.*, 2000). In addition, it was shown that preproteins could be transferred to the GIP of these complexes because bound precursors were protected from processing by added matrix processing peptidase (MPP). The TOM complex pore measures 20 to 26 Å in diameter by both electron microscopic analysis and size exculsion studies and is cation-selective and voltage gated (Hill *et al.*, 1998; Künkele *et al.*, 1998b; Künkele *et al.*, 1998a; Ahting *et al.*, 1999; Schwartz and Matouschek, 1999; Ahting *et al.*, 2001). When viewed by EM tomography, purified core TOM complex has been shown to contain two pores, while holo TOM complex preparations contain both two pore and three pore forms (Künkele *et al.*, 1998a; Ahting *et al.*, 1999). It was shown later that mitochondria lacking the protein Tom20 had TOM complexes that contained only two pores (Model *et al.*, 2002). This suggests that the random loss of Tom20 during purification of the holo complex probably gives rise to a mixed population of two and three pore structures.

Initial recognition and binding of precursor proteins to the TOM complex is thought to occur at the cytosolic face of the mitochondrial outer membrane at the *cis* protein-binding site (Fig. 2) (Mayer *et al.*, 1995b). Mayer *et al.* (1995a), using purified outer membrane vesicles (OMVs), showed precursor binding is dependent on receptors facing the cytosol because precursor binding is abolished if OMVs are pretreated with proteases. In addition to this finding, *cis* site binding requires the presence of both Tom20 and Tom22, as precursor binding was abolished if either Tom20 or Tom22 were inactivated. It was also determined that precursor binding was reversible, and that binding was highly sensitive to addition of salt, suggesting that initial recognition of mitochondrial preproteins may involve electrostatic interactions. A second precursor-binding site was identified on the intermembrane space face of the outer membrane and was termed the *trans* site (Mayer *et al.*, 1995c). This study, again using OMVs, demonstrated that presequences, but not the mature regions of preproteins, were capable of being translocated across the outer membrane in the absence of $\Delta\psi$ or the TIM

complexes, and that translocation and binding of presequences to the *trans* site stimulated unfolding of mitochondrial preproteins. In addition, precursors arrested at the *trans* site were stably bound to the TOM complex even after the addition of salt, suggesting that hydrophobic interactions between the mitochondrial presequence and the *trans* site may be important for recognition and binding at this stage of import (Rapaport *et al.*, 1998c). Tom40 was identified as a possible component of both the *cis* and *trans* binding sites, as preproteins arrested at these sites could be chemically cross-linked to Tom40 *in vitro* (Rapaport *et al.*, 1997).

1.2.4.1 The Tom20 receptor

Tom20 was the first mitochondrial import receptor identified and has a large C-terminal domain exposed to the cytosol (reviewed in Pfanner and Neupert, 1990; Koehler *et al.*, 1999b; Tokatlidis and Schatz, 1999; Voos *et al.*, 1999; Herrmann and Neupert, 2000; Paschen and Neupert, 2001; Pfanner and Geissler, 2001; Rehling *et al.*, 2001; Chacinska *et al.*, 2002; Pfanner and Wiedemann, 2002). Tom20 was identified in *N. crassa* as being important for import of mitochondrial preproteins, as Fab fragments against this protein were shown to inhibit the import of precursor proteins containing classical N-terminal targeting sequences as well as porin (Söllner *et al.*, 1990). Tom20 was also found to be specifically enriched in mitochondrial contact sites. The yeast homolog of Tom20 was identified later and was found not to be essential for viability of yeast but was required for growth on non-fermentable carbon sources (Ramage *et al.*, 1993). Inactivation of Tom20 in *N. crassa* resulted in strains which exhibited extremely slow growth (Harkness *et al.*, 1994b). Both Yeast and *N. crassa* mitochondria lacking Tom20 have a decreased ability to import precursor proteins with classical N-terminal targeting sequences, while import of AAC or the phosphate carrier protein (PiC), which contain internal targeting sequences, were only moderately affected (Ramage *et al.*, 1993; Harkness *et al.*, 1994b). Analysis of Tom20 *N. crassa* mutants showed that mitochondria lacking Tom20 had few cristae and were deficient in cytochromes and protein synthesis activity (Harkness *et al.*, 1994b). Tom20 has been shown to contain a TPR motif that may be important for preprotein interactions and for association of Tom20 with other members of the TOM complex (Blatch and Lassle, 1999).

Initial characterization of important domains of Tom20 was done using the rat (r) Tom20 protein (Iwahashi *et al.*, 1997). This study used a series of rTom20 truncation constructs to rescue the ability of a yeast (y) Tom20 mutant to grow on non-fermentable carbon sources. It was shown that rescue of the yeast mutant occurred only if the construct contained the Tom20 predicted membrane-spanning domain, while the TPR motifs and acidic regions of Tom20 were shown not to be essential for the function of the protein. Brix *et al.* (1997) expressed and purified cytosolic domains of the TOM complex receptors for use these in *in vitro* binding assays. yTom20 was found to bind precursors containing both N-terminal and internal targeting sequences. Precursor binding was enhanced by the addition of salt, and competed for by the addition of chemically synthesized presequence fragments. However, a different study showed that rTom20 required cytosolic Hsp70 and ATP to bind precursor proteins, and that binding was inhibited by the addition of salt (Komiya *et al.*, 1997). In addition, this group suggested that precursors initially bind rTom70/MSF before being passed to rTom20.

More detailed studies of the rTom20 structure revealed that the membrane-spanning domain of the protein encompassed amino acids 5 through 25, while the cytosolic region of the protein was divided into three distinct regions (Schleiff and Turnbull, 1998a,b). A region encompassing amino acids 30 through 50 was identified that existed in a loosely folded confirmation and was hypothesized to be involved in binding to the mitochondrial outer membrane. A second region was identified as being important for binding α-helical targeting sequences and encompassed amino acids 60 through 90 of Tom20. The third cytosolic region encompassed amino acids 90 through 145. This region was suggested to exist in a tightly folded globular structure and thought to be important for binding internal targeting sequences. Brix *et al.* (1999) studied the ability of the chemically purified cytosolic domain of Tom20 to bind to cellulose bound peptide fragments of cytochrome *c* oxidase subunit IV (COXIV), which contains an N-terminal targeting sequence or to PiC. Tom20 was found to preferentially bind the presequence of COXIV, and to bind multiple segments in PiC excluding the N-terminal region of the protein.

The NMR structure of a rΔ50Tom20 in complex with the presequence of ALDH was solved (Abe *et al.*, 2000). It was found that the cytosolic domain of Tom20 forms an

α-helical groove to accommodate presequences and precursor binding involves interactions with the hydrophobic face of the presequences and leucine residues in the presequence binding groove of Tom20. Interestingly, some of the residues within the hydrophobic pocket were found to reside within the TPR repeat and were well conserved between species. In an attempt to identify the segments of presequences involved in Tom20 binding Muto *et al.* (2001) monitored the chemical shift perturbations of NMR signals of five labeled presequences by addition of the cytosolic domain of rat or yeast Tom20. All of the matrix targeting signals were found to be unstructured in aqueous solution and Tom20 caused perturbations of only a subset of backbone amides suggesting that Tom20 only binds to small segments of presequences.

Tom20 homologs have been found in many species of fungi, mammals and plants (McBride *et al.*, 1996; Iwahashi *et al.*, 1997; Terada *et al.*, 1997; Jansch *et al.*, 1998; Macasev *et al.*, 2000; Werhahn *et al.*, 2001). For the most part, all of the animal and fungal Tom20 proteins are similar, and for mammalian and yeast Tom20, it has been shown the proteins can be functionally interchanged (McBride *et al.*, 1996; Iwahashi *et al.*, 1997; Kanaji *et al.*, 2000; Muto *et al.*, 2001). In humans, there is a family of processed Tom20 pseudogenes that have been studied in some detail and are thought to have arisen from retrotransposition events (Hernandez *et al.*, 1998, 1999a,b, 2000). The Tom20 genes found in plants are very different than the ones identified in other species (Jansch *et al.*, 1998; Macasev *et al.*, 2000; Werhahn *et al.*, 2001). For example, Tom20 from potato exhibited a reverse membrane topology from that of previously identified Tom20s and is slightly more acidic in nature. Purification of the TOM complex from *Arabidopsis* revealed four forms of Tom20 (Werhahn *et al.*, 2001). All of these Tom20s had large cytosolic hydrophilic domains and were highly conserved in the N- and C-termini of the proteins. It is thought that modification of Tom20 in plants may serve to increase specificity of the TOM complex for mitochondrial preproteins and prevent uptake of chloroplast proteins, most of which are encoded in the nucleus and must be imported and assembled into the correct organelle (Soll, 2002).

1.2.4.2 The Tom22 receptor

Tom22 is a highly negatively charged outer membrane protein which exposes domains to both the cytosol and the intermembrane space (Kiebler *et al.*, 1993a). It was first identified as a protein that interacted with Tom20 and Tom70 and required the presence of surface receptors for insertion into the outer membrane (Kiebler *et al.*, 1990; Keil and Pfanner, 1993). Antibodies raised against Tom22 blocked import of precursors with N-terminal targeting signals or internal targeting signals (Kiebler *et al.*, 1993a; Lithgow *et al.*, 1994). Tom22 deficient mitochondria were unable to import preproteins destined for most mitochondrial subcompartments except the outer mitochondrial membrane (Nargang *et al.*, 1995). Initially, Tom22 was thought to be essential for the viability of both yeast and *N. crassa*, but more recent characterization showed that while Tom22 may be required for yeast ascospore germination, a vegetatively growing strain containing a Tom22 disruption could be cured of a plasmid containing Tom22 (Lithgow *et al.*, 1994; Nargang *et al.*, 1995; van Wilpe *et al.*, 1999). The resulting yeast strain grew extremely slowly and contained TOM complexes with altered structures (see below). On the other hand, *N. crassa* nuclei lacking a functional copy of *tom22* maintained in a sheltered heterokaryon cannot give rise to viable homokaryotic strains (Nargang *et al.*, 1995). Taken together, these data suggest that Tom22 plays an important role in preprotein recognition, translocation and TOM complex organization.

The domains of Tom22 required for viability and efficient import of mitochondrial precursor proteins has been assessed by construction of a variety of mutant versions of the protein. Nakai *et al.* (1995) and Court *et al.* (1996) showed that Tom22 constructs lacking the intermembrane space domain of Tom22 were capable of rescuing both yeast and *N. crassa* Tom22 mutants but that a deletion that included the predicted membrane-spanning domain of Tom22 failed to rescue the yeast Tom22 mutant. Import of mitochondrial outer membrane and intermembrane space precursor proteins were not affected by deletions of the intermembrane space domain, while import of some inner membrane and matrix proteins showed slight import defects (Court *et al.*, 1996). It was suggested that the import defects observed were the result of inefficient transfer of precursor proteins to the TIM complexes as *trans* site binding was unaffected in the mutants (Moczko *et al.*, 1997).

Brix *et al.* (1997) showed that the purified cytosolic domain of Tom22 preferentially bound precursors carrying N-terminal targeting sequences. This binding was inhibited by salt and could be competed for by the addition of excess presequence. Nargang *et al.* (1998) assessed the role of negative charges in cytosolic domain of Tom22, and found that a series of mutants lacking 2 to 15 of the 19 total negative charges in the cytosolic domain was still able to rescue a *N. crassa* Tom22 mutant strain. In addition, it was found that isolated mitochondria from these strains import preproteins as efficiently as wild type mitochondria. Deletion constructs of the cytosolic domain were also constructed and it was found that deletions lacking part, but not all, of the negatively charged region were capable of rescuing the Tom22 mutants. Brix *et al.* (1999) studied the binding ability of chemically purified cytosolic domains of Tom22 to cellulose bound peptide scans of COXIV and the PiC and found that Tom22 bound the C-terminus of the COXIV presequence and the N-terminus of the mature protein but showed no binding to the PiC. Finally, Tom22 has been implicated in organization of the TOM complex as cells lacking Tom22 have no authentic TOM complexes, but only contain smaller 100 kDa complexes which probably correlate to dimers of Tom40 associated with the small Tom proteins (van Wilpe *et al.*, 1999; Model *et al.*, 2002).

Homologs of Tom22 have been identified in humans, rats, and *Drosophila*, and all proteins are fairly well conserved, showing similar topology and composition to fungal Tom22 (Saeki *et al.*, 2000; Vaskova *et al.*, 2000; Yano *et al.*, 2000). As in the case with Tom20, plant homologs of Tom22 are quite different from their fungal and animal counterparts (Jansch *et al.*, 1998; Macasev *et al.*, 2000; Werhahn *et al.*, 2001). The plant forms of Tom22 are smaller than fungal versions, ranging in size from 9.2 kDa to 11.1 kDa, and they lack the acidic regions characteristic of the fungal and metazoan receptors. As with Tom20, it has been suggested that the differences found in this receptor represent a modification of Tom22 to avoid recognition and import of chloroplast precursor proteins, which also possess N-terminal targeting sequences (Soll, 2002).

1.2.4.3 The Tom70 receptor

Tom70 is a mitochondrial outer membrane protein with a large cytosolic domain, and has been found to contain seven TPR-like motifs (Söllner *et al.*, 1990). Tom70 was identified when antibodies to the protein were found to inhibit import of mitochondrial precursor proteins with internal targeting signals. The receptor is not essential in either yeast or *N. crassa* (Steger *et al.*, 1990; Grad *et al.*, 1999). An additional homolog of Tom70 was found in *S. cerevisiae* and was shown to associate with the TOM complex (Schlossmann *et al.*, 1996). This protein, named Tom71, is not essential, though deletion of the gene affects growth of yeast cells at high temperatures on non-fermentable carbon sources. Deletion of the genes for both Tom70 and Tom71 does not exacerbate the growth phenotypes seen. The function of Tom70 was also assessed in *N. crassa* (Grad *et al.*, 1999). Strains lacking Tom70 showed only mild slow growth phenotypes, and isolated mitochondria from these strains showed defects in import of carrier class proteins. Surprisingly, cells lacking Tom70 contain enlarged mitochondria raising the possibility that Tom70 may play a role in regulation or maintenance of mitochondrial morphology or is needed for import of proteins that are involved in mitochondrial morphology.

Brix *et al.* (1997) used the purified cytosolic domain of Tom70 and determined that the protein binds presequences with internal targeting sequences. The binding is not inhibited by addition of excess N-terminal targeting signals or salt, and does not require additional cytosolic chaperones. In contrast to this, Komiya *et al.* (1997) found that the cytosolic domain of Tom70 only bound precursors in the presence of MSF. To determine the regions in precursor proteins important for binding to Tom70, the ability of the Tom70 cytosolic domain to bind peptides of COXIV and PiC was assessed in peptide scans (Brix *et al.*, 1999). Tom70 showed no binding to COXIV, a precursor protein containing an N-terminal targeting sequence, but bound to multiple regions of PiC. A stably folded 25 kDa core domain was identified in the middle of Tom70 which encompassed two of the seven TPR motifs found in the protein. This core domain bound preproteins in a manner that was indistinguishable from the full-length receptor.

1.2.4.4 Interactions and overlapping functions of the receptors

Various lines of evidence support the idea that Tom20 may have functional or physical interactions with the other TOM receptors. Deletions of Tom20 in *S. cerevisiae* were shown to be synthetically lethal when they occurred in conjunction with a Tom70 deletion (Ramage *et al.*, 1993). In addition, the loss of respiration seen in Tom20 mutants could be compensated for by overexpression of Tom70, suggesting that Tom20 and Tom70 may function together to import preproteins or that Tom20 and Tom70 have partially overlapping roles in protein import. Haucke *et al.* (1996) showed that Tom20 could be co-immunoprecipitated with or cross-linked to Tom70, and this association was dependent on a TPR motif found in Tom20. Mutations in the TPR motif of Tom20 were also shown to abrogate import of proteins recognized by Tom70. Tom20 was also shown to be involved in either the assembly or stability of Tom22 in the outer membrane as mitochondria deficient in Tom20 also showed decreased levels of Tom22 (Harkness *et al.*, 1994b). Tom20 and Tom22 could also be crosslinked to one another, indicating a direct physical interaction between these receptors (Mayer *et al.*, 1995b). Finally, TOM complexes devoid of Tom22 lack both the Tom20 and Tom70 receptors (van Wilpe *et al.*, 1999).

1.2.4.5 The small Tom proteins

The three small components of the TOM complex, Tom5, Tom6 and Tom7 have been most well studied in yeast. None of these proteins are essential for viability, but Tom5 deficient strains have been shown to have growth defects at 30°C on all carbon sources, with a three-fold reduction in growth seen on non-fermentable carbon sources (Kassenbrock *et al.*, 1993; Honlinger *et al.*, 1996; Dietmeier *et al.*, 1997). Tom6 and Tom7 are proposed to have opposite roles in the function of the TOM complex (Alconada *et al.*, 1995; Honlinger *et al.*, 1996; Dekker *et al.*, 1998). Tom6 is thought to promote associations of the TOM complex receptors with Tom40, while Tom7 is thought to destabilize these interactions. Tom5 is thought to play a role in the transfer of preproteins from the TOM receptors to Tom40 and the GIP (Dietmeier *et al.*, 1997). These small components have also been found associated with the TOM complex in *N. crassa*, and Tom6 and Tom7 have been cross-linked to Tom40 (Künkele *et al.*, 1998a,b; Ahting *et*

al., 1999; Dembowski *et al.*, 2001) (W. Neupert and S. Nussberger, personal communication).

1.2.4.6 Tom40

Tom40 is an essential gene in both *S. cerevisiae* and *N. crassa* (Baker *et al.*, 1990; Taylor *et al.*, 2003; this thesis). Tom40 was first identified as a protein that could be cross-linked to mitochondrial precursors as they traversed the mitochondrial outer membrane (Vestweber *et al.*, 1989; Kiebler *et al.*, 1990). Purified holo and core TOM complexes have structural and electrophysiological properties similar to TOM complexes from which all components but Tom40 have been removed, or to purified and reconstituted Tom40 dimers (Hill *et al.*, 1998b; Künkele *et al.*, 1998a,b; Ahting *et al.*, 1999). Mitochondrial preproteins arrested at the *cis* protein-binding site on the outer surface of the mitochondrial outer membrane could be cross-linked to Tom40, as well as to other TOM complex components, while preproteins arrested at the *trans* site were only cross-linked to Tom40 (Rapaport *et al.*, 1997, 1998c). In the TOM complex, Tom40 primarily exists as dimers (Dekker *et al.*, 1998; Hill *et al.*, 1998; Rapaport *et al.*, 1998c; Ahting *et al.*, 1999; Model *et al.*, 2001). Cross-linking studies showed that Tom40 dimers dissociate upon binding of mitochondrial precursor proteins and this dissociation is enhanced when preproteins bind at the *trans* site (Rapaport *et al.*, 1998c). Based on protease accessibility studies in whole mitochondria and mitoplasts, both the C- and N-termini of Tom40 appear to be located within the intermembrane space of *N. crassa* (Künkele *et al.*, 1998b). However, in *S. cerevisiae*, the N-terminus is susceptible to cleavage by trypsin (Hill *et al.*, 1998). Computer predictions suggest only one α-helical membrane-spanning domain in both *N. crassa* and yeast Tom40 (Kiebler *et al.* 1990) and favor the notion that the protein exists as a β-barrel, similar to bacterial outer membrane porins (Court *et al.*, 1995; Mannella *et al.*, 1996). These predictions suggest that Tom40 spans the outer membrane in a series of fourteen antiparallel β-sheets and is in agreement with CD spectral data obtained using bacterially expressed and refolded Tom40 (Hill *et al.*, 1998). In contrast, spectral analysis of Tom40 purified directly from mitochondria revealed less β-sheet content and predicted that Tom40 spans the membrane in as few as eight to ten strands (Ahting *et al.*, 2001).

1.2.4.7 Assembly of Tom40 into the TOM complex

The integration and assembly of Tom40 into the TOM complex is dependent on the presence of functional TOM complexes and requires that the protein exist in a partially folded state (Rapaport and Neupert, 1999). Tom40 assembly is thought to occur via a series of intermediates (Fig. 3) (Rapaport and Neupert, 1999; Model *et al.*, 2001). Tom40 first binds the mitochondrial surface receptors as a monomer. This monomer is then assembled into an intermediate of 250 kDa containing Tom37 (renamed Mas37 for mitochondrial assembly), Tom5, and other unknown proteins (Wiedemann, 2003). The Tom40 precursor in this complex has been shown to be partially inserted into the mitochondrial outer membrane (Model *et al.*, 2001; Taylor *et al.*, 2003). Full integration of Tom40 into the membrane seems to occur as the precursor protein progresses to a 100 kDa intermediate since Tom40 in this intermediate is resistant to carbonate extraction. The 100 kDa form most likely contains a dimer of Tom40, consisting of a newly imported Tom40 molecule in association with a pre-existing molecule of Tom40 as well as Tom5 and Tom6. The intermediate undergoes further assembly and becomes associated with other TOM components to give rise to the fully assembled TOM complex of 400 kDa. Conserved residues in the N-terminus of Tom40 are required for assembly and stability of Tom40 within the TOM complex, but do not seem to be required for targeting of Tom40 to the mitochondrial outer membrane (Rapaport *et al.*, 2001; Taylor *et al.*, 2003; this thesis).

Integration of Tom40, and other TOM complex subunits, into the membrane suggests questions specific for the precursors of these proteins. Do these subunits integrate into the bilayer and associate with a pool of assembly intermediates to form a new complex? Alternatively, newly imported subunits may assemble into the TOM complex that is importing them. In this case, to maintain a constant stoichiometry pre-existing subunits would be displaced. These displaced subunits may then form a pool of unassembled subunits in the bilayer. It has been shown that subunits can exchange between existing complexes or at least reform from existing subcomplexes (Rapaport *et al.*, 2001). As a result, it seems likely that there is a constant flux of subunits into and out

of assembled complexes. Since intermediates have not been detected in isolated mitochondria, pools of unassembled subunits must be small.

1.2.5 The translocases of the inner mitochondrial membrane

Following translocation of the initial portion of precursors destined for the matrix or mitochondrial inner membrane through the mitochondrial outer membrane, precursors are bound at the TOM complex *trans* protein-binding site. Preproteins bound at this site have been shown to interact with one of two translocase complexes in the inner mitochondrial membrane (Fig. 1) (reviewed in Neupert, 1997; Pfanner *et al.*, 1997; Rassow *et al.*, 1999; Pfanner and Wiedemann, 2002). Further translocation steps require a potential across the inner membrane (Gasser *et al.*, 1982; Schleyer and Neupert, 1982; Eilers *et al.*, 1987; Sirrenberg *et al.*, 1996; Endres *et al.*, 1999). Membrane potential is required for dimerization of TIM23 complex and function of both the TIM23 and TIM22 complexes (Bauer *et al.*, 1996). Membrane potential may also be required to "drive" the positively charged presequence across the intermembrane space and through the inner membrane (Martin *et al.*, 1991). Transfer of preproteins from the TOM complex to the TIM complexes is thought to occur at contact sites between the inner and outer membrane (Schleyer and Neupert, 1985; Rassow *et al.*, 1989; Donzeau *et al.*, 2000). It has been hypothesized that the process of protein translocation and protein transfer to the TIM complexes may stimulate formation of these sites. While, *in vivo*, the TIM complexes interact with preproteins that have been translocated across the outer membrane via the TOM complex, it has been shown *in vitro* that these complexes can function independently of the TOM complex (Hwang and Schatz, 1989; Hwang *et al.*, 1991; Segui-Real *et al.*, 1993; Paschen *et al.*, 2000).

1.2.5.1 Components of the TIM23 complex

Matrix destined precursors with N-terminal targeting sequences are imported into the matrix, the intermembrane space, or the inner membrane via the TIM23 complex (Fig. 1) (reviewed in Neupert, 1997; Pfanner *et al.*, 1997; Rassow *et al.*, 1999; Pfanner and Wiedemann, 2002). The TIM23 complex contains four known proteins, Tim17, Tim23, Tim44 and Tim50.

Tim23 was first identified in genetic screens designed to reveal defects in mitochondrial protein import (Dekker *et al.*, 1993; Emtage and Jensen, 1993). Tim23 is essential for viability of yeast at all temperatures and on all carbon sources. Further, characterization of Tim23 demonstrated that it could be cross-linked to precursors in transit thereby supporting its role in protein import (Ryan and Jensen, 1993; Kübrich *et al.*, 1994; Berthold *et al.*, 1995). Following identification of Tim23, a second mitochondrial protein essential for the import of precursors was identified and named Tim17 (Dekker *et al.*, 1993; Maarse *et al.*, 1994). Tim23 and Tim17 are predicted to span the inner membrane four times, with their carboxy and N-termini localized to the intermembrane space (Sirrenberg *et al.*, 1996). Tim23 and Tim17 are conserved, and homologs of these proteins have been found in a number of different species (reviewed in (Bömer *et al.*, 1996; Rassow *et al.*, 1999)). Although Tim17 and Tim23 are themselves homologous, they cannot be substituted for one another, suggesting that both proteins have unique roles in protein import (Maarse *et al.*, 1994; Ryan *et al.*, 1994; Blom *et al.*, 1995).

The most noticeable difference between the Tim17 and Tim23 proteins lies at their N-termini (Bauer *et al.*, 1996). *S. cerevisiae* Tim23 possesses a 100 amino acid hydrophilic N-terminal domain that extends into the intermembrane space, which is absent in Tim17. The region of Tim23 encompassing amino acids 61-83 is thought to encode a leucine zipper motif that is required for dimerization of the protein. Dimerization requires the presence of membrane potential, and Tim23 dimers are disrupted in the presence of mitochondrial presequences (Sirrenberg *et al.*, 1996). It has been suggested that the region encompassing amino acids 1-60 span mitochondrial intermembrane space and the mitochondrial outer membrane, exposing a few amino acids to the cytosol which are sensitive to the addition of exogenous protease (Donzeau *et al.*, 2000). This unique topology may keep the TIM23 complex close to/or associated with morphological contact sites. On the other hand, unusually high protease concentrations were necessary to see the clipping, and it should be noted that no similar mitochondrial outer membrane-spanning domain has been identified in the *Arabidopsis* (Murcha *et al.*, 2003) or *N. crassa* version of Tim23 (S. Hoppins and F. Nargang, personal communication).

Tim23 and Tim17 exist in equimolar amounts in a stable 90 kDa complex in the inner mitochondrial membrane (Dekker *et al.*, 1997; Moro *et al.*, 1999). This complex is termed the core TIM17/23 complex. Some data suggests that Tim23 and Tim17 form the pore through which preproteins traverse the mitochondrial inner membrane, while other data support a role for only Tim23 in pore formation. This channel has been termed MCC, for the **M**itochondrial inner membrane **C**onductance **C**hannel. Data suggesting that Tim17 and Tim23 together form the MCC include the evidence that both proteins have been shown to contact precursors in transit (Ryan and Jensen, 1993; Kübrich *et al.*, 1994). Depletion of either of these proteins reduces the number of inner membrane MCCs (Milisav *et al.*, 2001). Using reconstituted proteoliposomes, it was shown that Tim17 and Tim23 were able to insert AAC and Tim23 into liposome membranes in the presence of membrane potential (Haucke and Schatz, 1997). Surprisingly, this process did not require the addition of Tim44 or mitochondrial Hsp70 (see below). However, the role of Tim17 in MCC formation has recently been called into question because antibodies targeted against Tim23 alone are capable of blocking MCC conductance and MCC has shown to be affected in Tim23 mutants (Lohret *et al.*, 1997). Finally, chemically pure Tim23 reconstituted into liposomes has been shown to form a voltage-sensitive cation-selective channel with conductance characteristics similar to that of the authentic MCC (Truscott *et al.*, 2001). The MCC described in this study was estimated to be 13 to 24 Å in diameter, which is in agreement with previous data obtained using sized steric bulk probes attached to precursor proteins to assess the pore size of the core TIM23 complex (Schwartz and Matouschek, 1999).

Tim44 was identified when it was shown that mitochondria lacking the protein failed to import preproteins (Maarse *et al.*, 1992; Blom *et al.*, 1993, 1995). Most evidence suggests that Tim44 is a peripheral membrane protein, it is not abundant in the mitochondrial matrix, and has been shown to interact with both TIM23 complex, and mitochondrial Hsp70 (Berthold *et al.*, 1995; Blom *et al.*, 1995). Tim44 is thought to bind the TIM23 complex on the matrix side of the inner membrane where it acts to recruit mitochondrial Hsp70 to the translocation channel (reviewed in Neupert, 1997; Pfanner *et al.*, 1997; Rassow *et al.*, 1999; Pfanner and Wiedemann, 2002). It is thought that repeated rounds of mitochondrial Hsp70 binding to a preprotein in transit provides

directionality to the import process and that this binding prevents preproteins from moving backwards across the membranes (Gambill *et al.*, 1993; Voos *et al.*, 1993, 1994; Westermann *et al.*, 1995). There are several lines of evidence that support the importance of these proteins for import of mitochondrial proteins. First, precursors arrested in transit were shown to be bound to mitochondrial Hsp70 (Scherer *et al.*, 1990). Second, it was shown that mitochondrial Hsp70 was required for import of preproteins using temperature-sensitive mitochondrial Hsp70 mutants (Gambill *et al.*, 1993). Corroborating evidence for the importance of these proteins came from genetic screens aimed to identify proteins important for translocation of mitochondrial preproteins (Kübrich *et al.*, 1994). These screens identified Tim44 and mitochondrial Hsp70, in addition to the known mitochondrial import components Tim23 and Tim17. Finally, mutations were made in Tim44 that weaken the interaction between mitochondrial Hsp70 and Tim44, and these Tim44 mutants were not able to rescue a *S. cerevisiae* strain lacking wild type *TIM44* (Merlin *et al.*, 1997). Some evidence also suggests, at least *in vitro*, that the requirement for Tim44 and mitochondrial Hsp70 may vary depending on the type of preprotein being translocated. As described above, Haucke and Schatz (1997) suggested that the association of Tim44 and mitochondrial Hsp70 with the TIM23 complex was not important for the insertion of proteins into the mitochondrial inner membrane. In addition, it was found that mitochondria containing mutants of Tim44 were still able to import precursor proteins *in vitro*, but at a reduced rate compared to wild type controls (Bömer *et al.*, 1998). The efficiency of import of the preproteins tested was dependent on the folding state of the protein in question. More loosely folded preproteins did not require functional Tim44, while tightly folded proteins were more sensitive to loss of Tim44 activity.

An additional component of the TIM23 complex has recently been identified based on site-specific photocrosslinking and mass spectrometry of a ~50-56 kDa band from purified TIM complex preparations (Geissler *et al.*, 2002; Yamamoto *et al.*, 2002; Mokranjac *et al.*, 2003). This protein, termed Tim50, is highly abundant, and is a mitochondrial inner membrane protein with one predicted membrane-spanning domain. Tim50 may play a role in guiding preproteins with matrix targeting signals to the TIM23 complex (Geissler *et al.*, 2002). In addition, translocation intermediates arrested at the

TOM complex can be crosslinked to Tim50, suggesting that this protein may play a role in linking the outer and inner mitochondrial membranes (Yamamoto *et al.*, 2002).

It is interesting to note that both Tim17 and Tim23 have been co-immunoprecipitated with other proteins of unknown identity and function (Berthold *et al.*, 1995). As a result, it is likely that additional components of the TIM23 complex will be identified.

1.2.5.2 The role of mtHsp70 in mitochondrial protein import

Two theories for the mode of action of mitochondrial Hsp70 have been proposed (Matouschek *et al.*, 1997; Gaume *et al.*, 1998; Craig *et al.*, 1999; Moro *et al.*, 1999, 2002; Bauer *et al.*, 2000; Matouschek *et al.*, 2000; Geissler *et al.*, 2001; Neupert and Brunner, 2002; Okamoto *et al.*, 2002). The first model is based on a mechanism whereby the random motion of a translocating preprotein moves a precursor protein across the mitochondrial membranes where it is bound in the matrix space by mitochondrial Hsp70. In this "Brownian ratchet" model, mitochondrial Hsp70 becomes the arresting, or direction conferring, component of the translocation system, as once mitochondrial Hsp70 is bound to a translocating precursor, the protein can no longer move back through the translocation channels. Successive Brownian movements of the precursor may then expose more of the protein to the mitochondrial matrix, allowing for a second molecule of mitochondrial Hsp70 to bind. This cycle is repeated until the entire preprotein is translocated into the matrix. Forward movement of translocating preproteins is thought to be associated with spontaneous unfolding or "breathing" of the domains of the precursor still located outside of the mitochondrion. In the second model of mitochondrial Hsp70 action, it is proposed that a conformation change in mitochondrial Hsp70, associated with hydrolysis of ATP, pulls a translocating precursor across the membrane. Again, successive binding of mitochondrial Hsp70 would be required for complete translocation of a precursor across the mitochondrial membranes. In this model, the force generated through pulling the precursor across the membrane also aids in unfolding of the domains of the precursor remaining outside of the mitochondrion.

Evidence to support the Brownian ratchet model for the action of mitochondrial Hsp70 comes from a variety of sources and from more than one organelle and

translocation system. In mitochondria, it has been observed that preproteins are capable of spontaneous movement within the channels of both the TOM and TIM complexes (Mayer *et al.*, 1995c). Retrograde movement of precursor proteins has also been observed in mitochondria depleted of matrix ATP (Schneider *et al.*, 1994; Ungermann *et al.*, 1994; Gaume *et al.*, 1998). Import of membrane proteins that follow the "stop-transfer" pathway, which results in insertion of proteins into the inner membrane via the TIM23 complex, do not require matrix ATP or functional mitochondrial Hsp70 for insertion (Rojo *et al.*, 1998). Finally, Okamoto *et al.* (2002) used two different experimental approaches study the role of Hsp70 in import of matrix proteins. First, preproteins containing stretches of glutamate or glycine repeats in front of folded domains were imported into mitochondria. These proteins were successfully imported into mitochondria despite the fact that Hsp70 cannot bind repeated glutamate or glycine tracts. The second approach used was to import preproteins containing folded immunoglobulin-like domains. The force needed to unfold these immunoglobin-like domains was estimated to be ~200 pN, while the force generated by the pulling action of Hsp70 was estimated to be ~5 pN. Although these domains were tightly folded, the preproteins were successfully imported into mitochondria. These data taken together suggest that Hsp70 acts like a ratchet to import mitochondrial preproteins.

Studies using components of the translocation machinery from the endoplasmic reticulum also show evidence that this Brownian ratchet is sufficient to drive import into the lumen of this organelle (Matlack *et al.*, 1999; Liebermeister *et al.*, 2001). Matlack *et al.* (1999) showed that antibodies against the secretory protein prepro-α factor, enclosed in proteoliposomes in which the SEC import machinery was incorporated, were capable of translocating this precursor to a protease resistant location, indicative of bonafide translocation. As antibody binding to a preprotein should confer no conformational change to the antibody or the target protein, the most reasonable conclusion that can be drawn is that a Brownian ratchet is sufficient to achieve translocation.

Most precursor proteins are translocated across the mitochondrial membranes in an unfolded state, although the size of the GIP suggests that it may be able to tolerate two α-helices at one time (Hill *et al.*, 1998; Künkele *et al.*, 1998a,b; Schwartz and Matouschek, 1999). A commonly used argument in favor of the force-generating model

is that the rate of spontaneous unfolding of mitochondrial precursor proteins is not sufficient to explain the rate of import seen (Matouschek *et al.*, 2000; Geissler *et al.*, 2001; Lim *et al.*, 2001). Thus, some mechanism must exist to force unfolding of precursor proteins. It has been demonstrated that import and unfolding of preproteins by mitochondria can be significantly faster than their rate of spontaneous unfolding in solution (Matouschek *et al.*, 1997). In addition, Huang *et al.* (1999) have shown that mitochondria can change the rate of spontaneous unfolding of the ribonuclease barnase. The sequence of unfolding also changes in the presence of mitochondria unfolding of barnase occurred through the N-terminus of the protein in the presence of mitochondria while spontaneous unfolding in solution occured through unfolding of the middle section of the protein. These observations argue for a direct role for mitochondria in unfolding of precursor proteins but do not rule out the possibility that simple association of precursor proteins with the TOM complex is sufficient to catalyze this process. The force generating motor model also assumes that mitochondrial Hsp70 exerts a pulling force on presequences, and thus acts as a driving force in the process of import that would otherwise be absent in the Brownian motion model. The fact that import requires ATP in the matrix as well as mitochondrial Hsp70 are taken as support for the idea that mitochondrial Hsp70 takes a direct role in import and unfolding of preproteins (Gambill *et al.*, 1993; Wachter *et al.*, 1994). Finally, it has been shown that mitochondrial Hsp70 contributes directly to protein unfolding as mutations in mitochondrial Hsp70 have severe effects on the import of folded precursor proteins, but not of unfolded precursors (Kang *et al.*, 1990; Voisine *et al.*, 1999).

1.2.5.3 The TIM22 complex

The second translocase complex in the inner membrane is the TIM22 complex (Fig. 1) (reviewed in Rassow *et al.*, 1999; Tokatlidis and Schatz, 1999; Pfanner and Wiedemann, 2002). This complex is responsible for insertion of proteins with internal targeting sequences into the mitochondrial inner membrane. This class of proteins includes members of the metabolite carrier family such as AAC and PiC (Palmieri, 1994). Components of the TIM22 complex include Tim22, Tim54 and Tim18. Tim22 was identified in *S. cerevisiae* through database searches with the previously described

components of the TIM23 complex, Tim23 and Tim17 (Sirrenberg *et al.*, 1996). An open reading frame was identified with the potential to encode a transmembrane protein of approximately 22 kDa. This protein showed significant sequence similarity to Tim23, and antibodies raised against it selectively blocked import and assembly of the AAC family of proteins. Tim54 was originally identified in a potential interaction with MMM1, a protein required for interaction of *S. cerevisiae* mitochondria with the actin cytoskeleton, in a yeast two-hybrid screen (Kerscher *et al.*, 1997). Tim54 was subsequently found to be an essential import component and could be co-immunoprecipitated with Tim22 but not with members of the TIM23 complex. Tim18 is an integral inner membrane protein, and was identified independently by two groups (Kerscher *et al.*, 2000; Koehler *et al.*, 2000). Koehler *et al.* (2000) identified Tim18 as a protein that could be co-immunoprecipitated with Tim54. Unlike Tim22 or Tim54, Tim18 was found not to be essential, but mutations in Tim18 reduce the growth rate of yeast by a factor of two and impair import of carrier class proteins. Kerscher *et al.* (2000) identified Tim18 as a suppressor of a temperature-sensitive Tim54 strain of yeast, and also determined that it could physically interact with both Tim54 and Tim22.

The TIM22 complex exists in the mitochondrial inner membrane as a 300 kDa multi-subunit protein complex with an unknown stoichiometry (Koehler *et al.*, 2000). Purified Tim22 has been shown to form a voltage-activated channel in artificial membranes that responds specifically to proteins with internal targeting sequences (Kovermann *et al.*, 2002). The Tim22 channel has two pore sizes of 11 Å and 18 Å. The small opening is large enough to accommodate one polypeptide chain, while the larger opening would be able to accommodate a tightly packed polypeptide loop. The functions of the other components of this complex are not yet clear. Tim54 may be involved in stabilization of Tim22 in the inner membrane, while Tim18 may play a role in assembly and stabilization of the TIM22 complex (Koehler *et al.*, 2000; Kovermann *et al.*, 2002).

1.2.5.4 The role of the small Tim proteins

In addition to the membrane-associated components of the TIM22 complex, a number of small soluble intermembrane space proteins were identified as important for import of carrier class proteins, as well as a subset of other hydrophobic membrane proteins such as Tim23 itself (reviewed in Koehler *et al.*, 1999b; Rassow *et al.*, 1999; Tokatlidis and Schatz, 1999; Pfanner and Wiedemann, 2002). The proteins involved in the import of carrier class proteins are Tim9, Tim10, and Tim12, all of which are essential for viability. Tim10 and Tim12 were first identified in *S. cerevisiae*, when expressed from a multicopy plasmid, as genes capable of restoring respiration competence to yeast strains defective in splicing of mitochondrial group II introns (Jarosch *et al.*, 1996, 1997). It was later found that these proteins were essential for import of proteins with internal targeting signals (Koehler *et al.*, 1998b; Sirrenberg *et al.*, 1998). Both Tim10 and Tim12 have been shown to contain zinc-binding domains and have the ability to coordinate zinc *in vitro* (Sirrenberg *et al.*, 1998). Tim9 was discovered in a screen to recover suppressors of a temperature sensitive Tim10 mutation, and as a protein that could be co-immunoprecipitated with Tim10 (Koehler *et al.*, 1998a; Adam *et al.*, 1999). Tim9, Tim 10 and Tim12 are hypothesized to exist in two different 70 kDa complexes. Interestingly, the isolated 70 kDa complexes did not contain detectable amounts of zinc and instead, the cysteine residues in the zinc finger domains of Tim10 and Tim12 were shown to be important for intermolecular protein/protein interactions (Curran *et al.*, 2002). The two complexes differ with respect to the presence of Tim12; one form of the complex was shown to contain three subunits of Tim9 and three subunits of Tim10, while the other form of the complex was shown to contain three Tim9 subunits, two Tim10 subunits, and one Tim12 subunit. The Tim9/10 complex is soluble in the intermembrane space and has been shown to interact with preproteins as they exit the TOM complex translocation pore (Endres *et al.*, 1999; Curran *et al.*, 2002). The Tim9/10/12 complex is found associated with the TIM22 complex at the surface of the inner membrane. This complex has been shown to accept precursors from the Tim9/10 complex and facilitate their transfer to Tim22. In addition to Tim9/10/12, two more small Tim proteins have been identified (reviewed in (Koehler *et al.*, 1999b; Rassow *et*

al., 1999; Tokatlidis and Schatz, 1999; Pfanner and Wiedemann, 2002)). Tim8 was identified in *S. cerevisiae* as a homolog of a gene, *TIMM8*, that causes human deafness dystonia syndrome when mutated (Koehler *et al.*, 1999a). The *TIMM8* product was called DPP for "deafness dystonia protein". Tim8 was found to be homologous to Tim9/10/12, and database searches identified an additional protein, Tim13 (or DDP2). Neither Tim8 nor Tim13 are essential genes, but mutations in Tim8 are synthetically lethal when they occur in conjunction with a conditional mutation in Tim10. The Tim8 and Tim13 proteins also form a 70 kDa complex. Although both Tim8 and Tim13 have zinc finger domains, the purified Tim8/13 complex does not coordinate zinc (Curran *et al.*, 2002).

Non-carrier class proteins such as Tim23 are also imported via the TIM22 complex, and are dependent on the small Tim proteins for assembly into the mitochondrial inner membrane (Davis *et al.*, 1998; Kaldi *et al.*, 1998; Koehler *et al.*, 1998b; Sirrenberg *et al.*, 1998; Adam *et al.*, 1999; Leuenberger *et al.*, 1999). In addition, it is likely that Tim17 also uses the TIM22 complex as it is structurally related to Tim23, but no clear evidence exists for this hypothesis (Kaldi *et al.*, 1998). In fact, import of Tim17 was affected by depletion of both Tim22 and Tim23 and may be dependent on both complexes for insertion into the inner membrane. At least in some circumstances, import of Tim23 is dependent on the Tim8/13 complex, as yeast mitochondria lacking both Tim8 and Tim13 show reduced Tim23 import under conditions of lowered membrane potential (Paschen *et al.*, 2000). The Tim8/13 complex may facilitate translocation of Tim23 across the intermembrane space by binding the membrane spanning domains of the protein as they emerge from the TOM complex (Curran *et al.*, 2002)

1.2.6 Precursor processing and folding

Following the translocation of precursor proteins destined for the matrix space, precursor proteins must be matured (Gakh *et al.*, 2002). The process of precursor maturation is essential and involves the removal of mitochondrial targeting sequences and the folding of proteins to achieve their active conformation. The two proteins involved in cleavage of mitochondrial targeting sequences were first identified as temperature sensitive nuclear mutations that blocked the import of mitochondrial proteins

at non-permissive temperatures (Yaffe and Schatz, 1984). Later, these genes were shown to encode components of the mitochondrial processing peptidase (MPP) (Hawlitschek *et al.*, 1988; Witte *et al.*, 1988; Yang *et al.*, 1988). It was found that these two components function in a complex and are required for the cleavage of N-terminal targeting sequences, and may recognize different segments of the presequence than the TOM complex (Geli *et al.*, 1990; Arretz *et al.*, 1994).

Recently the crystal structure of the mitochondrial processing peptidase has been solved (Taylor *et al.*, 2001). It was found that MPP binds precursors in an extended confirmation, in contrast to the amphiphilic helical conformation required for recognition of presequences by Tom20 (Abe *et al.*, 2000).

A second protease in the matrix space is responsible for mediating removal of an octapeptide sequence found at the N-termini of a subset of mitochondrial precursors immediately following the targeting signal (Isaya *et al.*, 1994). This protein termed mitochondrial intermediate peptidase (MIP) is required for growth on non-fermentable carbon sources. The role of this octapeptide sequence is currently unknown. Finally, two proteases exist in the intermembrane space, and are involved in maturation of proteins found in this sub-compartment (Nunnari *et al.*, 1993).

Protein folding is accomplished by a number of chaperones found within the matrix (Cheng *et al.*, 1989; Ostermann *et al.*, 1989; Rowley *et al.*, 1994; Rassow *et al.*, 1995). One of these chaperones is mitochondrial Hsp60, which is essential for cell viability.

1.3 Major objectives of this study

Little is known about the domains of Tom40 that are required for its assembly and function within the TOM complex, or how its interactions with other components of the TOM complex are maintained. The initial goals of this study were to create a *tom40* null strain in *N. crassa* in order to examine and characterize the effects of Tom40 depletion in an organism other than *S. cerevisiae* (Baker *et al.*, 1990). Additional goals of this study have been to use this *tom40* null strain to determine the importance of conserved domains of Tom40 in the function and assembly of the TOM complex. Using this approach I have identified domains in the N-and C-termini that may play a role in the assembly and

stability of the TOM complex. I have also analyzed the Tom40 assembly pathway *in vitro* in *N. crassa*, using both wild type and mutant versions of the Tom40 protein.

In addition, I have begun a study to determine the membrane topology of Tom40 using the procedure of substituted-cysteine accessibility mapping (SCAM). I have tentatively mapped the last two membrane-spanning domains of the protein, and defined the loop domains that separate them.

Finally, I have begun experiments to determine the protein composition of the mitochondrial outer membrane in *N. crassa.* Using this approach I have identified five proteins not previously known to be associated with mitochondria in *N. crassa.* Interestingly, one of the proteins that I have identified is a homolog of the *S. cerevisiae* protein Ugo1p, which has been shown to play a role in mitochondrial fission and fusion events (Sesaki and Jensen, 2001).

Figure 1. **The protein translocases of the outer and inner mitochondrial membranes in *Neurospora crassa.*** The components of each complex are indicated. Preproteins are initially recognized by the receptor components of the TOM complex, the receptor Tom70 preferentially interacts with hydrophobic carrier proteins. The receptor Tom20 has overlapping precursor protein specificity and binds precursors with both amino terminal and internal targeting signals. Tom22 may also act as a receptor in conjunction with Tom20. All precursors are then translocated through the general import pore (GIP) consisting of Tom40, Tom22, Tom5, Tom6 and Tom7 which make up the TOM core complex. Precursors destined for the outer membrane are inserted at this point and some proteins destined for the intermembrane space compartment are released into the intermembrane space. Precursor proteins destined for the mitochondrial inner membrane or matrix space are transferred to the TIM complexes to complete the import process by mechanisms that depend on the presence of membrane potential. The TIM22 complex is responsible for insertion of proteins with internal targeting signals (such as carrier proteins) into the inner mitochondrial membrane, and accomplishes this with the aid of the small Tim proteins, Tim9/10/12. The Tim8/13 complex aids in the import of Tim23 and possibly other preproteins under conditions of low membrane potential. The TIM23 complex is responsible for translocation of matrix proteins, as well as a few proteins that are inserted into the inner membrane. Proteins using the TIM23 pathway have amino terminal targeting signals that must be cleaved following translocation. The signal sequence is removed by the matrix processing peptidase, or MPP. Finally, a subset of matrix targeted proteins, as well as mitochondrial encoded proteins are assembled into the inner membrane from the matrix via the OXA1 translocase.

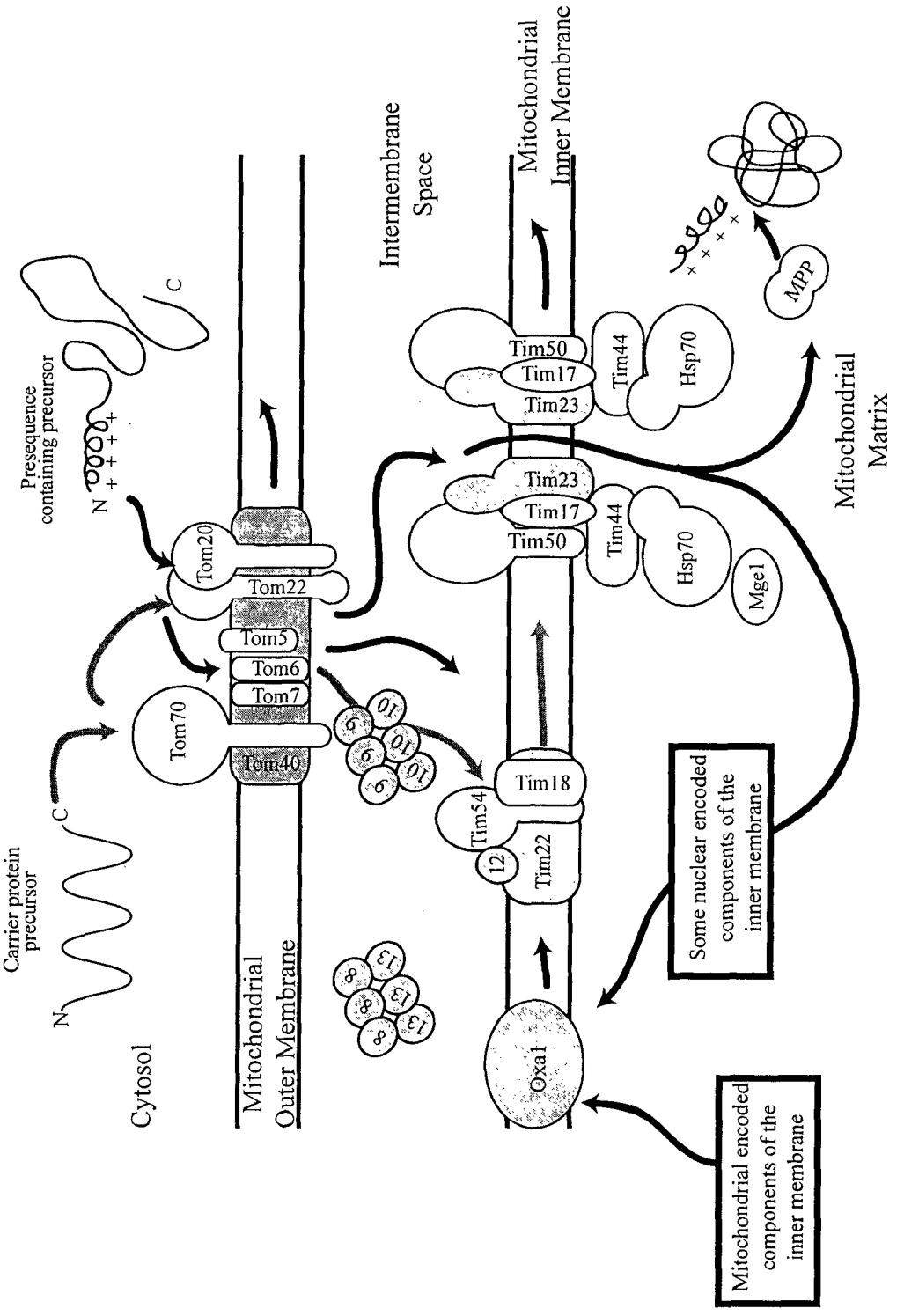

Figure 2. **The TOM complex.** The components of the TOM complex are indicated. Preproteins initially bind the TOM complex at the *cis* binding sites, which are composed of the TOM complex receptors, Tom70, Tom22, and Tom20. Tom40 may play a role in *cis* site binding as well. Following initial recognition of mitochondrial preproteins, proteins are translocated through the GIP consisting of Tom40, Tom22, Tom5, Tom6, and Tom7. Tom40 is the most abundant component of the TOM complex, and dimers of Tom40 are thought to constitute the pore through which preproteins traverse the outer membrane. Following preprotein translocation through the membrane, the preprotein is arrested at the *trans* protein binding site. This *trans* site probably consists primarily of Tom40, but may involve the intermembrane space domain of Tom22. From the *trans* site, preproteins are sorted via different routes to complete their translocation, depending on the features of the precursor.

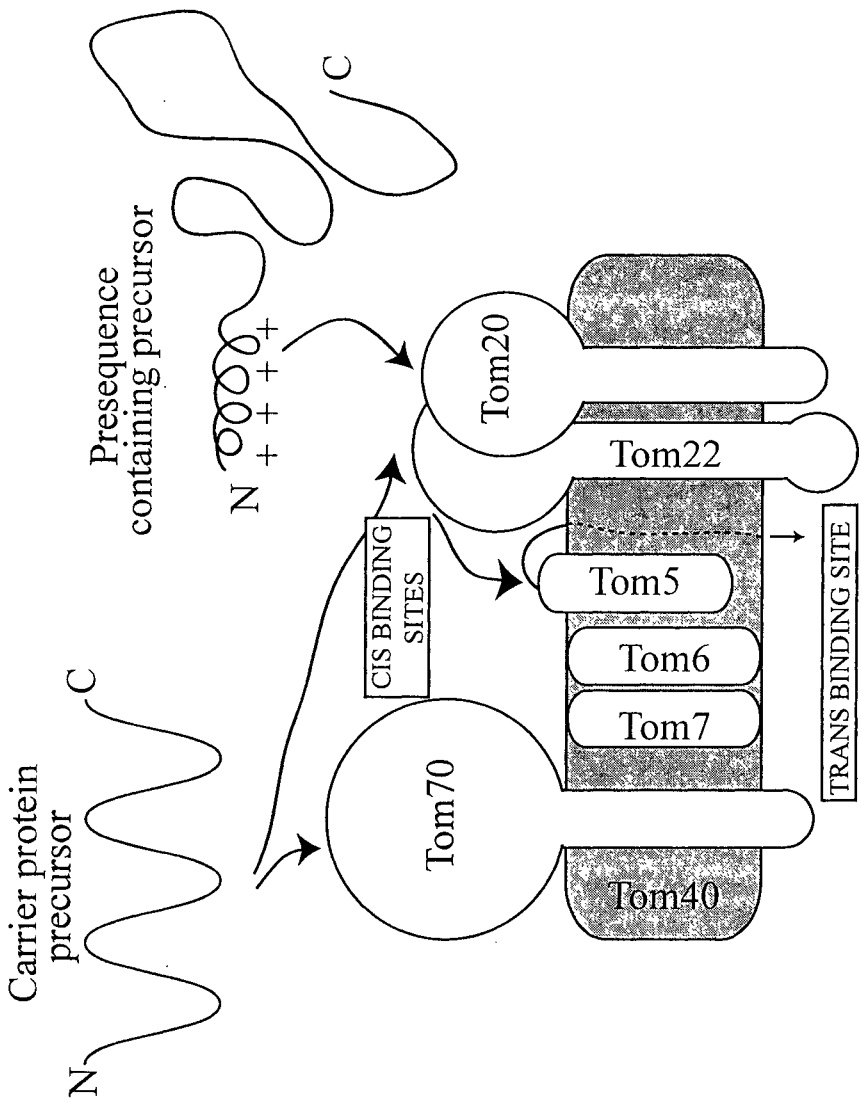

Figure 3. **The Tom40 assembly pathway. A.** Diagram of a typical blue native gel (BNG) Tom40 assembly assay. Arrow indicates the direction of electrophoresis. The Tom40 assembly intermediates are labeled in panel B (see section 2.7). **B.** The pathway for insertion of Tom40 is depicted diagrammatically. Tom40 initially binds the outer surface of mitochondria as a monomer, which is then incorporated into a high molecular weight intermediate of 250 kDa containing Tom5, Tom37/Mas37 and other unknown proteins. The Tom40 molecule in this intermediate is largely carbonate extractable, and is resistant to externally added protease. Conversion to the 250 kDa intermediate depends on the presence of Tom5. The Tom40 precursor in the 250 kDa intermediate then dissociates from this complex to form a 100 kDa complex, probably consisting of a dimer of Tom40, in conjunction with a molecule of Tom5. Conversion of the 250 kDa intermediate to the 100 kDa intermediate requires the presence of Tom6. From the 100 kDa intermediate, Tom40 is incorporated into authentic TOM complexes, through association with other TOM components.

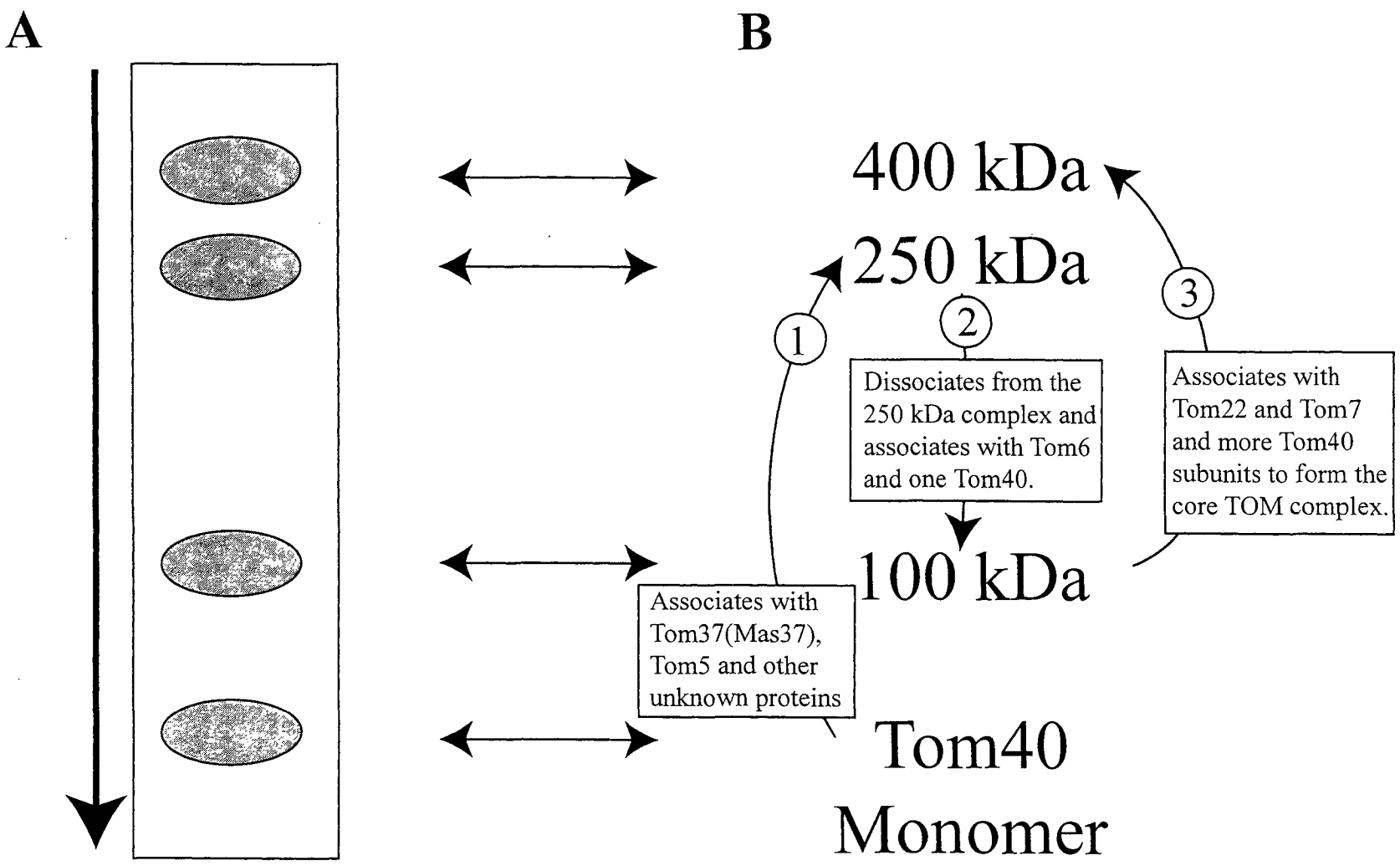

2. MATERIALS AND METHODS

2.1 Growth of *N. crassa* and strains used

Growth and handling of *N. crassa* strains was carried out as previously described (Davis and De Serres, 1970). Strains used in this study are listed in Table 1. Race tubes were constructed in 25 ml pipettes or 80 cm glass tubes as described previously (Davis and De Serres, 1970; White and Woodward, 1995). The extent of mycelial elongation was recorded every 24 hr.

2.2 Creation of sheltered RIP mutant

Repeat induced point mutation (RIP) occurs in *N. crassa* when one of the nuclei in a sexual cross carries a sequence duplication. RIP results in the generation of GC to AT transitions in both copies of the duplication, and can be used to generate strains containing essentially null alleles of targeted genes (Selker, 1990). RIP occurs during mating, after cells fuse, but before karyogamy has occurred, and thus only the duplicated sequence in one nucleus in a cross is affected. RIP is not 100% efficient but for duplications of about 2 kb, roughly 50% of the progeny will contain RIPed versions of the duplication. As Tom40 was predicted to be an essential protein, the more complex procedure of sheltered RIP was used to mutate the *tom40* gene (Metzenberg and Grotelueschen, 1992; Harkness *et al.*, 1994a). Sheltered RIP insures that nuclei containing non-functional alleles are present in a heterokaryon that also contains nuclei with a wild type copy of the gene. In the process of sheltered RIP, various nutritional and antibiotic resistance markers on the chromosome carrying the target gene are employed. In addition to these markers, both strains in the sheltered RIP cross must contain a *mei-2* mutation. This mutation eliminates meiotic recombination and results in formation of aneuploid ascospores. As a result of the mutations in *mei-2* the majority of the ascospores generated in a sheltered RIP cross are inviable, as they may lack one or more chromosomes. However, a fraction of the ascospores generated may be disomic for one or more chromosomes. The desired progeny of a sheltered RIP cross is an ascospore that contains a complete complement of chromosomes and is disomic for the chromosome on which the targeted gene is located. One chromosome of the disomic pair will possess a

wild type copy of the gene, while the other possesses a RIPed copy of the gene of interest. Disomic spores break down during vegetative growth to form heterokaryotic strains. The different but complementing, nutritional markers carried on each of the disomic chromosomes arising from the two parents in the cross allow for selection of the desired heterokaryotic progeny from the cross by growth on minimal medium. Once the sheltered heterokaryon is isolated, the drug resistance markers can be used to shift the ratio of nuclei in the strain, making it possible to assess the effects of deficiencies in essential gene products. (See section 3.1 and Fig. 4 for further explanation of sheltered RIP strains.)

To generate the RIP40het strain, molecular restriction fragment length polymorphism mapping studies were first performed (Metzenberg *et al.*, 1984; Metzenberg *et al.*, 1985) using a *tom40* containing cosmid as a probe. This revealed that the *tom40* gene was located on linkage group V of *N. crassa.* To create a duplication of *tom40*, spheroplasts of the HostV strain for sheltered RIP were transformed with a plasmid (pRIP-4) carrying hygromycin resistance (Staben *et al.*, 1989) and 1.8 kb of PCR-generated *tom40* genomic sequence. Transformants were selected on hygromycin, and strains containing duplications were identified by Southern analysis. One strain, 40Dupl, was crossed to the MateV strain. Any ascospores from this cross that were capable of growth on minimal medium should be heterokaryons. One nucleus of the heterokaryon would be expected to be wild type with respect to Tom40 function, whereas the other nucleus of the heterokaryon could contain either RIPed or wild type *tom40* alleles. The desired heterokaryotic strain is indicated in Fig. 4.

Several ascospore isolates from the sheltered RIP cross were screened for the predicted characteristics of $tom40^{RIP}$ sheltered heterokaryons. When heterokaryons with the genotype shown in Fig. 4 were grown in media containing lysine, leucine and cycloheximide (concentrations ranging from 30 to 50 μg/ml) the RIPed nucleus was forced to predominate the heterokaryon to provide resistance to the antibiotic. As a result, the growth rate was severely reduced, because Tom40 could not be supplied by the nucleus providing cycloheximide resistance. One strain (RIP40het), which grew slowly under these conditions, was analyzed further and found to be the desired strain (see "RESULTS", see section 3.1).

2.3 Transformation of *N. crassa*

DNA was transformed into *N. crassa* using spheroplasts as described previously (Schweizer *et al.*, 1981; Akins and Lambowitz, 1985) or by electroporation of conidia using modifications of a previously described technique (Margolin *et al.*, 1997; Margolin *et al.*, 2000). For electroporation, conidia (1 week old) were harvested, washed 3 times with 50 ml sterile ice-cold 1M sorbitol, and resuspended in 1M sorbitol at a concentration of 2 to 2.5 X 10^9 conidia/ml. Linearized plasmid DNA (5 μg, in a final volume of 5 μl) was mixed with 40 μl of conidia, placed in a pre-chilled electroporation cuvette and incubated on ice for 5 min prior to electroporation. A Gene Pulser (BioRad, Hercules, CA) was used with settings of 2.1 kV, 475 Ω, 25 microfarads. Immediately after the pulse (time constant varied from 11 to 12 ms), 1 ml of ice-cold sterile 1M sorbitol was added and the conidia were allowed to recover for 30 min to 1 hr at 30°C. Aliquots (10-100 μl) of the mixture were added to top agar (standard sorbose medium (Davis and De Serres, 1970) containing 1M sorbitol) containing the appropriate antibiotics for selection of transformants, and the mixture was poured onto plates containing the same medium without the sorbitol. The plates were placed at 30°C for 3 to 7 days to allow transformed colonies to form and transformants were purified as described in section 2.4.

2.4 Purification of single *N. crassa* colonies

To increase the likelihood of obtaining homokaryotic strains from transformed heterokaryons, individual transformed colonies were picked from transformation plates using sterile Pasteur pipets and transferred to slants of Vogel's medium containing the nutritional requirements of the desired homokaryon and the drug to which the homokaryon was resistant. The drug was used at 0.5 X concentration, as it was found that 1 X concentrations of most drugs reduced conidiation. The slants were placed at 30°C for three to four days and then transferred to room temperature for three to four days to allow conidiation. Conidia were then spread on viability plates containing 1 X concentration of the selective agent, and incubated at 30°C for several days. Colonies were picked as above and transferred to slants containing Vogel's media plus appropriate additives for the homokaryon but with no selection agent. These were allowed to grow,

and conidiate. Conidia from these isolates were then tested for their nutritional requirements to assure the recovery of the appropriate homokaryotic strain.

2.5 Creation of strains expressing mutant variants of Tom40

Mutant alleles of *tom40* were created by site directed mutagenesis of single-stranded DNA derived from a Bluescript plasmid containing the genomic version of *N. crassa tom40* and a bleomycin resistance gene. After confirmation of the desired mutation by DNA sequencing, plasmids were transformed (see section 2.3) into the $tom40^{RIP}$ sheltered heterokaryon, RIP40het. Transformants were selected on media containing cycloheximide (50 μg/ml), lysine and leucine (to select for transformants of the nucleus carrying the $tom40^{RIP}$ alleles), as well as bleomycin (1.5 μg/ml) to select for transformants and caffeine (0.5 mg/ml, to enhance the action of bleomycin), and purified through one round of single-colony isolation (section 2.4). Rescue of the RIPed nucleus was confirmed by testing for nutritional requirements. Plasmids that gave rise to homokaryons requiring lysine and leucine contain mutant alleles capable of restoring Tom40 function to levels sufficient for viability (Fig. 4). Integration of the mutant alleles were confirmed by DNA sequence analysis of PCR products generated from genomic DNA isolated from the transformants (see section 3.3).

2.6 Creation of Tom40 variants for *in vitro* import studies

A *tom40* cDNA was cloned into plasmid pGEM7Zf(+) and single stranded DNA was isolated. Mutant alleles were created by site-directed mutagenesis and used for *in vitro* transcription and translation to produce mutant Tom40 precursor proteins for import into isolated mitochondria.

2.7 Import of radiolabeled proteins into isolated mitochondria

For *in vitro* import studies, the isolation of mitochondria (Mayer *et al.*, 1993), and import of most mitochondrial precursor proteins (Harkness *et al.*, 1994b) were as described. Import was analyzed by SDS-polyacrylamide gel electrophoresis (PAGE) and gels were viewed by autoradiography. For *in vitro* import of Tom40 precursor proteins, mitochondria were incubated with radiolabeled preproteins that had been transcribed and

translated in rabbit reticulocyte lysate in the presence of [^{35}S]-methionine (ICN Biomedicals, Costa Mesa, CA). Import reactions were performed by incubation of 30 to 50 μg of mitochondria in import buffer (0.5% BSA [wt/vol], 250 mM sucrose, 80 mM KCl, 5 mM $MgCl_2$, 2 mM ATP, 10 mM MOPS-KOH, pH 7.2) with 2μl of labeled lysate at the indicated temperatures. If a proteinase K (PK) treatment of samples was performed, samples were incubated with 8μl of PK (2mg/ml) for 15 min on ice, followed by addition of 1 mM phenylmethylsulfonyl fluoride. Mitochondria were reisolated and import was analyzed by blue native gel electrophoresis (BNGE), or SDS-PAGE, and gels were viewed by autoradiography.

For some experiments, carbonate extraction was performed to determine if imported precursor proteins were inserted into the membranes. Mitochondria were suspended in 0.1 M sodium carbonate (pH 11.5) for 30 min at 0°C. The mixture was centrifuged at 20 000 rpm in a TLA55 rotor (Beckman Instruments, Palo Alto, CA) for 30 min at 2°C, and the pellets were processed for BNGE or SDS-PAGE.

2.8 Pulse import of Tom40 precursors

Mitochondria were isolated as in section 2.7. 50 μg of mitochondria, for each desired time point, were incubated in the presence of lysate containing radiolabeled Tom40 (2 μl for each 50 μg of mitochondrial protein) and import buffer (100 μl for each 50 μg of mitochondrial protein) at 25°C for 4 min (see section 2.7). Mitochondria were centrifuged at 15 000 rpm in a TLA55 rotor for 15 min at 1°C. The mitochondria were resuspended in fresh import buffer in the absence of radiolabeled preproteins and incubated at 25°C. Aliquots were taken at the appropriate time points (see figure legends for details) and added to 500 μl of ice-cold mitochondrial isolation buffer (0.25 M sucrose; 10 mM MOPS-KOH, pH 7.2; 1 mM EDTA) containing 1 mM phenylmethylsulfonyl fluoride. Mitochondria were then spun in a TLA55 rotor at 15 000 rpm for 15 min at 1°C, and the resulting pellets were processed for BNGE.

2.9 Blue native gel electrophoresis (BNGE)

Mitochondria (50-100 μg) were solubilized in 50 μl of buffer containing detergent (either 1% digitonin or 1% dodecylmaltoside in 20mM Tris-Cl, pH 7.4; 0.1 mM EDTA; 50 mM NaCl; 1% glycerol [vol/vol]; 1 mM phenylmethylsulfonyl fluoride). After gentle mixing at 4°C for 15 min and a clarifying spin (30 min, 14 000 g), 5 μl of sample buffer (5% Coomassie Brilliant Blue G-250 in 100 mM Bis-Tris, 500 mM 6-aminocaproic acid, pH 7.0) was added, and the mixture was analyzed on a 6-13% gradient blue native gel (BNG) as previously described (Schägger and von Jagow, 1991; Schägger *et al.*, 1994).

2.10 Electron microscopy

One milliliter of cell suspension from young liquid cultures (18 hrs for the control strain (HV), 18 hrs for RIP40het in the absence of cycloheximide, 24 hrs for the cycloheximide resistant control strain (HV) in the presence of cycloheximide, and 48 hrs for RIP40het in the presence of cycloheximide) was fixed in 1.5% $KMnO_4$ for 30 min at room temperature followed by several washes with distilled water. The sample was then suspended in 0.05 M sodium cacodylate buffer containing 2% glutaraldehyde and 30% sucrose, and incubated on ice for 30 min. The cells were then post-fixed in 1% OsO_4 [vol/vol] and 1.5% $K_2Cr_2O_7$ for 90 min on ice. Samples were then post-stained in 1% uranyl acetate overnight at room temperature. The steps of dehydration, embedding, and sectioning were performed by the Microscopy Unit, Department of Biological Sciences, University of Alberta. Sections were examined by transmission electron microscopy.

2.11 Isolation of purified mitochondrial outer membrane vesicles

Isolation of purified outer membrane vesicles was performed as outlined in (Mayer *et al.*, 1995a). In brief, mitochondria were isolated from large liquid cultures (Mayer *et al.*, 1993). The isolated mitochondria then were subjected to osmotic shock by incubation in a hypotonic solution (5 mM K_2PO4; 5 mM EDTA; 1 mM phenylmethylsulfonyl fluoride). The mitochondrial outer membrane was removed from the inner membrane by processing with a dounce homogenizer for 60 min on ice. Outer

membrane vesicles were purified by centrifuging the samples on two successive step sucrose gradients. The first gradient was prepared by overlaying 12 mls of 0.9 M sucrose in EMP buffer (2.5 mM EDTA; 10 mM MOPS-KOH, pH 7.2; 1 mM phenylmethylsulfonyl fluoride) with 9 mls of 0.25 M sucrose in EMP buffer. 15 mls of the dounced samples were added to the top of the gradient, and the tubes were spun for 1 hr at 28 K in a Beckman SW28 rotor at 2°C. The outer membrane vesicle fraction (OMV) was collected at the interface between the 0.25 M and 0.9 M solutions, while unruptured mitochondria and inner membrane vesicles sedimented. The OMV fraction collected was adjusted to 0.9 M by the addition of 2 M sucrose EMP buffer. 14 mls of this solution was loaded into each of four tubes and was overlayed with 19 mls of 0.72 M sucrose in EMP buffer, followed by 3 mls of EMP buffer. The tubes were spun for 12 hrs at 28 K in a Beckman SW28 rotor at 2°C. The OMV fraction was collected from between the 0 M and 0.72 M sucrose interface. The intermediate vesicle fraction (IMF), containing both the outer and inner membrane, was collected from between the 0.72 M and 0.9 M interface. The purity of the OMVs were tested by Western analysis for components of the outer and inner membranes (see section 2.17).

2.12 Silver staining

Purified OMVs or IMFs were subject to SDS-PAGE. Silver staining was then performed using a modified procedure adapted from (Rabilloud *et al.*, 1988). All solutions used in this procedure were made fresh for each use. The polyacrylamide gel was first fixed in a solution of 50% methanol, 10% acetic acid for 30 min at room temperature. The gel was then incubated for 15 min in a 50% methanol solution. Following incubation, the gel was washed five times in distilled water for 5 min each. The gel was then incubated in sodium thiosulfate (0.02%) for 1 min, and washed two times for 1 min each in distilled water. The gel was then incubated in silver nitrate (0.2%) for 25 min. Following silver nitrate treatment, the gel was washed twice again in distilled water for 1 min, and then developed in a solution of sodium carbonate (2%) and formaldehyde (0.015%) until the desired intensity of bands appeared. Developing was stopped by incubation in a 1.4% Na_2EDTA solution for 10 min.

2.13 Substituted cysteine accessibility mapping

Strains with single cysteine substitutions were grown in 500 ml liquid Vogel's media supplemented with 200 mg per liter lysine and leucine. Mitochondria were isolated as previously described (Mayer *et al.*, 1993) and resuspended in PBSSP buffer (137 mM NaCl; 2.7 mM KCl; 10 mM Na_2HPO_4; 2 mM KH_2PO_4; 0.25 M Sucrose; 1 mM phenylmethylsulfonyl fluoride; pH7.2) to a final concentration of 10 μg per μl. For each sample, 500 μg of mitochondria were diluted to a final volume of 500 μl in PBSSP. 5 μl of a 2 mg per 100 μl solution of freshly dissolved N^{α}-(3-maleimidylpropionyl) biocytin (biotin maleimide) (Molecular Probes, Eugene, OR) in dimethyl sulfoxide was added to the mitochondria and allowed to react for 1 hr with gentle shaking at room temperature (Tang *et al.*, 1998; Fujinaga *et al.*, 1999). Mitochondria were then reisolated by centrifugation, and washed once with 500 μl of PBSSP. Mitochondria were then lysed for immunoprecipitation.

2.14 Immunoprecipitation

Immunoprecipitations were performed as described in (Nargang *et al.*, 1988) with modifications. Mitochondria were lysed in 500 μl IP buffer (150 mM NaCl; 1% Triton X-100; 50 mM Tris-Cl, pH 7.0; 1 mM phenylmethylsulfonyl fluoride) for 30 min at 4°C with gentle rocking. Samples were then subjected to a clarifying spin (10 min; 14 000 rpm in a microcentrifuge) and supernatants were transferred to fresh tubes. For each immunoprecipitation to be performed, 4 mg protein A sepharose CL-4B (Amersham-Pharmacia, Piscataway, NJ) were prebound to 30 μl of antiserum (against the 12 C-terminal residues of Tom40 raised in rabbits) in the presence of IP buffer. The protein A sepharose-immunoglobulin complex was washed once in IP buffer, and resuspended in 50 μl IP buffer per 4 mg of protein A-sepharose used. 50 μl of the protein A sepharose-immunoglobulin complex solution were added to each clarified supernatant and allowed to incubate overnight with gentle shaking at 4°C. The protein A sepharose was pelleted by spinning at top speed for 2 min in an Eppendorf microcentrifuge. The pellets were washed three times with 1 ml of IP buffer. The final pellet was resuspended in 50 μl of buffer containing 100 mM Tris-Cl, pH 7.5, 5% SDS, 5% β-mercaptoethanol and boiled

for 5 min. The protein A sepharose was removed by centrifugation, and the supernatants were electrophoresed and transferred to nitrocellulose membranes as described below (see section 2.17).

Unless otherwise stated, all immunoprecipitations and immunodetections of Tom40 on Western blots were done using antiserum raised in rabbits to a peptide consisting of the last 12 amino acids of the Tom40 protein.

2.15 Detection of biotin labeled cysteine residues

Following electrophoresis and electroblotting to nitrocellulose membranes, membranes were incubated in blocking buffer (5% skim milk powder; 20 mM Tris-Cl pH 7.5; 150 mM NaCl; 2.5% Tween 20) for 30 min. Following incubation, a 1:2000 dilution of streptavidin biotinylated horseradish peroxidase complex (Amersham-Pharmacia, Piscataway, NJ) in blocking buffer was incubated with membranes for 4 hrs. Following streptavidin binding, membranes were washed twice with blocking buffer in the absence of the streptavidin complex for 5 min, and once in blocking buffer without 5% skim milk powder. Membranes were then subjected to enzyme catalyzed light generation and exposure to Kodak X-OMAT AR X-ray film (referred to from now on as ECL) (also see section 2.17).

2.16 Testing for immunoprecipitation efficiency

Following detection of the biotin labeled cysteine residues (section 2.15), membranes were then washed three times in TBS buffer (20 mM Tris-Cl pH 7.5; 150 mM NaCl; 2.5% Tween 20). The membranes were then incubated with blocking buffer for 30 min and immunodecorated with the mouse α-Tom40 antibody by standard techniques (see section 2.17) using a secondary antiserum-HRP conjugate to mouse IgGs. The mouse antiserum was directed against the same C-terminal peptide used to generate the immunoprecipitation antiserum.

2.17 Other techniques

The standard techniques of agarose gel electrophoresis, Southern and Northern blotting of agarose gels, preparation of radioactive probes, transformation of *Escherichia coli*, isolation of bacterial plasmid DNA, and the PCR using a mixture of *Taq* and *Vent* polymerase (New England Biolabs, Beverly, MA) to minimize replication errors, were all performed as described (Ausubel *et al.*, 1992; Sambrook and Russell, 2001). The following procedures were performed using the suppliers recommendations or previously described procedures: isolation of total RNA with the Qiagen RNeasy plant mini kit (Qiagen Inc., Santa Clarita, CA), separation of mitochondrial proteins by polyacrylamide gel electrophoresis (Laemmli, 1970), Western blotting (Good and Crosby, 1989), Western detection using LumiGLO chemiluminescent substrate (ECL) (Kirkegaard and Perry Laboratories, Gaithersburg, MD), genomic DNA isolation (Wendland *et al.*, 1996), protein determination with Coomassie dye binding assay (Bio-Rad, Hercules, CA), manual DNA sequencing using thermosequenase (Amersham Biosciences, Cleveland, OH), automated sequencing using a DyeNamic sequencing kit system (Amersham Biosciences) with a Model 373 stretch sequencer separation system (Applied Biosystems, Foster City, CA), and site directed mutagenesis using the Muta-Gene system (Bio-Rad) or a system based on the Muta-gene system assembled from individual reagents. Radioactive precursor proteins for import were generated by coupled *in vitro* transcription and translation using the Promega (Madison, WI) TnT reticulocyte lysate system in the presence of [^{35}S] methionine (ICN).

2.18 Oligonucleotides and plasmids

Oligonucleotides used in this study are listed in Table 2. Plasmids containing wild type copies of *tom40* are listed in Table 3, while plasmids containing mutant alleles of *tom40* are listed in Table 4.

Table 1: Strains used in this study.

SECTION A: STOCK STRAINS		
Strain	**Genotype**	**Origin or Source**
HostV	*a cyh-2 lys-2 leu-5 mei-2*	Fungal Genetics Stock Center #7255
MateV	*A am132 inl inv mei-2*	Fungal Genetics Stock Center #7265
NCN251 (also called 74*A*)	*A*	Fungal Genetics Stock Center #2489 (74-OR23-1VA)
40Dupl	As HV, but carries an ectopic copy of *tom40*. Hygromycin resistant	Transformation of Host V with the *tom40* plasmid pRIP-4
RIP40het[1] (strains studied F40-6, F46B-2)	Sheltered heterokaryon: (*cyh-2 lys-2 leu-5 mei-2* *tom40*^{RIP}+ *am132 inl inv mei-2*), mating type unknown. Both nuclei also contain an ectopic RIPed copy of *tom40*.	Cross of MateV x 40Dupl

SECTION B: Tom40 VARIANT STRAINS[2]		
Strain	**Genotype**	**Origin or Source**

[1] Two RIP40het strains were used in this study, F40-6, and F46B-2. F40-6 was found to be more reliable for transformation experiments because it consistently gave back lysine-leucine requiring strains with the correct introduced *tom40* allele, while F46B-2 gave back not only lysine-leucine requiring strains, but also leucine requiring strains.

[2] Strains are listed in the order of the mutations that they contain starting from the N- and proceeding to the C-terminus.

ΔNPGT (strain studied 8.5-2-1)	*cyh-2 lys-2 leu-5 mei-2 tom40*^{RIP} also contains an ectopic copy of *tom40* with a deletion of amino acids 40-43.	Transformation of RIP40het with plasmid p8.5
NPGT-AAAA (strain studied 9.7-1-1)	*cyh-2 lys-2 leu-5 mei-2 tom40*^{RIP} also contains an ectopic copy of *tom40* with residues NPGT at positions 40-43 changed to alanine residues.	Transformation of RIP40het with plasmid p9.7
Δ40-48 (strains studied C2962-1-1, C2962-2-1)	*cyh-2 lys-2 leu-5 mei-2 tom40*^{RIP} also contains an ectopic copy of *tom40* with a deletion of amino acids 40-48, and a change of codon 49 from Arg to Ala.	Transformation of RIP40het with plasmid p296.2
ΔRD (strain studied RD6-1)	*cyh-2 lys-2 leu-5 mei-2 tom40*^{RIP} also contains an ectopic copy of *tom40* with a deletion of amino acids 53-54.	Transformation of RIP40het with plasmid pRD
ΔRDTLL (strain studied RDT4-9-1)	*cyh-2 lys-2 leu-5 mei-2 tom40*^{RIP} also contains an ectopic copy of *tom40* with a deletion of amino acids 53-57.	Transformation of RIP40het with plasmid pRDTLL
Δ51-60 (strains studied 297-62-1, 297-68-1, 297-70-1)	*cyh-2 lys-2 leu-5 mei-2 tom40*^{RIP} also contains an ectopic copy of *tom40* with a deletion of amino acids 51-60, and a change of codon 50 from Glu to Ala.	Transformation of RIP40het with plasmid p297
YAF-AAA (strain studied 12-4-1)	*cyh-2 lys-2 leu-5 mei-2 tom40*^{RIP} also contains an ectopic copy of *tom40* with residues 94-96 with alanine	Transformation of RIP40het with plasmid p12.4

P-A (strain studied 10-7-1)	*cyh-2 lys-2 leu-5 mei-2 tom40*^{RIP} also contains an ectopic copy of *tom40* with residue 183 with alanine	Transformation of RIP40het with plasmid p10.7
WQQ (strain studied WQQ-8-1, WQQ-13-1)	*cyh-2 lys-2 leu-5 mei-2 tom40*^{RIP} also contains an ectopic copy of *tom40* with residues 237 and 238 changed from Lys to Glu.	Transformation of RIP40het with plasmid pWQQ
ΔCys (strain studied 170-6-12-1)	*cyh-2 lys-2 leu-5 mei-2 tom40*^{RIP} also contains an ectopic copy of *tom40* with residue 294 changed from Cys to Ser.	Transformation of RIP40het with plasmid p170-6
321AAA (strains studied 16.6-4-1, 16-18-1)	*cyh-2 lys-2 leu-5 mei-2 tom40*^{RIP} also contains an ectopic copy of *tom40* with residues KLG at positions 321-323 changed to alanine residues.	Transformation of RIP40het with plasmid p16.6
Δ329–349 (strains studied FC8-1, FC17-1)	*cyh-2 lys-2 leu-5 mei-2 tom40*^{RIP} also contains an ectopic copy of *tom40* with a deletion of amino acids 329-349.	Transformation of RIP40het with plasmid pΔC-ter
T40His (strain studied T40H-1-1)[1]	*cyh-2 lys-2 leu-5 mei-2 tom40*^{RIP} also contains an ectopic copy of *tom40* with the addition of a hexahistidyl tag at the carboxy terminus.	Transformation of RIP40het with plasmid pRT40H-9

[1] Created in the course of this study, but only used in collaboration at the Universiy of Munich

SECTION C: Tom40 SCAM[1] STRAINS

Strain	Genotype	Origin or Source
L10C (strain studied 10-2-1)	*cyh-2 lys-2 leu-5 mei-2 tom40*^{RIP} also contains an ectopic copy of *tom40* with residue 294 changed from Cys to Ala and residue 10 changed from Leu to Cys	Transformation of RIP40het with specific cysteine construct (see Plasmid table provided)
L292C (strain studied 292-1-1)	*cyh-2 lys-2 leu-5 mei-2 tom40*^{RIP} also contains an ectopic copy of *tom40* with residue 294 changed from Cys to Ala and residue 292 changed from Leu to Cys	Transformation of RIP40het with specific cysteine construct (see Plasmid table provided)
S293C (strain studied 293-3-1)	*cyh-2 lys-2 leu-5 mei-2 tom40*^{RIP} also contains an ectopic copy of *tom40* with residue 294 changed from Cys to Ala and residue 293 changed from Ser to Cys	Transformation of RIP40het with specific cysteine construct (see Plasmid table provided)
L295C (strain studied 295-1-1)	*cyh-2 lys-2 leu-5 mei-2 tom40*^{RIP} also contains an ectopic copy of *tom40* with residue 294 changed from Cys to Ala and residue 295 changed from Leu to Cys	Transformation of RIP40het with specific cysteine construct (see Plasmid table provided)
L296C (strain studied 296-2-1)	*cyh-2 lys-2 leu-5 mei-2 tom40*^{RIP} also contains an ectopic copy of *tom40* with residue 294 changed from Cys to Ala and residue 296 changed from Leu to Cys	Transformation of RIP40het with specific cysteine construct (see Plasmid table provided)
E297C (strain studied 297-2-1)	*cyh-2 lys-2 leu-5 mei-2 tom40*^{RIP} also contains an ectopic copy of *tom40* with residue 294 changed from Cys to Ala and residue 297 changed from Glu to Cys	Transformation of RIP40het with specific cysteine construct (see Plasmid table provided)

[1] SCAM, substituted cysteine accessibility mapping

K298C (Strain studied 298-4-1)	*cyh-2 lys-2 leu-5 mei-2 tom40*^{RIP} also contains an ectopic copy of *tom40* with residue 294 changed from Cys to Ala and residue 298 changed from Lys to Cys	Transformation of RIP40het with specific cysteine construct (see Plasmid table provided)
R299C (strain studied 299-6-1)	*cyh-2 lys-2 leu-5 mei-2 tom40*^{RIP} also contains an ectopic copy of *tom40* with residue 294 changed from Cys to Ala and residue 299 changed from Arg to Cys	Transformation of RIP40het with specific cysteine construct (see Plasmid table provided)
L300C (strain studied 300-1-1)	*cyh-2 lys-2 leu-5 mei-2 tom40*^{RIP} also contains an ectopic copy of *tom40* with residue 294 changed from Cys to Ala and residue 300 changed from Leu to Cys	Transformation of RIP40het with specific cysteine construct (see Plasmid table provided)
G301C (strain studied 301-3-1)	*cyh-2 lys-2 leu-5 mei-2 tom40*^{RIP} also contains an ectopic copy of *tom40* with residue 294 changed from Cys to Ala and residue 301 changed from Gly to Cys	Transformation of RIP40het with specific cysteine construct (see Plasmid table provided)
A302C (strain studied 302-1-1)	*cyh-2 lys-2 leu-5 mei-2 tom40*^{RIP} also contains an ectopic copy of *tom40* with residue 294 changed from Cys to Ala and residue 302 changed from Ala to Cys	Transformation of RIP40het with specific cysteine construct (see Plasmid table provided)
A303C (strain studied 303-9-1)	*cyh-2 lys-2 leu-5 mei-2 tom40*^{RIP} also contains an ectopic copy of *tom40* with residue 294 changed from Cys to Ala and residue 303 changed from Ala to Cys	Transformation of RIP40het with specific cysteine construct (see Plasmid table provided)
P304C (strain studied 304-1-1)	*cyh-2 lys-2 leu-5 mei-2 tom40*^{RIP} also contains an ectopic copy of *tom40* with residue 294 changed from Cys to Ala and residue changed from Pro to Cys	Transformation of RIP40het with specific cysteine construct (see Plasmid table provided)

V305C (strain studied 305-1-1)	*cyh-2 lys-2 leu-5 mei-2 tom40*^{RIP} also contains an ectopic copy of *tom40* with residue 294 changed from Cys to Ala and residue 305 changed from Val to Cys	Transformation of RIP40het with specific cysteine construct (see Plasmid table provided)
T306C (strain studied 306-1-1)	*cyh-2 lys-2 leu-5 mei-2 tom40*^{RIP} also contains an ectopic copy of *tom40* with residue 294 changed from Cys to Ala and residue 306 changed from Thr to Cys	Transformation of RIP40het with specific cysteine construct (see Plasmid table provided)
L307C (strain studied 307-2-1)	*cyh-2 lys-2 leu-5 mei-2 tom40*^{RIP} also contains an ectopic copy of *tom40* with residue 294 changed from Cys to Ala and residue 307 changed from Leu to Cys	Transformation of RIP40het with specific cysteine construct (see Plasmid table provided)
T308C (strain studied 308-4-1)	*cyh-2 lys-2 leu-5 mei-2 tom40*^{RIP} also contains an ectopic copy of *tom40* with residue 294 changed from Cys to Ala and residue 308 changed from Thr to Cys	Transformation of RIP40het with specific cysteine construct (see Plasmid table provided)
F309C (strain studied 309-4-1)	*cyh-2 lys-2 leu-5 mei-2 tom40*^{RIP} also contains an ectopic copy of *tom40* with residue 294 changed from Cys to Ala and residue 309 changed from Phe to Cys	Transformation of RIP40het with specific cysteine construct (see Plasmid table provided)
A310C (strain studied 310-10-1)	*cyh-2 lys-2 leu-5 mei-2 tom40*^{RIP} also contains an ectopic copy of *tom40* with residue 294 changed from Cys to Ala and residue 310 changed from Ala to Cys	Transformation of RIP40het with specific cysteine construct (see Plasmid table provided)
A311C (strain studied 311-1-1)	*cyh-2 lys-2 leu-5 mei-2 tom40*^{RIP} also contains an ectopic copy of *tom40* with residue 294 changed from Cys to Ala and residue 311 changed from Ala to Cys	Transformation of RIP40het with specific cysteine construct (see Plasmid table provided)

D312C (strain studied 312-2-1)	*cyh-2 lys-2 leu-5 mei-2 tom40*^{RIP} also contains an ectopic copy of *tom40* with residue 294 changed from Cys to Ala and residue 312 changed from Asp to Cys	Transformation of RIP40het with specific cysteine construct (see Plasmid table provided)
V313C (strain studied 313-1-1)	*cyh-2 lys-2 leu-5 mei-2 tom40*^{RIP} also contains an ectopic copy of *tom40* with residue 294 changed from Cys to Ala and residue 313 changed from Val to Cys	Transformation of RIP40het with specific cysteine construct (see Plasmid table provided)
D314C (strain studied 314-1-1)	*cyh-2 lys-2 leu-5 mei-2 tom40*^{RIP} also contains an ectopic copy of *tom40* with residue 294 changed from Cys to Ala and residue 314 changed from Asp to Cys	Transformation of RIP40het with specific cysteine construct (see Plasmid table provided)
H315C (strain studied 315-1-1)	*cyh-2 lys-2 leu-5 mei-2 tom40*^{RIP} also contains an ectopic copy of *tom40* with residue 294 changed from Cys to Ala and residue 315 changed from His to Cys	Transformation of RIP40het with specific cysteine construct (see Plasmid table provided)
V316C (strain studied 316-6-1)	*cyh-2 lys-2 leu-5 mei-2 tom40*^{RIP} also contains an ectopic copy of *tom40* with residue 294 changed from Cys to Ala and residue 316 changed from Val to Cys	Transformation of RIP40het with specific cysteine construct (see Plasmid table provided)
T317C (strain studied 317-4-1)	*cyh-2 lys-2 leu-5 mei-2 tom40*^{RIP} also contains an ectopic copy of *tom40* with residue 294 changed from Cys to Ala and residue 317 changed from Thr to Cys	Transformation of RIP40het with specific cysteine construct (see Plasmid table provided)
Q318C (strain studied 318-1-1)	*cyh-2 lys-2 leu-5 mei-2 tom40*^{RIP} also contains an ectopic copy of *tom40* with residue 294 changed from Cys to Ala and residue 318 changed from Gln to Cys	Transformation of RIP40het with specific cysteine construct (see Plasmid table provided)

Q319C (strain studied 319-7-1)	*cyh-2 lys-2 leu-5 mei-2 tom40*^{RIP} also contains an ectopic copy of *tom40* with residue 294 changed from Cys to Ala and residue 319 changed from Gln to Cys	Transformation of RIP40het with specific cysteine constructs (see Plasmid table provided)
A320C (strain studied 320-1-1)	*cyh-2 lys-2 leu-5 mei-2 tom40*^{RIP} also contains an ectopic copy of *tom40* with residue 294 changed from Cys to Ala and residue 320 changed from Ala to Cys	Transformation of RIP40het with specific cysteine constructs (see Plasmid table provided)
K321C (strain studied 321-2-1)	*cyh-2 lys-2 leu-5 mei-2 tom40*^{RIP} also contains an ectopic copy of *tom40* with residue 294 changed from Cys to Ala and residue 321 changed from Lys to Cys	Transformation of RIP40het with specific cysteine constructs (see Plasmid table provided)
L322C (strain studied 322-5-1)	*cyh-2 lys-2 leu-5 mei-2 tom40*^{RIP} also contains an ectopic copy of *tom40* with residue 294 changed from Cys to Ala and residue 322 changed from Leu to Cys	Transformation of RIP40het with specific cysteine constructs (see Plasmid table provided)
G323C (strain studied 323-5-1)	*cyh-2 lys-2 leu-5 mei-2 tom40*^{RIP} also contains an ectopic copy of *tom40* with residue 294 changed from Cys to Ala and residue 323 changed from Gly to Cys	Transformation of RIP40het with specific cysteine constructs (see Plasmid table provided)
M324C (strain studied 324-1-1)	*cyh-2 lys-2 leu-5 mei-2 tom40*^{RIP} also contains an ectopic copy of *tom40* with residue 294 changed from Cys to Ala and residue 324 changed from Met to Cys	Transformation of RIP40het with specific cysteine constructs (see Plasmid table provided)
S325C (strain studied 325-5-1)	*cyh-2 lys-2 leu-5 mei-2 tom40*^{RIP} also contains an ectopic copy of *tom40* with residue 294 changed from Cys to Ala and residue 325 changed from Ser to Cys	Transformation of RIP40het with specific cysteine constructs (see Plasmid table provided)

V326C (strain studied 326-1-1)	*cyh-2 lys-2 leu-5 mei-2 tom40*^{RIP} also contains an ectopic copy of *tom40* with residue 294 changed from Cys to Ala and residue 326 changed from Val to Cys	Transformation of RIP40het with specific cysteine constructs (see Plasmid table provided)
S327C (strain studied 327-1-1)	*cyh-2 lys-2 leu-5 mei-2 tom40*^{RIP} also contains an ectopic copy of *tom40* with residue 294 changed from Cys to Ala and residue 327 changed from Ser to Cys	Transformation of RIP40het with specific cysteine construct (see Plasmid table provided)
I328C (strain studied 328-1-1)	*cyh-2 lys-2 leu-5 mei-2 tom40*^{RIP} also contains an ectopic copy of *tom40* with residue 294 changed from Cys to Ala and residue 328 changed from Ile to Cys	Transformation of RIP40het with specific cysteine construct (see Plasmid table provided)
E329C (strain studied 329-7-1)	*cyh-2 lys-2 leu-5 mei-2 tom40*^{RIP} also contains an ectopic copy of *tom40* with residue 294 changed from Cys to Ala and residue 329 changed from Glu to Cys	Transformation of RIP40het with specific cysteine construct (see Plasmid table provided)
A330C (strain studied 330-1-1)	*cyh-2 lys-2 leu-5 mei-2 tom40*^{RIP} also contains an ectopic copy of *tom40* with residue 294 changed from Cys to Ala and residue 330 changed from Ala to Cys	Transformation of RIP40het with specific cysteine construct (see Plasmid table provided)
S331C (strain studied 331-4-1)	*cyh-2 lys-2 leu-5 mei-2 tom40*^{RIP} also contains an ectopic copy of *tom40* with residue 294 changed from Cys to Ala and residue 331 changed from Ser to Cys	Transformation of RIP40het with specific cysteine construct (see Plasmid table provided)
D332C (strain studied 332-1-1)	*cyh-2 lys-2 leu-5 mei-2 tom40*^{RIP} also contains an ectopic copy of *tom40* with residue 294 changed from Cys to Ala and residue 332 changed from Asp to Cys	Transformation of RIP40het with specific cysteine construct (see Plasmid table provided)

V333C (strain studied 333-1-1)	*cyh-2 lys-2 leu-5 mei-2 tom40*^{RIP} also contains an ectopic copy of *tom40* with residue 294 changed from Cys to Ala and residue 333 changed from Val to Cys	Transformation of RIP40het with specific cysteine construct (see Plasmid table provided)
D334C (strain studied 334-1-1)	*cyh-2 lys-2 leu-5 mei-2 tom40*^{RIP} also contains an ectopic copy of *tom40* with residue 294 changed from Cys to Ala and residue 334 changed from Asp to Cys	Transformation of RIP40het with specific cysteine construct (see Plasmid table provided)
L335C (strain studied 335-3-1)	*cyh-2 lys-2 leu-5 mei-2 tom40*^{RIP} also contains an ectopic copy of *tom40* with residue 294 changed from Cys to Ala and residue 335 changed from Leu to Cys	Transformation of RIP40het with specific cysteine construct (see Plasmid table provided)
Q336C (strain studied 336-1-1)	*cyh-2 lys-2 leu-5 mei-2 tom40*^{RIP} also contains an ectopic copy of *tom40* with residue 294 changed from Cys to Ala and residue 336 changed from Gln to Cys	Transformation of RIP40het with specific cysteine construct (see Plasmid table provided)
E337C (strain studied 337-2-1)	*cyh-2 lys-2 leu-5 mei-2 tom40*^{RIP} also contains an ectopic copy of *tom40* with residue 294 changed from Cys to Ala and residue 337 changed from Glu to Cys	Transformation of RIP40het with specific cysteine construct (see Plasmid table provided)
Q338C (strain studied 338-1-1)	*cyh-2 lys-2 leu-5 mei-2 tom40*^{RIP} also contains an ectopic copy of *tom40* with residue 294 changed from Cys to Ala and residue 338 changed from Gln to Cys	Transformation of RIP40het with specific cysteine construct (see Plasmid table provided)
Q339C (strain studied 339-1-1)	*cyh-2 lys-2 leu-5 mei-2 tom40*^{RIP} also contains an ectopic copy of *tom40* with residue 294 changed from Cys to Ala and residue 339 changed from Gln to Cys	Transformation of RIP40het with specific cysteine construct (see Plasmid table provided)

S344C (strain studied 344-4-1)	*Cyh-2 lys-2 leu-5 mei-2 tom40*^{RIP} also contains an ectopic copy of *tom40* with residue 294 changed from Cys to Ala and residue 344 changed from Ser to Cys	Transformation of RIP40het with specific cysteine construct (see Plasmid table provided)

Table 2: All primers used in this study are indicated. "P" indicates the presence of a phosphate.

PRIMER	SEQUENCE (5' - 3')	COMMENTS
FNA 93	TGTGGTGAGAGATGTCTATCGTTCCG	Tom40 sequencing primer, see Fig. 6.
FNA 94	CCGTTACAATCATGGCTTCGTTTTCC	Tom40 sequencing primer, see Fig. 6.
FNA 103	GCCATGGGAAAAATCGAAAGTCGGAC	Tom40 sequencing primer, see Fig. 6.
FNA 113	CGGTATCTTTGTCGGCGACTAC	Tom40 sequencing primer, see Fig. 6.
FNA 114	TGCCTTTGCTGCTCTCTACG	Tom40 sequencing primer, see Fig. 6.
FNA 115	GTTGAAGGCATCGGAAAGGCTCG	Tom40 sequencing primer, see Fig. 6.
FNA 116	GATGTCGATCTCCAGGAGCAGCAAGAG	Tom40 sequencing primer, see Fig. 6.
FNA 142	CTACAAGCTTGTAATACGACTCACTATA GGGCGAATTGGG	T7 - 40mer; primer for sequencing and PCR.
FNA 170	PCTTCTCGAGCAAGGCGCTGAGCTTG	Mutagenic primer to replace endogenous cysteine with alanine for genomic construct.
FNA 171	PCTTCTCGAGCAAGGAGCTGAGCTTG	Mutagenic primer to replace endogenous cysteine with serine for genomic construct.
FNA175	CGCCTATATCGCCGACATCACCGAT	Homologous to pBR322 region of pCSN44 and pRIP4
FNA 176	GTCCCTGTCTACTGCGACCGTTA	Tom40 sequencing primer, see Fig. 6.
FNA 181	GGCTTTCAGCCTCGCCCCTC	Tom40 sequencing primer, see Fig. 6.
FNA 182	CAAGATTCAACTACAGATGGG	Tom40 sequencing primer, see Fig. 6.
FNA 183	TTAAAAAGGGGATGTTGAGGG	Tom40 sequencing primer, see Fig. 6.
FNA194	PGGTGGGCATCGTGTGTGATTAGTGATG GTGATGGTGATGGATTACGTTGTCAACA CA	Mutagenic primer to create Tom40 C-terminal 6X-His tag.
FNA 247	PGAAGGTCTATGCGGCCGCGACAACCGA GGACTGCCC	Sequence after EcoRi site in pLR, from reverse primer sequence of pLR. Contains *NotI* site.

FNA 248	PGGTTGCGGATCCGCGGTAATGCATGATTGTAACGGTCGCAGTAG	Sequence at "ATG", contains created *NsiI* site at ATG and *BamHI* site further down stream for ligation of PCR product.
FNA 249	PGAGACTTGAGGATGCATTTCTCTGGCCTCCGCGCC	5' end PCR primer to create n-terminal deletion of Tom40. Contains *NsiI* site.
FNA 250	PCCATTACGCGGATCCTTGTATGCAAAGACCCAAGCC	3' PCR primer to create N-terminal deletion of Tom40. Contains *BamHI* site.
FNA 252	CAACGTACAGAGGGGCGAGGCTG	Tom40 sequencing primer, see Fig. 6.
FNA 253	GGCCTCCGCGCCGACGTCAC	Tom40 sequencing primer, see Fig. 6.
FNA 296	PATGGTGGCAGCAACGCACCGGCGGAAAGACCGAACTGTTTCC	Mutagenic primer for Δ40-48; R49A for genomic construct.
FNA 296-2	PATGTGTATGGTGGCAGCAACGCACCGGCGGAAAGACCGAACTGTTTCCTCCTTTC	Mutagenic primer for Δ40-48; R49A for genomic construct. (SEE FNA296)
FNA 297	PGCGCGGAGGCCAGAGAACATCGCTGTCAAGGCATTGTCAGCA	Mutagenic primer for Δ51-60; E50A for genomic construct.
RTA2	PCTTCATCCCCAATATACATATTCCAGTTTAAATGGAGACGGACATGCCGAGCTTGGCTTG	Mutagenic primer for ΔC-TERM for genomic and cDNA construct.
RTA3	PCATGATTGTAACGGTCGCAGTAGAC	Mutagenic primer for ΔN-1a for genomic construct.
RTA4	PTTCTCTGGCCTCCGCGCCGACGTC	Mutagenic primer for ΔN-1b for genomic construct.
RTA5	PGGATGTGTATGGTGGCAGCAACGCACCGCGCATGATTGTAACGGTCGCAGTAGACAGGG	Mutagenic primer for ΔN-2a for genomic construct.
RTA6	PGCCTTGGTGACGTCGGCGCGGAGGCCAGAGAACATGATTGTAACGGTCGCAGTAGACAGGG	Mutagenic primer for ΔN-2b for genomic construct.
RTA7	PCCCTATCCGTCAGCTGCTGCCAGAAGGAAGTGTTGAG	Mutagenic primer for WKK - WQQ for genomic and cDNA construct.
RTA8	PCGCGGGCGATGGTCTCGATGGAAAGACCGAACTGTTTCC	Mutagenic primer for ΔNPGT for genomic construct.
RTA9	PCGCGGGCGATGGTCTCGATCGCGGCGGCGGCGGAAAGACCGAACTGTTTCC	Mutagenic primer for NPGT - AAAA for genomic construct.

RTA10	PGAGGCCGAGTCTGGCAGTGACGGC	Mutagenic primer for VTPR- VTAR for genomic and cDNA construct.
RTA11	PGGTTCCGTAGAGAGCAGCAGGGTTCAACCTCTCGCC	Mutagenic primer for ΔYAF for genomic and cDNA construct.
RTA12	PGGTTCCGTAGAGAGCAGCCGCGGCAGCAGGGTTCAACCTCTCGCC	Mutagenic primer for YAF - AAA for genomic and cDNA construct.
RTA13	PGCAGCTGAGCTTGCCCTTCTGAGCCCTGAAGGTGG	Mutagenic primer for ΔIDS for genomic and cDNA construct.
RTA14	PGCAGCTGAGCTTGCCCTTGGCAGCGGCCTGAGCCCTGAAGGTGG	Mutagenic primer for IDS - AAA for genomic and cDNA construct.
RTA15	PCCTCAATGGAGACGGACATGGCTTGTTGCTTGAAGGGG	Mutagenic primer for ΔKLG for genomic construct.
RTA16	PCCTCAATGGAGACGGACATCGCGGCCGCGGCTTGTTGCTTGAAGGGG	Mutagenic primer for KLG - AAA for genomic construct.
RTA17	PGACGGGGGCGGCACCAAGGAGCAAGCAGCTGAGCTTC	Mutagenic primer for ΔEKR for genomic and cDNA construct.
RTA18	PGACGGGGGCGGCACCAAGGGCCGCCGCGAGCAAGCAGCTGAGCTTG	Mutagenic primer for ERK - AAA for genomic and cDNA construct.
RTA19	PGAGGCTGAAAGCCTTGGTGACAGAGAACATGTAGTTGGTGAGG	Mutagenic primer for ΔGLRAD for genomic and cDNA construct.
RTA20	PGAGGCTGAAAGCCTTGGTGACGGCTGCGGCTGCGGCAGAGAACATGTAGTTGGTGAGG	Mutagenic primer for GLRAD - AAAAA for genomic and cDNA construct.
RTA21	PCAACTCGCCCATGGCAAAAACTTGGAAGCTTGGGTTATAG	Mutagenic primer for ΔSHQ for genomic construct.
RTA22	PCAACCTCTCGCCCATGGCAAACGCGGCGGCAACTTGGAAGCTTGGGTTATAG	Mutagenic primer for SHQ -AAA for genomic construct.
RTA23	PGGTGAGGAGGGTTTGGACCTCTGTC	Mutagenic primer for ΔRD for genomic construct.
RTA24	PGAACATGTAGTTGGTTTGGACCTCTGTCAAGG	Mutagenic primer for ΔRDTLL for genomic construct.
RTA25	PGACGGCCTGGAGTTAGTCGCCGAC	Mutagenic primer for C4-Y STOP for cDNA construct.
RTA26	PCCTGACGTTGTCAGACGGCCTGG	Mutagenic primer for I5-W STOP for cDNA construct.

RTA27	PGGTGATGCCTTCCTAGGTAAGCCCAC	Mutagenic primer for I7-K STOP for cDNA construct.
RTA28	PGAAGGTGGACATTCAGAAGTCGTAC	Mutagenic primer for C7-RSTOP for cDNA construct.
RTA29	PGTGACGTGGTCAACCTAAGCAGCGAAG GTCAG	Mutagenic primer for M14-DSTOP for cDNA construct.
RTA30	CCTTTGGCGATGCTGCGCGACAATGCC	PCR primer, eliminates amplification of the endogenous RIP copy.
RTA31	GGTGACTGGGTTGCTAGCGCTCAGC	Tom40 sequencing primer, see Fig. 6.
RTA32	GAAAAACCGCTGACCTATAACCCAAG	Tom40 sequencing primer, see Fig. 6.
RTA33	CCTTAGCCCACAATTAGAATAAAGC	Tom40 sequencing primer, see Fig. 6.
RTA34	CCACGTCACTGTAAGTCACATGGCC	Tom40 sequencing primer, see Fig. 6.
RTA35	PCCAGAGAACATGTAGTTGGTTTGGACC TCGCGGGCGATGGTCTC	Mutagenic primer for ΔRDTLL for cDNA construct.
RTA36	PGAACATGTAGTTGGTGAGGAGGGTTTG GACCTCGCGGGCGATGGTATCG	Mutagenic primer for ΔRD for cDNA construct.
RTA37	PGAGGAGGGTATCGCGTTGGACCTCGGC GGAAAGACCGAACTGTTTCCTCC	Mutagenic primer for Δ40-48, R49A for cDNA construct.
RTA38	PCGTCGGCGCGGAGGCCAGAGAACATCG CGCGGGCGATGGTCTCGTGCC	Mutagenic primer for Δ51-60, E50A for cDNA construct.
RTA40	GGAACGAATTCGTTGTGTCCGCGTTCGC TTCCGCC	3' PCR primer for Tom6
RTA41	GTCGCTGTTTCAGAACTGGCTCGTCG	3' PCR primer for Tom6
RTA42	ATTCGACGTTCCCAGTATGCGATTGC	5' PCR primer for Tom6
RTA43	GTGCGCGGAAACAACAGAGCG	Tom40 sequencing primer, see Fig. 6. Same as FNA169.
RTA44	CGCCTCAATGGAGACGGACATGGCTTGT TGAGTGACGTGGTC	Mutagenic primer for ΔKLG for cDNA construct.
RTA45	CGCCTCAATGGAGACGGACATGGCGGCC GCGGCTTGTTGAGTGACGTGGTC	Mutagenic primer for KLG - AAA for cDNA construct.
RTA46	PGTCGAGAGAGCGCCCTCGTTCTGAGCG AAGATCTGTTGAC	Mutagenic primer for ΔGNLD for genomic construct.

RTA47	PGTCGAGAGAGCGCCCTCGTTGGCCGCG GCCGCCTGAGCGAAGATCTGTTGAC	Mutagenic primer for GNLD - AAAA for genomic construct.
RTA48	PCCACCAATCGAGAACTGCGTGATGGTC CTGTCACCCCATC	Mutagenic primer for ΔTK for genomic and cDNA construct.
RTA49	PCCACCAATCGAGAACTGCGCGGCGATG GTCCTGTCACCCCATC	Mutagenic primer for TK - AA for genomic and cDNA construct.
RTA50	PGAGGCACTGAAGTCGTCGCCAAGGTGG GCCATATCCTGGCCGCCACCAATCG	Mutagenic primer for ΔQHFEHE for genomic and cDNA construct.
RTA51	PGAGGCACTGAAGTCGTCGCCAAGGTGC GCGGCCGCGGCCGCGGCCATATCCTGGC CGCCACCAATCG	Mutagenic primer for QHEFE - AAAAA for genomic and cDNA construct.
RTA52	PCTGGAGACCGAGGCCGAGTCTGGCCTG GAGGTAGTCGCCGAC	Mutagenic primer for ΔVTP for genomic and cDNA construct.
RTA53	PCTGGAGACCGAGGCCGAGTCTGGCCGC GGCCTGGAGGTAGTCGCCGA	Mutagenic primer for VTP-AAA for genomic and cDNA construct.
RTA54	PCTGGAGACCGAGGCCGAGTCTAGTGAC GGCCTGGAGGTAGTC	Mutagenic primer for VTPR - VTR for genomic and cDNA construct.
RTA55	PGCCTGCACCCTATCCGTCAGCCAGAAG GAAGTGTTGAGAG	Mutagenic primer for ΔKK for genomic and cDNA construct.
RTA56	PGCCTGCACCCTATCCGTCAGCGCCGCC CAGAAGGAAGTGTTGAGAG	Mutagenic primer for KK-AA for genomic and cDNA construct.
RTA57	PCATGCCGAGCTTGGCTTGTTGCTAGACG TGGTCAACATCAGCAGC	Mutagenic primer for new C7-T STOP for cDNA construct.
RTA58	PGACGGGGGCGGCACCCTAACGCTTCTC GAGCAAGCAGC	Mutagenic primer for new I7-L STOP for cDNA construct.
RTA59	PCCTCTCGCCCATGGCAAACGCGGCCGC AACTTGGAAGAGAGGGGCG	Mutagenic primer for SHQ -AAA for cDNA construct.
RTA60	PCCTCTCGCCCATGGCAAAAACTTGGAA GAGAGGGGCG	Mutagenic primer for ΔSHQ for cDNA construct.
RTA61	PGCCGAGCTTGGCTTGTTGAGTAAGACG CTTCTCGAGCAAGCAGCTG	Mutagenic primer for ΔM13#1 for cDNA construct.
RTA62	PCATGCCGAGCTTGGCTTGTTGAGTGGA CATTCTGAAGTCGTACTTGGC	Mutagenic primer for ΔM13#2 for cDNA construct.
RTA63	PGTCGAGAGAGCGCCCTCGTTCTGAGCG AAGATCTGGTTGG	Mutagenic primer for ΔGNLD for cDNA construct.

RTA64	PGTCGAGAGAGCGCCCTCGTTCGCGGCC GCGGCCTGAGCGAAGATCTGGTTGG	Mutagenic primer for GNLD - AAAA for cDNA construct.
RTA65	PGGGGCGAGGCTGAAAGCCTTGGTGACG GCTGCGGCTGCGGCAGAGAACATGTAGT TGGTGAGGAGGG	Mutagenic primer for GLRAD - AAAAA for cDNA construct.
RTA66	PGGGGCGAGGCTGAAAGCCTTGGTGACA GAGAACATGTAGTTGGTGAGGAGGG	Mutagenic primer for ΔGLRAD for cDNA construct.
RTA67	GAGGTTACATGCGGCCGCCGATCCAGAT CCAAGAGAGTTCAAATGCGG	TOM40 5' cloning - For subclone pB3
RTA68	GAGGTTACATGCGGCCGCTAGCGAGGGA CGGTGAAAAGGTATGACCC	TOM40 3' cloning - For subclone pB3
RTA69	GAGGTTACATGAATTCATTAAAGAGGAG AAATTAACTATGGCTTCGTTTTCCACCGA GTCGCCTTTG	TOM40 5' N - His construct – *EcoRI*
RTA70	GAGGTTACATAAGCTTTTAATGGTGATG GTGATGGTGATGGTGATGGAGAGGGGCG AGGCTGAAAGCCTTGG	TOM40 3' N - 9 His construct *HinDIII*
RTA71	GAGGTTACATAAGCTTTTAATGGTGATG GTGATGGTGGAGAGGGGCGAGGCTGAA AGCCTTGG	TOM40 3' N - 6 His construct *HinDIII*
RTA72	PGACCGCCGTCAAGGAAAGAGATGGCCT TGAGGGAGGCAC	Mutagenic primer for ΔNP for genomic construct.
RTA73	PGAGCTTGGCTTGTTGAGTGACATCAGC AGCGAAGGTCAGAG	Mutagenic primer for ΔVDH for genomic and cDNA construct.
RTA74	PGACCGCCGTCAAGGAAAGAGGCGGCG ATGGCCTTGAGGGAGGCAC	Mutagenic primer for NP-AA for genomic and cDNA construct.
RTA75	PGAGCTTGGCTTGTTGAGTGACCGCGGC CGCATCAGCAGCGAAGGTCAGAG	Mutagenic primer for VDH-AAA for genomic and cDNA construct.
RTA76	PGTCGAGAGAGCGCCCTCGTTCTGAGCG AAGATCTGTTGAC	Mutagenic primer for ΔGNLD for cDNA construct.
RTA78	CGAGCGTTCTGAACAAATCCAG	Sequencing primer - pQE40 – DHFR
RTA79	GAGGTTACATGAATTCATTAAAGAGGAG AAATTAACTATGGCTTCGTTTTCCACCGA GTCGCC	TOM40 - New 5' His primer

RTA84	GAGGTTACATAAGCTTTTAGTGATGGTG ATGGTGATGAAAGGGGATGTTGAGGGAC TG	TOM40 extreme C-terminal 6 His tag
RTA85	TTTAAAAGGGGATGTTGAGGGAC	See Wt-TOM40 PCR Cter
RTA86	GAAAAGGTATGACCCACACCCTTTC	Tom40 sequencing primer, see Fig. 6.
RTA87	CACCATCCGCTGCGTCCTCGATTCCC	Tom40 sequencing primer, see Fig. 6.
WTPCR Nter	CCGATGCCTTCAACGCCTTTC	Used to eliminate ectopic RIP in PCR from potential transformants.
WTPCR Cter	TTTAAAAGGGGATGTTGAGGGAC	Used to eliminate endogenous RIP in PCR from potential transformants.

SECTION B: SCAM[1] PRIMERS

PRIMER	SEQUENCE (5' - 3')	COMMENTS
RTA80	PGCATTGTCGCGCAGCATCGCACAAGGC GACTCGGTGGAAAACG	Mutagenic primer for cysteine mutant L10C for genomic construct.
L292C	PCGCTTCTCGAGCAAGGCGCTACACTTGCCCT TGGAGTCGATCTG	Mutagenic primer for cysteine mutant L292C for genomic construct.
S293C	PGACGCTTCTCGAGCAAGGCACAGAGCTTGC CCTTGGAGTCGATC	Mutagenic primer for cysteine mutant S293C for genomic construct.
L295C	PGCACCAAGACGCTTCTCGAGACAGGCGCTG AGCTTGCCCTTGG	Mutagenic primer for cysteine mutant L295C for genomic construct.
L296C	PGCGGCACCAAGACGCTTCTCACACAAGGCG CTGAGCTTGCCCTTG	Mutagenic primer for cysteine mutant L296C for genomic construct.
E297C	PGGGCGGCACCAAGACGCTTACAGAGCAAGG CGCTGAGCTTGC	Mutagenic primer for cysteine mutant E297C for genomic construct.
K298C	PGGGGGCGGCACCAAGACGACACTCGAGCAA GGCGCTGAGCTTG	Mutagenic primer for cysteine mutant K292C for genomic construct.
R299C	PGACGGGGGCGGCACCAAGACACTTCTCGAG CAAGGCGCTGAGC	Mutagenic primer for cysteine mutant R299C for genomic construct.
L300C	PCAGAGTGACGGGGGCGGCACCACAACGCTT CTCGAGCAAGGCGCTG	Mutagenic primer for cysteine mutant L300C for genomic construct.

[1] SCAM, substituted cysteine accessibility mapping

G301C	PGTCAGAGTGACGGGGGCGGCACAAAGACGC TTCTCGAGCAAGGCG	Mutagenic primer for cysteine mutant G301C for genomic construct.
A302C	PGAAGGTCAGAGTGACGGGGGCACAACCAA GACGCTTCTCGAGCAAG	Mutagenic primer for cysteine mutant A302C for genomic construct.
A303C	PGCGAAGGTCAGAGTGACGGGACAGGCACCA AGACGCTTCTCGAGC	Mutagenic primer for cysteine mutant A303C for genomic construct.
P304C	PGCAGCGAAGGTCAGAGTGACACAGGCGGCA CCAAGACGCTTCTCG	Mutagenic primer for cysteine mutant P304C for genomic construct.
V305C	PCAGCACGCAAGGTCAGAGTACAGGGGGCGG CACCAAGACGCTTC	Mutagenic primer for cysteine mutant V305C for genomic construct.
T306C	PCATCAGCAGCGAAGGTCAGACAGACGGGGG CGGCACCAAGACGC	Mutagenic primer for cysteine mutant T306C for genomic construct.
L307C	PCAACATCAGCAGCGAAGGTACAAGTGACGG GGGCGGCACCAAGAC	Mutagenic primer for cysteine mutant L307C for genomic construct.
T308C	PGGTCAACATCAGCAGCGAAACACAGAGTGA CGGGGGCGGCACCAAG	Mutagenic primer for cysteine mutant T308C for genomic construct.
F309C	PCGTGGTCAACATCAGCAGCACAGGTCAGAG TGACGGGGGCGGCACC	Mutagenic primer for cysteine mutant F309C for genomic construct.
A310C	PGACGTGGTCAACATCAGCACAGAAGGTCAG AGTGACGGGGGCGGC	Mutagenic primer for cysteine mutant A310C for genomic construct.
A311C	PCAGTGACGTGGTCAACATCACAAGCGA AGGTCAGAGTGACGGG	Mutagenic primer for cysteine mutant A311C for genomic construct.
D312C	PTTACAGTGACGTGGTCAACACAAGCAG CGAAGGTCAGAGTGAC	Mutagenic primer for cysteine mutant D312C for genomic construct.
V313C	PGACTTACAGTGACGTGGTCACAATCAG CAGCGAAGGTCAGAGTG	Mutagenic primer for cysteine mutant V313C for genomic construct.
D314C	PATGTGACTTACAGTGACGTGACAAACA TCAGCAGCGAAGGTCAGA	Mutagenic primer for cysteine mutant D314C for genomic construct.
H315C	PGCCATGTGACTTACAGTGACACAGTCA ACATCAGCAGCGAAGGTC	Mutagenic primer for cysteine mutant H315C for genomic construct.
RTA81	PGAGGCCATGTGACTTACAGTACAGTGG TCAACATCAGCAGCG	Mutagenic primer for cysteine mutant V316C for genomic construct.
T317C	PGAAGAGGCCATGTGACTTACACAGACG TGGTCAACATCAGCAGCG	Mutagenic primer for cysteine mutant T317C for genomic construct.
Q318C	PGACATGCCGAGCTTGGCTTGACACTTG AAGGGGGTTAGCAGAAG	Mutagenic primer for cysteine mutant Q318C for genomic construct.

Q319C	PACGGACATGCCGAGCTTGGCACATTGC TTGAAGGGGGTTAGCAG	Mutagenic primer for cysteine mutant Q319C for genomic construct.
A320C	PAGACGGACATGCCGAGCTTACATTGTT GCTTGAAGGGGGTTAGC	Mutagenic primer for cysteine mutant A320C for genomic construct.
RTA82	PGGAGACGGACATGCCGAGACAGGCTTG TTGCTTGAAGGGGG	Mutagenic primer for cysteine mutant K321C for genomic construct.
L322C	PCTCAATGGAGACGGACATGGCACACTT GGCTTGTTGCTTGAAGG	Mutagenic primer for cysteine mutant L322C for genomic construct.
G323C	PCGCCTCAATGGAGACGGACATACAGAG CTTGGCTTGTTGCTTGA	Mutagenic primer for cysteine mutant G323C for genomic construct.
M324C	PGACGCCTCAATGGAGACGGAACAGCCG AGCTTGGCTTGTTGCTT	Mutagenic primer for cysteine mutant M324C for genomic construct.
S325C	PTCAGACGCCTCAATGGAGACACACATG CCGAGCTTGGCTTGTTGC	Mutagenic primer for cysteine mutant S325C for genomic construct.
V326C	PCATCAGACGCCTCAATGGAACAGGACA TGCCGAGCTTGGCTTG	Mutagenic primer for cysteine mutant V326C for genomic construct.
S327C	PCGAGATCAGACGCCTCAATACAGACGG ACATGCCGAGCTTGGCT	Mutagenic primer for cysteine mutant S327C for genomic construct.
I328C	PGATCGACATCAGACGCCTCACAGGAGA CGGACATGCCGAGCTTG	Mutagenic primer for cysteine mutant I328C for genomic construct.
E329C	PGGAGATCGACATCAGACGCACAAATGG AGACGGACATGCCGAGC	Mutagenic primer for cysteine mutant E329C for genomic construct.
A330C	PTCCTGGAGATCGACATCAGAACACTCA ATGGAGACGGACATGCCG	Mutagenic primer for cysteine mutant A330C for genomic construct.
S331C	PCTGCTCCTGGAGATCGACATCACACGC CTCAATGGAGACGGACATG	Mutagenic primer for cysteine mutant S331C for genomic construct.
C332D	PCTGCTCCTGGAGATCGACACAAGACGC CTCAATGGAGACG	Mutagenic primer for cysteine mutant D332C for genomic construct.
C333V	PCTTGCTGCTCCTGGAGATCACAATCAG ACGCCTCAATGGAG	Mutagenic primer for cysteine mutant V333C for genomic construct.
C334D	PCTCTTGCTGCTCCTGGAGACAGACATC AGACGCCTCAATGG	Mutagenic primer for cysteine mutant D334C for genomic construct.
C335L	PCCCTCTTGCTGCTCCTGACAATCGACAT CAGACGCCTCAATG	Mutagenic primer for cysteine mutant L335C for genomic construct.
C336Q	PGGGCACCCTCTTGCTGCTCACAGAGAT CGACATCAGACGC	Mutagenic primer for cysteine mutant Q336C for genomic construct.

C337E	PGACTGGGCACCCTCTTGCTGACACTGG AGATCGACATCAGA	Mutagenic primer for cysteine mutant E337C for genomic construct.
C338Q	PGACTGGGCACCCTCTTGACACTCCTGG AGATCGACATCAG	Mutagenic primer for cysteine mutant Q338C for genomic construct.
C339Q	PGGGACTGGGCACCCTCACACTGCTCCT GGAGATCGACATC	Mutagenic primer for cysteine mutant Q339C for genomic construct.
RTA83	PGTTTAAAAGGGGATGTTGAGACACTGG GCACCCTCTTGCTGC	Mutagenic primer for cysteine mutant S344C for genomic construct.

Table 3: Plasmids used for initial Tom40 work.

Plasmid name	Genomic or cDNA	Cloned into	Made by	Comments
pBJ5	Genomic	pNEB-193	B.J. McHale	First cloning attempt for Tom40. Contains a 8 kb genomic *KpnI-ClaI* fragment.
pLR	Genomic	pBluescript	L. Corrigan	First subcloning of Tom40 from pBJ5. Fragment cloned was ~6 kb *EcoRI-PmeI* cloned into pBluescript cut with *EcoRI* and *HincII*.
pRIP4	Genomic	pGEMT	B.J. McHale	Cloning of Tom40 derived from PCR with FNA94 and FNA93 approximately 1.8 kb with a hyg resistance marker.
pLS4	Genomic	pBluescript	L. Corrigan	Subclone of Tom40 from pLR, *EcoRI – ClaI* 5.5 kb Fragment. Contains Bleo from Bleo520, *EcoRI* fragment
P15	Genomic	pBluescript	R. Taylor	Subclone of Tom40 from pLS4. PCR based cloning, primers used were RTA67 and RTA68.
pB3	Genomic	pBluescript	R. Taylor	As for p15 with Bleo520 inserted. Used for site directed mutagenesis
pChBr	cDNA	PCSN44	M. Kiebler, Neupert lab	Tom40 cDNA, hyg resistance marker
pSnPy4, 10	cDNA	pGEM7ZF(+)	R. Taylor	Tom40 cDNA, used for site directed mutagenesis. SP6 promoter used for transcription.
pAsterix	cDNA	pGEM	M. Kiebler, Neupert lab	Tom40 cDNA, for *in vitro* translation, SP6 promoter used for transcription.
pRT40H9	Genomic	pBluescript	R. Taylor	pLS4 with 6X C-terminal his tag
pC8	Genomic	pBluescript	R. Taylor	Tom40 gDNA as pB3, No endogenous cysteine, to use for SCAM

Table 4: List of all mutations made in Tom40 with corresponding genomic and cDNA plasmids listed.

Mutation name	Amino Acids Affected	cDNA Plasmid	Genomic Plasmid
ΔC-ter	Deletion of aa[1] 330-349	ΔC2	pTOM40ΔC-3, -19, -22, -27
ΔN-ter	Deletion of aa 2-61	Rapaport *et al.* 2001.	pB40N12
Δ40-50	Deletion of aa 40-48; R49A	pRTCΔ40-14	p296.2
Δ50-60	E50A; Deletion of aa 51-60	p38-12	p297.4
ΔNPGT	Deletion of aa 40-43	pRTC8-1,-6	p8-5
NPGT-AAAA	Replacement of aa 40-43 with Ala	pRTC9-1,-3	p9-7
ΔRD	Deletion of aa 53-54	p36-19	pRD1, pRD7
ΔRDTLL	Deletion of aa 53-57	p35-16	pRDT4
ΔGLRAD	Deletion of aa 64-68	p19-12	P19-8
GLRAD-AAAA	Replacement of aa 64-68 with Ala	p20-12	p20-19
ΔGNLD	Deletion of aa 109-112	p63.2	p46-7
GNLD-AAAA	Replacement of aa 109-112 with Ala	p64-6	p47-8
ΔQFEHE	Deletion of aa 145-149	p50.4	p50-3
QFEHE-AAAAA	Replacement of aa 145-149 with Ala	p51-7	p51-6
ΔVTP	Deletion of aa 183-185	p52-4	p52-6
VTP-AAA	Replacement of aa 183-185 with Ala	p53-1	p53-1
VTPR-VTR	Deletion of aa 183	p54-2	p54-3

[1] aa, amino acid number

VTPR-VTAR	Replacement of aa 183 with Ala	p10-9	p10.7
ΔERK	Deletion of aa 297-299	p17.9	Old p17-1 New p17-5
ERK-AAA	Replacement of aa 297-299 with Ala	p18.3	Old p18-1 New p18-3
ΔSHQ	Deletion of aa 82-84	pΔS-2	p21-3
SHQ-AAA	Replacement of aa 82-84 with Ala	pA3.1, 3.2	p22-10
ΔYAF	Deletion of aa 94-96	pC11.8	11.6
YAF-AAA	Replacement of aa 94-96 with Ala	pC12-1	p12.4
ΔIDS	Deletion of aa 286-288	pC13-8	p13.6
IDS-AAA	Replacement of aa 286-288 with Ala	pC14-7, -8	p14.4
ΔKLG	Deletion of aa 321-323	p44-15	p15.3
KLG-AAA	Replacement of aa 321-323 with Ala	p45-14	p16.6
ΔTK	Deletion of aa 131-132	p48-6	p48-7
TK-AA	Replacement of aa 131-132 with Ala	p49-9	p49-1
ΔNP	Deletion of aa 163-164	pN1	p72-2
NP-AA	Replacement of aa 163-164 with Ala	pNA7	p74-1
ΔKK	Deletion of aa 237-238	p55-1, -7	p55-2
KK-AA	Replacement of aa 237-238 with Ala	p56-20	p56-1
WKK-WQQ	Replacement of aa 237-238 with Gln	p7-1	pWQQ11-2
ΔVDH	Deletion of aa 312-314	pV3	p73-3
VDH-AAA	Replacement of aa 312-314 with Ala	pVA1	p75-6
I5-W	Stop inserted at aa 195	pI5W-4	**NA**
C7-Threonine	Stop inserted at aa 317	pC7-9	**NA**
I7-Threonine	Stop inserted at aa 300	pI7-3, -8	**NA**
M13#1	Deletion of aa 301-315	p61-5	**NA**
M13#2	Deletion of aa 281-315	p62-4	**NA**

SECTION B: SCAM[1] Plasmids

Mutation name	Amino Acids Affected	cDNA Plasmid	Genomic Plasmid
L10C	Replacement of Leu at position 10 with Cys in pC8 plasmid.	**NA**	p10-5, -8
L292C	Replacement of Leu at position 292 with Cys in pC8 plasmid.	**NA**	p292-1
S293C	Replacement of Ser at position 293 with Cys in pC8 plasmid.	**NA**	p293-2
L295C	Replacement of Leu at position 295 with Cys in pC8 plasmid.	**NA**	p295-5
L296C	Replacement of Leu at position 296 with Cys in pC8 plasmid.	**NA**	p296-1
E297C	Replacement of Glu at position 297 with Cys in pC8 plasmid.	**NA**	p297-1
K298C	Replacement of Lys at position 298 with Cys in pC8 plasmid.	**NA**	p298-1
R299C	Replacement of Arg at position 299 with Cys in pC8 plasmid.	**NA**	p299-1
L300C	Replacement of Leu at position 300 with Cys in pC8 plasmid.	**NA**	p300-1
G301C	Replacement of Gly at position 301 with Cys in pC8 plasmid.	**NA**	p301-2
A302C	Replacement of Ala at position 302 with Cys in pC8 plasmid.	**NA**	p302-3

[1] SCAM, substituted cysteine accessibility mapping

A303C	Replacement of Ala at position 303 with Cys in pC8 plasmid.	**NA**	p303-10
P304C	Replacement of Pro at position 304 with cys in pC8 plasmid.	**NA**	p304-2
V305C	Replacement of Val at position 305 with Cys in pC8 plasmid.	**NA**	p305-1
T306C	Replacement of Thr at position 306 with Cys in pC8 plasmid.	**NA**	p306-5
L307C	Replacement of Leu at position 307 with Cys in pC8 plasmid.	**NA**	p307-1
T308C	Replacement of Thr at position 308 with Cys in pC8 plasmid.	**NA**	p308-8
F309C	Replacement of Phe at position 309 with Cys in pC8 plasmid.	**NA**	p309-1
A310C	Replacement of Ala at position 310 with Cys in pC8 plasmid.	**NA**	p310-4
A311C	Replacement of Ala at position 311 with Cys in pC8 plasmid.	**NA**	p311 Quiagen
D312C	Replacement of Asp at position 312 with Cys in pC8 plasmid.	**NA**	p312-2, -4
D314C	Replacement of Asp at position 314 with Cys in pC8 plasmid.	**NA**	p314-1, -2, -4
V316C	Replacement of Val at position 316 with Cys in pC8 plasmid.	**NA**	p316-7, -8
T317C	Replacement of Thr at position 317 with Cys in pC8 plasmid.	**NA**	p317-1
Q319C	Replacement of Gln at position 319 with Cys in pC8 plasmid.	**NA**	p319-3

K321C	Replacement of Lys at position 321 with Cys in pC8 plasmid.	**NA**	p321-4, -7
L322C	Replacement of Leu at position 322 with Cys in pC8 plasmid.	**NA**	p322-1
G323C	Replacement of Gly at position 323 with Cys in pC8 plasmid.	**NA**	p323-1M, p323-2M
S325C	Replacement of Ser at position 325 with Cys in pC8 plasmid.	**NA**	p325-1, -2
S327C	Replacement of Ser at position 327 with Cys in pC8 plasmid.	**NA**	p327-2
E329C	Replacement of Glu at position 329 with Cys in pC8 plasmid.	**NA**	p329-2
S331C	Replacement of Ser at position 331 with Cys in pC8 plasmid.	**NA**	p331-1, -2, -3
D332C	Replacement of Asp at position 332 with Cys in pC8 plasmid.	**NA**	p332-2
V333C	Replacement of Val at position 333 with Cys in pC8 plasmid.	**NA**	p333-1
D334C	Replacement of Asp at position 334 with Cys in pC8 plasmid.	**NA**	p334-1
L335C	Replacement of Leu at position 335 with Cys in pC8 plasmid.	**NA**	p335-4
Q336C	Replacement of Gln at postion 336 with Cys in pC8 plasmid.	**NA**	p336-2
E337C	Replacement of Glu at position 337 with Cys in pC8 plasmid.	**NA**	p337-1
Q338C	Replacement of Gln at position 338 with Cys in pC8 plasmid.	**NA**	p338-1

Q339C	Replacement of Gln at position 339 with Cys in pC8 plasmid.	**NA**	p339-1
S344C	Replacement of Ser at position 344 with Cys	**NA**	p344-3, -6

Figure 4. **Sheltered heterokaryon for the *tom40*^{RIP} mutant.** The box symbolizes the heterokaryotic RIP40het strain used in this study, containing two distinct nuclei indicated by circles. Nucleus 1 contains no functional copies of *tom40*; Nucleus 2 contains a wild type allele of the gene. Only markers necessary for the manipulation of the heterokaryon are indicated in each nucleus. The complete genotype is listed in Table 1. The mutant allele of the *cyh-2* gene provides resistance to cycloheximide. The heterokaryon was produced as described in section 2.2.

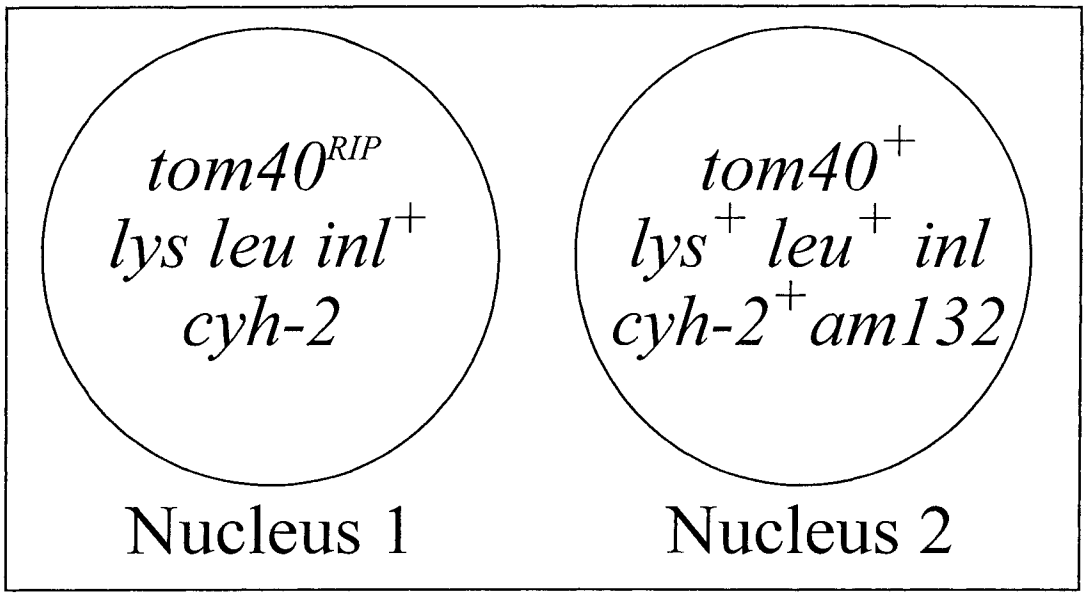

3. RESULTS

3.1 Generation and isolation of the *tom40* null mutant

Tom40 is the major component of the TOM complex. It is thought to form the pore through which preproteins traverse the outer membrane (Hill *et al.*, 1998; Ahting *et al.*, 2001), and it is known to be an essential gene in yeast (Baker *et al.*, 1990). Therefore, the procedure of sheltered RIP was used to obtain *N. crassa tom40* mutants. As described in section 2.2, the result of this technique is a heterokaryotic strain in which one nucleus contains *tom40* alleles inactivated by RIP, while the other nucleus retains a wild type copy of the gene (Fig. 4). Following the RIP cross that generated the sheltered heterokaryon, one strain (RIP40het) was chosen for further study.

Southern analysis (Fig. 5) indicated that, in addition to the gene at the endogenous *tom40* locus, the ectopically integrated RIP substrate was also present in the strain. Using specific primers (FNA176 and FNA177 for the endogenous locus, FNA94 and FNA175 from the ectopic copy), both RIPed versions of the gene were amplified by PCR. The gene at the endogenous locus was cloned and sequenced to completion (Fig. 6), and a total of 92 RIP mutations were identified, including one that created a stop codon at amino acid 35. DNA sequence from approximately 270 bp of the ectopic *tom40* allele was determined directly from PCR products. Nine RIP mutations were observed, including one that created a stop codon at residue 30 of the Tom40 protein. The wild type *tom40* sequence is shown in Fig. 6, and the position of the RIP mutations are also indicated. For both RIPed alleles, the stop codons occur before the first predicted membrane-spanning domain of Tom40 (Court *et al.*, 1995).

To determine if *tom40* is an essential gene in *N. crassa*, conidiaspores from the RIP40het strain were streaked onto medium containing all the nutritional requirements for both nuclei in the heterokaryon (see Table 1 and Fig. 7). Conidiaspores produced by *N. crassa* are usually multinucleate (2 to 5 nuclei per spore (Davis and De Serres, 1970)) and are produced by the random segregation of nuclei into spores. As a result, the heterokaryon should produce three types of conidiaspores: spores that are homokaryons for the lysine-leucine-requiring $tom40^{RIP}$ nucleus, spores that are homokaryons for the

inositol-leucine-requiring sheltering nucleus, and spores that contain both nuclei. A total of 181 single colony isolates were tested for nutritional requirements. No lysine-leucine strains were identified, indicating that the *tom40*^{RIP} nucleus was not viable as a homokaryon. In contrast, 120 heterokaryotic colonies and 61 leucine-inositol requiring colonies were recovered from this experiment. These data demonstrate that *tom40* is essential for viability of *N. crassa.* To confirm that the effects of RIP were specific to the *tom40* gene, the RIP40het strain was transformed with a plasmid containing a genomic copy of *tom40* on a bleomycin resistance vector. When transformants were selected on media containing lysine, leucine, cycloheximide, and bleomycin, viable lysine-leucine-requiring homokaryotic strains were recovered.

3.2 Characterization of the *tom40* null mutant

As shown in Fig. 4, the two nuclei in the RIP40het strain differ with regard to auxotrophic and antibiotic resistance markers. These differing markers make it possible to force the *tom40*^{RIP} bearing nucleus to predominate the heterokaryon by growing in medium containing lysine, leucine and cycloheximide (Fig. 8). When RIP40het was grown under these conditions, growth of the heterokaryon was severely reduced (Fig. 9A), as a result of the inability of the cycloheximide resistance-conferring *tom40*^{RIP} nucleus to supply Tom40 protein when it predominates the heterokaryon. Mitochondria isolated from RIP40het, following growth in media containing lysine, leucine and cycloheximide, show a decrease in Tom40 levels on Western blots (Fig. 9B). BNGE of the TOM complex from these Tom40 deficient mitochondria revealed no differences in complex size or stability compared to control strains (Fig. 9C). This indicates that the TOM complex forms normally in the Tom40 deficient strain but in reduced amounts.

The Tom40 deficient mitochondria were also analyzed for levels of other mitochondrial proteins, including additional members of the TOM complex (Fig. 9B). In Tom40 deficient mitochondria the levels of TOM complex receptors Tom70 and Tom20, as well as mitochondrial Hsp70 and porin are unaffected by reduction in Tom40 levels. In contrast, levels of Tom22, and Tom6 were reduced in the Tom40 deficient mitochondria. To determine if transcription of these genes was affected, Northern blots were analyzed for the presence of *tom22*, *tom40* and *tom6* transcripts (Fig. 10). mRNA

levels were severely reduced for *tom40* in the RIP40het strain grown in cycloheximide as has been previously observed for RIPed genes (Rountree and Selker, 1997; Grad *et al.*, 1999), while transcript levels of *tom22* were unaffected. Transcripts were not detected for Tom6 in mutant or control strains suggesting that this may be a rarely produced, or unstable transcript. However, there is no reason to expect that the control of expression of *tom6* differs from *tom22* and the data suggest that either the import or stability of Tom22 and, by analogy, Tom6 within mitochondria is dependent on assembly with Tom40. It should be noted that the reduction in these components was not due to a generalized decrease in import capacity that would be expected in Tom40 deficient mitochondria, as other mitochondrial proteins were present at wild type levels (Fig. 9B).

To determine the effects of reduced levels of Tom40 on import of preproteins into mitochondria, *in vitro* import assays were performed using the precursor forms of $F_1\beta$ and the matrix processing peptidase (MPP). Both precursors contain an N-terminal targeting signal and are imported into the matrix space. The precursor of AAC was also used in these experiments. It contains an internal targeting signal and is assembled into the inner membrane by the TIM22 complex. Import of all the mitochondrial preproteins tested was reduced in Tom40 deficient mitochondria compared to control mitochondria (Fig. 11).

To determine the structure and morphology of Tom40 deficient mitochondria, cells grown under conditions where the $tom40^{RIP}$ nucleus predominates the RIP40het strain were examined by electron microscopy (Fig. 12). Mitochondria with reduced levels of Tom40 were smaller than the control mitochondria and contained virtually no cristae.

3.3 Creation of *tom40* variant plasmids and mutant strains

Little is known about the regions of Tom40 required for its targeting to the mitochondrial outer membrane or for its assembly into the TOM complex. An alignment of Tom40 protein sequences from a variety of different species was performed to identify conserved domains in Tom40 that may be important for its function and assembly (Fig. 13). Domains that were fairly well conserved were targeted for site-directed mutagenesis. These Tom40 mutant alleles were created in different plasmids containing

either the cDNA or genomic versions of *tom40*. A list of specific mutations made in both the cDNA and genomic versions of Tom40 is given in Table 4.

The mutant *tom40* genomic alleles were used to transform the RIP40het strain. Plasmids that gave rise to lysine-leucine requiring, cycloheximide resistant homokaryotic colonies were assumed to restore Tom40 function to a level sufficient for viability (Fig. 14). The presence of mutant alleles was confirmed through PCR of genomic DNA isolated from the resulting strains, with primers that were designed to specifically amplify the newly introduced version of *tom40*, and sequencing of the resulting PCR product (Fig. 15). The detailed characterization of specific *tom40* variants is discussed next. Some of the variants have not yet been characterized in detail, and are mentioned at the end of the "RESULTS" (section 3.7). The mutant *tom40* cDNA constructs were used for Tom40 *in vitro* assembly assays to assess the effects of specific mutations on targeting and assembly of Tom40 into the mitochondrial outer membrane and the TOM complex.

3.4 A region near the N-terminus of Tom40 affects assembly and stability of the TOM complex

3.4.1 A conserved region identified in the N-terminus

A previous study had shown that Tom40 precursor proteins lacking amino acid residues 2-60 failed to be integrated into the TOM complex *in vitro* (Rapaport and Neupert, 1999). Alignments of Tom40 in this region from several different organisms revealed the existence of a conserved region of the protein near the N-terminus of Tom40 spanning amino acids 40-60 of the *N. crassa* protein, while no conservation of sequence between organisms prior to amino acid 38 of the *N. crassa* protein was observed (Fig 13). This is in agreement with the results from *in vitro* experiments showing that the first 40 amino acids of Tom40 are dispensable for Tom40 assembly (Rapaport and Neupert, 1999; Rapaport *et al.*, 2001). Conserved residues in the 40-60 region were targeted for site-directed mutagenesis as described above.

Amino acids 40-50 are well conserved between all species, while amino acids 50-60, are well conserved in fungal versions of the protein. To determine the role of these regions in Tom40 assembly and function, cDNA and genomic versions of the *tom40* gene

of the gene was constructed with various alterations (Fig. 16). These altered *tom40* alleles include those with a deletion of the NPGT residues at positions 40-43 (ΔNPGT), replacement of the conserved NPGT residues with alanine (AAAA), constructs lacking the RD at positions 53-54 (ΔRD) and RDTLL at positions 53-57 residues (ΔRDTLL). Larger deletions were also constructed encompassing amino acids 40-48 (with a single amino acid change of R49A) (Δ40-48), and deletion of amino acids 51-60 (with a single replacement of amino acid E50A) (Δ51-60) (Fig. 16).

3.4.2. TOM complex assembly

The ability of the mutant Tom40 proteins to assemble into the TOM complex was assessed using Tom40 *in vitro* assembly assays. cDNA versions of wild type and variant Tom40 precursors were transcribed and translated *in vitro* in the presence of [^{35}S]methionine. Tom40 import assays were then performed with the labeled proteins, and the degree of assembly was assayed by BNGE (Fig. 17). Wild type Tom40 predominantly accumulates in a 250 kDa intermediate when import assays are carried out at 0°C. Further assembly is seen when import is performed at 25°C, as the protein assembles into both a 100 kDa intermediate, and authentic TOM complexes of approximately 400 kDa (Fig. 17A and B). As noted previously, residues 1-40 are not required for assembly (Rapaport and Neupert, 1999), and a variant lacking residues 2-20 (Δ2-20) assembles like the wild type version of the protein. All of the N-terminal variant proteins analyzed with alterations between amino acids 40-60, show a decrease in their ability to assemble into the authentic 400 kDa TOM complex at 25°C, and significant proportions of the precursors remain in the 250 kDa intermediate (Fig. 17A and B). However, for the ΔNPGT, AAAA, Δ40-48, ΔRD and ΔRDTLL mutants, some assembly into the 400 kDa complex is observed suggesting that these mutations have a relatively mild effect on Tom40 assembly. In contrast, assembly of the Δ51-60 variant into the TOM complex is more severely affected (Fig. 17B) as this variant fails to assemble past the 250 kDa intermediate even after 60 min of import at 25°C (discussed in section 3.6, Fig. 26A). There is also an effect on formation of the 100 kDa intermediate which was

not present as a discrete band at either temperature when the Δ51-60 variant protein was imported.

3.4.3 Rescue of RIP40het with N-terminal mutant alleles

Genomic Tom40 plasmids were constructed with the specific mutations shown in Fig. 16, and these constructs were used to assess the ability of these mutant *tom40* alleles to rescue the *tom40*^{RIP} nucleus in RIP40het (Fig. 14). It was found that a *tom40* allele encoding a protein lacking amino acid residues 2 to 60 was not able to restore viability to the nucleus harboring the RIPed version of *tom40* which supports *in vitro* findings (Rapaport and Neupert, 1999) that the first 60 residues of the N-terminal domain of Tom40 contain crucial assembly information. The remaining mutant alleles of the N-terminus, including both the Δ40-48 and the Δ51-60 alleles, were able to rescue the *tom40*^{RIP} nucleus in RIP40het and gave rise to homokaryons requiring lysine and leucine. This suggests that although the Δ51-60 Tom40 protein is unable to progress past the 250 kDa intermediate in *in vitro* assembly assays (Fig. 17B), it must be at least partially capable of assembling into TOM complexes *in vivo*.

3.4.4 Growth phenotypes of strains containing mutations in the N-terminus of Tom40

Mutant strains expressing the different mutant alleles showed highly variable growth phenotypes (see below), but all showed a reduced ability to climb the walls of growth flasks and to produce asexual conidia spores. Examples of this growth phenotype are shown in Fig. 18 for mutants of the 40-48 region. Mutants in the 51-60 region have a similar phenotype (data not shown). It is interesting to note that the strains that showed the most aberrant assembly phenotypes in the *in vitro* assembly assays (such as Δ40-48 and Δ51-60), grew and conidiated more poorly than strains that showed only slight assembly defects (such as ΔNPGT and ΔRD) (Fig. 18). Thus, the severity of assembly defects seen *in vitro* correlates well with the *in vivo* phenotypes observed in the mutant strains.

Strains containing the ΔRD and ΔRDTLL forms of Tom40 exhibited only a slightly reduced growth rate compared to control strains but strains containing either the Δ40-48 or Δ51-60 mutations grew much slower than controls. The Δ40-48 strain showed

a much slower growth rate that was easily distinguished from the other mutants based on rate of mycelial elongation in race tubes at room temperature (Fig. 19A). The Δ51-60 strain also showed mild growth defects in race tubes at room temperature (data not shown), but these growth defects were enhanced when the strain was grown in liquid culture at 15°C, where it grew at roughly half the rate of wild type cultures (Fig. 19B).

The ΔNPGT and AAAA mutants displayed a complex growth phenotype. A total of 18 different lysine-, leucine-requiring transformants of the AAAA type and 13 of the ΔNPGT type were analyzed for growth characteristics in race tubes. Nine of the AAAA strains and five of the ΔNPGT strains displayed a "stop-start" growth phenotype. These strains grew at near normal rates for a few days and then grew very slowly or not at all for 1 or 2 days before they resumed their initial growth rate (see ΔNPGT strain in Fig. 19A for an example of this growth phenotype). The strains exhibiting this behavior are remarkably consistent, because the stop phase of growth was observed to begin on the same day in up to six different race tubes of an individual strain. The rest of the strains analyzed from both groups grew slightly slower than control strains for 12 days without evidence of stopping (see AAAA strain in Fig. 19A for an example of this growth phenotype). Tom40 levels in all strains were similar, regardless of their growth phenotype (data not shown), though it is conceivable that subtle differences in expression, not identified in the analysis of Western blots, may explain the different growth characteristics. This could be due to locus-specific effects at different integration points of the transformed mutant alleles in the individual strains. Regardless, no differences between the strains have been found except for this behavior. For further analysis one stopper type of the ΔNPGT strains and one non-stopper growth type of the AAAA strains were chosen.

3.4.5 Function of the TOM complex in N-terminal mutant strains

The role of residues 40-60 of Tom40 in function of the TOM complex was further analyzed. Mitochondria isolated from the ΔNPGT, AAAA and Δ51-60 strains were assessed for function of the TOM complex by assaying their ability to import mitochondrial preproteins *in vitro*. The Δ40-48, ΔNPGT and AAAA strains showed a

decrease in the ability to import mitochondrial preproteins, with the greatest deficiency seen in the Δ40-48 strain (Fig. 20). The Δ51-60 strain showed a very mild import defect, suggesting that function of the TOM complex is only slightly affected in this strain, even though assembly of the complex may be more significantly impaired (section 3.4.2). Taken together, the data suggest that although the phenotypes overlap to some extent, the 40-50 region may be more important for TOM complex function, while the 50-60 region appears to have a greater role in TOM complex assembly.

3.4.6 Affects of Tom40 N-terminal mutations on levels of mitochondrial proteins

The level of TOM complex components and other mitochondrial proteins from the ΔNPGT, AAAA, and Δ40-48 strains were analyzed and found to be similar to the levels in controls (Fig. 21). This suggests that despite the import deficiencies observed in these strains, they still accumulate mitochondrial proteins at ratios similar to controls. This is a typical observation for mutants (Alconada *et al.*, 1995; Nargang *et al.*, 1995; Grad *et al.*, 1999). It seems likely the growth defects seen in these strains represent the increased time needed to accumulate proteins at levels sufficient for mitochondrial function and cellular growth.

3.4.7 Mutations in residues 40-60 of Tom40 result in a more fragile TOM complex

The role of the residues spanning amino acids 40-60 was analyzed further by assessing the stability and structure of the TOM complex in each of the mutant strains. Mitochondria containing the ΔNPGT, AAAA, Δ40-48, ΔRD, ΔRDTLL, and Δ51-60 Tom40 variants were dissolved in 1% digitonin, subjected to BNGE, blotted to PVDF membrane and were decorated with antibody to Tom40. The ΔNPGT, AAAA, Δ40-48, and Δ51-60 classes of mutants were found to contain a TOM complex with slightly increased electrophoretic mobility when mitochondria were solubilized in 1% digitonin (Fig. 22A and B). Mitochondria from all of the mutants strains analyzed appeared to contain a TOM complex that was more fragile than control strains when solubilized with 1% dodecylmaltoside. The TOM complexes in these mutants break down into a series of

smaller complexes with at least some fraction of the Tom40 molecules migrating as monomers. A striking deficiency of Tom40 also appears in the lanes containing mitochondria from the Δ51-60 strain, especially when mitochondria are solubilized with dodecylmaltoside despite the fact that equal amounts of mitochondrial protein were loaded in each lane. When mitochondria from this strain were solubilized in SDS no difference in the amount of Tom40 was observed relative to controls (Fig. 22C). Therefore, the deficiency of Tom40 observed following BNGE may have been due to aggregation of Tom40 molecules from this strain, resulting in an inability of Tom40 to enter the gel. These results demonstrate that residues 40-60 play an important role in the stability of the TOM complex. Blots of blue native gels for the ΔNPGT, AAAA and Δ40-48 strains were also examined using antibodies directed against two other TOM core complex components, Tom6 and Tom22. In both cases, the samples solubilized in digitonin showed the same electrophoretic mobility alteration seen in the blots examined with Tom40 antibodies (data not shown). For samples dissolved in 1% dodecylmaltoside, the patterns were similar to those seen with Tom40 antibodies, except that only trace amounts of Tom6 monomers were released from the mutant complexes.

3.5 Effects of mutations in the C-terminal region of Tom40

To examine effects of mutations in Tom40 outside the N-terminus of the protein mutations were made in the last block of conserved residues in the C-terminus of the protein (Fig. 13, Fig. 23A). These residues are predicted to lie within the last membrane-spanning domain of Tom40 in two computer predictions of Tom40 structure (T. Schirmer via D. Rapaport, personal communication) (Mannella *et al.*, 1996) but are not in a third model (Court *et al.*, 1995). Variant cDNA and genomic versions of *tom40* were constructed in which the conserved KLG residues (amino acids 321-323) were either deleted (Δ321-3) or changed to alanine residues (321AAA) (see section 3.3, Table 4). In addition to these mutations, a deletion of the fungal specific C-terminal extension (ΔC-term), spanning amino acids 329-349 of *N. crassa* Tom40 was also created (Fig. 23A).

The Tom40 cDNA constructs were used in *in vitro* assembly assays as described in section 3.4.2. Import of the 321AAA construct was similar to wild type Tom40, with some accumulation of precursor protein at the 250 kDa intermediate when imported at

25°C suggesting a mild assembly defect (Fig. 23B). The Δ321-3 variant showed a more dramatic assembly phenotype, as the mutant precursor did not assemble past the monomer stage of Tom40 assembly at 0°C, and did not progress past the 250 kDa intermediate at 25°C (Fig. 23B). As observed with the Δ51-60 mutation, failure to progress past the 250 kDa intermediate in Δ321-3 prevented formation of the 100 kDa intermediate, suggesting that this intermediate forms after the appearance of the 250 kDa complex. Thus, the deletion of the KLG residues dramatically affects the ability of Tom40 precursors to assemble into the TOM complex whereas changing the residues to alanines has little effect. Assembly of the ΔC-terminal (Tom40ΔC) construct was also assessed and to moderately affect assembly of Tom40 (Fig. 24A).

Genomic Tom40 plasmids were constructed with the specific mutations shown in Fig. 23A. These constructs were used to assess the ability of the mutant *tom40* alleles to rescue the $tom40^{RIP}$ nucleus in the RIP40het strain (see section 3.3). It was found that the Δ321-3 *tom40* allele was unable to rescue the $tom40^{RIP}$ nucleus, which is in keeping with the severe assembly defects observed *in vitro*. The 321AAA and ΔC-term alleles were able to rescue the $tom40^{RIP}$ nucleus in RIP40het and gave rise to homokaryons requiring lysine and leucine.

The 321AAA strains grew slightly slower than controls at room temperature (Fig. 23C). However, at 15°C the growth of the 321AAA strain was reduced to about half that of the control (Fig. 23C). The role of residues 321-323 in the function of the TOM complex was further demonstrated by the fact that mitochondria containing the 321AAA variant imported mitochondrial precursors less efficiently than control mitochondria (Fig. 23D). BNGE analysis of mitochondria isolated from 321AAA strains revealed striking defects in TOM complex stability (Fig. 23E). When mitochondria from 321AAA were solubilized in the mild detergent digitonin, a substantial fraction of Tom40 was not present in the 400 kDa fully assembled form and migrated at a position that would correspond roughly to a Tom40 dimer. From these data, it is impossible to determine if the smaller form of the complex forms during solubilization in digitonin and BNGE or if it is present *in vivo*. Solubilization of mitochondria containing the 321AAA Tom40 variant in dodecylmaltoside results in all of Tom40 in the TOM complex being released as a monomer.

Strains expressing the ΔC-term Tom40 (Fig. 23A) variant failed to climb the walls of growth flasks, produced few asexual conidiaspores, and grew at rates somewhat slower than wild type (Fig. 24B and C). The presence of the ΔC-term allele was confirmed through Western blots of mitochondria isolated from control strains (Dupl 40) and three ΔC-term strains (FC2-1, FC8-1, and FC17-1). Three antibodies directed against the complete Tom40 protein, the N-terminus of the protein and the C-terminus of the protein were used (Fig. 24D). As expected only the N-terminal and complete protein antibodies recognized the Tom40 protein in the ΔC-term strains. These blots also show that the ΔC-terminal protein was smaller than wild type and that no wild type protein existed within these strains. Strains expressing the ΔC-term Tom40 allele showed no defects in import of mitochondrial preproteins (Fig. 24E). Deletion of the C-terminal extension found in fungal Tom40 proteins has a moderate affect on assembly since the precursor appears to accumulate at the 250 kDa stage (Fig. 24A). Mitochondria containing Tom40 with the C-terminal deletion are still able to efficiently import precursors so the TOM complex is still functional (Fig. 24E). TOM complex isolated from strains expressing this variant was virtually indistinguishable from controls in terms of TOM complex stability on blue native gels (Fig. 23E, middle section). Thus, the instability of the complex observed in the 321AAA strain is not caused by general perturbations of the protein at the C-terminus.

3.6 Assembly of Tom40 into the TOM complex

The Tom40 assembly pathway was previously characterized in *S. cerevisiae* (Model *et al.*, 2001) and *N. crassa* (Rapaport and Neupert, 1999) but some aspects remain controversial. It is thought that Tom40 initially binds to the mitochondrial outer membrane as a monomer, and is then incorporated into a 250 kDa intermediate of unknown composition (Fig. 3). Based on sodium carbonate extraction experiments and resistance of the Tom40 precursor in the 250 kDa intermediate to externally added proteases, it was suggested that in this stage, the precursor lies within the mitochondrial intermembrane space, and is only peripherally associated with the outer mitochondrial membrane (Model *et al.*, 2001). In the next step of assembly, Tom40 dissociates from the 250 kDa complex and forms a 100 kDa complex that is probably a dimer of Tom40

associated with a molecule of Tom5. During formation of the 100 kDa intermediate, Tom40 is thought to insert into the membrane. Following formation of the 100 kDa intermediate, the protein is thought to interact with other components of the TOM complex and is assembled into the final 400 kDa complex (Model *et al.*, 2001). In another model of Tom40 biogenesis, the precursor was thought to progress directly from the 250 kDa intermediate to the 400 kDa complex (Rapaport and Neupert, 1999). The 100 kDa intermediate in this model was thought to be a non-productive step in the pathway of Tom40 biogenesis. I have attempted to address various aspects of these models in *N. crassa*. In addition to this, I attempted to address the relevance of a high molecular weight band (approximately 500 kDa) that was consistently observed on blue native gels of Tom40 import experiments. This band has not been discussed in previous reports.

As seen on previous import figures, a 500 kDa band is consistently observed on BNGs of Tom40 import experiments. The band did not appear in substantial amounts when import was stalled at the 250 kDa stage (Figs. 17B, 22B). To assess the relevance of the 500 kDa band, Tom40 precursor was imported into mitochondria for a 4 min pulse at 25° C. Mitochondria were immediately reisolated and the kinetics of precursor assembly were followed over a period of 240 min at 25° C. As seen in Fig. 25A, the amount of the 500 kDa form did not change appreciably over the course of the experiment. Thus, the 500 kDa band most likely represents Tom40 precursor in a non-productive state.

The above experiment also showed the precursor to product relationship of the 100 kDa and 250 kDa intermediates to the fully assembled 400 kDa form since the amount of radioactive Tom40 precursor in the intermediates gradually decreases as more radioactivity accumulates in the 400 kDa form (Fig. 25A and B). Inspection of the bands and quantification of the levels of radioactivity in the intermediates did not show that the appearance of Tom40 precursor in the 250 kDa form precedes its appearance in the 100 kDa intermediate as previously reported (Model *et al.*, 2001). In these experiments the Tom40 precursor appeared in both intermediates simultaneously. The rate of disappearance of the precursor from each intermediate, as Tom40 assembled to the 400 kDa form, was also virtually identical. Attempts to delay the appearance of the

intermediates by lowering the temperature of import to 10° or 15° C and shortening the pulse time to 1 min, reduced the rate of assembly but revealed no differences in precursor product relationships (data not shown). However, results obtained during studies of import and assembly of mutant Tom40 precursors did support the hypothesis that the 250 kDa intermediate is formed prior to the 100 kDa form (see below and section 3.4.2).

It has been suggested that the Tom40 precursor in the 250 kDa intermediate is only peripherally associated with the mitochondrial outer membrane, and it is only after formation of the 100 kDa intermediate that the precursor is assembled into the outer membrane (Model *et al.*, 2001). In an attempt to confirm the carbonate extractability following import of wild type precursor protein into wild type mitochondria at 0°C and 25°C it was observed that the amount of Tom40 in the 250 kDa intermediate was reduced following extraction (compare Tom40wt experiments on Fig. 26A and B; 250 kDa band). Despite this finding, interpretation of the data is not straightforward as it appears that carbonate stimulates assembly of Tom40 into the 400 kDa complex in *N. crassa* (compare Tom40wt experiments on Fig. 26A and B; 400 kDa band). The trivial explanation that further assembly to the 400 kDa form occurs as a result of the extra time at 0°C during incubation with carbonate cannot account for the data, since the untreated samples were handled in an identical fashion except for addition of carbonate. To determine if these newly assembled complexes contained correctly inserted Tom40, control and carbonate extracted samples were treated with proteinase K. This treatment should give rise to characteristic 26 and 12 kDa cleavage products if the protein is correctly folded and assembled into the TOM complex (Künkele *et al.*, 1998b). The characteristic bands can be seen in the non-carbonated extracted samples, while the carbonate treated samples show some evidence of these bands (Fig. 25C). In the carbonate treated samples, both cleavage products are reduced in amount, and the 26 kDa fragment is present in a series of smaller bands. The presence of extra bands is likely a result of carbonate treatment exposing greater portions of Tom40 to the protease in membrane sheets produced by carbonate extraction. Thus it appears that the protein present in the 400 kDa complex that arose by the action of carbonate represents correctly assembled Tom40.

3.6.1 Accumulated assembly intermediates of Tom40 variants are extractable by carbonate

As was previously shown in Fig. 17B, the Δ51-60 Tom40 variant fails to assemble to the 400 kDa complex during a standard 20 min *in vitro* import experiment. It was of interest to determine if this Tom40 variant could also be assembled into the 400 kDa complex during carbonate treatment. Wild type Tom40 and the Δ51-60 variant were imported into wild type mitochondria for 15, 30 or 60 min. The Δ51-60 form of the protein accumulates at the 250 kDa intermediate even after 60 min of import at 25°C (Fig. 26A). In contrast to wild type Tom40, following carbonate treatment, most of the Δ51-60 protein in the 250 kDa intermediate is removed though a fraction does remain associated in the 250 kDa complex (Fig. 26B). Interestingly, some of the Δ51-60 Tom40 does assemble past the 250 kDa intermediate, as can be seen by a discrete 100 kDa band which appears somewhat smaller than the wild type version.

It was previously shown that the Δ321-3 Tom40 variant also fails to assemble past the 250 kDa intermediate (Fig. 23B). To further confirm that Tom40 in the 250 kDa intermediate is extractable, similar experiments were performed with this Tom40 variant (Fig. 27). In contrast to the Δ51-60 variant, the Δ321-3 Tom40 variant is completely extractable by sodium carbonate and is not converted to an assembled form of Tom40 (Fig. 27B). Even long exposures (5 days) performed with a phosphorimager screen did not reveal any trace of the 250 kDa intermediate, 100 kDa intermediate, or fully assembled 400 kDa complex following carbonate treatment (data not shown).

It is interesting to note that although both variant forms of Tom40 seem to arrest at the 250 kDa intermediate, only Δ321-3 is fully carbonate extractable. This may suggest that the Δ321-3 and Δ51-60 variants arrest at two different stages of Tom40 assembly, and that the 250 kDa intermediate is composed of two distinct populations, a partially membrane inserted version which makes up part of the population in the 250 kDa intermediate of the Δ51-60 variant, and a peripherally associated intermediate that comprise the entire population of the Δ321-3 variant. Structural prediction programs suggest that the region encompassing amino acids 321 through 323 lies within the last membrane-spanning domain of Tom40 [Mannella, 1996 #1527; T Schirmer, via D.

Rapaport, personal communication, also see section 3.9]. The lack of assembly of the Δ321-3 variant could be explained by the fact that it may not be capable of inserting into the mitochondrial outer membrane and thus remains accessible to carbonate extraction. Thus, a possible model could be that the C-terminal membrane-spanning domain may enter into the membrane first, and the shortened membrane-spanning domain in the Δ321-3 variant may prevent insertion. On the other hand, it is thought that Tom6 is required for conversion of the precursor protein in the 250 kDa intermediate to the 100 kDa intermediate (Model *et al.*, 2001). Another conceivable model is that the Δ321-3 variant may not be able to associate with this protein.

Both the Δ321-3 and Δ51-60 mutant variants of Tom40 accumulate at the 250 kDa intermediate stage of the assembly pathway. Although a smear in the region from Tom40 monomer up to the 100 kDa form is often seen during the assembly of these mutants (Figs. 17B, 20D, 26, and 27), no clear band corresponding to the 100 kDa form seen following the import of the wild type precursor is observed. These observations support the notion that formation of the 250 kDa form precedes the formation of the 100 kDa intermediate.

3.6.2 An alternative pathway for Tom40 assembly in mitochondria containing mutant TOM complexes

To examine the process of Tom40 precursor assembly into TOM complexes containing mutant Tom40 molecules, I performed import of wild type Tom40 protein into the mutant mitochondria isolated from the Δ40-48 strain (see section 3.4). Surprisingly, Tom40 precursor proteins did not follow the normal import pathway, but assembled to a high molecular weight intermediate of approximately 450 kDa when import was performed at 0°C (Fig. 28A). A small amount of 250 kDa intermediate was detected, but no 100 kDa intermediate was seen. The larger intermediate was also seen in samples where the precursor was imported at 25°C. These results suggested that the normal 250 kDa and 100 kDa complexes were not formed in the mutant strains. It should also be noted that the 450 kDa form does not co-migrate with the 500 kDa non-productive form seen during import into mitochondria containing wild type Tom40 (see section 3.6.1) described earlier (Fig. 28A)

To determine if the 450 kDa intermediate could be chased into fully assembled TOM complexes, a time course experiment was designed. Mitochondria and Tom40 precursor protein were initially incubated for 20 min at 0°C to allow accumulation of the 450 kDa complex. Mitochondria were then reisolated and suspended in import mix. Samples were shifted to 25°C, and aliquots were taken over a time course from 0 to 120 min. It appeared that conversion of the 450 kDa intermediate to the 400 kDa complex did occur although the amount accumulated in the 400 kDa form is higher than the amount initially present at 450 kDa (Fig. 28B, left panel). Carbonate extraction of the import samples, performed at 0 min and 10 min, revealed that the Tom40 precursor in the 450 kDa complex is carbonate extractable, while Tom40 in the final 400 kDa complex (as seen previously) was resistant to carbonate. PK digestion of import samples showed that the 450 kDa form of Tom40 was not correctly assembled, and that the presence of the characteristic 26 kDa and 12 kDa bands corresponded to the appearance of the 400 kDa complex (Fig. 28B, right panel). The experiments were repeated with strains that contained different N-terminal mutations in Tom40 (Fig. 28C, D, and E). Consistent with the results for the Δ40-48 strain, the ΔNPGT (Fig. 28B), NPGT-AAAA (Fig. 28B) and the Δ51-60 (Fig. 28D) strains all showed a similar Tom40 assembly pathway.

To determine if this was a general phenomenon for all Tom40 variant TOM complexes, another mutant strain of *N. crassa* was analyzed. The mutant strain chosen contained Tom40 in which two conserved lysine residues were changed to glutamine at positions 237 and 238 (WQQ) (Fig. 13). Import into mitochondria isolated from this strain showed a normal import pathway with the 250 kDa and 100 kDa intermediates (Fig. 29). These results suggest a role for the N-terminus of Tom40 in proteins that are being imported (see Fig. 17A and B), as well as for Tom40 molecules in preexisting TOM complexes, for correct assembly of Tom40 precursor proteins.

3.7 Additional mutations made in Tom40

To assess the role of additional residues in the assembly and function of Tom40, mutations were created that changed many of the residues at conserved positions throughout the protein (Table 5; Fig. 30). These were made in both cDNA and genomic versions of *tom40* as described previously (section 3.3).

3.7.1 *in vitro* assembly of Tom40 variants

cDNAs encoding variant Tom40s were translated in the presence of [^{35}S]methionine and the products were imported into mitochondria (see section 2.18 and 3.3). Following import, mitochondria were solubilized in digitonin and run on BNGs. Five different assembly phenotypes were seen in the assembly pathway of the variant Tom40 molecules (Table 6). One representative strain for each type is shown in Fig. 31 panels B through F. Two variants failed to assemble, and remained peripherally bound to the mitochondrial outer membrane in the monomer binding stage (Fig. 31B). Others variant forms arrested at the 250 kDa intermediate, and formed no 400 kDa complex even after extended incubation at 25°C (Fig. 31C). A third class of variant proteins showed an accumulation of the 250 kDa intermediate (Fig. 31D) and showed variation in the amount of 400 kDa complex formed. A fourth class showed an accumulation of the 100 kDa intermediate with less 400 kDa complex and 250 kDa intermediate present (Fig. 31E). Finally some of the Tom40 variants showed a wild type assembly pattern (compare Fig. 31A and Fig. 31F).

3.7.2 Creation and characterization of other Tom40 variant strains

As stated above, a number of mutations in Tom40 at conserved positions in genomic versions of the gene were created (see Table 5). Most of the Tom40 mutations were capable of rescuing the *tom40*^{RIP} nucleus. Three of these mutations have been characterized in detail and are described below. Characterization of the remainder of these strains is currently being performed by another graduate student in the laboratory.

The Tom40 variants that were characterized in detail contained a change of conserved lysines to glutamines at position 237-238 (WQQ), a change of a conserved proline to alanine at position 183 (P-A), and a change of a conserved tyrosine and phenylalanine at positions 94 and 96 to alanine (YAF-AAA). See Figs. 15 and 30 for the positions of these mutations. It is interesting to note that the corresponding deletion of the three amino acids spanning 94-96 failed to rescue the *tom40*^{RIP} nucleus and that this region is predicted to lie within a membrane spanning domain of Tom40, similar to the 321-323 region of Tom40 discussed above (see section 3.5; Table 5). The growth rates

of the mutant strains were assessed by growth on race tubes compared to a control strain (Dupl40) at room temperature. Both the WQQ and YAF-AAA strains grew at rates only slightly slower than the control strain (Fig. 32A and B), while the P-A strain showed a more significant growth defect. Isolated mitochondria from the mutant strains were subjected to BNGE and immunoblotted for Tom40 (Fig. 32C). As with the mutations in the Δ51-60 residues in the N-terminus of Tom40 (see section 3.4), the level of TOM complex in the P-A and YAF-AAA strains seems to be considerably less than the control strain. All of the mutant strains had a more fragile TOM complex than the wild type strains as judged by migration of the complex following solubilization in dodecylmaltoside. To ensure that protein levels were similar in all the strains characterized, isolated mitochondria from the mutant and control (Dupl40) strains were subjected to SDS-PAGE and immunodecorated for proteins of the TOM complex, as well as mtHsp70, and CCHL. As with the strains expressing Tom40 mutations in the N-terminus of the protein, levels of mitochondrial proteins, including Tom40, in the mutant and control strains were similar (Fig. 32D). Thus, the reduced levels of TOM complex seen in the BNGs of the P-A and YAF-AAA strains are likely due to aggregates of Tom40 not entering the BNG. Finally, the ability of these mutant strains to import mitochondrial preproteins was assessed. It appears that none of these mutations has a dramatic effect on import of the mitochondrial precursors tested (Fig. 33). Thus, the phenotype of the YAF-AAA mutation is similar to the Δ51-60 form. The mutant proteins have assembly defects, but once assembled import is unaffected.

3.8 The protein content of the mitochondrial outer membrane

It has been suggested that the Tom37(Mas37) protein of yeast is an assembly factor for the TOM complex (Wiedemann, 2003). Since Tom37(Mas37) has not been identified in *N. crassa*, I wished to examine the proteins of *N. crassa* OMVs in an attempt to identify this protein. We were informed by the N. Pfanner laboratory that a potential *N. crassa* homolog was found in the *Neurospora* genome database (website - www.mips.biochem.mpg.de/proj/neurospora/). This protein was somewhat larger than the yeast protein, having a predicted molecular weight of 48.6 kDa.

Purified OMVs and IMFs were prepared and subjected to SDS-PAGE. One portion of the gel was silver stained (Fig. 34A), while the other portion of the gel was transferred to nitrocellulose membrane and immunodecorated to detect proteins of the outer membrane, inner membrane and matrix space (Fig. 34B). The OMVs were shown to be enriched over the IMFs in the outer membrane components, Tom70, Tom40, Tom22, and Tom5, while the IMFs were enriched in AAC, a component of the inner membrane (Fig. 34B). Neither fraction contained detectable amounts of a mitochondrial matrix protein Hsp70. Based on the Western blots, the positions of Tom40 and Tom70 could be located on the silver stained gel (Fig. 34A). Mitochondrial porin is one of the ten most abundant proteins in mitochondria, and is the most abundant protein in the outer membrane (Krimmer *et al.*, 2001). Thus, based on the known molecular weight of the protein (30 kDa) and the intensity of staining, it could also be localized on the gel. A total of 17 protein bands were excised from the region between Tom40 and Tom70, and these were subjected to mass spectroscopy (procedure done by the Institute for Biomolecular Design, Department of Biochemistry, University of Alberta). A number of proteins were identified (Table 7) including six proteins that have not been characterized in *N. crassa*. Two of these proteins are related to bacterial proteins, while three proteins are well conserved between yeast and *N. crassa*, though their function is unknown. The final new *Neurospora* protein identified was the homolog of the yeast Ugo1 protein (Sesaki and Jensen, 2001). This protein is thought to play a role in mitochondrial fusion in yeast, and likely plays a similar role in *N. crassa.* Unfortunately, the 48.6 kDa homolog to *S. cerevisiae* Tom37(Mas37) was not identified.

3.9 Cysteine-Scanning Mutagenesis

As described in section 1.2.4.8, Tom40 exists as an oligomer, with dimers as its basic structure (Dekker *et al.*, 1998; Hill *et al.*, 1998; Rapaport *et al.*, 1998c; Ahting *et al.*, 1999; Model *et al.*, 2001). It is known that Tom40 is an integral membrane protein, but little is known about its structure. Computer predictions of Tom40 structure suggest that the protein exists as a β-barrel, with 14 anti-parallel β-strands spanning the outer membrane (Court *et al.*, 1995; Mannella *et al.*, 1996) (T, Schirmer, via D. Rapaport, personal communication) (Fig. 35). These predictions vary somewhat with respect to

both the positions and lengths of the predicted β-strands. Also, as discussed in section 1.2.4.8, two studies have attempted to experimentally determine the relative amounts of β-sheet versus α-helical content in Tom40 and have found significantly different percentages of each structure (Hill *et al.*, 1998; Ahting *et al.*, 2001). Due to the conflicting nature of the experimental data pertaining to Tom40 structure, I have started the process of cysteine-scanning mutagenesis (cys-scanning) also called substituted cysteine accessibility mapping (SCAM), in an attempt to determine the topology of Tom40 (reviewed in (van Geest, 2000)).

To begin the process of cys-scanning, a genomic plasmid construct of *tom40* (plasmid pB3) was mutagenized (Table 3) to replace the single endogenous cysteine residue in Tom40 with alanine. The resulting construct (pC-8) was then used to create a number of plasmids with *tom40* encoding single cysteine residues at specific locations of the protein by site-directed mutagenesis (Table 4). The residues chosen for cys-scanning are shown in Fig. 36. Plasmids containing individual cysteine mutations were transformed into RIP40het and were shown to rescue the lysine-leucine requiring $tom40^{RIP}$ nucleus (called SCAM strains, see Table 1). To insure that strains chosen following transformation were not contaminants, the introduced *tom40* gene was amplified by PCR and sequenced to verify the presence of the cysteine substitution. To verify that the single cysteine substitutions did not grossly affect the structure or stability of the TOM complex, isolated mitochondria from the strain expressing only the cysteineless version of Tom40 and a series of SCAM strains were lysed in buffer containing the detergent digitonin and subject to BNGE. The proteins were then transferred to PVDF membrane and blotted for Tom40 (Fig. 37). The cysteineless strain serves as a control because the TOM complex in this strain is indistinguishable from the wild type complex (data not shown). The structure of the TOM complex in the SCAM strains was indistinguishable from the control strain, indicating that, in general, TOM complex structure is not greatly affected by single cysteine substitutions.

The SCAM procedure is detailed in Fig. 38. In brief, mitochondria were isolated from the SCAM strains and incubated with a cysteine-specific modifying reagent. The cysteine modifying reagent employed in this study was N^{α}-(3-maleimydylpropionyl) biocytin (biotin maleimide) (Fig. 39A) which labels cysteines (Fig. 39B) that are exposed

to the aqueous environment but not those that are membrane embedded (Tang *et al.*, 1998; Fujinaga *et al.*, 1999). Following labeling of isolated mitochondria with biotin maleimide, mitochondria were lysed and Tom40 was immunoprecipitated with antiserum raised in rabbits. The immunoprecipitated protein was subjected to SDS-PAGE and blotted to nitrocellulose membrane. The presence of the biotin maleimide modification was detected using a streptavidin-conjugated horseradish peroxidase protein and ECL (Fig. 40A). The efficiency of the immunoprecipitation was tested by washing the membranes following detection of cysteine labeling and decorating with a mouse-derived antiserum to the same C-terminal peptide used to generate the immunoprecipitation antibody (see section 2.16). As shown in Fig. 40B, the effectiveness of the immunoprecipitation for each lane was similar.

The membrane-spanning domains of Tom40 are predicted to be in the form of β-strands forming a β-barrel structure. Thus, the R-groups of the β-strands should be arranged in opposite directions (Voet, 1990) so that within a given membrane-spanning β-strand there should be an alternating arrangement of hydrophobic residues embedded in the bilayer followed by hydrophilic residues exposed in the aqueous pore (Fig 41). As only those amino acids that are in the aqueous environment should label, SCAM should reveal an alternating pattern of labeled and unlabeled residues in the cysteine-substituted Tom40 molecules. This prediction is based on the assumption that biotin maleimide (523.6 Da) is small enough to fit inside the pore of the TOM complex. This seems likely as the pores in the complex have been sized at 20-26 nm based on both EM tomography and size exclusion studies (Künkele *et al*, 1998a,b; Ahting *et al.*, 1999). The predicted alternating pattern of labeling was seen between amino acid residues 319-327, suggesting that this region forms a β-strand that spans the outer membrane (Fig. 40A). It is also highly likely that the region spanning amino acids 306-316 also forms a membrane-spanning β-strand, although amino acids 308 and 310 do not show the alternating pattern of labeling expected for a β-sheet spanning a membrane (see section 4.7). The intervening loop domains seem to encompass amino acids 300 (or earlier) to 306, and residues 316 to 319. Residues 329 to 349 are all predicted to exist in the intermembrane space. A representation of the topology of residues 300-349 of *N. crassa* Tom40 based on the SCAM data is shown in Fig. 42.

Table 5: A list of genomic Tom40 variants created and status of rescue. ✔ indicates rescue of *tom40*^{RIP} nucleus of the RIP40het strain, X indicates constructs unable to give rise to viable strains. Refer to Fig. 13 and 30 for the location of the mutations in the predicted Tom40 structure.

Mutation	Amino Acid Residues Affected	Region[1]	Rescues
ΔC-ter	Deletion of aa[2] 330-349	Intermembrane Space	✔
ΔN-ter	Deletion of aa 2-61	Intermembrane Space	X
Δ40-48	Deletion of aa 40-48; R49A	Intermembrane Space	✔
Δ51-60	E50A; Deletion of aa 51-60	Intermembrane Space	✔
ΔNPGT	Deletion of aa 40-43	Intermembrane Space	✔
NPGT-AAAA	Replacement of aa 40-43 with Ala	Intermembrane Space	✔
ΔRD	Deletion of aa 53-54	Intermembrane Space	✔
ΔRDTLL	Deletion of aa 53-57	Intermembrane Space	✔
ΔGLRAD	Deletion of aa 64-68	Intermembrane Space	✔
GLRAD-AAAA	Replacement of aa 64-68 with Ala	Intermembrane Space	✔
ΔGNLD	Deletion of aa 109-112	Intermembrane Space	✔
GNLD-AAAA	Replacement of aa 109-112 with Ala	Intermembrane Space	✔
ΔQFEHE	Deletion of aa 145-149	Intermembrane Space	✔
QFEHE-AAAAA	Replacement of aa 145-149 with Ala	Intermembrane Space	✔
ΔVTP	Deletion of aa 183-185	Intermembrane Space	X
VTP-AAA	Replacement of aa 183-185 with Ala	Intermembrane Space	✔
VTPR-VTR	Deletion of aa 183	Intermembrane Space	✔
VTPR-VTAR	Replacement of aa 183 with Ala	Intermembrane Space	✔
ΔEKR	Deletion of aa 297-299	Intermembrane Space	X

[1] Predicted based on the model of T. Schirmer, via D. Rapaport, personal communication.
[2] aa, amino acid number.

EKR-AAA	Replacement of aa 297-299 with Ala	Intermembrane Space	✔
ΔSHQ	Deletion of aa 82-84	Membrane Spanning	X
SHQ-AAA	Replacement of aa 82-84 with Ala	Membrane Spanning	✔
ΔYAF	Deletion of aa 94-96	Membrane Spanning	X
YAF-AAA	Replacement of aa 94-96 with Ala	Membrane Spanning	✔
ΔIDS	Deletion of aa 286-288	Membrane Spanning	X
IDS-AAA	Replacement of aa 286-288 with Ala	Membrane Spanning	X
ΔKLG	Deletion of aa 321-323	Membrane Spanning	X
KLG-AAA	Replacement of aa 321-323 with Ala	Membrane Spanning	✔
ΔTK	Deletion of aa 131-132	Cytosol	✔
TK-AA	Replacement of aa 131-132 with Ala	Cytosol	✔
ΔNP	Deletion of aa 163-164	Cytosol	✔
NP-AA	Replacement of aa 163-164 with Ala	Cytosol	✔
ΔKK	Deletion of aa 237-238	Cytosol	X
KK-AA	Replacement of aa 237-238 with Ala	Cytosol	✔
WKK-WQQ	Replacement of aa 237-238 with Gln	Cytosol	✔
ΔVDH	Deletion of aa 312-314	Cytosol	✔
VDH-AAA	Replacement of aa 312-314 with Ala	Cytosol	✔

Table 6: cDNA variants used in *in vitro* assembly assays, and their assembly phenotypes

Mutation	Assembly Phenotype	Region[1]
ΔC-ter	Like wild type.	Intermembrane Space
ΔN-ter	No assembly.	Intermembrane Space
Δ40-48	Assembles to 400 kDa, but accumulates at 250 kDa	Intermembrane Space
Δ51-60	Stops at 250 kDa	Intermembrane Space
ΔNPGT	Assembles to 400 kDa, but accumulates at 250 kDa	Intermembrane Space
NPGT-AAAA	Assembles to 400 kDa, but accumulates at 250 kDa	Intermembrane Space
ΔRD	Assembles to 400 kDa, but accumulates at 250 kDa	Intermembrane Space
ΔRDTLL	Assembles to 400 kDa, but accumulates at 250 kDa	Intermembrane Space
ΔGLRAD	Stops at 250 kDa	Intermembrane Space
GLRAD-AAAA	Stops at 250 kDa	Intermembrane Space
ΔGNLD	Like wild type	Intermembrane Space
GNLD-AAAA	Assembles to 400 kDa, but accumulates at 250 kDa	Intermembrane Space
ΔQFEHE	Stops at 250 kDa	Intermembrane Space
QFEHE-AAAAA	Stops at 250 kDa	Intermembrane Space
ΔVTP	Stops at 250 kDa	Intermembrane Space
VTP-AAA	Stops at 250 kDa	Intermembrane Space

[1] Predicted based on the model of T. Schirmer, via D. Rapaport, personal communication.

VTPR-VTR	Assembles to 400 kDa, but accumulates at 250 kDa	Intermembrane Space
VTPR-VTAR	Like wild type	Intermembrane Space
ΔEKR	Stops at 250 kDa	Intermembrane Space
EKR-AAA	Accumulates at 100 kDa	Intermembrane Space
ΔSHQ	Assembles to 400 kDa, but accumulates at 250 kDa	Membrane Spanning
SHQ-AAA	Assembles to 400 kDa, but accumulates at 250 kDa	Membrane Spanning
ΔYAF	Stops at 250 kDa	Membrane Spanning
YAF-AAA	Stops at 250 kDa	Membrane Spanning
ΔIDS	Stops at 250 kDa	Membrane Spanning
IDS-AAA	Stops at 250 kDa	Membrane Spanning
ΔKLG	Stops at 250 kDa	Membrane Spanning
KLG-AAA	Assembles to 400 kDa, but accumulates at 250 kDa	Membrane Spanning
ΔTK	Assembles to 400 kDa, but accumulates at 250 kDa	Cytosol
TK-AA	Assembles to 400 kDa, but accumulates at 250 kDa	Cytosol
ΔNP	Assembles to 400 kDa, but accumulates at 250 kDa	Cytosol
NP-AA	Assembles to 400 kDa, but accumulates at 250 kDa	Cytosol
ΔKK	Stops at 250 kDa	Cytosol
KK-AA	Assembles to 400 kDa, but accumulates at 250 kDa	Cytosol
WKK-WQQ	Like wild type	Cytosol

ΔVDH	Like wild type	Cytosol
VDH-AAA	Accumulates at 100 kDa	Cytosol
C7 Stop[1]	No assembly	Cytosol
I7 Stop[2]	No assembly	Intermembrane space

[1] Replacement of a threonine residue at position 317 with a stop codon generating a truncated protein.
[2] Replacement of a threonine residue at position 300 with a stop codon generating a truncated protein.

Table 7: Results of mass spectroscopy of excised bands from gel in Fig. 32A.

Band	Significant Hits	MOWSE Score[1]	Proteins Identified	Description some proteins identified
Band 1	1	399	*N. crassa* Tom40	Known mitochondrial outer membrane protein
Band 2	3	69	*N. crassa* Tom40	Known mitochondrial outer membrane protein
		54	*N. crassa* putative disulfide isomerase ERP38 precursor	
		49	Human keratin	
Band 3	1	103	*N. crassa* ketol-acid reductoisomerase	Mitochondrial precursor
Band 4	1	110	*N. crassa* probable delta-sterol C methyltransferase	Imported
Band 5	5	87	*N. crassa* zinc metallo-protease	
		82	*N. crassa* gamma actin	
		72	Hypothetical protein RV1155 (An *N. crassa* homolog does exist)	Reminiscent of stress protein. *Mycobacterium*, *Streptomyces*, and *Listeria*
		68	Actin1	
		66	Actin	
Band 6	1	293	*N. crassa* zinc metallo-protease	

[1] A commonly accepted threshold is that an event is significant if it would be expected to occur at random with a frequency of less than 5%, this corresponds to a score of greater than 45.

Band 7	4	118	*N. crassa* conserved hypothetical protein	Unknown function, conserved in Saccharomyces
		105	Hypothetical protein RV1155	See above
		104	*N. crassa* citrate synthase	Known mitochondrial protein
		62	*N. crassa* probable zinc metallo-protease	
Band 8	3	212	Elongation factor 1-alpha	
		67	Elongation factor 1-alpha	Protein found in *Heliothis subflexa*
		49	Similar to eukaryotic elongation factor	
Band 9	1	48	*N. crassa* conserved hypothetical protein	Unknown function, conserved in *Magnetospirillum*, and *Desulfitobacterium*
Band 10	2	101	*N. crassa* Tom70	
		45	Sugar ABC transporter permease protein	
Band 11	3	114	Serine hydroxy methyltransferase	Known cytosolic protein
		70	ATP citrate lyase, subunit 2	Protein found in *Sordaria macrospora*
		57	*N. crassa* Tom70	
Band 12	2	117	ATP synthase alpha chain	Mitochondrial precursor
		49	ATP synthase alpha chain	Protein found in *Coccidioides posadasii*
Band 13	2	545	*N. crassa* conserved hypothetical protein	Unknown function, very conserved
		157	*N. crassa* conserved hypothetical protein	AMP binding domain, very conserved

Band 14	3	116	*N. crassa* probable sphingosine-1-phosphate lyase	
		63	Protein disulfide isomerase precursor	
		48	*N. crassa* conserved hypothetical protein	Ugo1 - required for mitochondrial fission found in yeast MOM
Band 15	2	148	*N. crassa* Tom70	Known mitochondrial outer membrane protein
		45	Aldehyde dehydrogenase	Protein found in *Caenorhabditis elegans*
Band 16	1	106	78 kDa Glucose-regulated protein (GRP78)	
Band 17	2	549	*N. crassa* Tom70	Known mitochondrial outer membrane protein

Figure 5. **Southern blots of RIP40het reveal two copies of *tom40* within the *tom40*^{RIP} nucleus. A.** Genomic DNAs (10 μg) from the parental strains of the RIP cross, MateV, and Dupl40, as well as the *tom40*^{RIP} strain (RIP40het) were digested with *Xho*I. Following electrophoresis, DNA was blotted onto nylon membrane and probed with a [^{32}P]-labeled *tom40* specific cDNA or genomic (gDNA) probe. *Xho*I is predicted to cut once within the *tom40* gene, so strains containing only the endogenous copy of the gene should display two bands on the Southern blot. Strains that also contain the ectopic copy of the *tom40* gene will display an additional two bands on the Southern blot. The disappearance of the bands associated with the ectopic copy of *tom40* in Dupl40, and the appearance of a slightly higher molecular weight band above the largest endogenous *tom40* band in RIP40het, as well as the presence of one band of a higher molecular weight than either ectopic band can be explained by the fact that the process of RIP is associated with an increase in methylation of DNA in sequences affected by RIP (Selker, 1990). Digestion of DNA by the restriction enzyme *Xho*I is inhibited by DNA methylation, and the two novel bands in RIP40het represent the ectopic, and endogenous *tom40* RIP alleles. The different alleles of *tom40* represented in the Southern blot are indicated on the left (wt, wild type). It should be noted that RIP40het also contains the unRIPed endogenous tom40 bands from the *tom40*$^{+}$ allele in the sheltering nucleus (see Fig. 4). The position and size of bands from a λ *Hin*dIII marker are shown on the right. **B.** A diagram of the *Xho*I restriction map of genomic DNA in the region of *tom40*. Molecular weights of cleavage fragments are shown below the diagram. The grey regions in the *tom40* gene indicate the positions of the exons, while the black regions indicate introns. The regions used as probes are indicated.

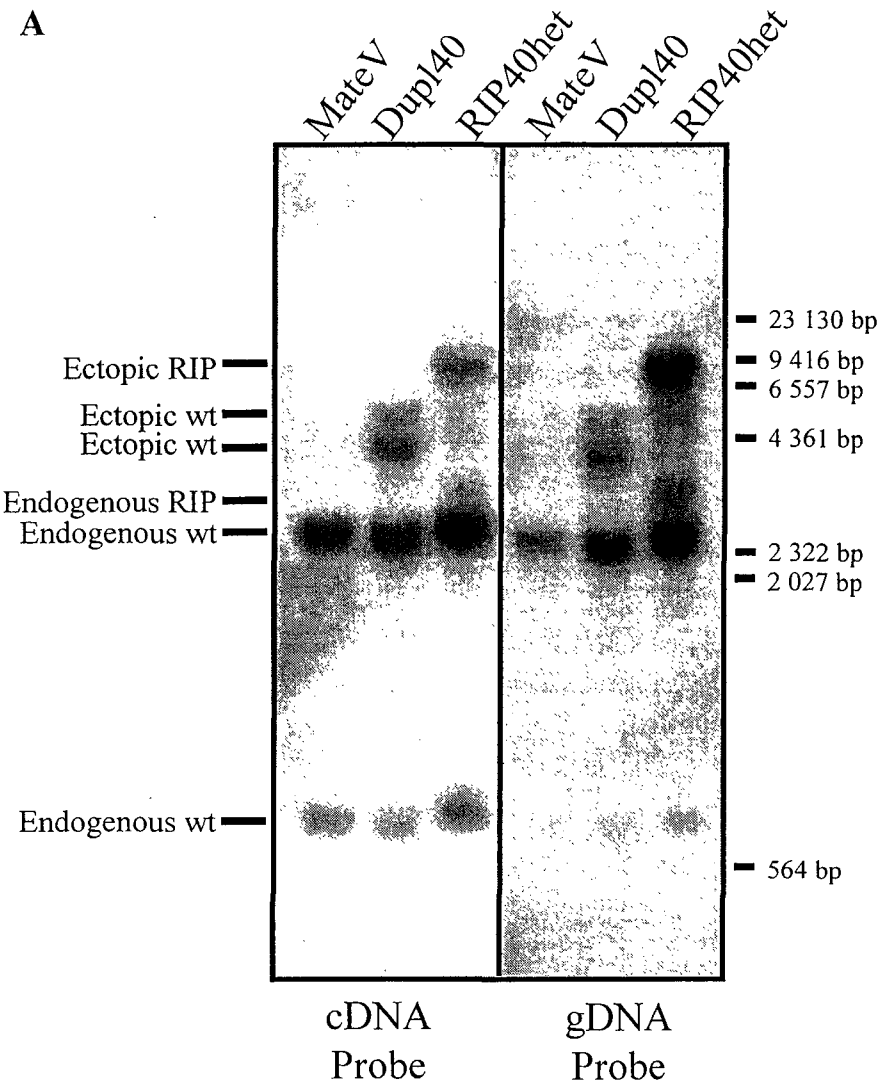

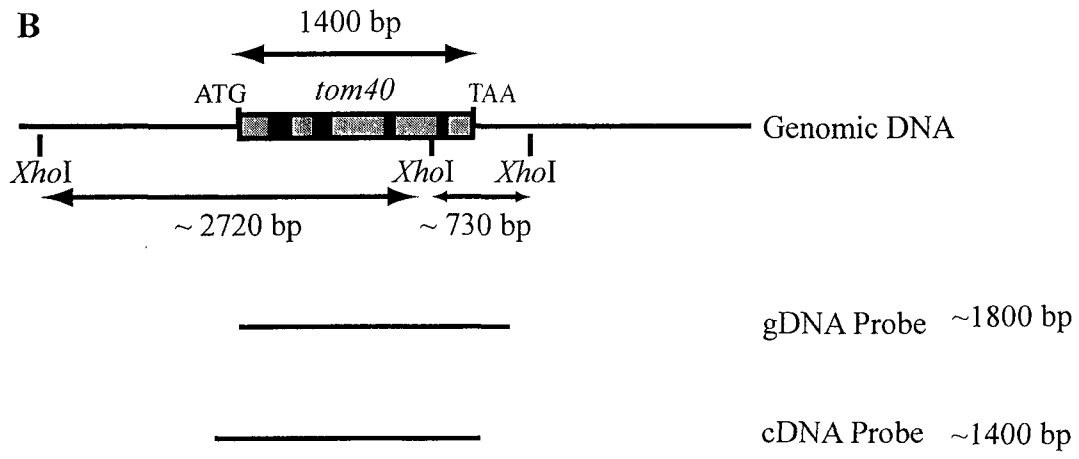

Figure 6. **The sequence of the *tom40* gene and protein.** A subclone (plasmid pLS-4) from a cosmid derived from an $su^{[mi\text{-}3]}$ (Gessert *et al.*, 1994) library was sequenced to obtain the genomic sequence for *tom40*. The positions of primers used for sequencing are indicated below the appropriate region of the sequence. In addition to the wild type genomic sequence, the sequence of both the endogenous (endogen) and ectopic $tom40^{RIP}$ alleles are indicated above the wild type sequence by showing positions altered by RIP. A solid line indicates the region of the RIP alleles that have been sequenced and correspond to the wild type sequence. RIP substitutions leading to stop codons are indicated by the boxed "STOP" above both the endogenous and ectopic RIP sequences. Nucleotide polymorphisms between this sequenced version of the gene, and the published sequence (Kiebler *et al.*, 1990) (also see www.mips.biochem.mpg.de/proj/neurospora/) are also indicated as blue nucleotides in the wild type genomic sequence. Downward pointing arrows indicate intron cleavage sites. Introns are shown in yellow highlight. Nucleotides shown in red on the genomic sequence indicate the *XhoI* restriction site used for Southern analysis (Fig. 5).

Translation of Nctom40gDNA(1-1932)
Universal code

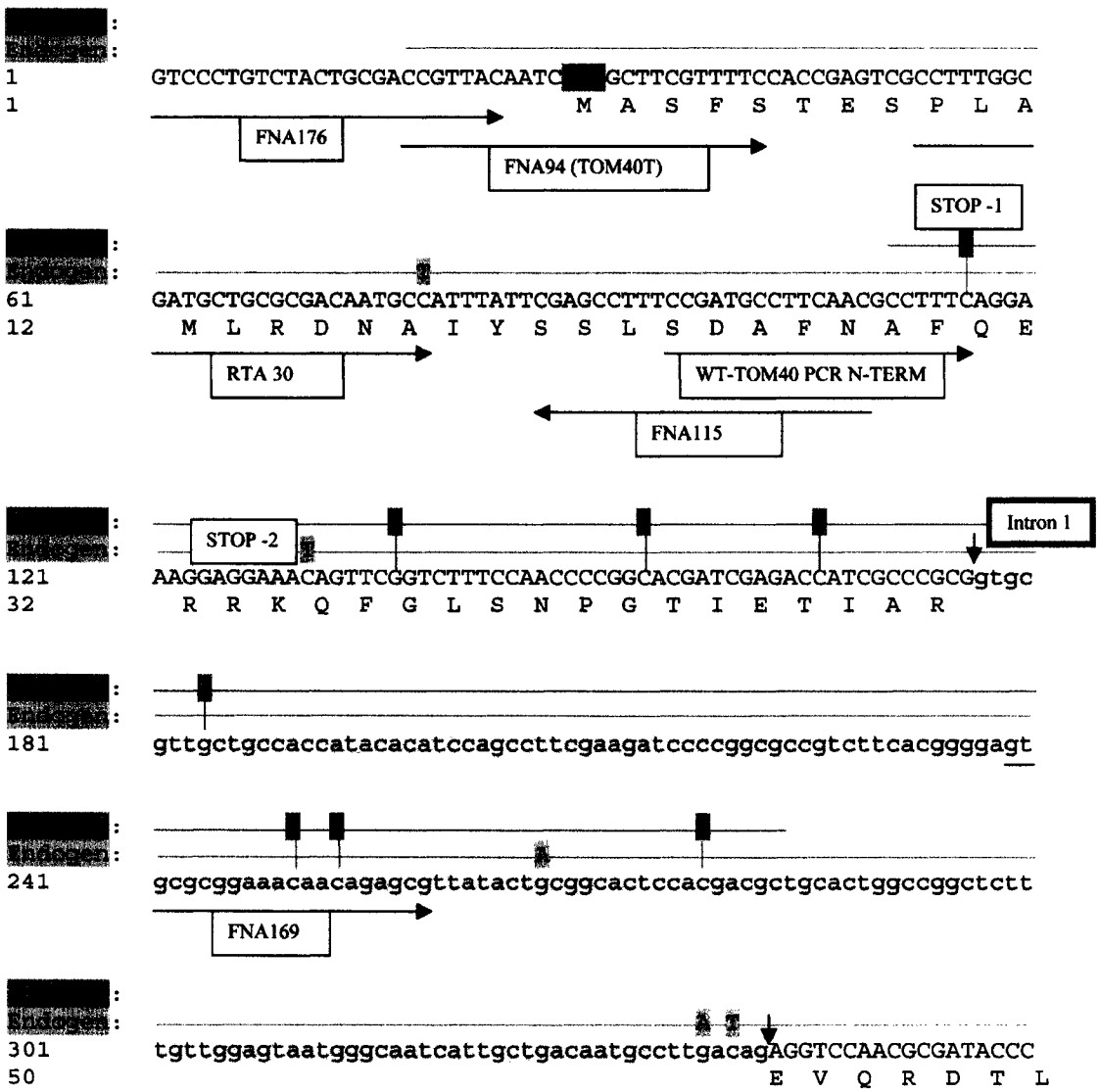

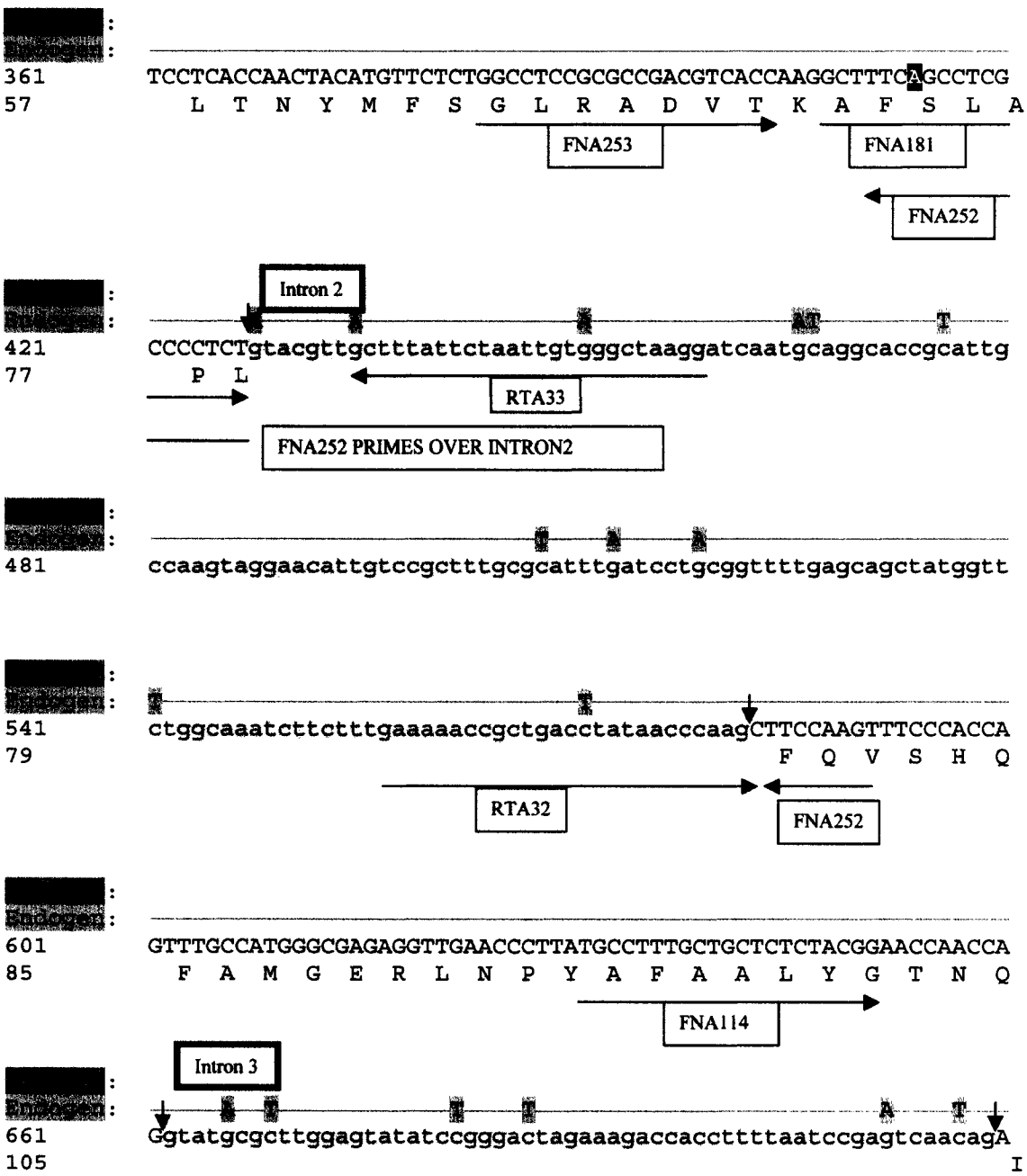

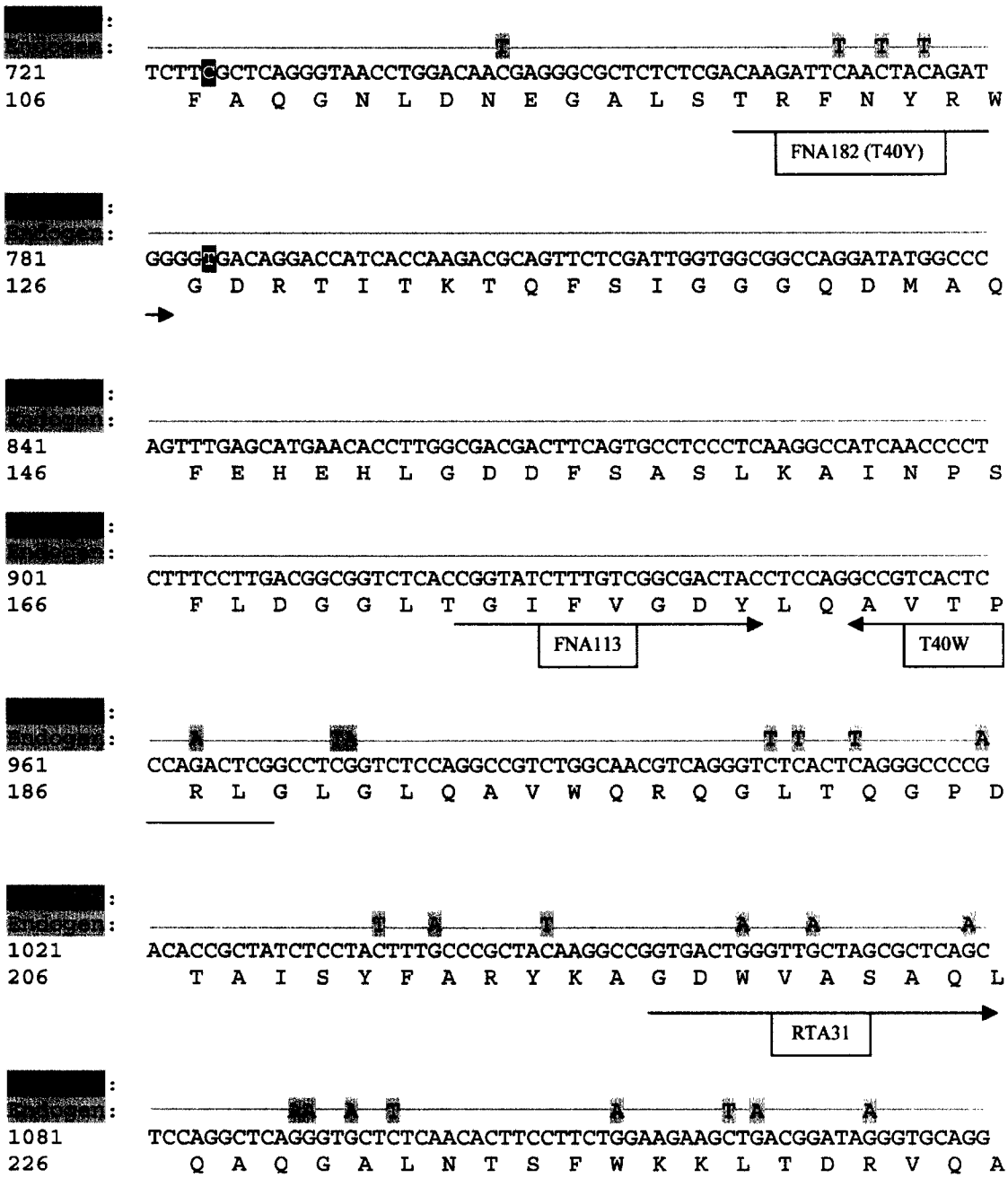

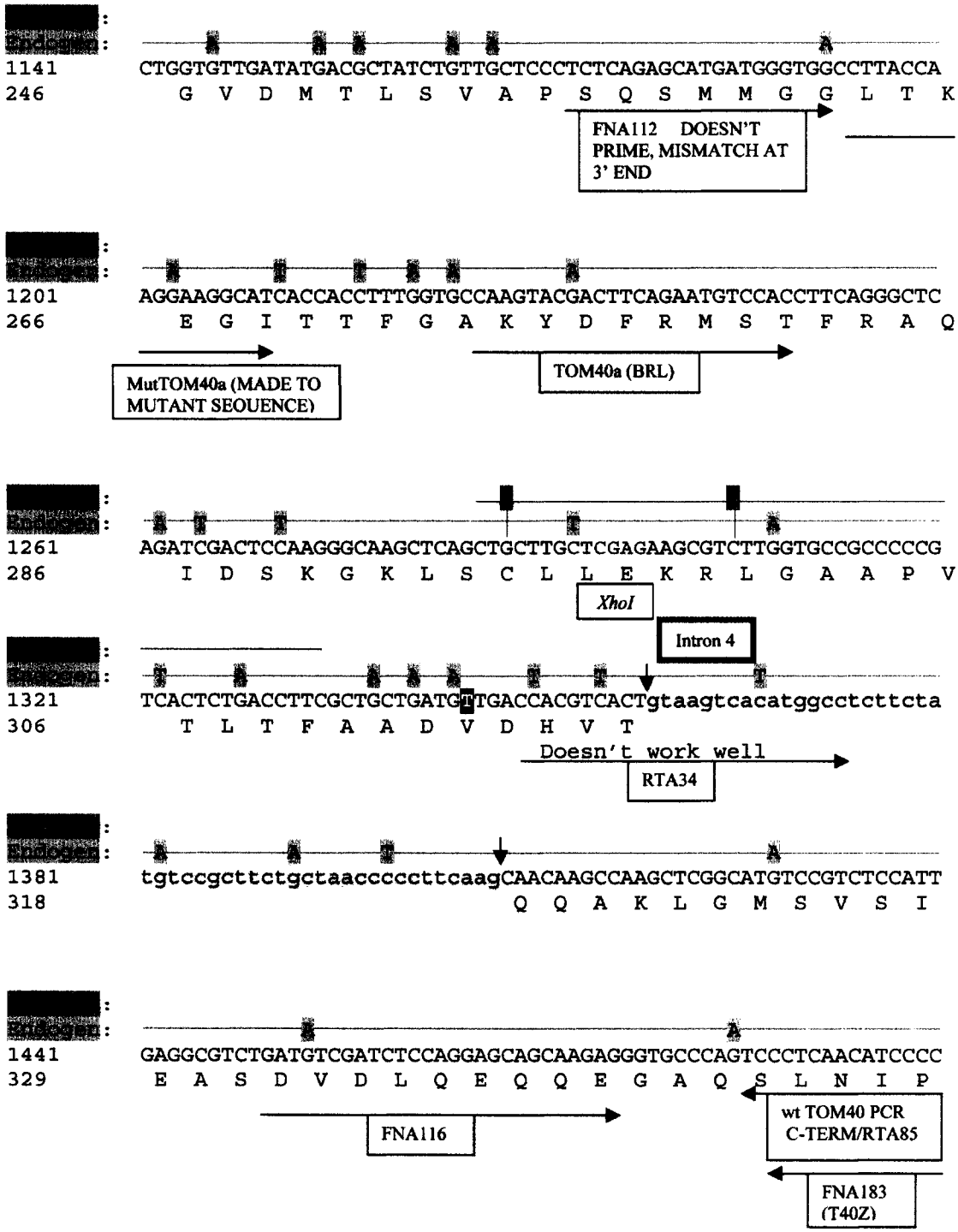

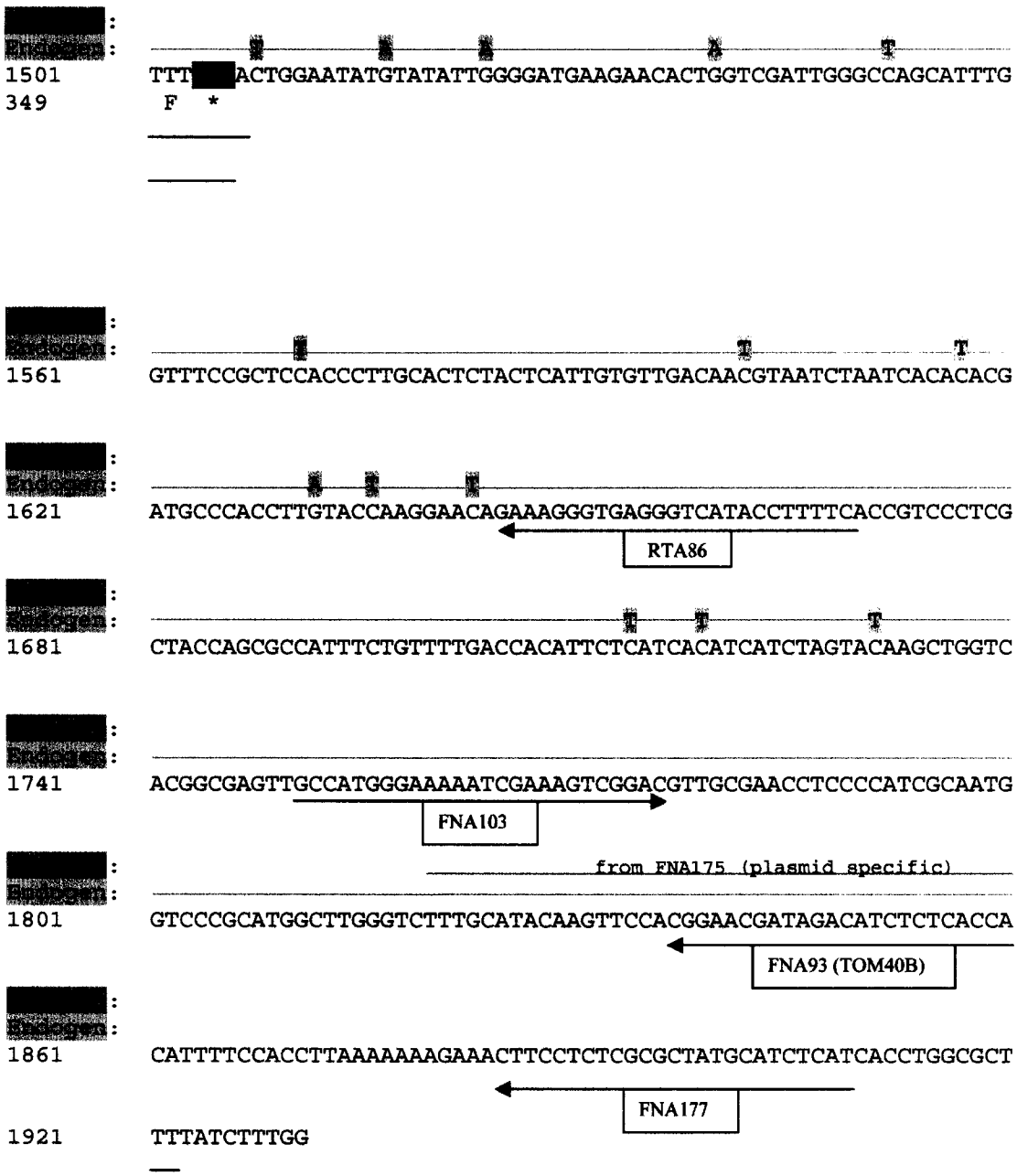

Yellow = introns, red = *XhoI* site, blue = nucleotide polymorphisms

Figure 7. **Genetic testing reveals that *tom40* is an essential gene. A.** Due to random segregation of conidia from the heterokaryotic strain (RIP40het), three types of conidiaspores should be produced: homokaryons for the lysine-leucine-requiring $tom40^{RIP}$ nucleus (nucleus 1), homokaryons for the inositol-leucine-requiring sheltering nucleus (nucleus 2), and heterokaryotic conidia containing both nuclei. **B.** Conidiaspores from the RIP40het strain were streaked onto medium containing all the nutritional requirements for both nuclei in the heterokaryon (see Fig. 4, and Table1). Single colonies were isolated and tested for nutritional requirements. The numbers of each type of colony recovered are indicated.

A

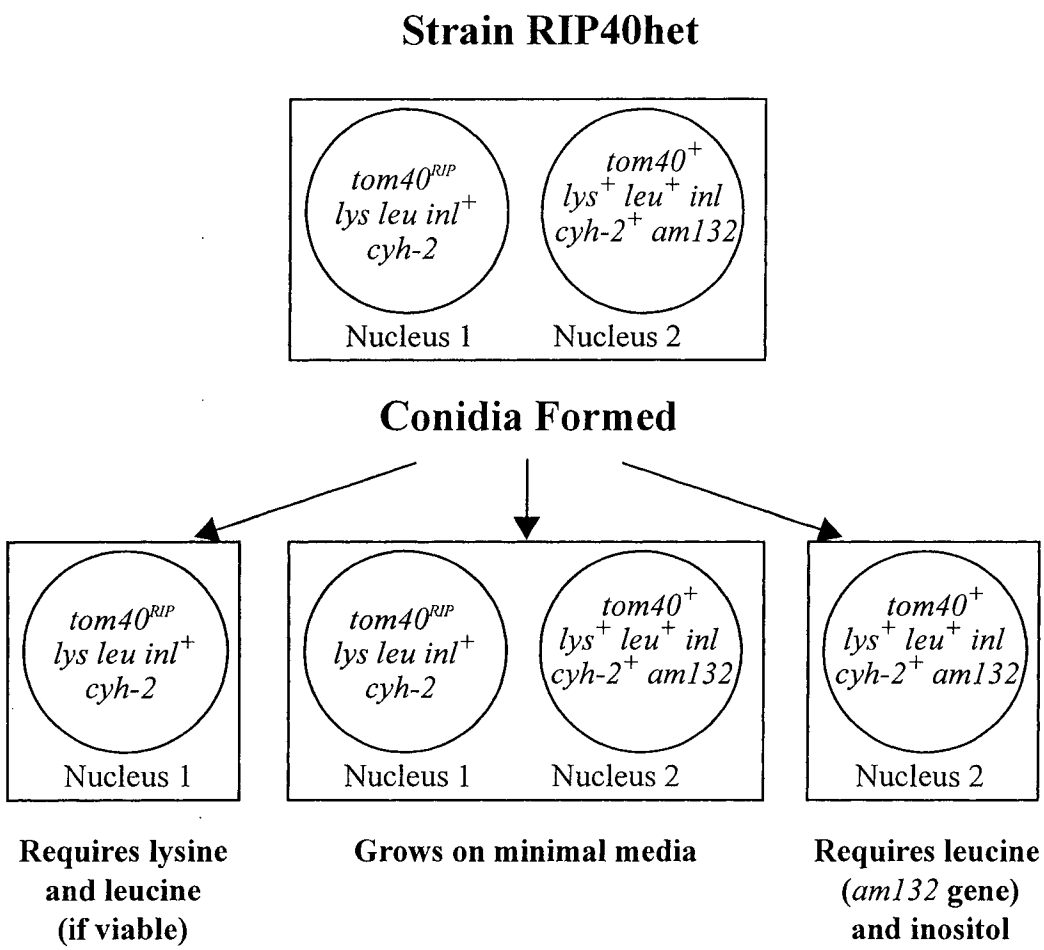

B

Strain	Colonies Tested	Growth on Minimal (heterokaryon)	Growth on Lysine/Leucine (*tom40*^{RIP} homokaryon)	Growth on Leucine/Inositol (*tom40*$^{+}$ homokaryon)
F46B-2	181	120	0	61

Figure 8. **Forcing the *tom40*^{RIP} nucleus to predominate RIP40het.** The *tom40*^{RIP} nucleus (grey shading) is auxotrophic for lysine (lys), leucine (leu) and is resistant to cycloheximide (CHI), while the *tom40*$^{+}$ nucleus is auxotrophic for inositol (inos), and is sensitive to cycloheximide (CHI). Because of the different nutritional markers located in each nucleus it is possible to manipulate the ratio of the nuclei in the heterokaryon. Growth in minimal media requires the presence of both nuclei and forces maintenance of the heterokaryotic strain. Growth of RIP40het in media containing lysine (lys), leucine (leu), and cycloheximide (CHI) force the *tom40*^{RIP} nucleus to predominate the strain to supply resistance to the drug and results in Tom40 deficiency. It is important to note that if *tom40* is an essential gene, at least a few nuclei containing the *tom40*$^{+}$ allele are required for growth of RIP40het, even in the presence of cycloheximide (CHI).

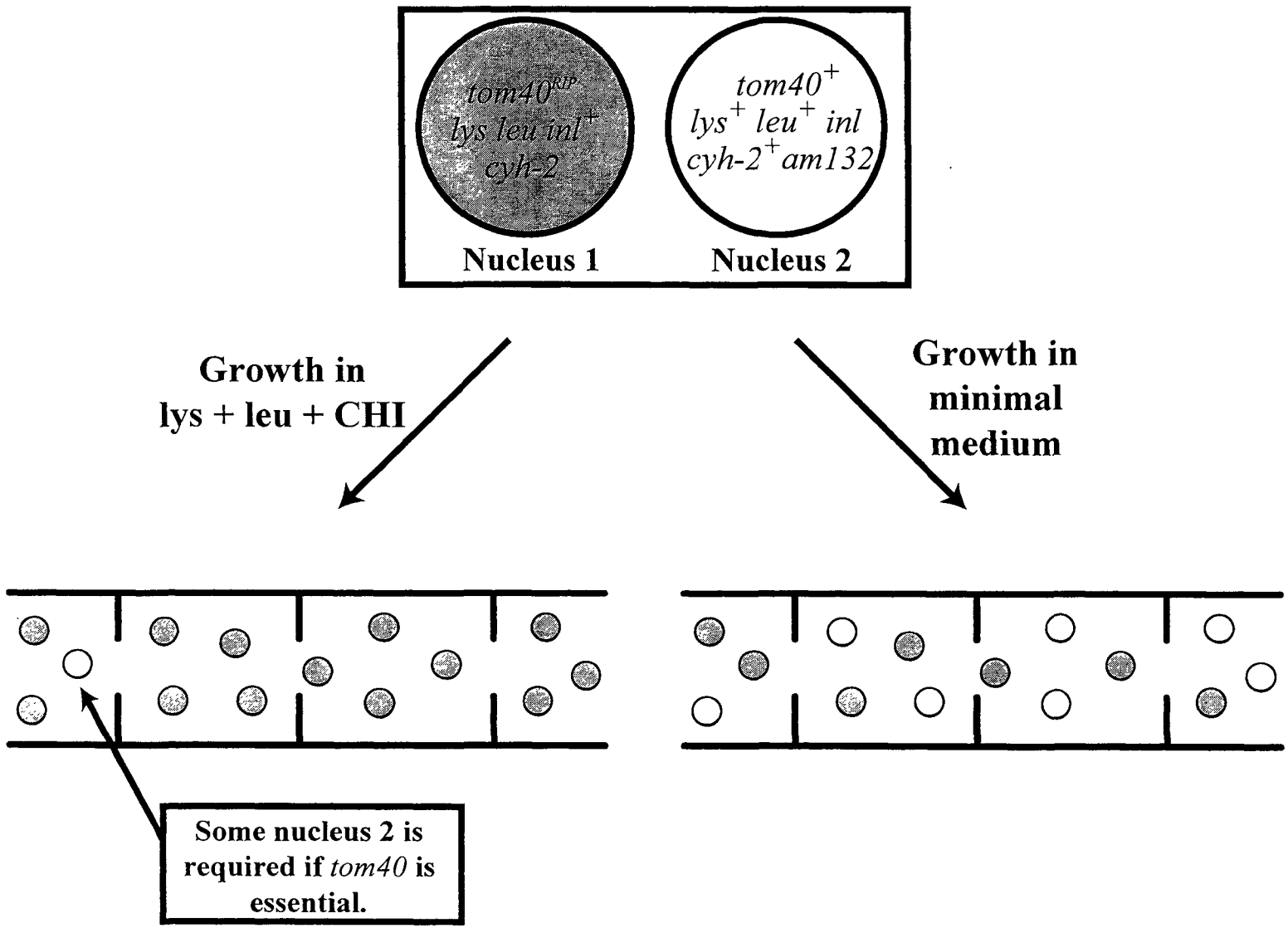

Figure 9. **Characteristics of Tom40-deficient cells. A.** The control strain (Dupl40) was grown in the presence of lysine and leucine (control, diamonds) and RIP40het was grown in minimal media (RIP40het, triangles) to compare their growth under conditions where complementation of Tom40 function occurs in the sheltered heterokaryon. To assess the growth rate of Tom40 deficient cells, the RIP40het strain was grown in medium containing lysine, leucine and cycloheximide (50 μg/ml) (RIP40het +CHI, squares), which forces the *tom40*^{RIP} nucleus to predominate the culture (see Fig. 8). The cycloheximide resistant control strain (HV) was grown under similar conditions (Control +CHI, crosses). **B.** Mitochondria were isolated from the indicated strains grown under conditions described in **A**. Mitochondrial proteins were separated by SDS-PAGE, blotted to nitrocellulose, and immunodecorated with antisera directed against the indicated proteins (mt, mitochondrial). **C.** Mitochondria from the control strain (Dupl40) and RIP40het grown in the presence of lysine, leucine, and cycloheximide were solubilized in either digitonin (DIG), or dodecyl maltoside (DDM) and analyzed by BNGE. The gel was transferred to PVDF membrane and immunodecorated with antisera against Tom40. The positions of molecular weight markers are indicated on the left.

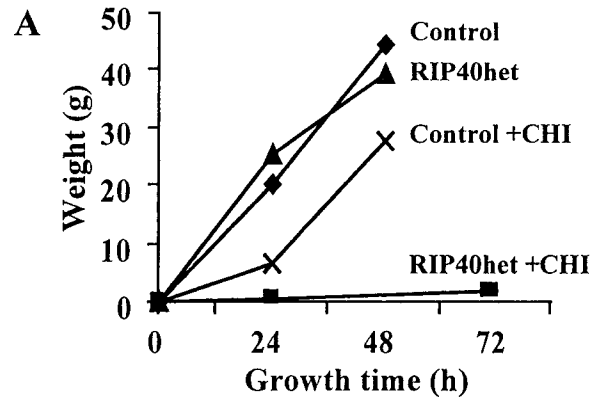

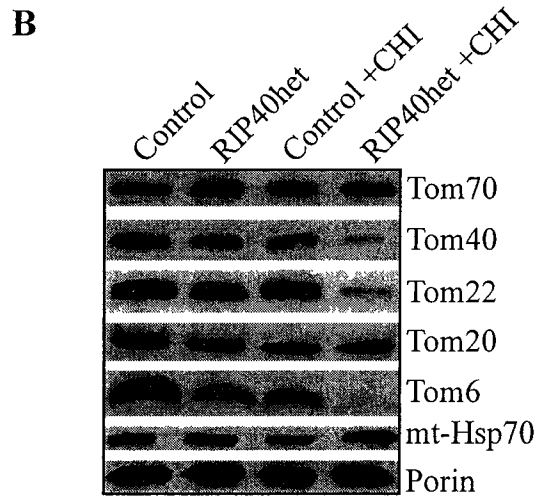

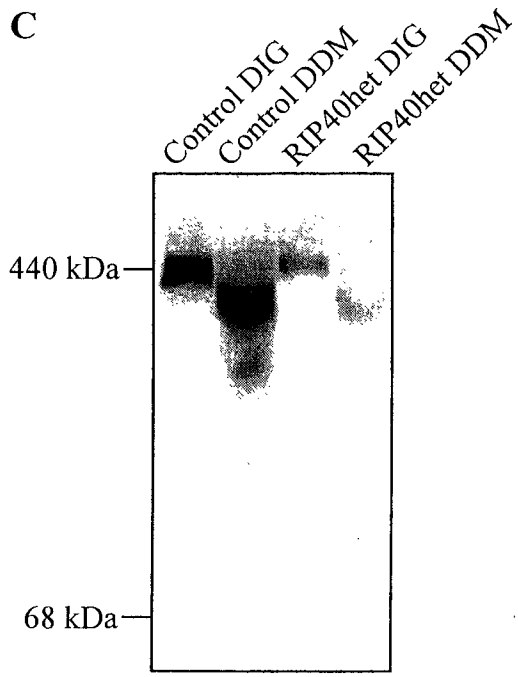

Figure 10. **The mRNA for Tom22 is not deficient in cells lacking Tom40.** Control cells (Dupl40) and RIP40het cells were grown as described for Fig. 9A. RNA was isolated from the cultures and electrophoresed on formaldehyde-agarose gels. The gel was stained with ethidium bromide, photographed, and transferred to nitrocellulose. The blot was cut in half and hybridized with ^{32}P-labeled DNA specific for *tom40* or *tom22*. **Top portion:** ethidium bromide stained gel. **Bottom portion:** autoradiogram of the blots following hybridization with the probe indicated at the bottom of the figure. The positions of the molecular weight markers (kb) are indicated on the left.

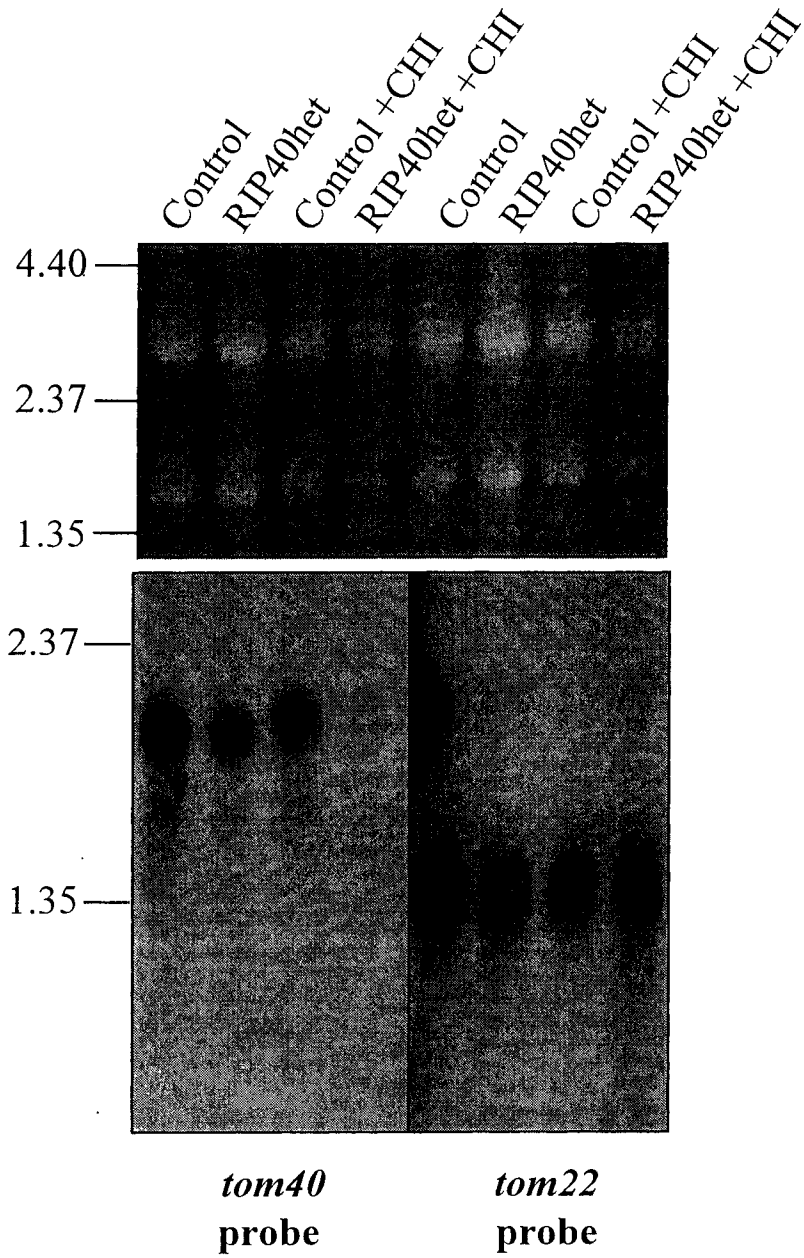

Figure 11. **Import of mitochondrial preproteins is reduced in Tom40 deficient mitochondria.** Mitochondria were isolated from the control strain (Dupl40) and RIP40het following growth in lysine, leucine and cycloheximide (30 μg/ml) so that mitochondria in RIP40het contained reduced levels of Tom40. Import of radiolabeled precursors ($F_1\beta$, the β-subunit of the F_1-ATP synthase; MPP, the matrix processing peptidase; AAC, the ATP/ADP carrier protein) was performed at 20°C for the times shown. Following a post-import treatment with proteinase K to remove non-imported precursors, mitochondria were re-isolated and subjected to SDS-PAGE. The gels were transferred to nitrocellulose membranes and exposed to x-ray film. The lysate lane contains 33% of the input lysate used in each import reaction. The precursor (p) and mature (m) forms of MPP and $F_1\beta$ are indicated. One sample from each lane was treated with trypsin prior to import (Pre-trypsin) to demonstrate that import was receptor dependent.

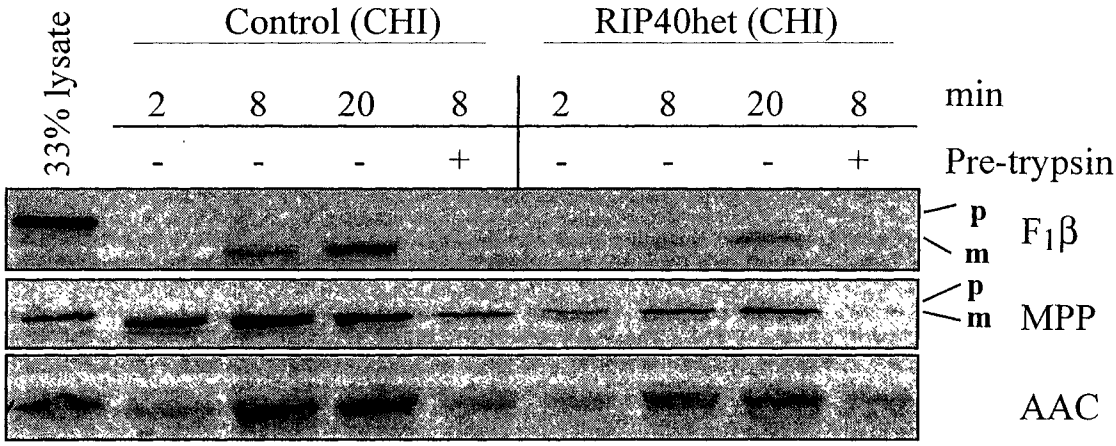

Figure 12. **Appearance of Tom40-deficient mitochondria.** The cycloheximide-resistant control strain (Dupl40) and RIP40het were grown under conditions described in the legend to Fig. 9A. At the indicated times, mycelium was harvested and processed for electron microscopy as described in section 2.10. Double membrane bound structures in panel D were assumed to mitochondria, although this assumption was not verified.

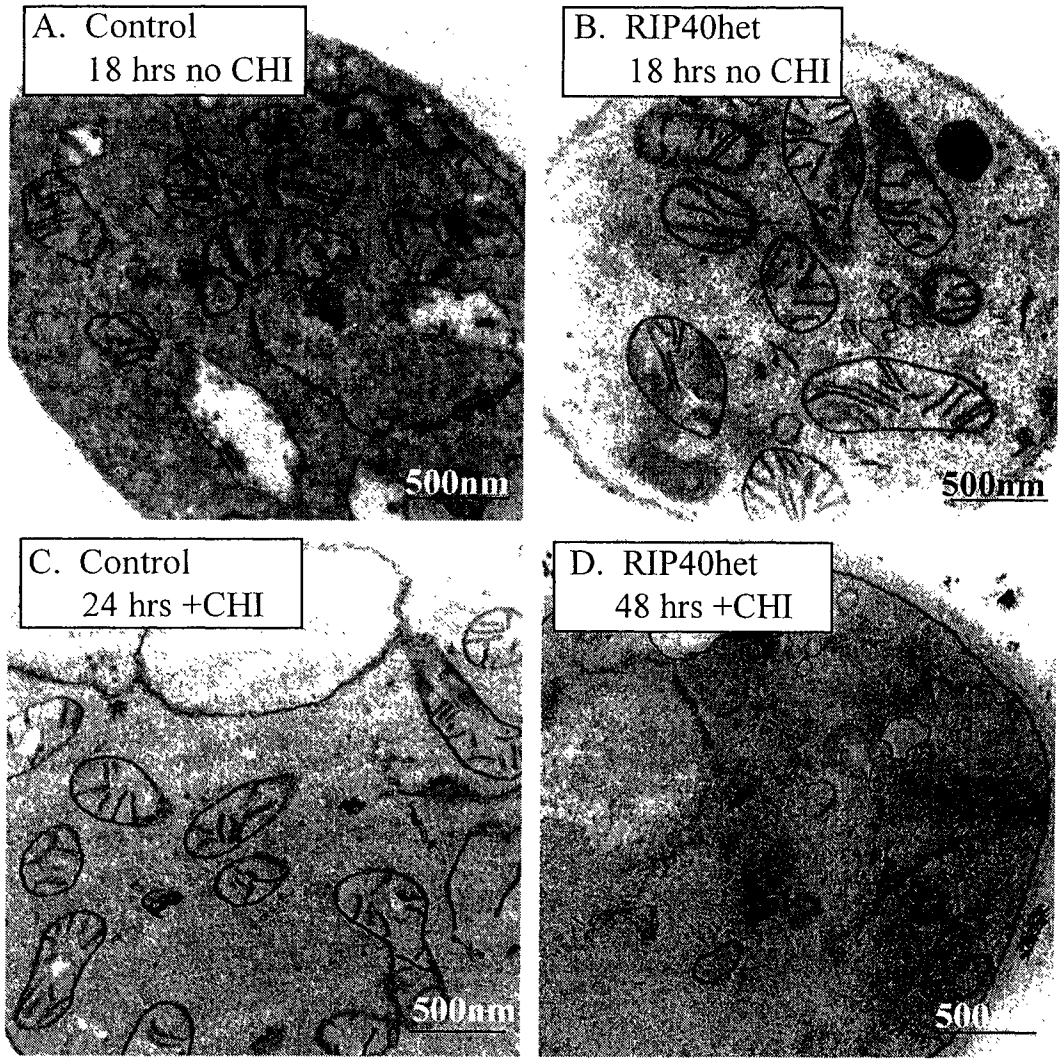

Figure 13. **Alignment of Tom40 proteins.** The Tom40 proteins from *Neurospora crassa* (Nc), *Saccharomyces cerevisiae* (Sc), *Schizosaccharomyces pombe* (Sp), *Mus musculus* (Mm), *Caenorhabditis elegans* (Ce), and *Drosophila melanogaster* (Dm) are shown. The number of residues in each protein is indicated on the right. Black shading indicates amino acid identity in at least four of the six species shown. Gray shading indicates amino acids of the same family in at least four of the six species. Starred residues indicate regions chosen for site-directed mutagenesis studies.

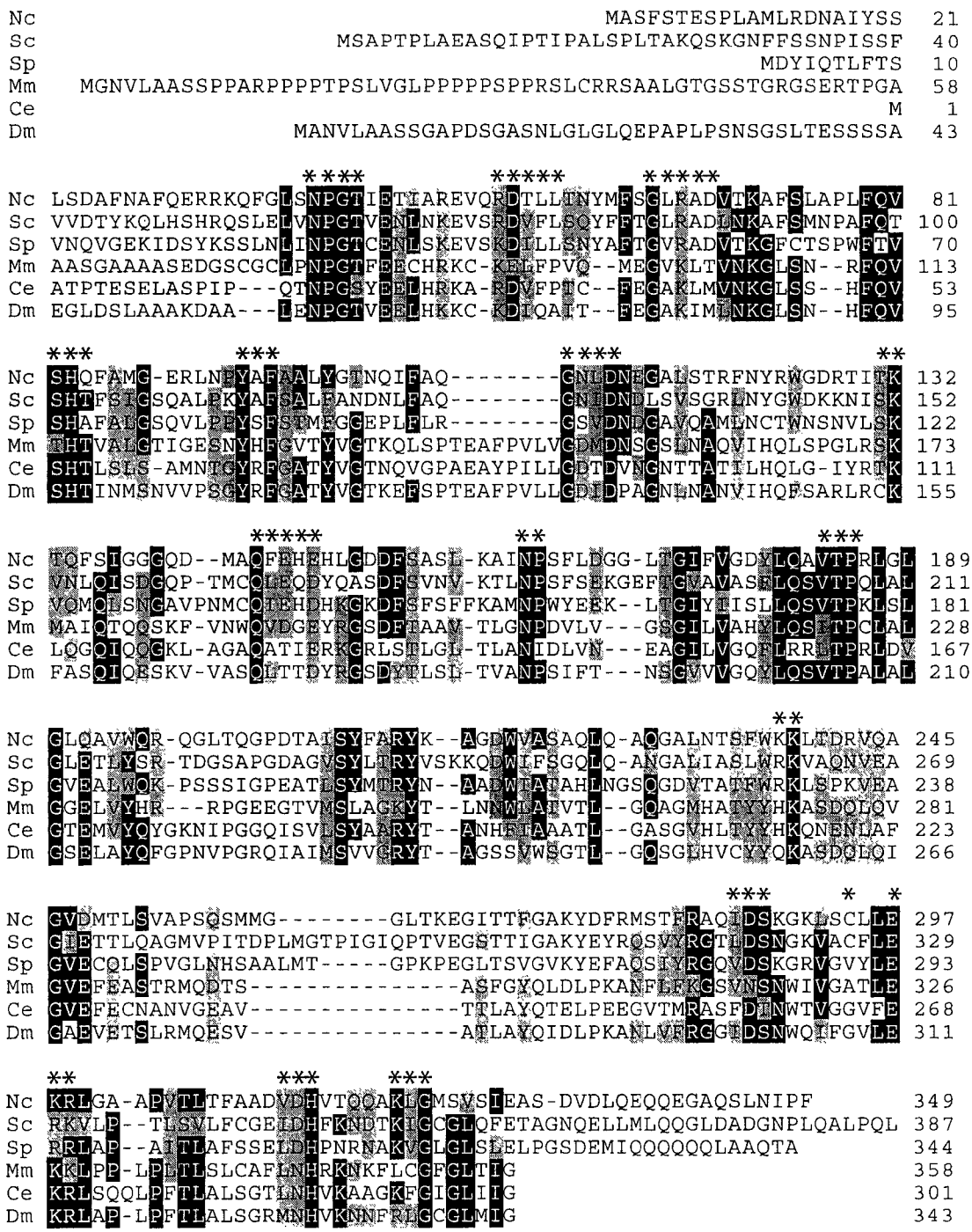

Figure 14. **Creation of *Neurospora crassa* strains expressing Tom40 variants.** Transformation of RIP40het with mutant alleles of *tom40*, carried on a bleomycin resistance plasmid, followed by selection on media containing bleomycin (3.7 μg/ml), cycloheximide (50 μg/ml), caffeine (0.5 mg/ml to enhance the action of bleomycin), lysine, and leucine resulted in homokaryons expressing only the predicted mutant alleles of *tom40*. Only *tom40* variants supplying enough activity for viability would be capable of giving rise to lysine-, leucine- requiring homokaryons.

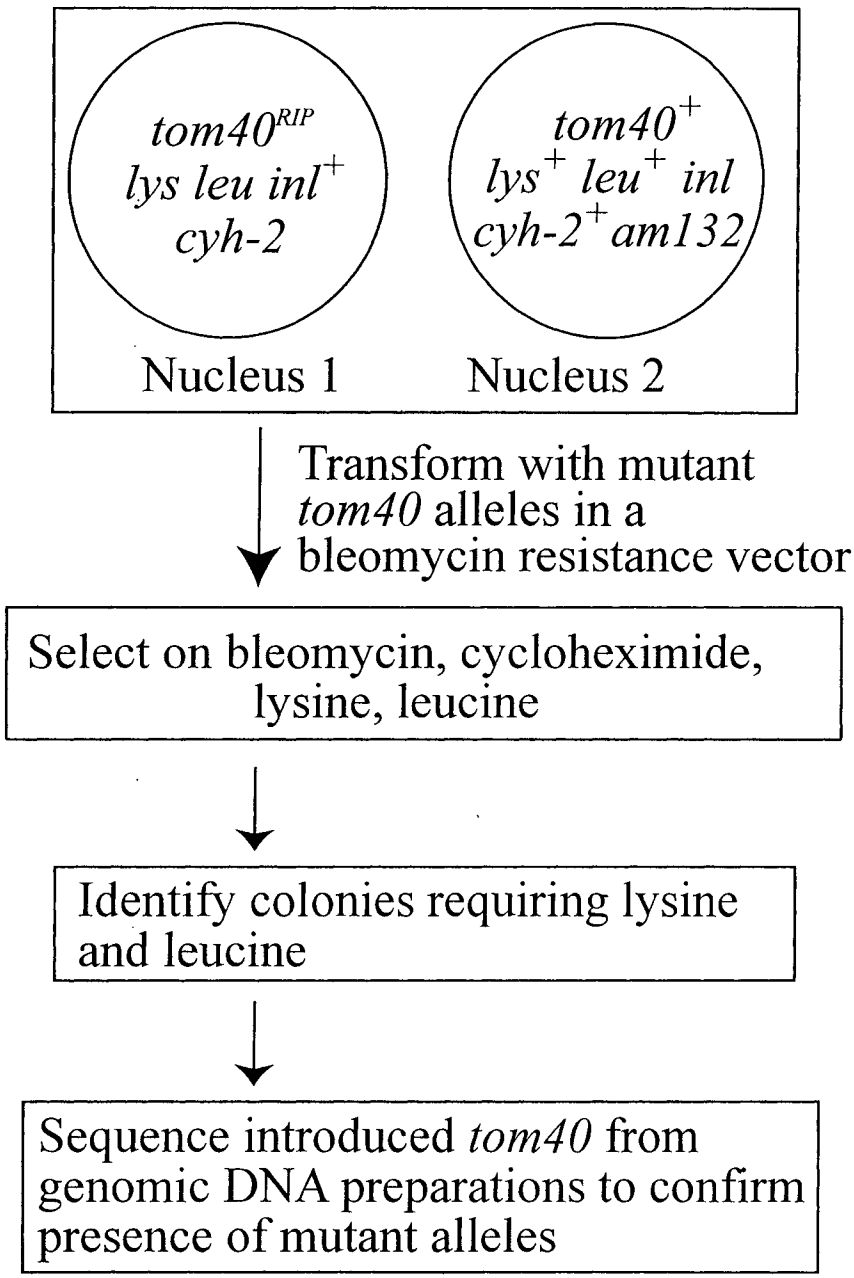

Figure 15. **PCR specific for the introduced (ectopic) copy of *tom40* in the *tom40* transformant strains. A.** Genomic DNA was isolated from lysine, leucine requiring strains following transformation of RIP40het with a plasmid containing an altered version of *tom40* on a bleomycin resistance plasmid. The three copies of *tom40* expected to be present in the *tom40* transformant strains are the endogenous RIP allele, the ectopic RIP allele, and the introduced allele containing specific mutations. For all three, *tom40* is shown in GREEN, while the RED regions depict the *tom40* specific flanking region surrounding the gene in each of the versions of *tom40.* The ectopic RIP allele has no *tom40* specific region upstream of the start codon. WtPCRNter cannot prime the ectopic RIP allele because the 3' end of the primer corresponds to a position containing a RIP mutation in that allele. Similarly, RTA85 cannot prime at the endogenous RIP allele because its 3' end corresponds to a position containing a RIP mutation in that allele. The position of the oligonucleotides is shown on the three versions of *tom40* only where they are capable of priming. **B.** The process for amplifying the introduced altered copy of *tom40* is shown. The first round of PCR will amplify only the endogenous RIP and introduced copies of *tom40* as there is insufficient flanking region for primer FNA176 to anneal to the ectopic RIP copy of *tom40* (only 6 bp of overlap). The second round of PCR is designed to eliminate both the ectopic and endogenous RIP copies of *tom40* as primer WtPCRNter will not amplify the ectopic RIP copy of *tom40*, while RTA85 will not amplify the endogenous *tom40* RIP allele. While it is possible to amplify the introduced copy of *tom40* using only PCR amplification step 2, it was found that two rounds of PCR were necessary to provide enough template for subsequent sequencing steps.

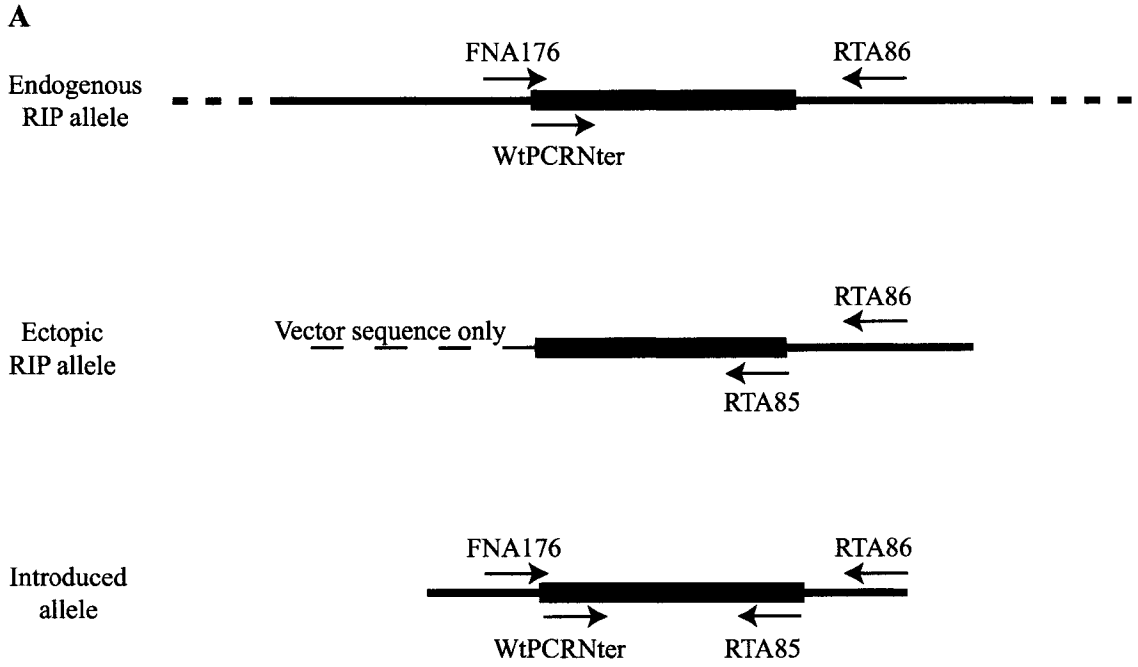

B

Step 1
Conidial DNA Isolation

↓

Step 2
First Round PCR
FNA176/RTA86
Eliminates Ectopic RIP copy

↓

Step 3
Second Round PCR
WtPCRNter/RTA85
Amplifies Only Introduced *tom40*

↓

Step 4
Sequence with appropriate *tom40* primer to confirm presence of desired *tom40* allele

Figure 16. **Alignment near the amino terminus of the Tom40 protein.** A region near the amino terminus of Tom40 proteins from *Neurospora crassa* (Nc), *Saccharomyces cerevisiae* (Sc), *Schizosaccharomyces pombe* (Sp), *Mus musculus* (Mm), *Caenorhabditis elegans* (Ce), and *Drosophila melanogaster* (Dm) is shown. Residues on the Nc protein are numbered at the top of the figure. Black shading indicates amino acid identity in at least four of the six species shown. Gray shading indicates amino acids of the same family in at least four of the six species. Residues affected in the amino terminal Tom40 variants are indicated below the alignment. Deleted residues are indicated by dashes, while amino acid substitutions are shown in lower case.

ΔNPGT: FGLS----IETIAREVQRDTLLTNYMFSG

AAAA: FGLSaaaaIETIAREVQRDTLLTNYMFSG

Δ40-48: FGLS---------aEVQRDTLLYNYMFSG

ΔRD: FGLSNPGTIETIAREVQ--TLLTNYMFSG

ΔRDTLL: FGLSNPGTIETIAREVQ-----TNYMFSG

Δ51-60: FGLSNPGTIETIARa----------MFSG

Figure 17. **Assembly of Tom40 amino terminal variants into the TOM complex.** Radiolabeled precursors of a wild type Tom40 (Tom40wt) or the indicated variants were incubated at either 0^{o} or $25^{o}C$ with wild type mitochondria (strain NCN251) for 20 min. Mitochondria were re-isolated and solubilized in buffer containing 1% digitonin. The samples were subject to BNGE, transferred to PVDF membrane, and analyzed by autoradiograpy. The positions of the 400 kDa, 250 kDa, 100 kDa, and monomer forms (M) are shown. **A.** Tom40 variants spanning amino acids 40-50. **B.** Tom40 variants spanning amino acids 50-60. (Note: Fig. 17A was supplied by Dr. Doron Rapaport, University of Munich.)

A

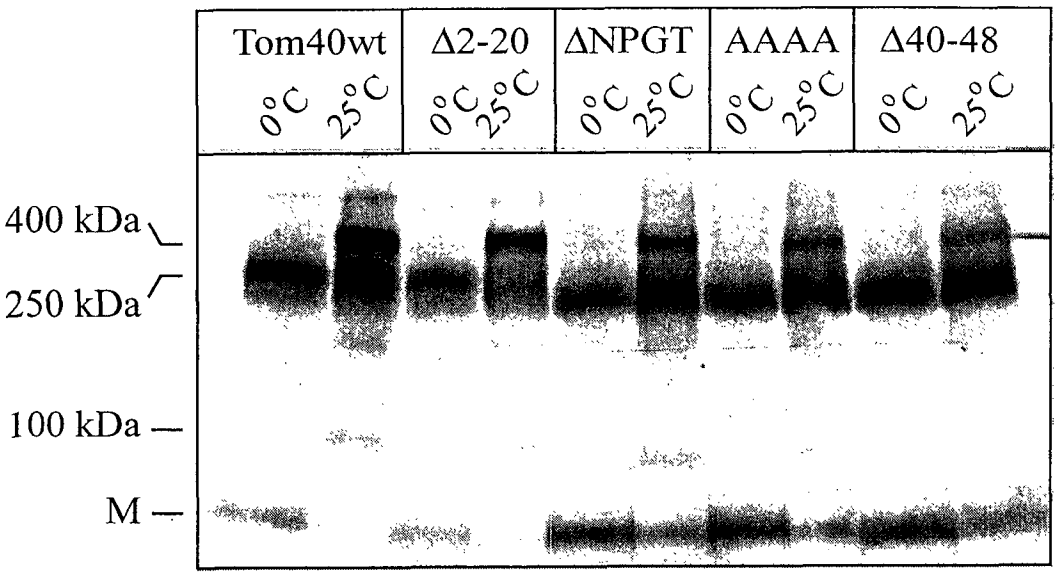

B

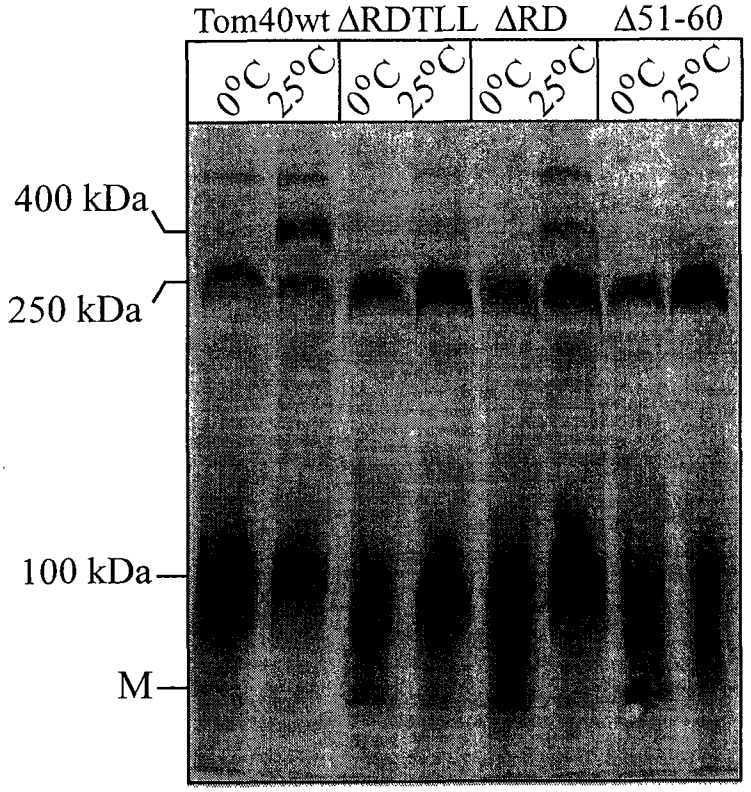

Figure 18. **Growth phenotypes of Tom40 variants spanning amino acids 40-50.** Strains containing mutations affecting amino acids 40-50 of Tom40 are unable to climb the walls of growth flasks and produce fewer asexual conidia spores compared to the parental control strains, MateV and Dupl40.

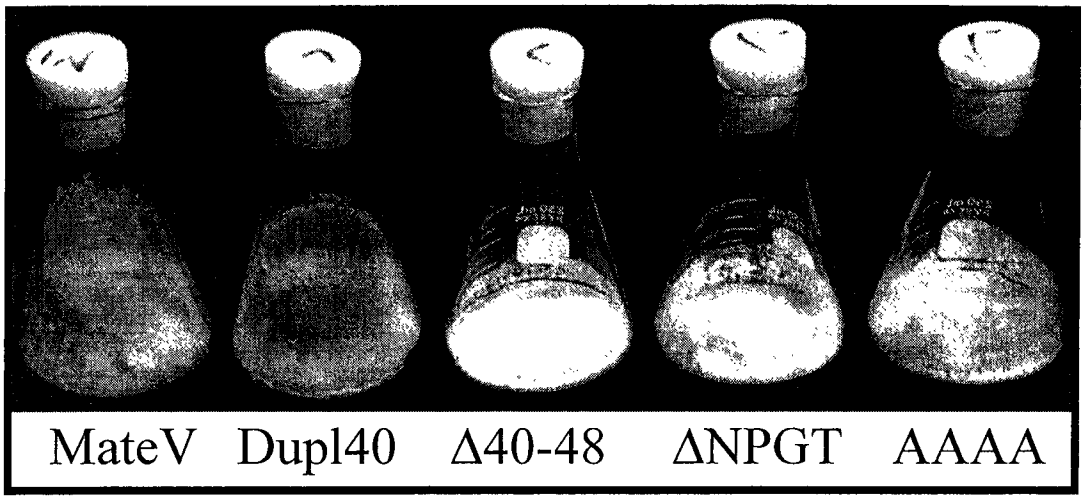

Figure 19. **Growth rate defects observed in strains containing Tom40 variants. A.** Mycelial elongation rate of a control strain (Dupl40, closed diamonds) and Tom40 variants spanning amino acids 40-50 as measured in race tubes. A representative of the Δ40-48 (closed squares), AAAA (open circles) and ΔNPGT (closed triangles) strains are shown, but it should be noted that some strains containing the AAAA mutation grow in the manner shown for ΔNPGT, and vice versa. **B.** The growth phenotype of Δ51-60 strains. Conidia from a Δ51-60 strain (open squares) and a control (Dupl40, closed circles) were inoculated into flasks containing 50 ml liquid medium, grown with shaking at 15°C, harvested at the indicated times, and the fresh weight was measured.

A

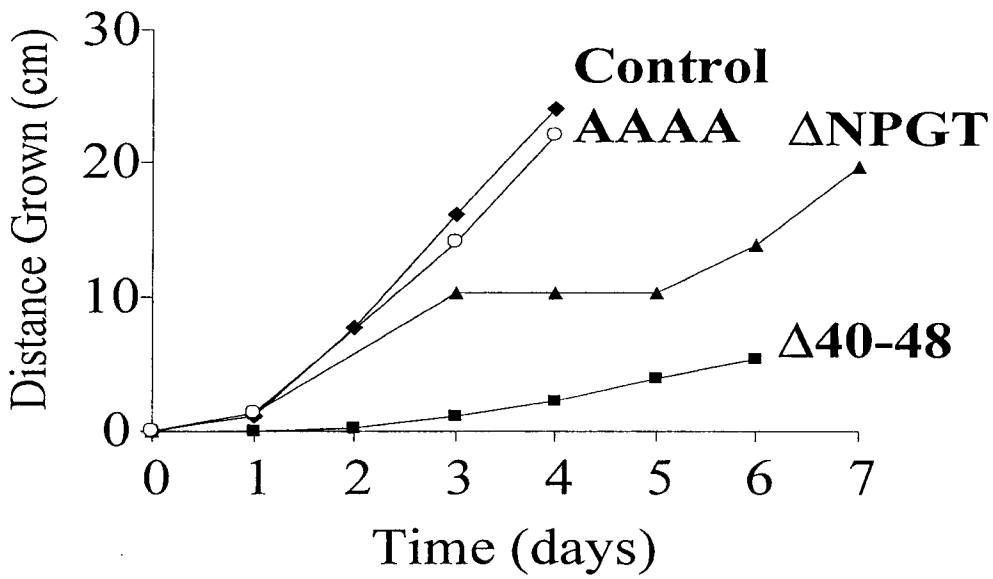

B

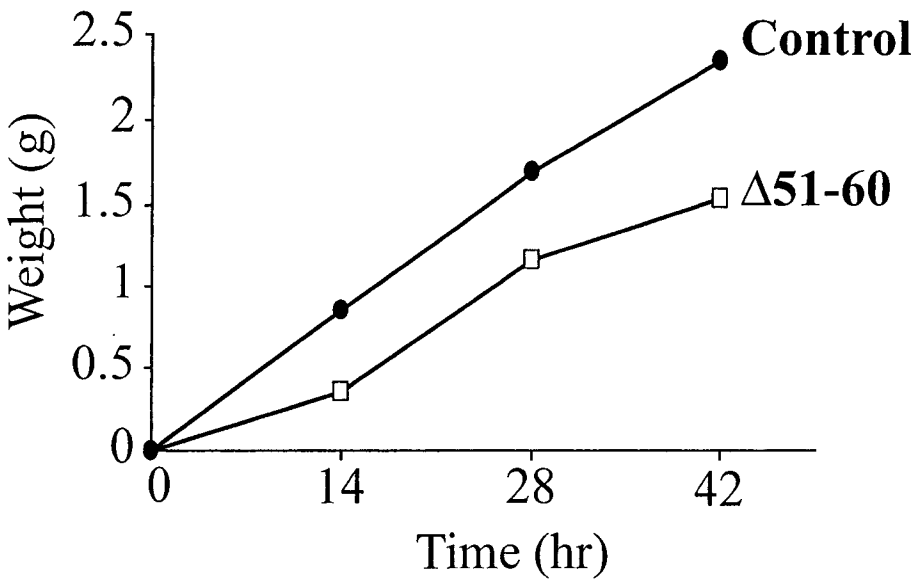

Figure 20. **Import defects in N-terminal mutant strains.** Mitochondria were isolated from the control strains (Dupl40) and the Tom40 variant strains indicated to the left. Import of radiolabeled precursors (CCHL, the cytochrome *c* heme lyase; F1β, the β subunit of the F_1 ATP synthase; MPP, the matrix processing peptidase; Porin, the voltage dependent anion conducting channel; Su9-DHFR, the first 69 amino acids of subunit 9 of the F_0 ATP synthase fused to dihydrofolate reductase) was performed at 20°C for the times shown. Following a post-import treatment with proteinase K to remove non-imported precursors, mitochondria were re-isolated and subjected to SDS-PAGE. The gels were transferred to nitrocellulose membranes and exposed to x-ray film. The lysate lane contains 33% of the input lysate used in each import reaction. The precursor (p) and mature (m) forms of $F_1\beta$, MPP and Su9-DHFR are indicated. One sample from each lane was treated with trypsin prior to import to demonstrate that import was receptor dependent.

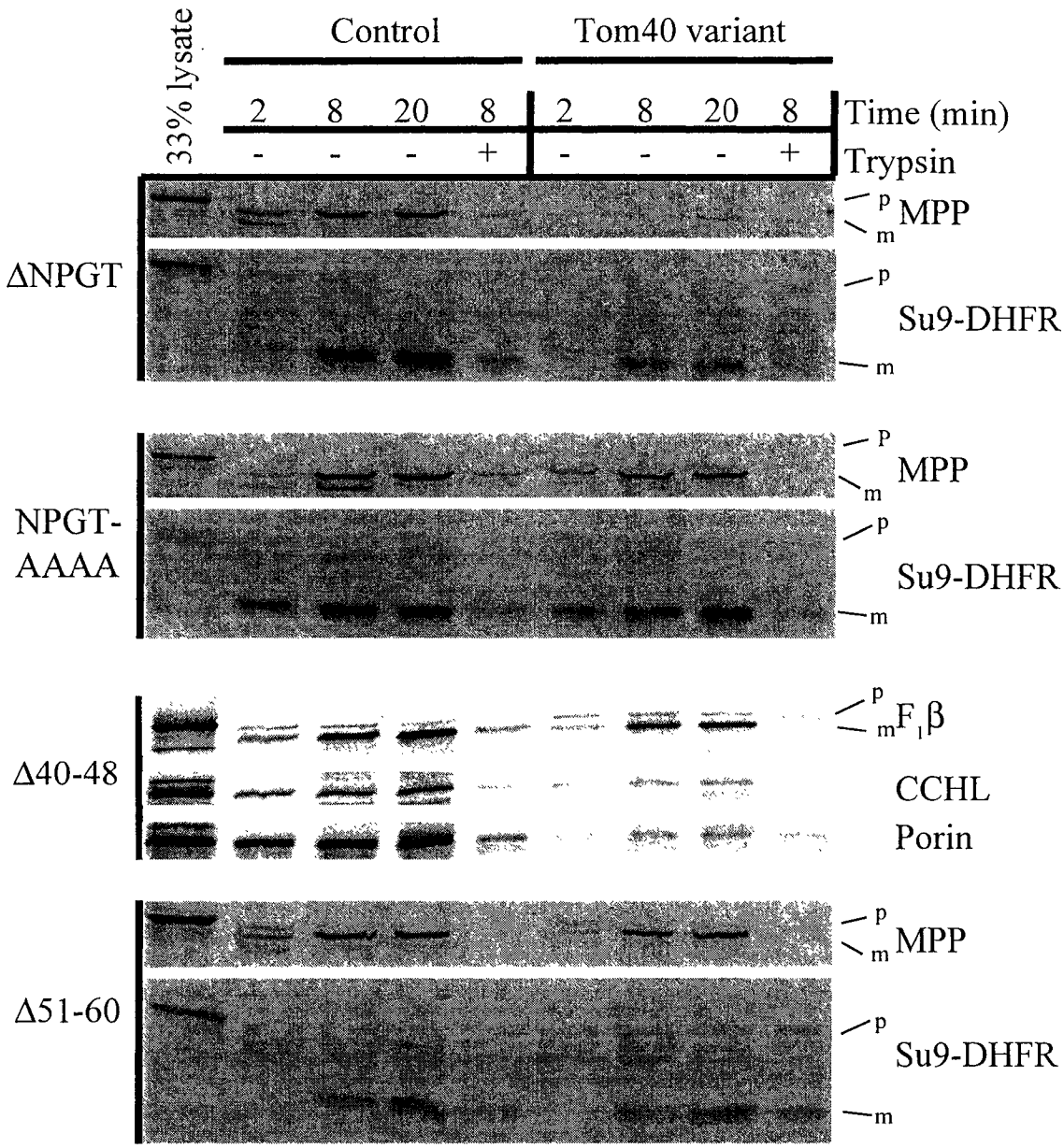

Figure 21. **Mitochondrial protein levels are unaffected in Tom40 variant strains.** Mitochondria isolated from the control (Dupl40) and mutant strains were subjected to SDS-PAGE, and transferred to nitrocellulose membrane. Membranes were immunodecorated with antisera to TOM complex components, as well as, the mitochondrial outer membrane protein porin, the intermembrane space protein cytochrome *c* heme lyase (CCHL), and the matrix protein, mitochondrial (mt)Hsp70.

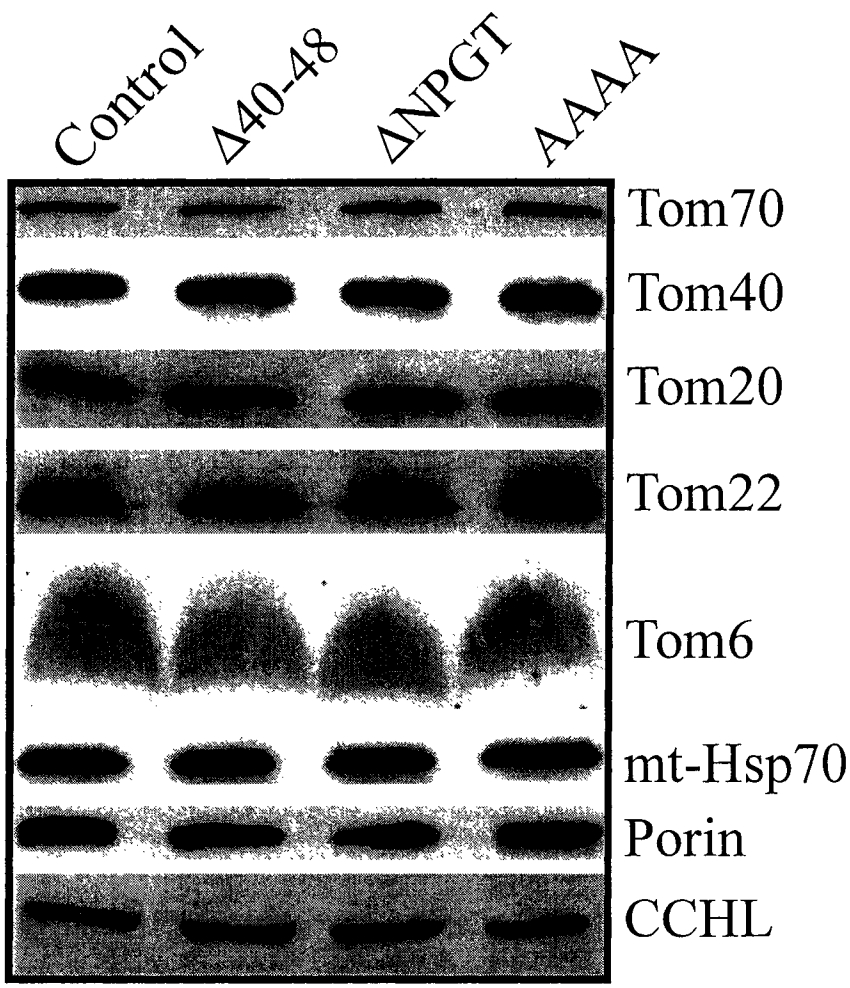

Figure 22. **Stability of the TOM complex is affected in strains containing variant Tom40s.** Mitochondria were dissolved in 1% digitonin (DIG) or 1 % dodecylmaltoside (DDM) and subjected to BNGE. The gels were transferred to PVDF membrane and decorated with antisera against Tom40. The positions of molecular weight markers are indicated on the left. **A.** Tom40 variants spanning amino acids 40 through 50. **B.** Tom40 variants spanning amino acids 50 through 60. **C.** SDS-PAGE analysis. Mitochondria from a control strain and a Δ51-60 strain were dissolved in Laemmli gel cracking buffer and subjected to SDS-PAGE. The gel was transferred to nitrocellulose and immunodecorated with antisera to Tom40 and Tom22. In all panels the control strain was Dupl40.

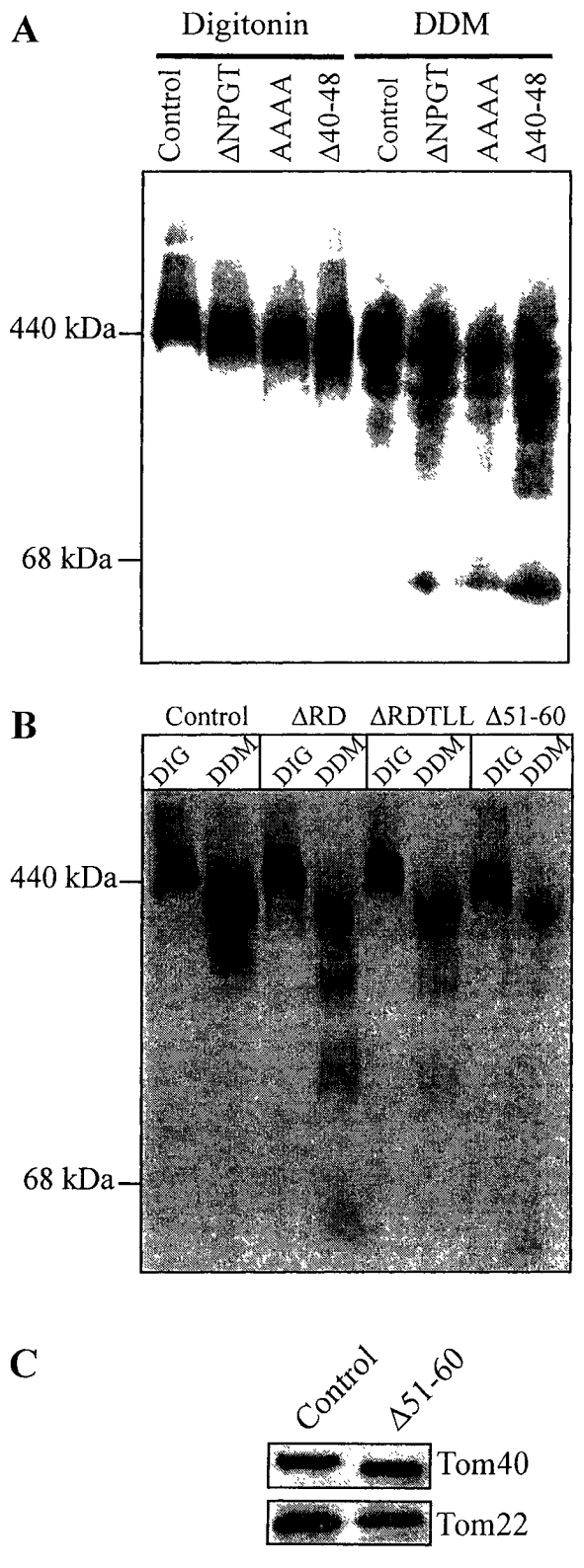

Figure 23. **Characteristics of the Δ321-3 and the 321AAA variants of Tom40. A.** Sequences at the carboxy terminus of Tom40 proteins from *Neurospora crassa* (Nc), *Saccharomyces cerevisiae* (Sc), *Schizosaccharomyces pombe* (Sp), *Mus musculus* (Mm), *Caenorhabditis elegans* (Ce), and *Drosophila melanogaster* (Dm) are shown. Residues in the Nc protein are numbered at the top of the figure. Black shading indicates amino acid identity in at least four of the six species shown. Gray shading indicates amino acids of the same family in at least four of the six species. Residues affected in the carboxy terminal Tom40 variants are indicated below the alignment. Deleted residues are indicated by dashes, while amino acid substitutions are shown in lower case. **B.** Radiolabeled precursors of wild type (Tom40wt) and variants Δ321-3 and 321AAA were imported into wild type mitochondria (NCN251) for 20 min at the indicated temperature. Mitochondria were reisolated and solubilized in buffer containing 1% digitonin. The samples were subject to BNGE, transferred to PVDF membrane, and analyzed by autoradiograpy. The positions of the 400 kDa, 250 kDa, 100 kDa, and monomer (M) species are shown. **C.** Growth of the 321AAA mutant. A control strain (Dupl40, squares) and a 321AAA mutant strain (circles) were inoculated in race tubes and incubated at either room temperature (22°C, filled symbols) or 15°C (open symbols). The extent of mycelial elongation was recorded every 24 hrs. **D.** Import of precursors into 321AAA mitochondria. Import into mitochondria isolated from a control strain (Dupl40), and a 321AAA strain was performed as described in the legend to Fig. 20. **E.** BNGE analysis of C-terminal mutant strains. Mitochondria were isolated from a control (Dupl40) and strains expressing the Tom40 variants 321AAA or the C-terminal deletion of amino acids 329-349 (ΔC-term). Mitochondria were solubilized with either 1% digitonin (DIG) or 1% dodecyl maltoside (DDM) and examined by BNGE. The gel was transferred to PVDF membrane, and immunodecorated with antiserum to the amino terminus of Tom40. The position of the molecular weight markers are indicated on the left.

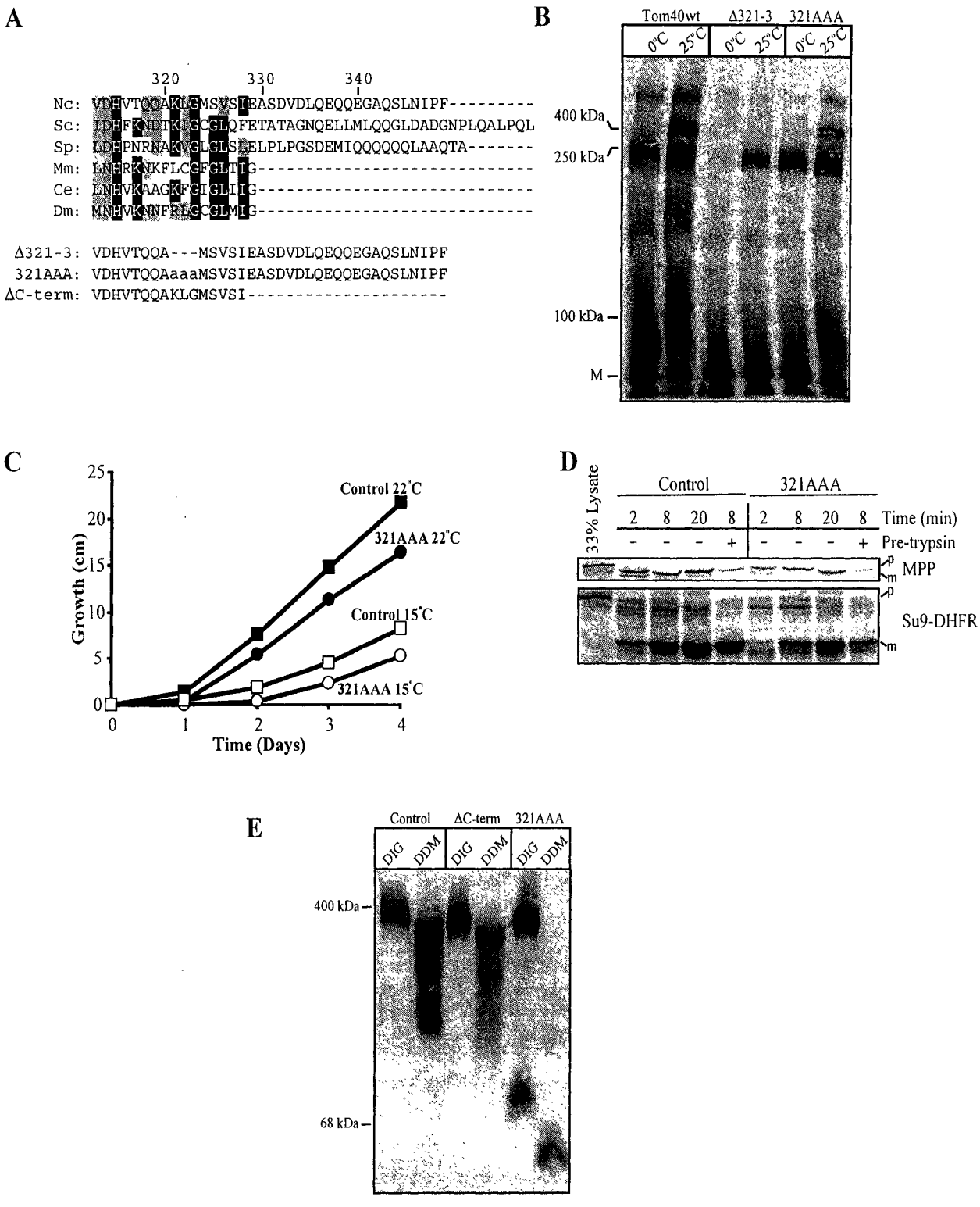

Figure 24. **Deletion of the fungal specific C-terminal extension of Tom40. A.** Import of Tom40wt protein and a Tom40 variant protein containing a deletion of the C terminus of Tom40 (Tom40ΔC), as shown in Fig. 23A, into control mitochondria (NCN251). Imports were performed as in Fig. 17. **B.** Strains containing a deletion of the fungal specific C-terminal extension (ΔC-term) of Tom40 fail to climb the walls of growth flasks and produce fewer asexual conidiaspores compared to the control strain (Dupl40). **C.** Growth rate of the ΔC-term mutant. A control strain (Dupl40, open diamonds) and a ΔC-term mutant strain (FC17-1, filled squares) were inoculated in race tubes and incubated at room temperature. The extent of mycelial elongation was recorded every 24 hrs. **D.** Isolated mitochondria from a control strain (Dupl40) and three strains containing the ΔC-term mutation (FC2-1, FC8-1, and FC17-1) were subjected to SDS-PAGE, transferred to nitrocellulose membrane and decorated with antisera to either the entire Tom40 protein (Total), the C terminus of Tom40 (C terminal) or the N terminus of Tom40 (N terminal). **E.** Mitochondria were isolated from a control strain (Dupl40) and a ΔC-term strain (FC17-1). Radiolabled precursor proteins were imported as detailed in Fig. 20. The precursors used in this experiment were the β-subunit of the F_1ATP synthase ($F_1\beta$), and cytochrome *c* heme lyase (CCHL).

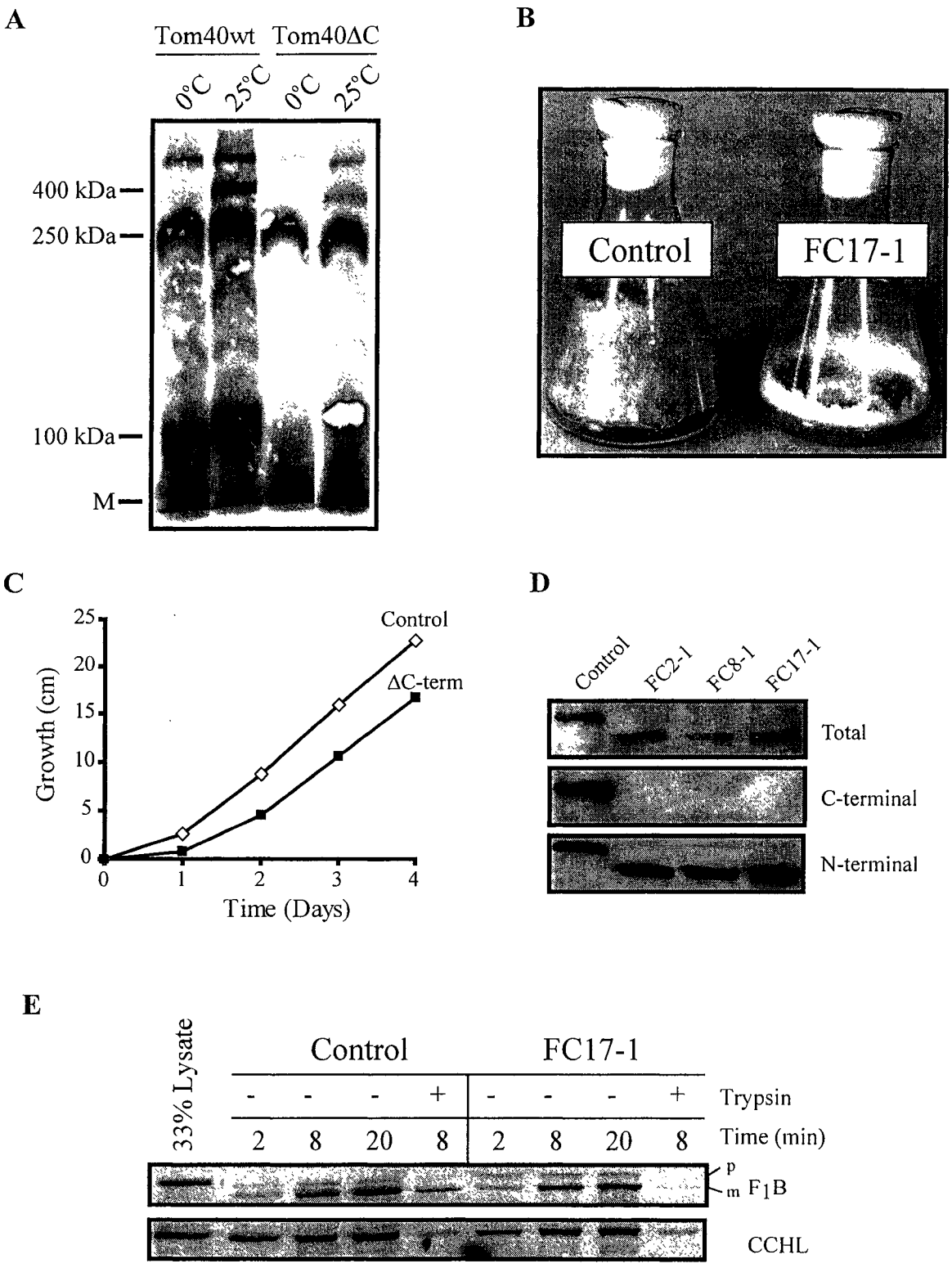

Figure 25. **Kinetics of Tom40 assembly. A.** Import of radiolabeled wild type Tom40 precursor was allowed to proceed into wild type mitochondria (NCN251) for 4 min at 25°C. Mitochondria were re-isolated at 1°C and resuspended in fresh import mix containing no additional Tom40 precursor. Import was allowed to proceed at 25°C with aliquots removed at the times indicated. Mitochondria were re-isolated and processed for BNGE. The gel was transferred to PVDF membrane and analyzed by autoradiography. The sizes and positions of the bands are indicated on the left. **B.** The experiment in panel A was quantified on a phosphorimager and plotted to show the disappearance of radioactive precursor from the 250 and 100 kDa intermediates, and accumulation of radiation in the assembled 400 kDa complex.

A

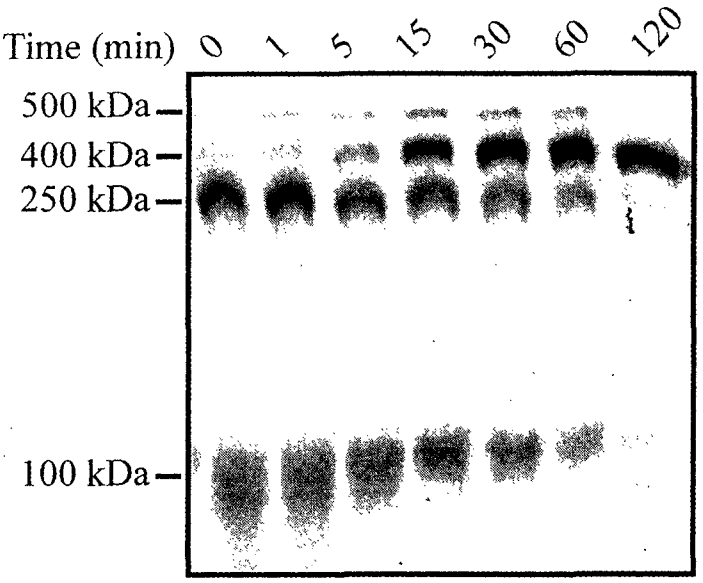

B

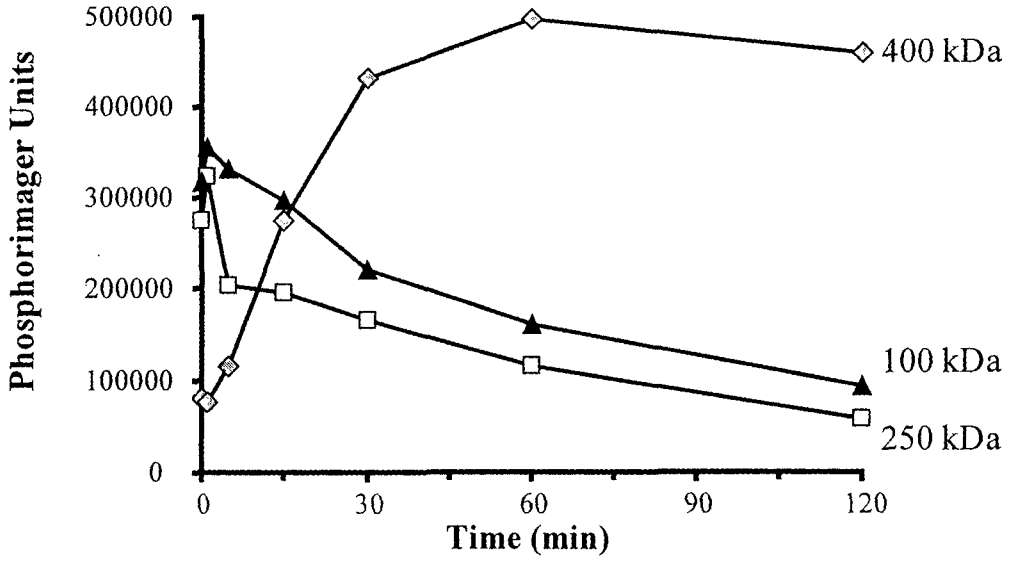

Figure 26. **Sodium carbonate treatment results in assembly of Tom40 precursors into the TOM complex.** For **A** and **B**, radiolabeled precursors of wild type Tom40 or variant Δ51-60, were imported into wild type mitochondria (NCN251) at 0° and 25°C for the times indicated at the bottom of each panel. The samples were divided equally, and mitochondria were pelleted. One tube from each sample was suspended in mitochondrial isolation buffer (Mayer *et al.*, 1993) and was held on ice at 0°C while mitochondria in the other samples were treated with 0.1 M sodium carbonate (pH 11.5). After 30 min on ice, the membrane fraction from the carbonate-treated samples and the untreated mitochondrial samples were pelleted at 2°C. Both pellets were suspended in 1% digitonin and processed for BNGE. **A.** BNGE of untreated samples. **B.** BNGE of carbonate treated samples. **C.** Import of wild type Tom40 precursor into wild type mitochondria (NCN251) was done for 20 min at 0° or 25°C. Each experiment was performed in quadruplicate, and mitochondria were pelleted. In the first set of samples mitochondria were pelleted and the pellets were solubilized in 1% digitonin and processed for BNGE. In the second set of samples, mitochondria were treated with 0.1 M sodium carbonate (pH 11.5). The resulting membrane sheets were pelleted and lysed in digitonin and prepared for BNGE. For the third set of samples, pellets were resuspended in import buffer and treated with proteinase K (0.1 μg/μl) for 15 min at 0°C. Mitochondria were then re-isolated and processed for SDS-PAGE. Finally, the fourth set of samples were subjected to extraction with 0.1 M sodium carbonate (pH 11.5), resuspended in import buffer, and treated with proteinase K as for samples 3. These samples again were processed for SDS-PAGE. Samples not treated with proteinase K and analyzed by BNGE are shown on the left, while samples treated with proteinase K and analyzed by SDS-PAGE are shown on the right as indicated by the numbers below the blots. Gels were transferred to PVDF (BNGE) or nitrocellulose (SDS-PAGE) and analyzed by autoradiography. For all panels, the positions and size of bands are indicated on the left. M, Tom40 monomer. Sample sets are indicated below the panels. The supernatants of the all the carbonate treated samples were analyzed by SDS-PAGE and autoradiography.

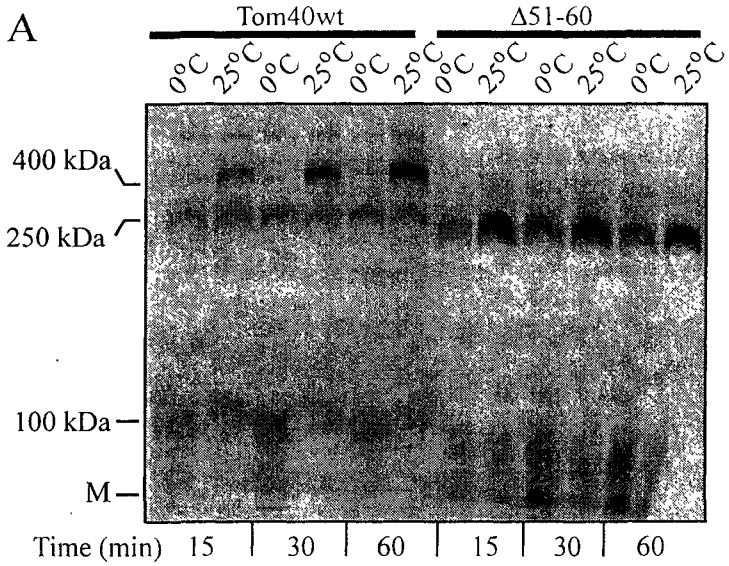

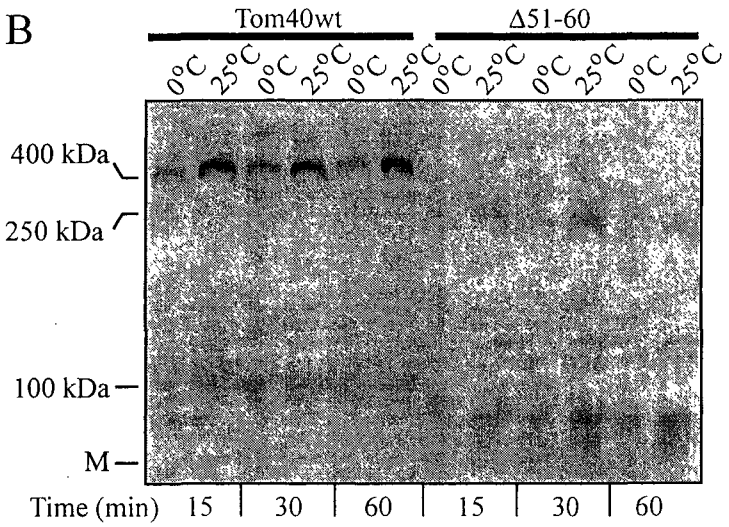

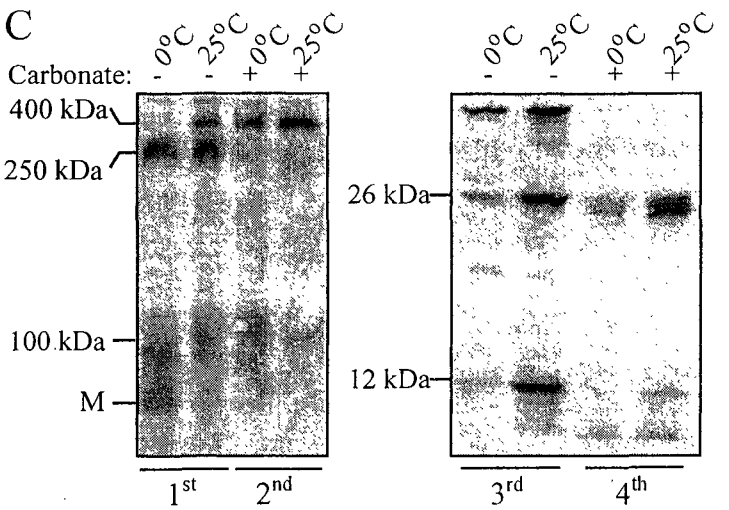

Figure 27. **The Δ321-3 Tom40 precursor is fully extracted from the 250 kDa intermediate by sodium carbonate.** Radiolabeled wild type and Δ321-3 Tom40 precursors were imported into wild type mitochondria (NCN251) and analyzed as described for panels A and B of Fig. 26. The positions and size of bands are indicated on the left. M, Tom40 monomer.

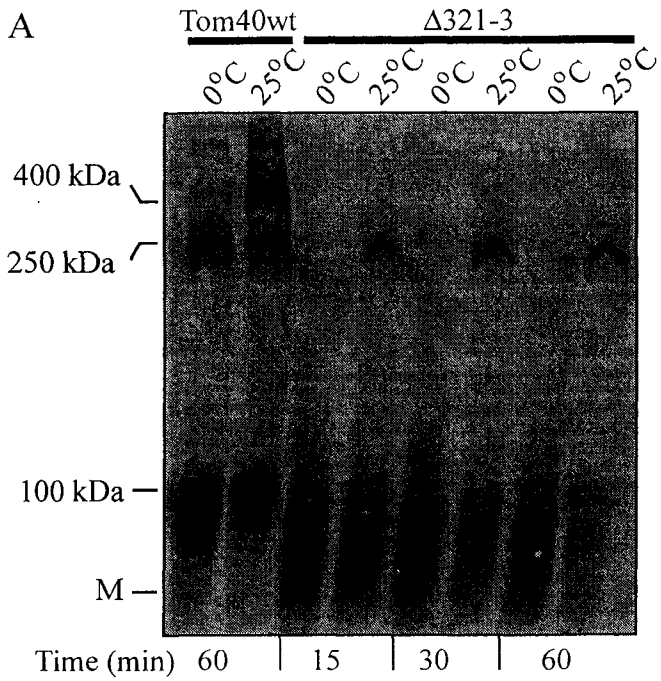

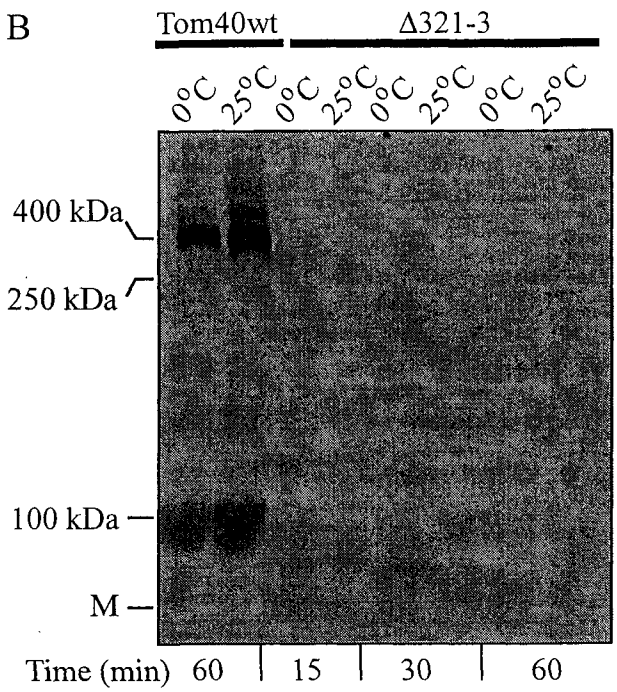

Figure 28. **An alternate pathway of Tom40 assembly in mitochondria containing Tom40 molecules with mutations at the N-terminus. A.** Radiolabeled wild type Tom40 precursor was imported for 20 min at either 0^{o} or 25^{o}C into mitochondria isolated from either control cells (NCN251) or cells expressing only the Δ40-48 mutant version of Tom40. Mitochondria were re-isolated and processed for BNGE. The gel was blotted to PVDF membrane and analyzed by autoradiography. **B.** Samples were processed as described in the legend for Fig. 25, except that the radiolabeled wild type Tom40 precursor was imported into mitochondria isolated from cells expressing only the Δ40-48 mutant form of the Tom40 protein. Duplicates of the 0 min and 10 min samples were subjected to sodium carbonate extraction following import and re-isolation of mitochondria (+carb). A second set of identical samples was treated with proteinase K (PK) after import and reisolation. The samples were processed for SDS-PAGE as described in the legend to Fig. 26. The positions and size of the bands are indicated on the left of all panels. **C.** Mitochondria were isolated from the ΔNPGT (ΔNPGT or ΔN) and AAAA (NPGT-AAAA or N-A) strains and treated as described for panel B, except that no PK digestion was performed. **D.** Mitochondria from the Δ51-60 strain were isolated and treated as described in panel B. M, Tom40 monomer.

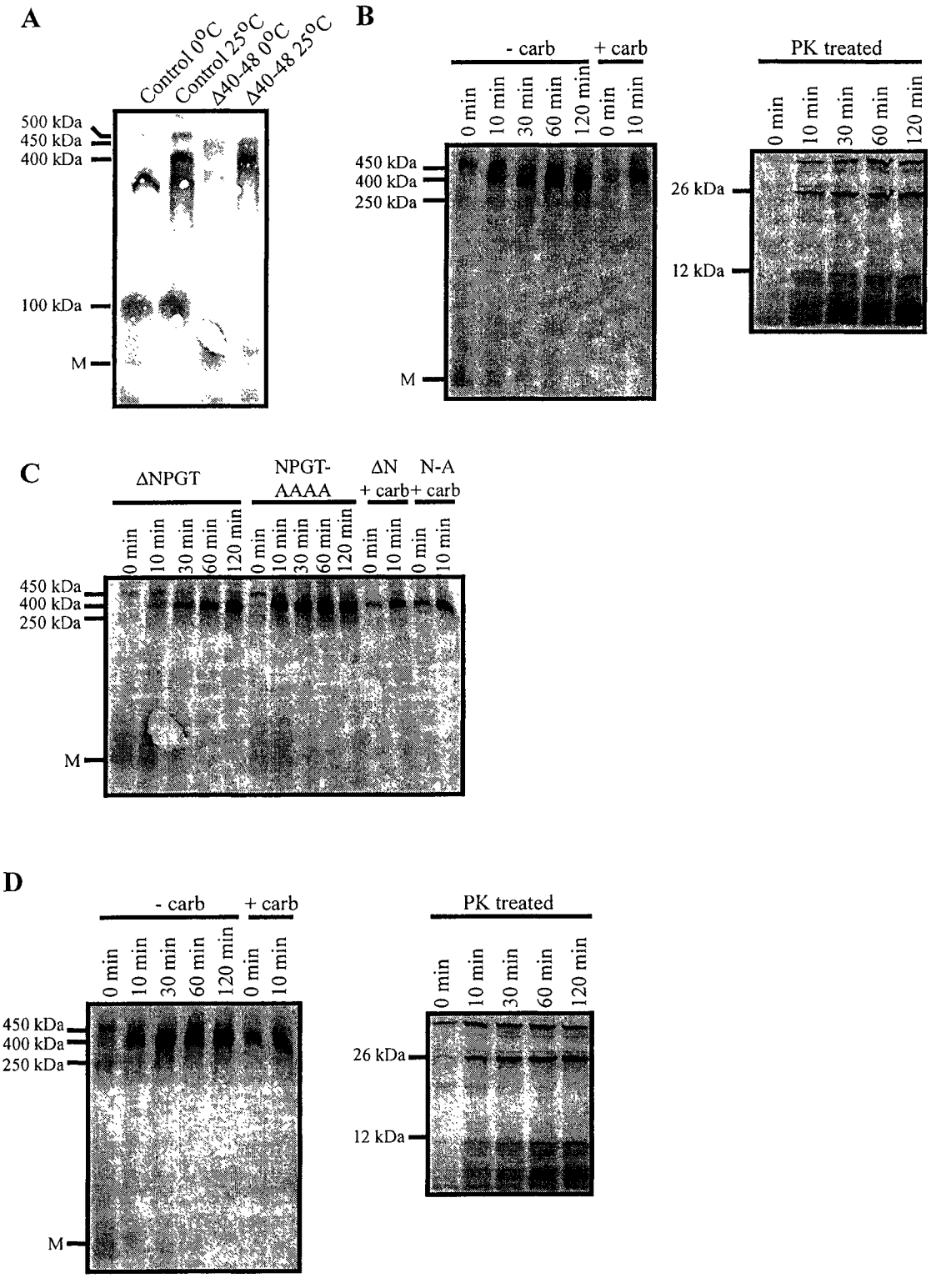

Figure 29. **Not all mitochondria containing mutant forms of Tom40 show the altered assembly pathway. A.** Samples were prepared as described in the legend for panel A, Fig. 28, except that the mitochondria used for import contained a replacement of two conserved lysine residues with glutamine at positions 237 and 238 of Tom40 (WQQ). **B.** Protease treated samples were prepared as described in the legend for panel B, Fig. 28, with the substitutions described in **A.** The positions and size of the bands are indicated on the left of each panel.

A

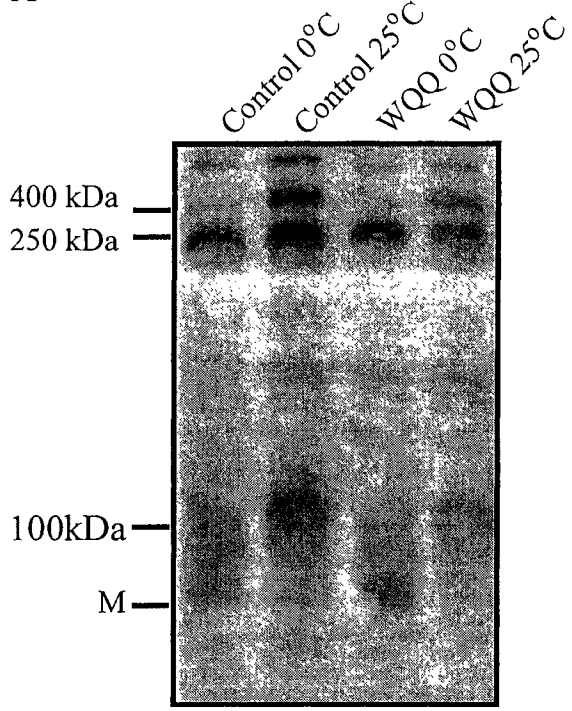

B

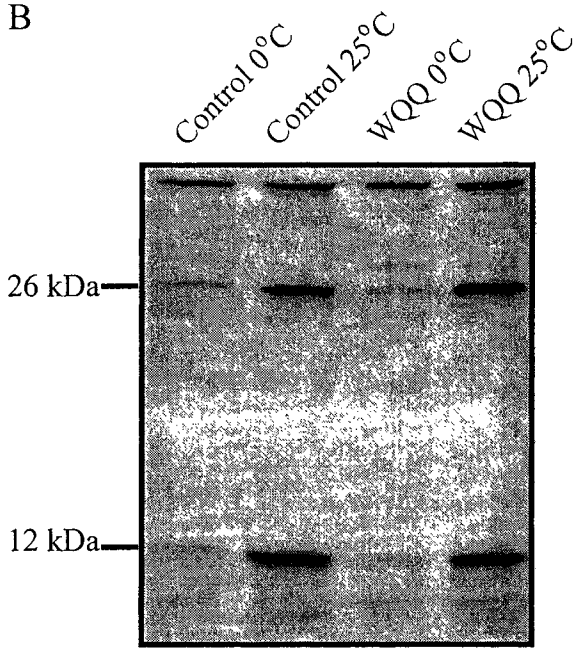

Figure 30. **Predicted topology of TOM40.** This model for the topology of Tom40 was provided by T. Schirmer, via D. Rapaport. Tom40 is indicated by dotted lines. The numbers in the white boxes indicate the span of amino acids predicted to span the outer mitochondrial membrane as β-strands. The shaded boxes refer to those amino acids targeted for mutagenesis (see Text).

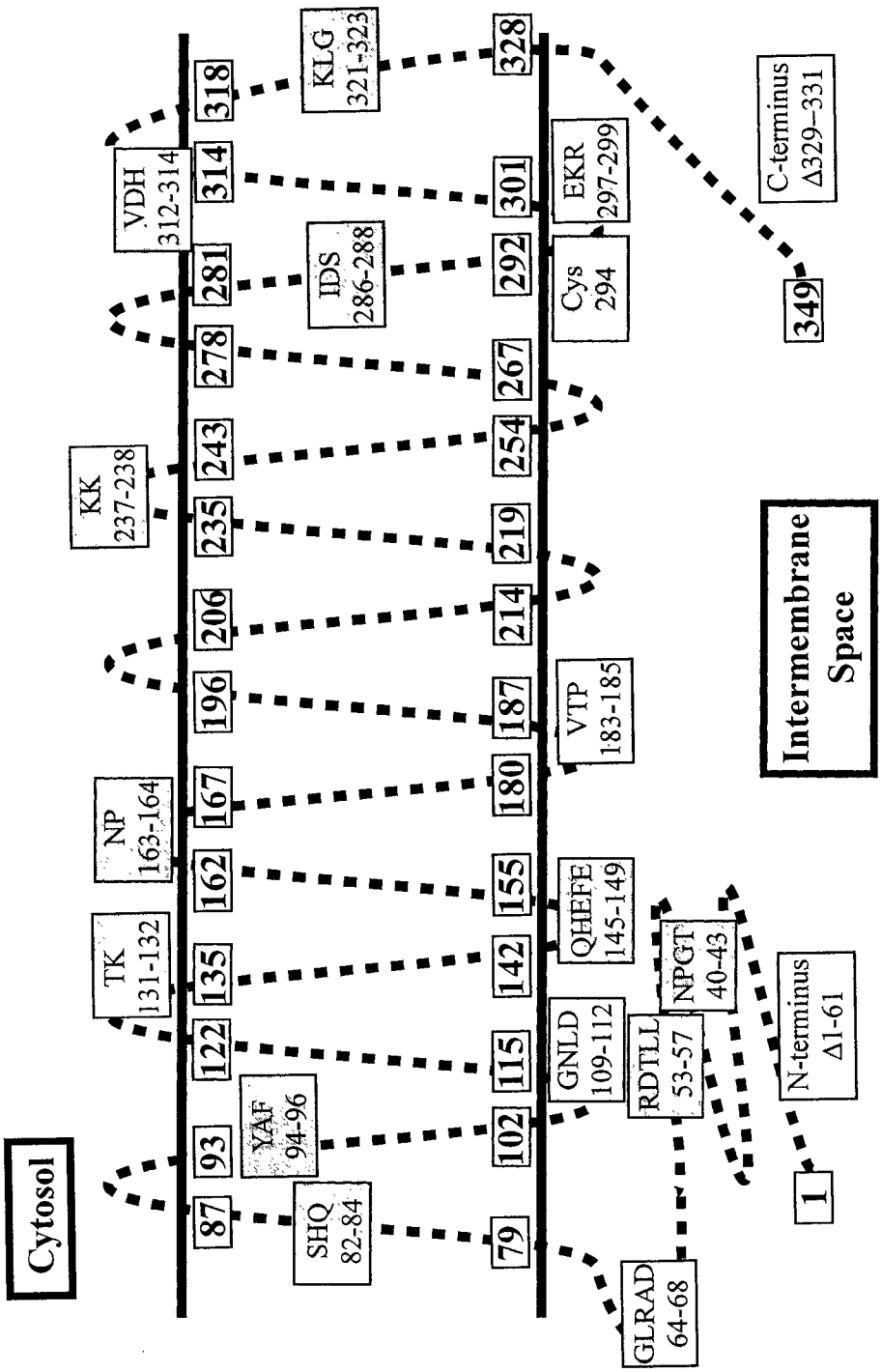

Figure 31. **Examples of classes of *in vitro* assembly phenotypes identified for the Tom40 proteins.** Import was performed as described in Fig. 17. Five classes of assembly mutants were identified. For a full listing of all mutations tested and the assigned assembly class, see Table 6. **A.** Assembly of wild type Tom40 protein (Wild type). **B.** No assembly past initial binding of mitochondrial receptors. The C7 stop mutation produces a stop codon at amino acid 317 of the protein, and results in deletion of the last predicted membrane-spanning domain of Tom40 (Fig. 30). **C.** As shown previously in Figs.17, and 26, a Tom40 variant containing the Δ51-60 mutation does not progress past the 250 kDa intermediate of Tom40 assembly. **D.** A class of mutations in Tom40 that result in accumulation of precursors at the 250 kDa intermediate, while some precursor still progresses to the 400 kDa complex. The examples shown here are Tom40 variant proteins with either deletion of amino acids 163-164 (ΔNP) or replacement of these amino acids with alanine (NP-AA) **E.** A class of mutations which result in accumulation of precursor protein in the 100 kDa intermediate. The example used in this panel is a Tom40 variant protein with a replacement of amino acids 297-299 with alanine (EKR-AAA). **F.** The final class of assembly phenotype is wild type assembly. The example used in this panel is a Tom40 variant containing a deletion of amino acids 109-112 (ΔGNLD).

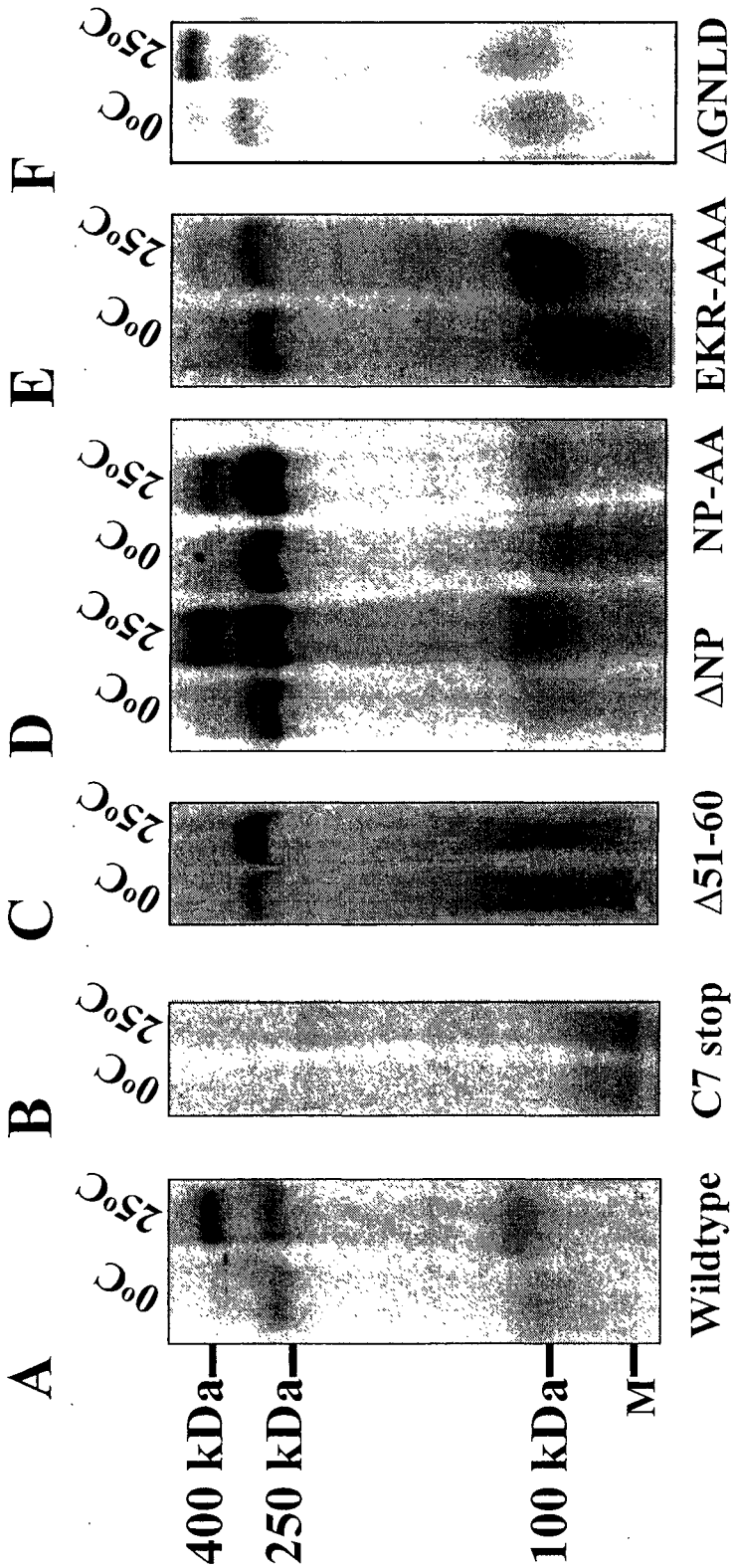

Figure 32. **Strains containing additional mutations made in the Tom40 protein. A.** Growth rates of the WQQ strain were performed as in Fig. 19 at room temperature. A control strain (Dupl40, black squares) is compared to the WQQ strain (open circles). **B.** Growth rates of P-A (open squares) and YAF-AAA (grey triangles) were performed as described in panel A compared to a control strain (Dupl40, black diamonds). **C.** Mitochondria were prepared and examined on BNGs as for Fig. 22. Positions of molecular weight markers are indicated on the left of the panel. **D.** Isolated mitochondria from the indicated strains were subjected to SDS-PAGE, blotted to nitrocellulose membranes and immunodecorated with antisera directed against the indicated proteins. (Control, Dulp40.)

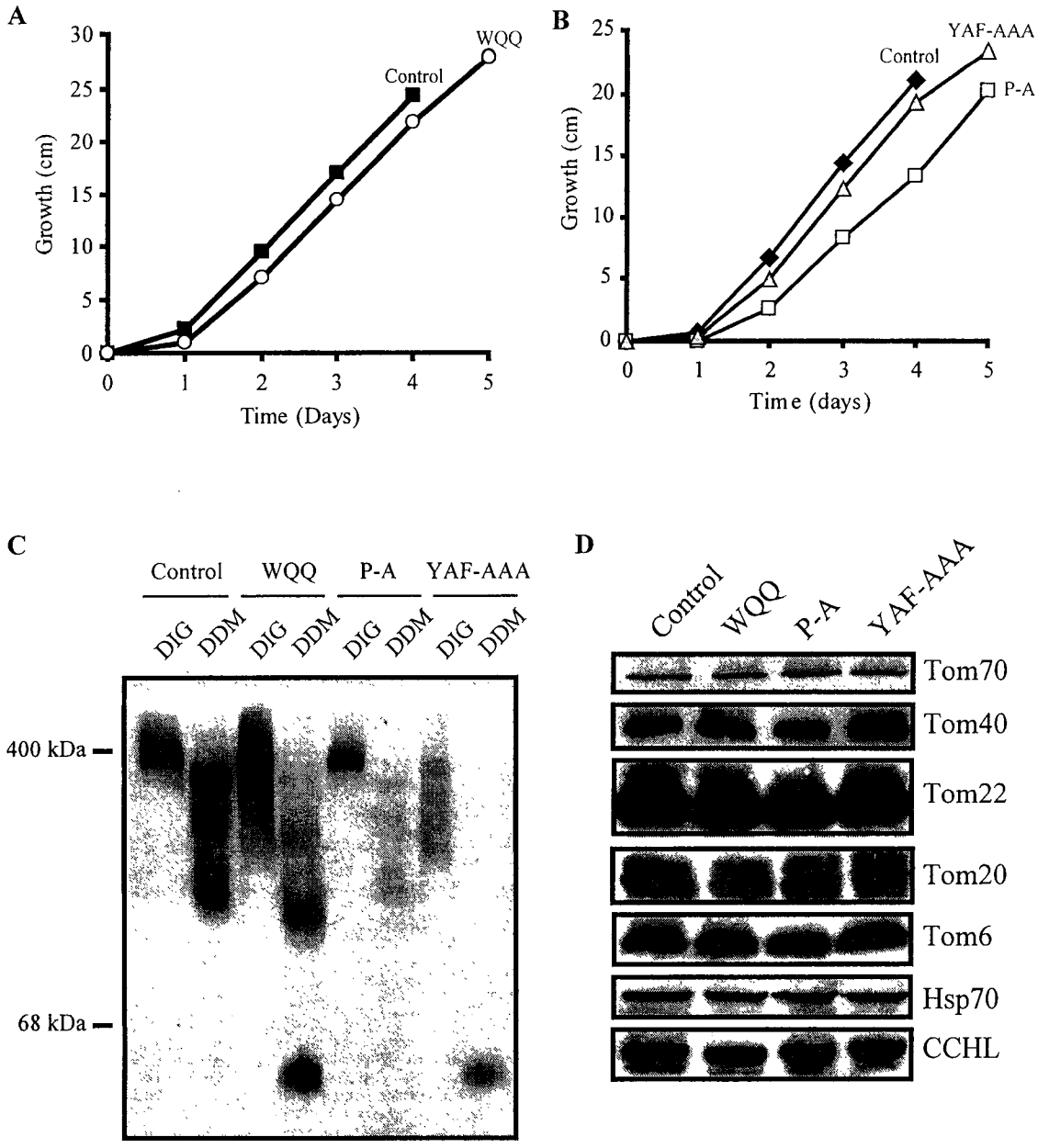

Figure 33. **Import of radiolabeled precursor proteins into additional Tom40 mutant strains.** Import was performed as for Fig. 20 with the exception that the radiolabeled precursors used were the matrix processing peptidase (MPP), cytochrome *c* heme lyase (CCHL), the first 69 amino acids of subunit 9 of the F_0 ATP synthase fused to mouse dihydrofolate reductase (Su9-DHFR), the β subunit of the F_1 ATP synthase ($F_1\beta$), or cytochrome *c* heme lyase (CCHL). The control strains for these experiments is Dupl40. The mutant strain for each set of panels is indicated on the left of the figure. (p, precursor form; m, mature form.)

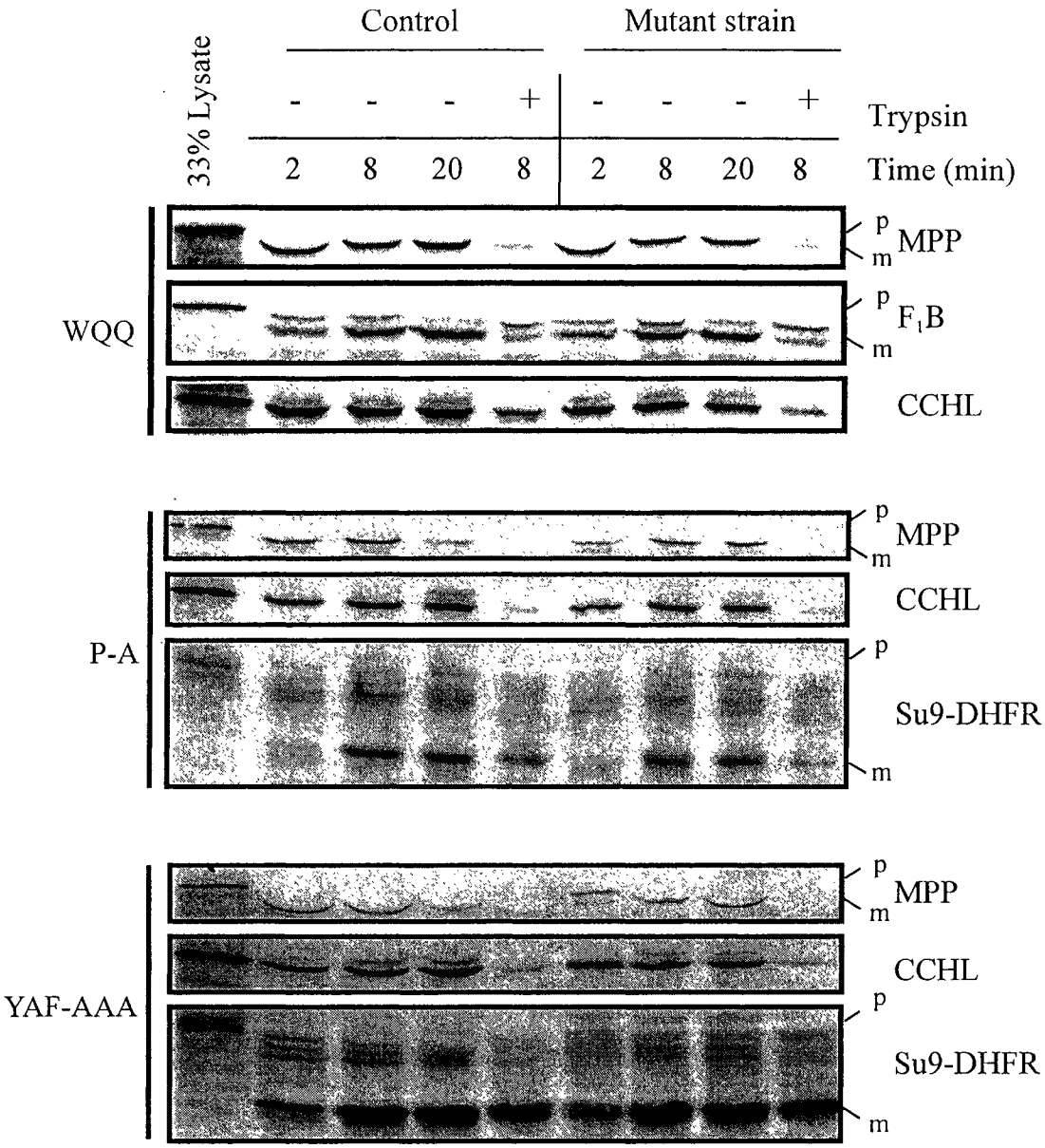

Figure 34. **Isolated mitochondrial outer membrane vesicles**. **A.** Proteins of purified OMVs and IMFs from wild type mitocondria were subjected to SDS-PAGE and silver stained. The positions of Tom70, Tom40 and porin (deduced as described in the text) are shown on the left hand side of the figure. The region from which the bands were excised for mass spectroscopy (MS) is indicated. **B.** Western analysis of OMVs and IMFs. Membranes were decorated for proteins of the outer membrane Tom70, Tom40, Tom22 and Tom5, a protein of the inner membrane, the ATP/ADP carrier (AAC), and a mitochondrial matrix protein, Hsp70.

A

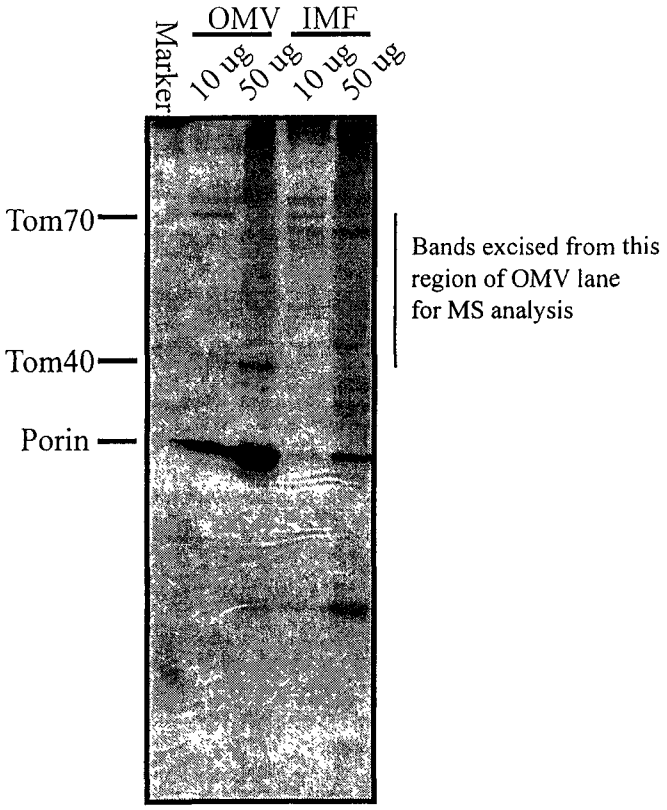

B

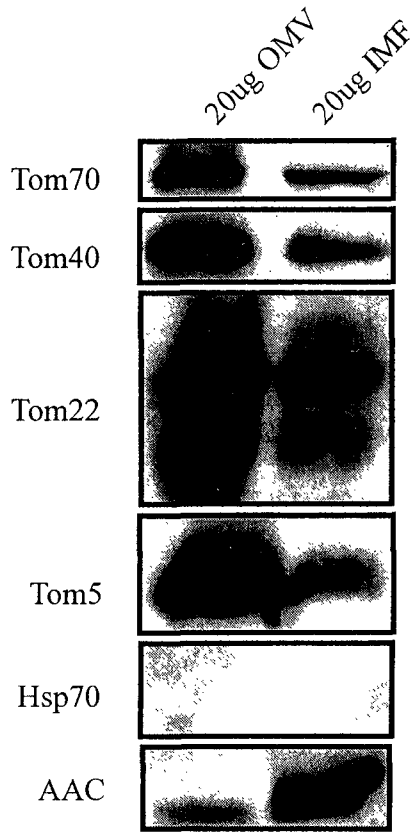

Figure 35. **Two computer predicted topologies for *N. crassa* Tom40.** Predicted membrane-spanning domains of Tom40 are shown in boxes on the protein sequence. **A.** Predicted topology as in (Court *et al.*, 1995). **B.** Predicted topology by T. Schirmer (D. Rapaport, personal communication). Also shown in Fig. 30.

A

```
  1  MASFSTESPL AMLRDNAIYS SLSDAFNAFQ ERRKQFGLSN PGTIETIARE
 51  VQRDTLLTNY MFSGLRADVT KAFSLAPLFQ VSHQFAMGER LNPYAFAALY
101  GTNQIFAQGN LDNEGALSTR FNYRWGDRTI TKTQFSIGGG QDMAQFEHEH
151  LGDDFSASLK AINPSFLDGG LTGIFVGDYL QAVTPRLGLG LQAVWQRQGL
201  TQGPDTAISY FARYKAGDWV ASAQLQAQGA LNTSFWKKLT DRVQAGVDMT
251  LSVAPSQSMM GGLTKEGITT FGAKYDFRMS TFRAQIDSKG KLSCLLEKRL
301  GAAPVTLTFA ADVDHVTQQA KLGMSVSIEA SDVDLQEQQE GAQSLNIPF
```

B

```
  1  MASFSTESPL AMLRDNAIYS SLSDAFNAFQ ERRKQFGLSN PGTIETIARE
 51  VQRDTLLTNY MFSGLRADVT KAFSLAPIFQ VSHQFAMGER LNPYAFAALY
101  GTNQIFAQGN LDNEGALSTR FNYRWGDRTI TKTQFSIGGG QDMAQFEHEH
151  LGDDFSASLK AINPSFLDGG LTGIFVGDYL QAVTPRLGLG LQAVWQRQGL
201  TQGPDTAISY FARYKAGDWV ASAQLQAQGA LNTSFWKKLT DRVQAGVDMT
251  LSVAPSQSMM GGLTKEGITT FGAKYDFRMS TFRAQIDSKG KLSCLLEKRL
301  GAAPVTLTFA ADVDHVTQQA KLGMSVSIEA SDVDLQEQQE GAQSLNIPF
```

Figure 36. **Regions in Tom40 chosen for initial cysteine scanning mutagenesis.** Boxed residues indicate those chosen for cysteine scanning.

```
  1 MASFSTESPL AMLRDNAIYS SLSDAFNAFQ ERRKQFGLSN PGTIETIARE
 51 VQRDTLLTNY MFSGLRADVT KAFSLAPLFQ VSHQFAMGER LNPYAFAALY
101 GTNQIFAQGN LDNEGALSTR FNYRWGDRTI TKTQFSIGGG QDMAQFEHEH
151 LGDDFSASLK AINPSFLDGG LTGIFVGDYL QAVTPRLGLG LQAVWQRQGL
201 TQGPDTAISY FARYKAGDWV ASAQLQAQGA LNTSFWKKLT DRVQAGVDMT
251 LSVAPSQSMM GGLTKEGITT FGAKYDFRMS TFRAQIDSKG KLSCLLEKRL
301 GAAPVTLTFA ADVDHVTQQA KLGMSVSIEA SDVDLQEQQE GAQSLNIPF
```

Figure 37. **The structure of the TOM complex in SCAM strains.** BNGE of isolated mitochondria from a selection of SCAM strains, compared with a the TOM complex containing the cysteineless version of Tom40. The gel was transferred to PVDF membrane and blotted for Tom40. The positions of molecular weight markers are indicated on the left of the blot.

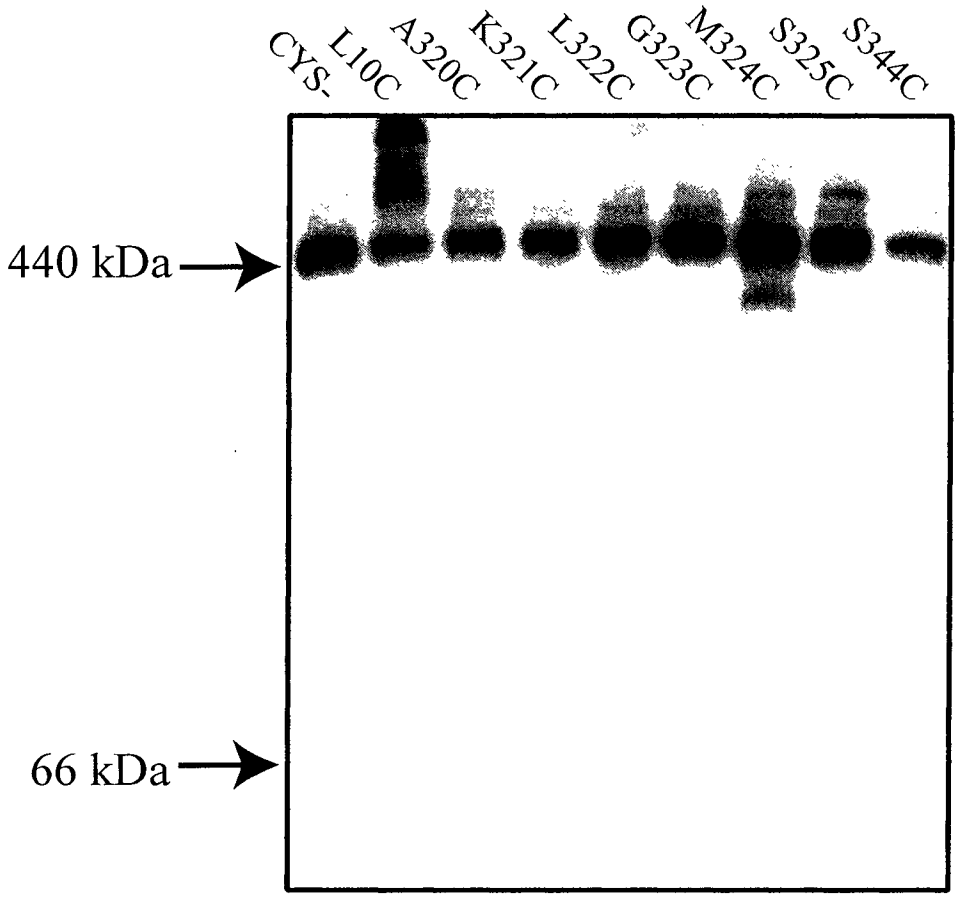

Figure 38. **The procedure of cysteine scanning mutagenesis.** Outline of the SCAM procedure which is described in detail in the text (see section 3.9).

Step 1

Create series of strains expressing Tom40 with single-cysteine replacements in each protein

Step 2

Grow strains and isolate mitochondria

Step 3

Treat with biotin maleimide

Step 4

Wash mitochondria to remove excess label

Step 5

Lyse in IP buffer plus TritonX-100, immunoprecipitate Tom40 with C-terminal peptide antibody

Step 6

Subject immunoprecipitated samples to SDS-PAGE and transfer to nitrocellulose membranes.

Step 7

Detected presence of label with streptavidin-biotinylated HRP conjugate and ECL

Figure 39. **N^{α}-(3-maleimydylpropionyl) biocytin (biotin maleimide). A.** The chemical structure of biotin maleimide. **B.** The sulfhydryl specific cysteine modification reaction with biotin maleimide.

A

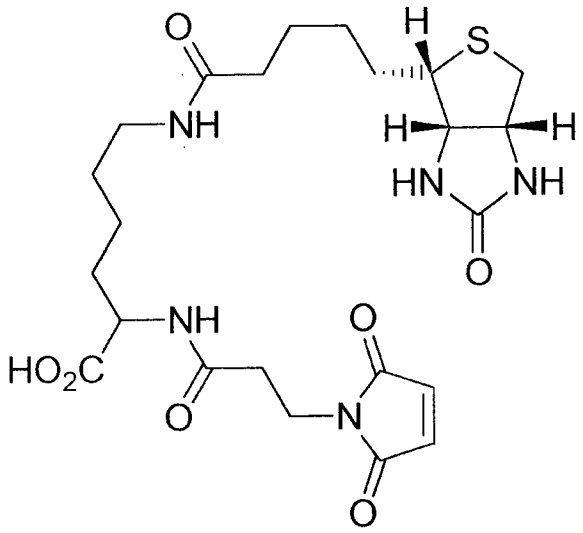

B

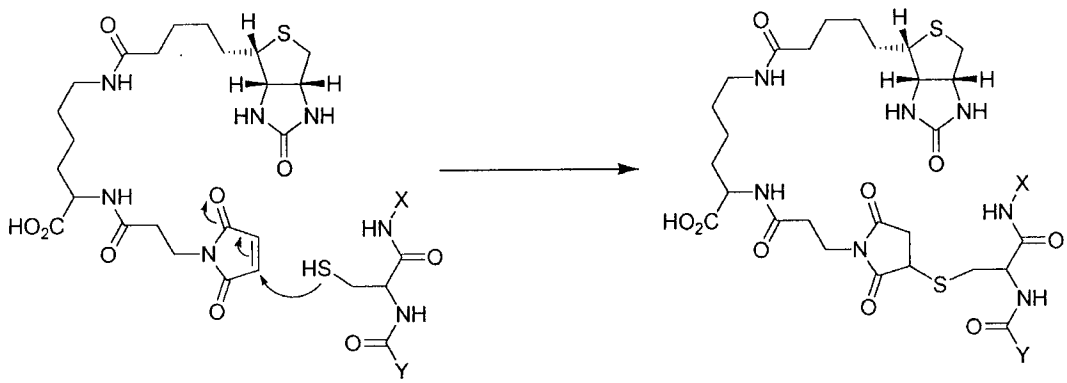

Figure 40. **Results of the cysteine scanning mutagenesis procedure. A.** Biotin maleimide labeling of specific cysteine substitution strains. The name of the strain corresponding to each lane is listed above. The CYS- strain is a strain that lacks the single endogenous cysteine residue in Tom40, and serves as a negative control. The L10C, and S344C strains contain single cysteine replacements in the extreme N- and C-termini of the protein, respectively, and are predicted to be accessible to biotin labeling since they exist in the intermembrane space. Thus, these strains act as positive controls for the experiment. Controls are indicated by a horizontal bracket on each gel. The D334C residue (bottom of panel A) is indicated by bracketed vertical bars because this lane was taken from a different gel. **B.** The cysteine scanning experiment from the V316C-G323C trial was used for immunodecoration with α-Tom40 antiserum derived from mouse. This verifies that the Tom40 immunoprecipitation was efficient, and Tom40 is present in each lane of the gel.

A

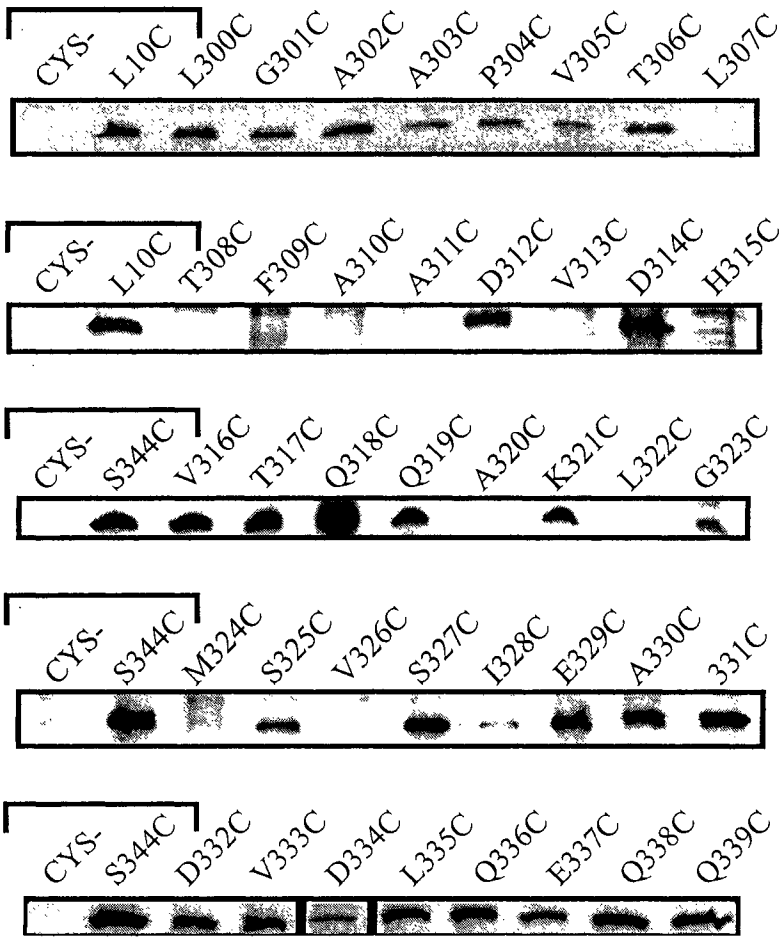

B

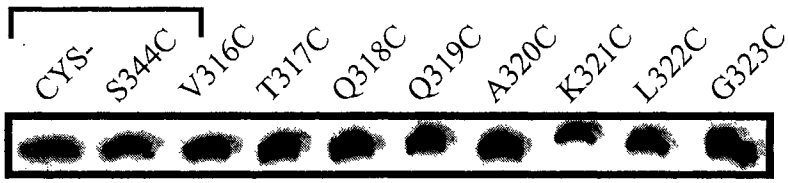

Figure 41. **A model of R-group orientation in antiparallel β-strands.** Depicted is a pair of anti-parallel β-strands, the GREEN arrows indicated the N- to C- terminal arrangement of the amino acids within each strand. DASHED lines indicate hydrogen bonds between the two strands. The R-groups of the polypeptide chains alternate between each side of the β-strand. Figure adapted from (Voet, 1990).

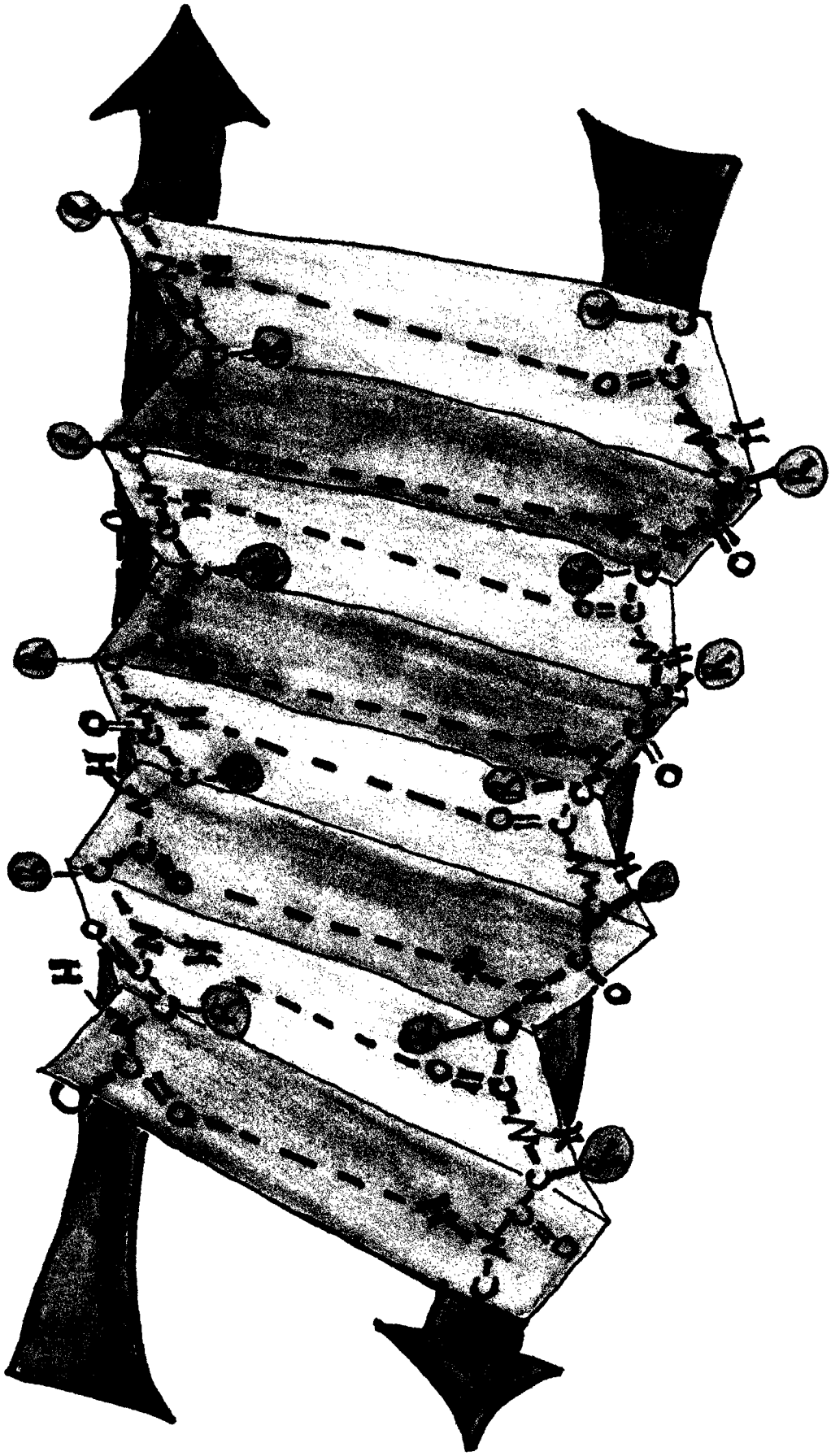

Figure 42. **Model of Tom40 topology determined by SCAM.** β-sheets are depicted spanning the bilayer of the mitochondrial outer membrane. Residues in blue represent those protruding into the Tom40 pore. Those in red are in the bilayer.

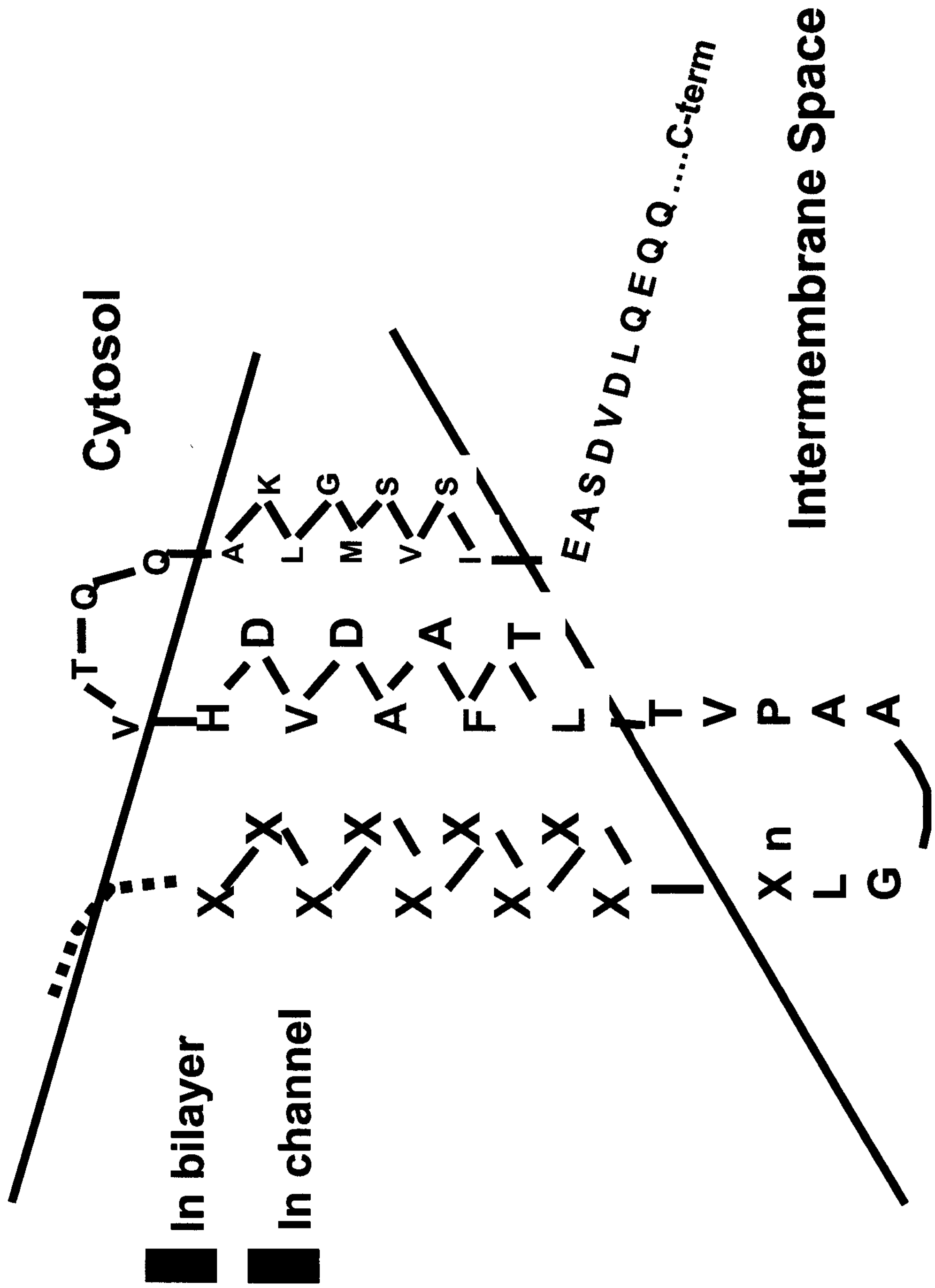

4. DISCUSSION

4.1 The *tom40* null strain

Tom40 was previously shown to be essential for the viability of *S. cerevisiae* cells and reduced levels of Tom40 resulted in the accumulation of mitochondrial precursors in the cytosol of mutant cells (Baker *et al.*, 1990). I have confirmed these results, showing that *tom40* is an essential gene in *N. crassa* and that mitochondria containing reduced levels of Tom40 are deficient in their capacity to import precursor proteins *in vitro*. When the sheltered heterokaryon, RIP40het, was made deficient in Tom40, it grew slowly compared to control strains. This is most likely related to a decreased capacity of the deficient strain to accumulate essential mitochondrial factors. The original findings in yeast by Baker *et al.* (1990), have been extended, as I have shown that mitochondria with lowered levels of Tom40 are smaller than normal and are devoid of cristae. These results are reminiscent of mitochondria observed in slow growing cells deficient in other important components of the TOM complex such as Tom20 and Tom22 (Harkness *et al.*, 1994b; Nargang *et al.*, 1995). Mitochondria deficient in Tom40 also have reduced levels of the TOM core complex components Tom22 and Tom6. These deficiencies are most likely due to the inability to import and/or assemble the proteins in the absence of Tom40. I have ruled out the possibility that reduced levels of Tom40 might signal reduced transcription of these genes by demonstrating that the mRNA for Tom22 is present at normal levels.

4.2 Role of a conserved region in the N-terminus of *tom40* on Tom40 assembly

Very little is known about the processes of Tom40 membrane insertion, and TOM complex assembly. Previous work has suggested that Tom40 must exist in a partially folded conformation for recognition and assembly into the TOM complex and is dependent on the receptors Tom20 and Tom70 for initial precursor binding (Rapaport and Neupert, 1999). More recent evidence has implicated the small Tom proteins in the assembly process as well (Model *et al.*, 2001). To determine which domains of Tom40 may be important for this process I mutagenized conserved regions of *N. crassa* Tom40 and characterized the variant proteins with regard to their ability to assemble into the

TOM complex *in vitro*. A subset of these mutations was further analyzed to determine their effects on TOM complex function and stability *in vivo*.

Previous findings showed that the highly conserved region containing amino acid residues 41-60 of Tom40 was not needed for binding of the Tom40 precursor to the receptors or for membrane insertion but was crucial for the assembly of the protein into the TOM complex (Rapaport *et al.*, 2001). Various mutations in cDNA clones were made so that the import of variants could be assessed by *in vitro* assembly assays. First, mutations were made affecting the residues 40-48. Mutations were made that deleted the highly conserved NPGT (ΔNPGT) domain, replaced NPGT with alanine (AAAA) and deleted amino acids 40-48 while replacing amino acid 49 with alanine (Δ40-48). The Δ40-48 variant of Tom40 had the most severe *in vitro* import defect, showing reduced assembly to the 400 kDa complex. The smaller mutations resulted in a slight inhibition of assembly of Tom40 to the 400 kDa assembled form.

To determine the importance of the 40-50 region of Tom40 *in vivo,* genomic versions of the cDNA alleles described above were constructed. All mutant alleles were capable of rescuing the *tom40* null strain, but resulted in the formation of TOM complexes with altered electrophoretic mobility and stability *in vivo*. The changes in mobility likely reflect changes in conformation of the TOM complex as all mutants analyzed displayed similar mobility changes, whereas the molecular weight of Tom40 in the AAAA mutant is not significantly different from that of the wild type form. The TOM complexes in all the mutant strains are also less stable than wild type as Tom40 monomers were lost from the mutant strains after solubilization in dodecylmaltoside. It seems likely that the highly conserved NPGT sequence, which is affected in all three strains, may play a role in mediating stability of the TOM complex. The *N. crassa* strains expressing the Tom40 variants were also altered in their ability to form conidia and exhibited growth defects. The region spanning amino acids 40-50 may also play a role in import of mitochondrial preproteins, as mitochondria expressing only ΔNPGT and AAAA forms of Tom40 showed a decreased ability to import preproteins *in vitro* compared to control strains.

Mutations were also made in the region encompassing amino acids 50-60 of Tom40. Deletion of the entire region (Δ51-60) resulted in a form of the Tom40 protein that was unable to progress past the 250 kDa intermediate assembly stage in *in vitro* assays, and was unable to progress to the fully assembled TOM complex even after 60 min of import at 25° C. The deletion of residues 51-60 does not totally abrogate assembly *in vivo* since strains expressing only this form of the protein are viable. Strains expressing a deletion of the conserved RD residues (ΔRD), RDTLL residues (ΔRDTLL) and the Δ51-60 mutant (Fig. 19B) all display growth defects and alterations in TOM complex stability. It is surprising to note that mitochondria from the Δ51-60 strain, do not show a reduction in import of mitochondrial preproteins in *in vitro* import assays. This may suggest that the region spanning amino acids 40 to 50 is more important for function of Tom40 within the TOM complex, whereas the region spanning amino acids 50 to 60 is important for assembly of Tom40 into the TOM complex. Regardless, the regions encompassed by both the Δ40-48 and Δ51-60 mutations play an important role for achieving the interactions necessary for progression past the 250 kDa intermediate on the Tom40 assembly pathway.

Several observations support the view that the impaired assembly of Tom40 mutant variants reflects a specific function of the affected amino acid residues rather than simple misfolding of the mutant forms. Wild type Tom40 that is appropriately assembled into the TOM complex yields characteristic 26 kDa and 12 kDa fragments upon treatment of mitochondria with proteinase K (Künkele *et al.*, 1998b). These cleavage products can be generated from all of the Tom40 mutant constructs used in this study (data not shown). The same fragments can be generated after integration of full-length Tom40 precursor into the membrane of isolated mitochondria at a stage when Tom40 is not yet assembled into the complex (Rapaport and Neupert, 1999; Rapaport *et al.*, 2001). Thus, Tom40 appears to reach its final, or near final, conformation rather early in its assembly pathway, and the actual integration of Tom40 precursor into the core of the TOM complex may not induce major conformational changes.

Many unanswered questions remain in regards to the N-terminal Tom40 mutants. How does a region in the N-terminus of Tom40, predicted to lie within the

intermembrane space, affect the import of mitochondrial precursor proteins, the stability of the TOM complex, and the assembly of incoming Tom40 precursor molecules? It is possible that this region of the protein contributes to the dimerization of Tom40. If true, mutations in this region would likely affect stability of the TOM complex. The 40-50 region may play a role in *trans* site binding, so that these mutations would affect the efficiency of import of preprotein destined to all mitochondrial subcompartments, with the possible exception of those residing in the outer membrane. Finally, this region may play some role in establishing interactions with other components of the TOM complex such as Tom6 and Tom22. Both of these proteins have been implicated in either stability of the TOM complex or establishing higher order TOM complex structures. In support of this hypothesis, Tom6 is lost from the mitochondria isolated from strains containing mutations in the 40-50 region, in the same manner that Tom40 is lost (data not shown).

4.3. Role of a conserved region in the C-terminus of Tom40

Mutations were also made in the conserved KLG residues near the C-terminus of Tom40. Two computer predictions of Tom40 structure place this region within the last membrane-spanning domain of Tom40 (T Schirmer, via D. Rapaport, personal communication) (Mannella *et al.*, 1996) while one does not (Court *et al.*, 1995). Two different Tom40 variants were constructed, one lacking the KLG residues (Δ321-3) and one replacing these residues with alanine (321AAA). Both types of cDNA Tom40 variants were used in *in vitro* Tom40 assembly assays, and genomic variant constructs were used to determine the *in vivo* relevance of the mutated residues. The lack of assembly to any high molecular weight intermediate of the Δ321-3 variant at 0° C in *in vitro* Tom40 assembly assays was striking. At this temperature the altered protein may not be in an import competent conformation. At 25° C, the precursor can be imported to the 250 kDa intermediate but cannot proceed to the membrane integration step of the assembly pathway. The severity of the assembly defects *in vitro* are supported by the observation that the genomic *tom40* construct bearing the Δ321-3 mutation cannot rescue the *tom40* null nucleus. There are a number of possible reasons that the Δ321-3 variant fails to assemble past monomer binding at 0°C and arrests at the 250 kDa intermediate at 25°C. It has been shown that Tom40 must be in a partially folded state for effective

integration into the membrane (Rapaport and Neupert, 1999). It is possible that the Δ321-3 variant may be unable to achieve the correct conformation for integration. However, it seems unlikely that there are gross overall changes in conformation at 25° C since the protein assembles past the initial precursor recognition stage and into the 250 kDa intermediate *in vitro*. Another possibility is that the KLG residues might provide a specific signal for Tom40 integration into the membrane or assembly with other TOM complex components, but this seems unlikely as changing the residues to alanine has little effect on *in vitro* assembly. In addition, a *tom40* gene encoding the 321AAA variant can restore viability to the $tom40^{RIP}$ nucleus, although the resulting strains have growth and TOM complex defects. Finally, it is conceivable that the KLG residues form part of a membrane-spanning domain. In this case, a reasonable explanation for the drastically different behavior of the deletion and substitution variants could be that replacement with alanine residues still allows the region to span the membrane, while loss of the residues does not allow membrane spanning and prevents integration. Such a membrane-spanning region might also be important for channel formation. It should be noted that the results of the cys-scanning experiments strongly support the idea that these residues occur in a membrane-spanning β-strand.

Given its position near the C-terminus and the striking fragility of the TOM complex from the 321AAA strain, it is conceivable that the region could also be involved in maintaining interactions between TOM complex subunits. The presence of the Tom40 dimer sized complex in digitonin treated samples is reminiscent of the subcomplexes of Tom40 dimers seen in Tom22 deficient yeast cells (van Wilpe *et al.*, 1999). Thus, the 321AAA Tom40 mutant might have weakened interactions with Tom22. The breakdown of the complex in 321AAA mitochondria to Tom40 monomers following solubilization with dodecylmaltoside suggests that the region could also contribute to the formation and maintenance of Tom40 dimers.

4.4 The nature of Tom40 assembly intermediates in *N. crassa*

Tom40 assembly into the TOM complex is thought to occur through a variety of translocation intermediates. It has been suggested that Tom40 initially binds the TOM complex as a monomer. This monomer then progresses to a 250 kDa complex of unknown composition. At this stage Tom40 is thought not yet to be incorporated into the mitochondrial outer membrane. The Tom40 precursor molecule then progresses to a 100 kDa intermediate, which most likely consists of the Tom40 precursor protein in association with a pre-existing molecule of Tom40 (Model *et al.*, 2001). Another model suggests that assembly occurs directly from the 250 kDa to 400 kDa complexes and that the 100 kDa form is non-productive (Rapaport and Neupert, 1999). The experiments presented in this thesis are consistent with the notion that both the 100 kDa and the 250 kDa forms are on the assembly pathway to the 400 kDa complex. However, the temporal relationship of the two intermediates in time course experiments using wild type Tom40 precursor could not be confirmed because both the 250 kDa and 100 kDa forms appeared and decreased at the same time. When the assembly of mutant Tom40 molecules was examined, many variants gave rise to both the 250 kDa and the 100 kDa intermediates, although the two largest classes of assembly defects seen were either failure of precursors to progress past the 250 kDa complex, or accumulation of precursors at the 250 kDa intermediate with some progression past this point of the pathway. The existence of variants that arrest at the 250 kDa intermediate with no discernable evidence of the 100 kDa intermediate (see Figs. 17B, 22, 26, and 27) supports the model in which the Tom40 precursor appears in the 250 kDa form first and then progresses to the 100 kDa form.

It has also been proposed that Tom40 precursor in the 250 kDa intermediate is associated with the outer membrane on the intermembrane space side and is extractable with sodium carbonate (Model *et al.*, 2001). My data from carbonate extraction of mitochondria following import of wild type Tom40 into wild type mitochondria do not allow conformation of this aspect of the model due to the unexpected finding that carbonate enhances assembly of Tom40 precursors in the intermediates to the final 400 kDa form. However, the observation that precursors of the Δ51-60 form of Tom40 in the 250 kDa intermediate were mostly extractable by carbonate and the precursors of the Δ321-3 variant were entirely extractable does support the notion that the Tom40

precursor is only peripherally associated with the membrane at this stage. It also suggests that there may be two distinct pools of 250 kDa intermediates, one pool that is only peripherally associated with the outer membrane, and one which is in the process of integrating into the membrane. One explanation for the action of sodium carbonate on wild type precursors might be that protein-protein interactions hold the molecule at the 250 kDa intermediate stage of assembly, and these are disrupted in the presence of carbonate. It is also conceivable that interactions between Tom40 molecules in existing TOM complexes may be weakened, facilitating replacement of existing subunits with incoming molecules.

4.5 Alternate assembly pathway identified in mitochondria bearing mutations in the N-terminus of Tom40

Analysis of the import and assembly of wild type Tom40 precursors into mitochondria containing only Tom40 with mutations in the N-terminus of the protein revealed differences from the normal assembly pathway. Following import of wild type Tom40 precursor protein into mutant mitochondria, very little of the precursor was seen in the 250 kDa intermediate and none of the 100 kDa intermediate was detectable. Instead, the precursor was found in a 450 kDa complex which appeared to assemble directly into the 400 kDa form. The Tom40 precursor in the 450 kDa form is completely sensitive to digestion with proteinase K, and the simplest interpretation is that 450 kDa complex represents a Tom40 precursor molecule associated with a pre-existing TOM complex. As most of the precursor at this stage was extractable with sodium carbonate, its initial association with the TOM complex must precede integration into the membrane. It seems likely that the Tom40 precursor at this stage integrates directly into the existing TOM complex by displacing a pre-existing Tom40 subunit. This interpretation suggests that amino acid residues 40-60 of Tom40 molecules in the wild type TOM complex normally interact with incoming subunits. Although this hypothesis seems difficult to reconcile with the predicted intermembrane space localization of these residues in the topology of Tom40 it has been suggested that the Tom40 precursor in the 250 kDa intermediate is on the intermembrane space side of the mitochondrial outer membrane (Model *et al.*, 2001). Another interpretation could be that the mutation in the

N terminus alters the confirmation of the TOM complex, making direct integration into the TOM complex possible. Although it may be surprising that an alternate Tom40 assembly pathway exists, it is also possible that a small amount of assembly occurs by this pathway under normal conditions, but is not easily detected by BNGE. Although others have shown that the N-terminus of Tom40 is not required for stable interactions between Tom40 molecules (Gordon *et al.*, 2001), my results suggest that the region is important for assembly of the protein into the TOM complex since alterations in the N-terminus of both Tom40 precursors and Tom40 molecules within the TOM complex have an affect on the assembly pathway.

It was also observed that more radioactivity was found in the final 400 kDa intermediate than could be accounted for by the initial amount of 450 kDa present in the initial 0°C time point following the pulse of import. It is possible that the Tom40 monomer seen on the lower portion of the BNGs in Fig. 28 also progresses directly to the 400 kDa complex by a mechanism similar to Tom40 in the 450 kDa intermediate, as this monomer form also disappears over the time course in all of the N-terminal mutant strains tested. It would be difficult to quantitate the amount of protein this monomer form contributes to the final complex, as the monomer does not form a discrete band, but is more diffuse in nature. As with the 450 kDa intermediate, the Tom40 precursor at this stage of assembly also appears to be completely sensitive to PK, and is carbonate extractable.

4.6 The protein content of the mitochondrial outer membrane

In an attempt to find the *N. crassa* homolog of Tom37(Mas37), the putative yeast TOM complex assembly factor (Wiedemann, 2003), OMVs were isolated and subjected to SDS-PAGE. Bands were excised between the molecular weights of ~38 kDa, and ~70 kDa and analyzed by mass spectroscopy. This region of the gel was chosen because information from the laboratory of N. Pfanner suggested that the *N. crassa* homolog had a molecular weight of 48.6 kDa. Although Tom37(Mas37) was not identified, a number of novel proteins were found (see Table 7). As the molecular weights of the proteins analyzed were restricted to a narrow molecular weight range, it is likely that a number of unidentified proteins remain to be discovered in the *N. crassa* mitochondrial outer

membrane. There are a number of observations that support this notion. For example Fzo1p, a mitochondrial outer membrane protein required for mitochondrial fusion, is known to exist in an 800 kDa complex, the composition of which is largely unknown (Rapaport *et al.*, 1998a). Also, unknown proteins involved in import and assembly of mitochondrial precursors may exist. For example, Tom37(Mas37) may be part of a separate assembly complex, of unknown composition, responsible for the insertion of β-barrel proteins into the mitochondrial outer membrane in *S. cerevisiea* (Wiedemann, 2003). Since the process of Tom40 assembly is well conserved between *N. crassa* and yeast, it seems likely that a similar complex exists in *N. crassa*. Further, both EM tomography and conventional EM have shown close associations between the endoplasmic reticulum and mitochondria (Mannella *et al.*, 1998; Rizzuto *et al.*, 1998). It is conceivable that these interactions are maintained by a yet uncharacterized protein or protein complex either in mitochondria, the endoplasmic reticulum, or both organelles. Finally, morphological contact sites, where outer and inner mitochondrial membranes associate closely, are permanent structures (Hackenbrock, 1966; Hackenbrock, 1968; Hackenbrock and Caplan, 1969; Hackenbrock *et al.*, 1971). It is thought that the IMF fraction recovered during isolation of OMVs represents the association of the outer and inner membranes at these contact sites (Mayer *et al.*, 1995a). As these structures seem to be permanent, it is likely that this membrane contact is mediated by an unknown protein or protein complex. Following identification of unknown proteins, further work would need to be done to prove the proteins are localized to the mitochondrial outer membrane. Mutations could then be made to assess the effects on cell viability, mitochondrial morphology, inheritance, and import of mitochondrial preproteins.

4.7 Cys scanning mutagenesis to determine the position of β-strands in Tom40

Current models of Tom40 structure are based almost entirely on computer predictions (Court *et al.*, 1995; Mannella *et al.*, 1996) (T. Schirmer, via D. Rapaport, personal communication). One experimental observation regarding *N. crassa* Tom40 structure localizes the extreme N- and C-termini to the intermembrane space (Künkele *et al.*, 1998b), though this conflicts with data from yeast suggesting that the N-terminus is

exposed to the cytosol (Hill *et al.*, 1998). Spectral evidence on the α-helix versus β-strand content of the protein also has given conflicting results (Hill *et al.*, 1998; Ahting *et al.*, 2001). Thus, it would be of interest to demonstrate directly which residues of Tom40 lie within the membrane, the aqueous channel, the intermembrane space and the cytosol.

Cys-scanning has several advantages over other techniques for topological studies. The substitutions of amino acids residues with cysteines have been shown not to result in gross changes in the structures of proteins being studied and the function of the protein is likely to be maintained, as only a single residue at a time is replaced by cysteine. During the procedure, the protein remains in its natural environment and in its normal confirmation. Finally, channel proteins with cysteine-substituted amino acids can be labeled with charged sulfhydryl reagents and examined by electrophysiology (Maloney *et al.*, 1994; Zhou *et al.*, 1997). This technique may be useful for elucidating those residues which function to form the pore of the TOM complex.

As previously discussed, two computer models of Tom40 structure place the highly conserved KLG residues (amino acids 321-323 of *N. crassa* Tom40) in the last membrane-spanning β-strand of Tom40 [T Schirmer, via D. Rapaport, personal communication; Mannella, 1996 #1527]. The inability of the Δ321-3 mutant form to assemble *in vitro* or to rescue the *tom40*^{RIP} nucleus while the 321AAA form does assemble and does rescue, adds further support for these two models. Using SCAM, I have verified that these residues are part of β-strand, as the region that encompasses residues 316-327 shows the alternate pattern of labeling predicted for amino acids in a membrane-spanning β-strand. It is interesting to note that some of the other mutations that have been made in other regions of the genomic *tom40* plasmid show the same pattern of non-rescue (for the deleted form) and rescue (for the alanine form) of the *tom40*^{RIP} nucleus (see Table 5). As with the 321-323 region, it is possible that these amino acids are also part of membrane spanning domains of Tom40. Cysteine scanning of these regions should verify this suggestion.

The predicted pattern of label/non-label for a β-sheet spanning a lipid bilayer is not evident in the entire region spanning amino acids 306-316. Rather the pattern was seen for amino acids 311-316, but none of residues 306-310 were labeled (Fig. 40). This is not entirely unexpected, as the technique of cys-scanning has been shown in previous

studies not to be able to label all expected residues. For example, residues in small loop domains of membrane proteins are not labeled with equal efficiency even though all these residues should be in the aqueous environment (Tang *et al.*, 1998; Fujinaga *et al.*, 1999). In these studies, it was suggested that a steric hindrance in the region surrounding the specific non-labeling residues might prevent access of biotin maleimide to the residue in question. As the Tom40 protein is part of a multi-subunit complex, it is possible that similar steric hindrances may exist within the TOM complex, preventing labeling patterns of certain residues of the protein.

The occurrence of such problems in generating topological data by cys-scanning, suggests that supporting evidence for the models produced will be beneficial. Supporting evidence for the position of predicted β-strands could be generated by mutational analysis of the regions. As seen in the case of the 321-323 region, small deletions within the membrane-spanning domains would be predicted not to rescue the *tom40*^{RIP} nucleus, while the corresponding replacement of residues with alanine would allow the β-strand to span the membrane. Insertion of a string of hydrophilic amino acids into a membrane-spanning domain would also be predicted to fail to rescue the *tom40*^{RIP} nucleus. Another type of evidence would be electrophysiological verification of residues predicted to exist in the aqueous pore. TOM complexes containing Tom40 with cysteines at positions predicted to line the pore could be isolated, reacted with a charged sulfhydryl-labeling reagent, and analyzed electrophysiologically. It has been found that such adducts in the pores of channel proteins and channel protein complexes perturb or block normal conductance (Maloney *et al.*, 1994; Zhou *et al.*, 1997). These experiments will be done in conjunction with collaborators at the University of Munich, Munich, Germany.

4.8 Future directions

Tom40 is an essential protein and is highly conserved between divergent species (Fig. 13). In conjunction with a new graduate student, I have started a study to both delete and change to alanine all the highly conserved domains of the *tom40* gene. The results of certain mutations have been discussed above, but a number of domains remain to be characterized (Table 5). The genomic versions of the mutations have been created, and the new student is in the process of determining the effects these mutations have with

respect to growth phenotypes, TOM complex morphology, and the ability of mitochondria isolated from these strains to import mitochondrial precursor proteins. *In vitro* assembly assays have already identified domains that may be important for Tom40 assembly. In this study we are particularly interested in mutations that do not appear to affect Tom40 assembly in hopes that we identify domains primarily responsible for preprotein import. This may allow us to define domains that participate in the formation of the *cis* site, the *trans* site or regions of the protein that are responsible for translocation of preproteins.

Tom22 is required for assembly of Tom40 into the TOM complex, and is required for maintaining higher order structures within the TOM complex (Rapaport *et al.*, 1998b; van Wilpe *et al.*, 1999). Our laboratory has previously generated a variety of mutant strains containing only mutant versions of Tom22 (Court *et al.*, 1996; Nargang *et al.*, 1998; Rodriguez-Cousino *et al.*, 1998). It would be interesting to determine if regions of Tom22 are required for Tom40 assembly into the TOM complex, and to determine the effects of these mutations on TOM complex structural stability. Initial experiments with a mutant version of Tom22 lacking the intermembrane space domain of the protein suggest that the Tom40 assembly pathway in these mitochondria is unaffected by deletion of this domain (data not shown) (Court *et al.*, 1996), but the cytosolic and membrane-spanning domains may be involved in TOM complex assembly.

Virtually nothing is known about how the components of the TOM complex are spatially arranged. Using various strain supplied by our lab, collaborators at the University of Munich are trying to crystallize the TOM complex to determine it's three-dimensional structure. This structure would offer great insight into how different components of the TOM complex interact, and how precursor proteins interact at both the *cis* and *trans* binding sites. The SCAM strains described in this thesis may help generate the X-ray structure by providing TOM complexes with specific Tom40-cysteine substitutions that will be useful for obtaining phasing data following interactions with Hg^{2+} ions.

5. BIBLIOGRAPHY

Abdul, K.M., Terada, K., Yano, M., Ryan, M.T., Streimann, I., Hoogenraad, N.J. and Mori, M. (2000) Functional analysis of human metaxin in mitochondrial protein import in cultured cells and its relationship with the Tom complex. *Biochem Biophys Res Commun*, **276**, 1028-1034.

Abe, Y., Shodai, T., Muto, T., Mihara, K., Torii, H., Nishikawa, S., Endo, T. and Kohda, D. (2000) Structural basis of presequence recognition by the mitochondrial protein import receptor Tom20. *Cell*, **100**, 551-560.

Adam, A., Endres, M., Sirrenberg, C., Lottspeich, F., Neupert, W. and Brunner, M. (1999) Tim9, a new component of the TIM22:54 translocase in mitochondria. *EMBO J.*, **18**, 313-319.

Ahting, U., Thieffry, M., Engelhardt, H., Hegerl, R., Neupert, W. and Nussberger, S. (2001) Tom40, the pore-forming component of the protein-conducting TOM channel in the outer membrane of mitochondria. *J. Cell Biol.*, **153**, 1151-1160.

Ahting, U., Thun, C., Hegerl, R., Typke, D., Nargang, F., Neupert, W. and Nussberger, S. (1999) The TOM core complex: The general protein import pore of the outer membrane of mitochondria. *J. Cell Biol.*, **147**, 959-968.

Akins, R.A. and Lambowitz, A.M. (1985) General method for cloning *Neurospora crassa* nuclear genes by complementation of mutants. *Mol. Cell. Biol.*, **5**, 2272-2278.

Alconada, A., Kübrich, M., Moczko, M., Hönlinger, A. and Pfanner, N. (1995) The mitochondrial receptor complex: The small subunit Mom8b/Isp6 supports association of receptors with the general insertion pore and transfer of preproteins. *Mol. Cell. Biol.*, **15**, 6196-6205.

Armstrong, L.C., Komiya, T., Bergman, B.E., Mihara, K. and Bornstein, P. (1997) Metaxin is a component of a preprotein import complex in the outer membrane of the mammalian mitochondrion. *J Biol Chem*, **272**, 6510-6518.

Armstrong, L.C., Saenz, A.J. and Bornstein, P. (1999) Metaxin 1 interacts with metaxin 2, a novel related protein associated with the mammalian mitochondrial outer membrane. *J Cell Biochem*, **74**, 11-22.

Arnheim, N. and Cortopassi, G. (1992) Deleterious mitochondrial DNA mutations accumulate in aging human tissues. *Mutat Res*, **275**, 157-167.

Arretz, M., Schneider, H., Guiard, B., Brunner, M. and Neupert, W. (1994) Characterization of the mitochondrial processing peptidase of *Neurospora crassa*. *J. Biol. Chem.*, **269**, 4959-4967.

Attardi, G. and Schatz, G. (1988) Biogenesis of mitochondria. *Annu Rev Cell Biol*, **4**, 289-333.

Ausubel, R.A., Brent, R., Kingston, R.E., Moore, D.D. and Seidman, J.G. (1992) *Current Protocols in Molecular Biology.* Greene and Wiley Interscience, New York.

Baker, K.P., Schaniel, A., Vestweber, D. and Schatz, G. (1990) A yeast mitochondrial outer membrane protein is essential for protein import and cell viability. *Nature*, **348**, 605-609.

Bauer, M.F., Gempel, K., Reichert, A.S., Rappold, G.A., Lichtner, P., Gerbitz, K.D., Neupert, W., Brunner, M. and Hofmann, S. (1999a) Genetic and structural characterization of the human mitochondrial inner membrane translocase. *J. Mol. Biol.*, **289**, 69-82.

Bauer, M.F., Hofmann, S., Neupert, W. and Brunner, M. (2000) Protein translocation into mitochondria: the role of TIM complexes. *Trends Cell Biol*, **10**, 25-31.

Bauer, M.F. and Neupert, W. (2001) Import of proteins into mitochondria: a novel pathomechanism for progressive neurodegeneration. *J Inherit Metab Dis*, **24**, 166-180.

Bauer, M.F., Rothbauer, U., Muhlenbein, N., Smith, R.J., Gerbitz, K., Neupert, W., Brunner, M. and Hofmann, S. (1999b) The mitochondrial TIM22 preprotein translocase is highly conserved throughout the eukaryotic kingdom. *FEBS Lett.*, **464**, 41-47.

Bauer, M.F., Sirrenberg, C., Neupert, W. and Brunner, M. (1996) Role of Tim23 as voltage sensor and presequence receptor in protein import into mitochondria. *Cell*, **87**, 33-41.

Becker, K., Guiard, B., Rassow, J., Söllner, T. and Pfanner, N. (1992) Targeting of a chemically pure preprotein to mitochondria does not require the addition of a cytosolic signal recognition factor. *J. Biol. Chem.*, **267**, 5637-5643.

Bernardi, P. (1999) Mitochondrial transport of cations: channels, exchangers, and permeability transition. *Physiol Rev*, **79**, 1127-1155.

Bernardi, P., Petronilli, V., Di Lisa, F. and Forte, M. (2001) A mitochondrial perspective on cell death. *Trends Biochem Sci*, **26**, 112-117.

Berridge, M.J., P. Lipp, and M.D. Bootman. (2000) The versatility and universality of calcium signaling. *Nat. Mol. Cell Biol.*, **1**, 11-21.

Berthold, J., Bauer, M.F., Schneider, H.-C., Klaus, C., Dietmeier, K., Neupert, W. and Brunner, M. (1995) The MIM complex mediates preprotein translocation across the mitochondrial inner membrane and couples it to the mt-Hsp70/ATP driving system. *Cell*, **81**, 1085-1093.

Blanchard, J.L. and Lynch, M. (2000) Organellar genes: why do they end up in the nucleus? *Trends Genet*, **16**, 315-320.

Blatch, G.L. and Lassle, M. (1999) The tetratricopeptide repeat: a structural motif mediating protein- protein interactions. *Bioessays*, **21**, 932-939.

Bleazard, W., McCaffery, J.M., King, E.J., Bale, S., Mozdy, A., Tieu, Q., Nunnari, J. and Shaw, J.M. (1999) The dynamin-related GTPase Dnm1 regulates mitochondrial fission in yeast. *Nat Cell Biol*, **1**, 298-304.

Blom, J., Dekker, P. and Meijer, M. (1995) Functional and physical interactions of components of the yeast mitochondrial inner-membrane import machinery (MIM). *Euro. J. Biochem.*, **232**, 309-314.

Blom, J., Kübrich, M., Rassow, J., Voos, W., Dekker, P.J., Maarse, A.C., Meijer, M. and Pfanner, N. (1993) The essential yeast protein MIM44 (encoded by MPI1) is involved in an early step of preprotein translocation across the mitochondrial inner membrane. *Mol. Cell. Biol.*, **13**, 7364-7371.

Bömer, U., Maarse, A.C., Martin, F., Geissler, A., Merlin, A., Schonfisch, B., Meijer, M., Pfanner, N. and Rassow, J. (1998) Separation of structural and dynamic functions of the mitochondrial translocase: Tim44 is crucial for the inner membrane import sites in translocation of tightly folded domains, but not of loosely folded preproteins. *EMBO J*, **17**, 4226-4237.

Bömer, U., Pfanner, N. and Dietmeier, K. (1996a) Identification of a third yeast mitochondrial Tom protein with tetratrico peptide repeats. *FEBS Lett*, **382**, 153-158.

Bömer, U., Rassow, J., Zufall, N., Pfanner, N., Meijer, M. and Maarse, A.C. (1996) The preprotein translocase of the inner mitochondrial membrane: evolutionary conservation of targeting and assembly of TIM17. *J. Mol. Biol.*, **262**, 389-395.

Bootman, M.D., P. Lipp, and M.J. Berridge. (2001) The organization and functions of local Ca2+ signals. *J. Cell. Sci.*, **114**, 2213-2222.

Brix, J., Dietmeier, K. and Pfanner, N. (1997) Differential recognition of preproteins by the purified cytosolic domains of the mitochondrial import receptors Tom20, Tom22, and Tom70. *J. Biol. Chem.*, **272**, 20730-20735.

Brix, J., Rudiger, S., Bukau, B., Schneider-Mergener, J. and Pfanner, N. (1999) Distribution of binding sequences for the mitochondrial import receptors Tom20, Tom22, and Tom70 in a presequence-carrying preprotein and a non-cleavable preprotein. *J. Biol. Chem.*, **274**, 16522-16530.

Brunk, U.T. and Terman, A. (2002) The mitochondrial-lysosomal axis theory of aging: accumulation of damaged mitochondria as a result of imperfect autophagocytosis. *Eur J Biochem*, **269**, 1996-2002.

Capaldi, R.A. (2000) The changing face of mitochondrial research. *Trends Biochem Sci*, **25**, 212-214.

Cartwright, P., Beilharz, T., Hansen, P., Garrett, J. and Lithgow, T. (1997) Mft52, and acid-bristle protein in the cytosol that delivers precursor proteins to yeast mitochondria. *J. Biol. Chem.*, **272**, 5320-5325.

Catlett, N.L. and Weisman, L.S. (2000) Divide and multiply: organelle partitioning in yeast. *Curr Opin Cell Biol*, **12**, 509-516.

Chacinska, A., Pfanner, N. and Meisinger, C. (2002) How mitochondria import hydrophillic and hydrophobic proteins. *Trends Cell Biol.*, **12**, 299-303.

Cheng, M.Y., Hartl, F.-U., Martin, J., Pollock, R.A., Kalousek, F., Neupert, W., Hallberg, E.M., Hallberg, R.L. and Horwich, A.L. (1989) Mitochondrial heat-shock protein hsp60 is essential for assembly of proteins imported into yeast mitochondria. *Nature*, **337**, 620-625.

Claros, M.G. and Vincens, P. (1996) Computational method to predict mitochondrially imported proteins and their targeting sequences. *Eur J Biochem*, **241**, 779-786.

Cortopassi, G.A., Shibata, D., Soong, N.W. and Arnheim, N. (1992) A pattern of accumulation of a somatic deletion of mitochondrial DNA in aging human tissues. *Proc Natl Acad Sci U S A*, **89**, 7370-7374.

Cortopassi, G.A. and Wong, A. (1999) Mitochondria in organismal aging and degeneration. *Biochim Biophys Acta*, **1410**, 183-193.

Court, D.A., Lill, R. and Neupert, W. (1995) The protein import apparatus of the mitochondrial outer membrane. *Can. J. Bot.*, **73 (Suppl. 1)**, S193-S197.

Court, D.A., Nargang, F.E., Steiner, H., Hodges, R.S., Neupert, W. and Lill, R. (1996) Role of the intermembrane space domain of the preprotein receptor Tom22 in protein import into mitochondria. *Mol. Cell. Biol.*, **16**, 4034-4042.

Craig, E.A., Voisine, C. and Schilke, B. (1999) Mitochondrial iron metabolism in the yeast Saccharomyces cerevisiae. *Biol Chem*, **380**, 1167-1173.

Criddel, R.S., and G. Schatz. (1969) Protomitochondria of anaerobically grown yeast. I. Isolation and biochemical properties. *Biochemistry*, **8**, 322-344.

Curran, S.P., Leuenberger, D., Oppliger, W. and Koehler, C.M. (2002) The Tim9p-Tim10p complex binds to the transmembrane domains of the ADP/ATP carrier. *EMBO J.*, **21**, 942-953.

Davis, A.J., Ryan, K.R. and Jensen, R.E. (1998) Tim23p contains separate and distinct signals for targeting to mitochondria and insertion into the inner membrane. *Mol. Biol. Cell*, **9**, 2577-2593.

Davis, R.H. and De Serres, F.J. (1970) Genetic and microbiological research techniques for *Neurospora crassa*. *Methods Enzymol.*, **17**, 79-143.

de Grey, A.D. (2002a) The reductive hotspot hypothesis of mammalian aging: membrane metabolism magnifies mutant mitochondrial mischief. *Eur J Biochem*, **269**, 2003-2009.

de Grey, A.D. (2002b) Three detailed hypotheses implicating oxidative damage to mitochondria as a major driving force in homeotherm aging. *Eur J Biochem*, **269**, 1995.

Dekker, P.J., Martin, F., Maarse, A.C., Bömer, U., Muller, H., Guiard, B., Meijer, M., Rassow, J. and Pfanner, N. (1997) The Tim core complex defines the number of mitochondrial translocation contact sites and can hold arrested preproteins in the absence of matrix Hsp70-Tim44. *EMBO J.*, **16**, 5408-5419.

Dekker, P.J., Ryan, M.T., Brix, J., Müller, H., Honlinger, A. and Pfanner, N. (1998) Preprotein translocase of the outer mitochondrial membrane: molecular dissection and assembly of the general import pore complex. *Mol. Cell. Biol.*, **18**, 6515-6524.

Dekker, P.J.T., Keil, P., Rassow, J., Maarse, A.C., Pfanner, N. and Meijer, M. (1993) Identification of *MIM23*, a putative component of the protein import machinery of the mitochondrial inner membrane. *FEBS Lett.*, **330**, 66-70.

Dembowski, M., Künkele, K.-P., Nargang, F., Neupert, W. and Rapaport, D. (2001) Assembly of Tom6 and Tom7 into the TOM core complex of *Neurospora crassa*. *J. Biol. Chem.*, **276**, 17679-17685.

Deshaies, R.J., Koch, B.D. and Schekman, R. (1988a) The role of stress proteins in membrane biogenesis. *Trends Biochem. Sci.*, **13**, 384-388.

Deshaies, R.J., Koch, B.D., Werner-Washburne, M., Craig, E.A. and Schekman, R. (1988b) A subfamily of stress proteins facilitates translocation os secretory and mitochondrial precursor polypeptides. *Nature*, **332**, 800-805.

Di Lisa, F. and Bernardi, P. (1998) Mitochondrial function as a determinant of recovery or death in cell response to injury. *Mol Cell Biochem*, **184**, 379-391.

Diekert, K., Kispal, G., Guiard, B. and Lill, R. (1999) An internal targeting signal directing proteins into the mitochondrial intermembrane space. *Proc. Natl. Acad. Sci. USA*, **96**, 11752-11757.

Dietmeier, K., Honlinger, A., Bömer, U., Dekker, P.J., Eckerskorn, C., Lottspeich, F., Kubrich, M. and Pfanner, N. (1997) Tom5 functionally links mitochondrial preprotein receptors to the general import pore [see comments]. *Nature*, **388**, 195-200.

Dolan, M.F., Guerrero, R. and Margulis, L. (2000) Endosymbioses: cyclical and permanent in evolution.[comment]. *Proc Natl Acad Sci U S A*, **97**, 6954-6959.

Donzeau, M., Kaldi, K., Adam, A., Paschen, S., Wanner, G., Guiard, B., Bauer, M.F., Neupert, W. and Brunner, M. (2000) Tim23 links the inner and outer mitochondrial membranes. *Cell*, **101**, 401-412.

Drubin, D.G., Jones, H.D. and Wertman, K.F. (1993) Actin structure and function: roles in mitochondrial organization and morphogenesis in budding yeast and identification of the phalloidin- binding site. *Mol Biol Cell*, **4**, 1277-1294.

Eaton, S., Pourfarzam, M. and Bartlett, K. (1996a) The effect of respiratory chain impairment of beta-oxidation in rat heart mitochondria. *Biochem J*, **319**, 633-640.

Eaton, S., Zaitoun, A.M., Record, C.O. and Bartlett, K. (1996b) beta-Oxidation in human alcoholic and non-alcoholic hepatic steatosis. *Clin Sci (Lond)*, **90**, 307-313.

Eaton, S.a.K.B. (1996) Inhibition of mitochondrial b-oxidation in the heart by increased redox state of the ubiquinone pool. *Biochem. Soc. Trans.*, **24**, 457S.

Eilers, M., Oppliger, W. and Schatz, G. (1987) Both ATP and an energized inner membrane are required to import into mitochondria. *EMBO J.*, **6**, 1073-1077.

Eilers, M. and Schatz, G. (1988) Protein unfolding and the energetics of protein translocation across biological membranes. *Cell*, **52**, 481-483.

Emtage, J.L.T. and Jensen, R.E. (1993) *MAS6* encodes an essential inner membrane component of the yeast mitochondrial protein import pathway. *J. Cell Biol.*, **122**, 1003-1012.

Endres, M., Neupert, W. and Brunner, M. (1999) Transport of the ADP/ATP carrier of mitochondria from the TOM complex to the TIM22:54 complex. *EMBO J.*, **18**, 3214-3221.

Frey, T.G. and Mannella, C.A. (2000) The internal structure of mitochondria. *Trends Biochem Sci*, **25**, 319-324.

Fritz, S., Rapaport, D., Klanner, E., Neupert, W. and Westermann, B. (2001) Connection of the mitochondrial outer and inner membranes by Fzo1 is critical for organellar fusion. *J Cell Biol*, **152**, 683-692.

Fuchs, F., Prokisch, H., Neupert, W. and Westermann, B. (2002) Interaction of mitochondria with microtubules in the filamentous fungus Neurospora crassa. *J Cell Sci*, **115**, 1931-1937.

Fujiki, M. and Verner, K. (1991) Coupling of protein synthesis and mitochondrial import in a homologous yeast in-vitro system. *J. Biol. Chem.*, **266**, 6841-6847.

Fujiki, M. and Verner, K. (1993) Coupling of cytosolic protein synthesis and mitochondrial protein import in yeast. Evidence for cotranslational import in vivo. *J Biol Chem*, **268**, 1914-1920.

Fujinaga, J., Tang, X.B. and Casey, J.R. (1999) Topology of the membrane domain of human erythrocyte anion exchange protein, AE1. *J Biol Chem*, **274**, 6626-6633.

Gakh, O., Cavadini, P. and Isaya, G. (2002) Mitochondrial processing peptidases. *Biochim Biophys Acta*, **1592**, 63.

Gambill, B.D., Voos, W., Kan, P.J., Miao, B., Langer, T., Craig, E.A. and Pfanner, N. (1993) A dual role for mitochondrial heat shock protein 70 in membrane translocation of preproteins. *J. Cell Biol.*, **123**, 109-117.

Gasser, S.M., Daum, G. and Schatz, G. (1982) Import of proteins into mitochondria: Energy-dependent uptake of precursors by isolated mitochondria. *J. Biol. Chem.*, **257**, 13034-13041.

Gaume, B., Klaus, C., Ungermann, C., Guiard, B., Neupert, W. and Brunner, M. (1998) Unfolding of preproteins upon import into mitochondria. *EMBO J.*, **17**, 6497-6507.

Geissler, A., Chacinska, A., Truscott, K.N., Wiedemann, N., Brandner, K., Sickmann, A., Meyer, H.E., Meisinger, C., Pfanner, N. and Rehling, P. (2002) The mitochondrial presequence translocase: an essential role of Tim50 in directing preproteins to the import channel. *Cell*, **111**, 507-518.

Geissler, A., Rassow, J., Pfanner, N. and Voos, W. (2001) Mitochondrial import driving forces: Enhanced trapping by matrix Hsp70 stimulates translocation and reduces the membrane potential dependence of loosely folded proteins. *Mol. Cell. Biol.*, **21**, 7097-7104.

Geli, V., Yang, M.J., Suda, K., Lustig, A. and Schatz, G. (1990) The MAS-encoded processing peptidase of yeast mitochondria: overproduction and characterization of its two non-identical subunits. *J. Biol. Chem.*, **265**, 19216-19222.

Gessert, S.F., Kim, J.H., Nargang, F.E. and Weiss, R.L. (1994) A polyprotein precursor of two mitochondrial enzymes in *Neurospora crassa*. *J. Biol. Chem.*, **269**, 8189-8203.

Gillespie, L.L., Argan, C., Taneja, A.T., Hodges, R.S., Freeman, K.B. and Shore, G.C. (1985) A synthetic signal peptide blocks import of precursor proteins destined for the mitochondrial inner membrane or matrix. *J. Biol. Chem.*, **260**, 16045-16048.

Good, A.G. and Crosby, W.L. (1989) Anaerobic induction of alanine aminotransferase in barley root tissue. *Plant Physiol.*, **90**, 1305-1309.

Gordon, D.M., Wang, J., Amutha, B. and Pain, D. (2001) Self-association and precursor protein binding of Saccharomyces cerevisiae Tom40p, the core component of the protein translocase channel of the mitochondrial outer membrane. *Biochem. J.*, **356**, 207-215.

Grad, L., Descheneau, A., Neupert, W., Lill, R. and Nargang, F. (1999) Inactivation of the Neurospora crassa mitochondrial outer membrane protein TOM70 by repeat-induced point mutation (RIP) causes defects in mitochondrial protein import and morphology. *Curr. Genet.*, **36**, 137-146.

Gray, M.W. (1989) Origin and evolution of mitochondrial DNA. *Annu. Rev. Cell Biol.*, **5**, 25-50.

Gray, M.W. (1999) Evolution of organellar genomes. *Curr Opin Genet Dev*, **9**, 678-687.

Gray, M.W., Burger, G. and Lang, B.F. (1999) Mitochondrial evolution. *Science*, **283**, 1476-1481.

Gray, M.W., Burger, G. and Lang, B.F. (2001) The origin and early evolution of mitochondria. *Genome Biol*, **2**.

Griparic, L. and van der Bliek, A.M. (2001) The many shapes of mitochondrial membranes. *Traffic*, **2**, 235-244.

Gross, A., McDonnell, J.M. and Korsmeyer, S.J. (1999) BCL-2 family members and the mitochondria in apoptosis. *Genes Dev*, **13**, 1899-1911.

Hachiya, N., Alam, R., Sakasegawa, H., Sakaguchi, M., Mihara, N. and Omura, T. (1993) A mitochondrial import factor purified from rat liver cytosol is an ATP-dependent conformational modulator for precursor proteins. *EMBO J.*, **12**, 1579-1586.

Hachiya, N., Komiya, T., Alam, R., Iwahasi, J., Sakaguchi, M., Omura, T. and Mihara, K. (1994) MSF, a novel cytoplasmic chaperone which functions in precursor targeting to mitochondria. *EMBO J.*, **13**, 5146-5154.

Hackenbrock, C.R. (1966) Ultrastructural bases for metabolically linked mechanical activity in mitochondria. I. Reversible ultrastructural changes with change in metabolic steady state in isolated liver mitochondria. *J Cell Biol*, **30**, 269-297.

Hackenbrock, C.R. (1968) Ultrastructural bases for metabolically linked mechanical activity in mitochondria. II. Electron transport-linked ultrastructural transformations in mitochondria. *J Cell Biol*, **37**, 345-369.

Hackenbrock, C.R. and Caplan, A.I. (1969) Ion-induced ultrastructural transformations in isolated mitochondria. The energized uptake of calcium. *J Cell Biol*, **42**, 221-234.

Hackenbrock, C.R., Rehn, T.G., Weinbach, E.C. and Lemasters, J.J. (1971) Oxidative phosphorylation and ultrastructural transformation in mitochondria in the intact ascites tumor cell. *J Cell Biol*, **51**, 123-137.

Hagen, T.M., Yowe, D.L., Bartholomew, J.C., Wehr, C.M., Do, K.L., Park, J.Y. and Ames, B.N. (1997) Mitochondrial decay in hepatocytes from old rats: membrane potential declines, heterogeneity and oxidants increase. *Proc Natl Acad Sci U S A*, **94**, 3064-3069.

Halestrap, A.P. and Dunlop, J.L. (1986) Intramitochondrial regulation of fatty acid beta-oxidation occurs between flavoprotein and ubiquinone. A role for changes in the matrix volume. *Biochem J*, **239**, 559-565.

Hallermayer, G., Zimmermann, R. and Neupert, W. (1977) Kinetic studies on the transport of cytoplasmatically synthesized proteins into mitochondria in intact cells of *Neurospora crassa*. *Eur. J. Biochem.*, **81**, 523-532.

Hammen, P.K., Gorenstein, D.G. and Weiner, H. (1996a) Amphiphilicity determines binding properties of three mitochondrial presequences to lipid surfaces. *Biochemistry*, **35**, 3772-3781.

Hammen, P.K., Waltner, M., Hahnemann, B., Heard, T.S. and Weiner, H. (1996b) The role of positive charges and structural segments in the presequence of rat liver aldehyde dehydrogenase in import into mitochondria. *J Biol Chem*, **271**, 21041-21048.

Harkness, T.A.A., Metzenberg, R.L., Schneider, H., Lill, R., Neupert, W. and Nargang, F.E. (1994a) Inactivation of the *Neurospora crassa* gene encoding the mitochondrial protein import receptor MOM19 by the technique of "sheltered RIP". *Genetics*, **136**, 107-118.

Harkness, T.A.A., Nargang, F.E., Van der Klei, I., Neupert, W. and Lill, R. (1994b) A crucial role of the mitochondrial protein import receptor MOM19 for the biogenesis of mitochondria. *J. Cell Biol.*, **124**, 637-648.

Harmey, M.A., Hallermayer, G., Korb, H. and Neupert, W. (1977) Transport of cytoplasmically synthesized proteins into mitochondria in a cell-free system from *Neurospora crassa*. *Eur. J. Biochem.*, **81**, 533-544.

Harris, D.J., Fetzner, J.W., Jr. and Harris, M.H. (2000) The role of the Bcl-2 family in the regulation of outer mitochondrial membrane permeability. *Proceedings of the Royal Society of London - Series B: Biological Sciences*, **267**, 1679-1686.

Haucke, V., Horst, M., Schatz, G. and Lithgow, T. (1996) The Mas20p and Mas70p subunits of the protein import receptor of yeast mitochondria interact via the tetratricopeptide repeat motif in Mas20p. Evidence for a single hetero-oligomeric receptor. *EMBO J.*, **15**, 1231-1237.

Haucke, V. and Schatz, G. (1997) Reconstitution of the protein insertion machinery of the mitochondrial inner membrane. *EMBO J.*, **16**, 4560-4567.

Hawlitschek, G., Schneider, H., Schmidt, B., Tropschug, M., Hartl, F.-U. and Neupert, W. (1988) Mitochondrial protein import: identification of processing peptidase and of PEP, a processing enhancing protein. *Cell*, **53**, 795-806.

Hermann, G.J., King, E.J. and Shaw, J.M. (1997) The yeast gene, MDM20, is necessary for mitochondrial inheritance and organization of the actin cytoskeleton. *J Cell Biol*, **137**, 141-153.

Hermann, G.J. and Shaw, J.M. (1998) Mitochondrial dynamics in yeast. *Annu Rev Cell Dev Biol*, **14**, 265-303.

Hermann, G.J., Thatcher, J.W., Mills, J.P., Hales, K.G., Fuller, M.T., Nunnari, J. and Shaw, J.M. (1998) Mitochondrial fusion in yeast requires the transmembrane GTPase Fzo1p. *J Cell Biol*, **143**, 359-373.

Hernandez, J.M., Blat, B., Iruela, C., Vila, F. and Hernandez-Yago, J. (1998) Identification of two processed psuedogenes of the human Tom20 gene. *Mol Gen Genet*, **258**, 117-122.

Hernandez, J.M., Blesa, J.R. and Hernandez-Yago, J. (2000) Comments on nomenclature of TOM genes/proteins and characterization of psi4Tom20, a novel processed pseudogene of the human Tom20 gene. *Genomics*, **67**, 107-108.

Hernandez, J.M., Giner, P. and Hernandez-Yago, J. (1999a) Gene structure of the human mitochondrial outer membrane receptor Tom20 and evolutionary study of its family of processed pseudogenes. *Gene*, **239**, 283-291.

Hernandez, J.M., Hernandez, C.S., Giner, C.P., Donat, V. and Hernandez-Yago, J. (1999b) Identification of psi3Tom20, a novel processed pseudogene of the human Tom20 gene, and complete characterization of psi1Tom20 and psi2Tom20. *Mol Gen Genet*, **262**, 207-211.

Herrmann, J. and Neupert, W. (2000) Protein transport into mitochondria. *Curr. Opin. Microbiol.*, **3**, 210-214.

Hicke, L. and Schekman, R. (1989) Yeast Sec23p acts in the cytoplasm to promote protein transport from the ER to the Golgi complex in vovo and in vitro. *EMBO J.*, **8**, 1677-1684.

Hill, K., Model, K., Ryan, M.T., Dietmeier, K., Martin, F., Wagner, R. and Pfanner, N. (1998) Tom40 forms the hydrophilic channel of the mitochondrial import pore for preproteins. *Nature*, **395**, 516-521.

Hines, V., Brandt, A., Griffiths, G., Horstmann, H., Brütsch, H. and Schatz, G. (1990) Protein import into yeast mitochondria is accelerated by the outer membrane protein *MAS70. EMBO J.*, **9**, 3191-3200.

Hoffmann, H.P. and Avers, C.J. (1973) Mitochondrion of yeast: ultrastructural evidence for one giant, branched organelle per cell. *Science*, **181**, 749-751.

Honlinger, A., Bömer, U., Alconada, A., Eckerskorn, C., Lottspeich, F., Dietmeier, K. and Pfanner, N. (1996) Tom7 modulates the dynamics of the mitochondrial outer membrane translocase and plays a pathway-related role in protein import. *EMBO J*, **15**, 2125-2137.

Hoogenraad, N.J., Ward, L.A. and Ryan, M.T. (2002) Import and assembly of proteins into mitochondria of mammalian cells. *Biochim Biophys Acta*, **1592**, 97-105.

Horwich, A.L., Kalousek, F., Fenton, W.A., Pollock, R.A. and Rosenberg, L.E. (1986) Targeting of pre-ornithine transcarbamylase to mitochondria: definition of critical regions and residues in the leader peptide. *Cell*, **46**, 451-459.

Horwich, A.L., Kalousek, F., Mellman, I. and Rosenberg, L.E. (1985) A leader peptide is sufficient to direct mitochondrial import of a chimeric protein. *EMBO J.*, **4**, 1129-1135.

Huang, S., Ratcliff, K.S., Schwartz, M.P., Spenner, J.M. and Matouschek, A. (1999) Mitochondria unfold precursor proteins by unraveling them from their N-termini. *Nature Struct. Biol.*, **6**, 1132-1138.

Hurt, E.C., Müller, U. and Schatz, G. (1985) The first twelve amino acids of a yeast mitochondrial outer membrane protein can direct a nuclear encoded cytochrome oxidase subunit to the mitochondrial inner membrane. *EMBO J.*, **4**, 3509-3518.

Hwang, S.T. and Schatz, G. (1989) Translocation of proteins across the mitochondrial inner membrane, but not into the outer membrane, requires nucleotide triphosphates in the matrix. *Proc. Natl. Acad. Sci U.S. A.*, **86**, 8432-8436.

Hwang, S.T., Wachter, C. and Schatz, G. (1991) Protein import into the yeast mitochondrial matrix. *J. Biol. Chem.*, **266**, 21083-21089.

Isaya, G., Miklos, D. and Rollins, R.A. (1994) *MIP1*, a new yeast gene homologous to the rat mitochondrial intermediate peptidase gene, is required for oxidative metabolism in *Saccharomyces cerevisiae*. *Mol. Cell. Biol.*, **14**, 5603-5616.

Iwahashi, J., Takaichi, S., Mihara, K. and Omura, T. (1994) Reconstitution of import-competent outer membrane vesicles from mammalian mitochondria. *J. Biochem.*, **116**, 156-163.

Iwahashi, J., Yamazaki, S., Komiya, T., Nomura, N., Nishikawa, S., Endo, T. and Mihara, K. (1997) Analysis of the functional domain of the rat liver mitochondrial import receptor Tom20. *J. Biol. Chem.*, **272**, 18467-18472.

Jansch, L., Kruft, V., Schmitz, U.K. and Braun, H.P. (1998) Unique composition of the preprotein translocase of the outer mitochondrial membrane from plants. *J Biol Chem*, **273**, 17251-17257.

Jarosch, E., Rodel, G. and Schweyen, R.J. (1997) A soluble 12-kDa protein of the mitochondrial intermembrane space, Mrs11p, is essential for mitochondrial biogenesis and viability of yeast cells. *Mol Gen Genet*, **255**, 157-165.

Jarosch, E., Tuller, G., Daum, G., Waldherr, M., Voskova, A. and Schweyen, R.J. (1996) Mrs5p, an essential protein of the mitochondrial intermembrane space, affects protein import into yeast mitochondria. *J Biol Chem*, **271**, 17219-17225.

Jascur, T., Goldenberg, D.P., Vestweber, D. and Schatz, G. (1992) Sequential translocation of an artificial precursor protein across the two mitochondrial membranes. *J. Biol. Chem.*, **267**, 13636-13641.

Jensen, R.E., Hobbs, A.E., Cerveny, K.L. and Sesaki, H. (2000) Yeast mitochondrial dynamics: fusion, division, segregation, and shape. *Microsc Res Tech*, **51**, 573-583.

Jin, H., Kendall, E., Freeman, T.C., Roberts, R.G. and Vetrie, D.L. (1999) The human family of Deafness/Dystonia peptide (DDP) related mitochondrial import proteins. *Genomics*, **61**, 259-267.

Johnson, A.E. and Haigh, N.G. (2000) The ER translocon and retrotranslocation: is the shift into reverse manual or automatic? *Cell*, **102**, 709-712.

Kaldi, K., Bauer, M.F., Sirrenberg, C., Neupert, W. and Brunner, M. (1998) Biogenesis of Tim23 and Tim17, integral components of the TIM machinery for matrix-targeted preproteins. *EMBO J.*, **17**, 1569-1576.

Kanaji, S., Iwahashi, J., Kida, Y., Sakaguchi, M. and Mihara, K. (2000) Characterization of the signal that directs Tom20 to the mitochondrial outer membrane. *J Cell Biol*, **151**, 277-288.

Kang, P.-J., Ostermann, J., Shilling, J., Neupert, W., Craig, E.A. and Pfanner, N. (1990) Requirement for hsp70 in the mitochondrial matrix for translocation and folding of precursor proteins. *Nature*, **348**, 137-142.

Kassenbrock, C.K., Cao, W. and Douglas, M.G. (1993) Genetic and biochemical characterization of *ISP6*, a small mitochondrial outer membrane protein associated with the protein translocation complex. *EMBO J.*, **12**, 3023-3034.

Keil, P. and Pfanner, N. (1993) Insertion of MOM22 into the mitochondrial outer membrane strictly depends on surface receptors. *FEBS Lett.*, **321**, 197-200.

Kerscher, O., Holder, J., Srinivasan, M., Leung, R.S. and Jensen, R.E. (1997) The Tim54p-Tim22p complex mediates insertion of proteins into the mitochondrial inner membrane. *J. Cell Biol.*, **139**, 1663-1675.

Kerscher, O., Sepuri, N.B. and Jensen, R.E. (2000) Tim18p is a new component of the Tim54p-Tim22p translocon in the mitochondrial inner membrane. *Mol. Biol. Cell*, **11**, 103-116.

Kiebler, M., Becker, K., Pfanner, N. and Neupert, W. (1993a) Mitochondrial protein import: Specific recognition and membrane translocation of preproteins. *J. Membrane Biol.*, **135**, 191-207.

Kiebler, M., Keil, P., Schneider, H., van der Klei, I., Pfanner, N. and Neupert, W. (1993b) The mitochondrial receptor complex: A central role of MOM22 in mediating transfer of preproteins from receptors to the general insertion pore. *Cell*, **74**, 483-492.

Kiebler, M., Pfaller, R., Söllner, T., Griffiths, G., Horstmann, H., Pfanner, N. and Neupert, W. (1990) Identification of a mitochondrial receptor complex required for recognition and membrane insertion of precursor proteins. *Nature*, **348**, 610-616.

Knox, C., Sass, E., Neupert, W. and Pines, O. (1998) Import into mitochondria, folding and retrograde movement of fumarase in yeast. *J Biol Chem*, **273**, 25587-25593.

Koehler, C., Merchant, S., Oppliger, W., Schmid, K., Jarosch, E., Dolfini, L., Junne, T., Schatz, G. and Tokatlidis, K. (1998a) Tim9p, an essential partner subunit of Tim10p for the import of mitochondrial carrier proteins. *EMBO J.*, **17**, 6477-6486.

Koehler, C.M., Jarosch, E., Tokatlidis, K., Schmid, K., Schweyen, R.J. and Schatz, G. (1998b) Import of mitochondrial carriers mediated by essential proteins of the intermembrane space. *Science*, **279**, 369-373.

Koehler, C.M., Leuenberger, D., Merchant, S., Renold, A., Junne, T. and Schatz, G. (1999a) Human deafness dystonia syndrome is a mitochondrial disease. *Proc. Natl. Acad. Sci. USA*, **96**, 2141-2146.

Koehler, C.M., Merchant, S. and Schatz, G. (1999b) How membrane proteins travel across the mitochondrial intermembrane space. *Trends Biochem. Sci.*, **24**, 428-432.

Koehler, C.M., Murphy, M.P., Bally, N.A., Leuenberger, D., Oppliger, W., Dolfini, L., Junne, T., Schatz, G. and Or, E. (2000) Tim18p, a new subunit of the TIM22 complex that mediates insertion of imported proteins into the yeast mitochondrial inner membrane. *Mol. Cell. Biol.*, **20**, 1187-1193.

Komiya, T., Hachiya, N., Sakaguchi, M., Omura, T. and Mihara, K. (1994) Recognition of mitochondria-targeting signals by a cytosolic import stimulation factor, MSF. *J. Biol. Chem.*, **269**, 30893-30897.

Komiya, T., Rospert, S., Schatz, G. and Mihara, K. (1997) Binding of mitochondrial precursor proteins to the cytoplasmic domains of the import receptors Tom70 and Tom20 is determined by cytoplasmic chaperones. *EMBO J.*, **16**, 4267-4275.

Komiya, T., Sakaguchi, M. and Mihara, K. (1996) Cytoplasmic chaperones determine the targeting pathway of precursor proteins to mitochondria. *EMBO J.*, **15**, 399-407.

Kovermann, P., Truscott, K.N., Guiard, B., Rehling, P., Sepuri, N.B., Müller, H., Jensen, R.E., Wagner, R. and Pfanner, N. (2002) Tim22, the essential core of the mitochondrial proteininsertion complex, forms a voltage-activated and signal-gated channel. *Molec. Cell*, **9**, 363-373.

Krimmer, T., Rapaport, D., Ryan, M.T., Meisinger, C., Kassenbrock, C.K., Blachly-Dyson, E., Forte, M., Douglas, M.G., Neupert, W., Nargang, F.E. and Pfanner, N. (2001) Biogenesis of porin of the outer mitochondrial membrane involves an import pathway via receptors and the general import pore of the TOM complex. *J Cell Biol*, **152**, 289-300.

Kübrich, M., Keil, P., Rassow, J., Dekker, P., Blom, J., Meijer, M. and Pfanner, N. (1994) The polytopic mitochondrial inner membrane proteins MIM17 and MIM23 operate at the same preprotein import site. *FEBS Lett*, **349**, 222-228.

Künkele, K.-P., Heins, S., Dembowski, M., Nargang, F.E., Benz, R., Thieffry, M., Walz, J., Lill, R., Nussberger, S. and Neupert, W. (1998a) The preprotein translocation channel of the outer membrane of mitochondria. *Cell*, **93**, 1009-1019.

Künkele, K.P., Juin, P., Pompa, C., Nargang, F.E., Henry, J.P., Neupert, W., Lill, R. and Thieffry, M. (1998b) The isolated complex of the translocase of the outer membrane of mitochondria. Characterization of the cation-selective and voltage-gated preprotein-conducting pore. *J Biol Chem*, **273**, 31032-31039.

Laemmli, U.K. (1970) Cleavage of structural proteins during the assembly of the head of bacteriophage T4. *Nature*, **227**, 680-685.

Lang, B.F., Gray, M.W. and Burger, G. (1999) Mitochondrial genome evolution and the origin of eukaryotes. *Annu Rev Genet*, **33**, 351-397.

Lee, C.M., Sedman, J., Neupert, W. and Stuart, R.A. (1999) The DNA helicase, Hmi1p, is transported into mitochondria by a C-terminal cleavable targeting signal. *J Biol Chem*, **274**, 20937-20942.

Leuenberger, D., Bally, N.A., Schatz, G. and Koehler, C.M. (1999) Different import pathways through the mitochondrial intermembrane space for inner membrane proteins. *EMBO J.*, **18**, 4816-4822.

Liebermeister, W., Rapoport, T.A. and Heinrich, R. (2001) Ratcheting in post-translational protein translocation: a mathematical model. *J Mol Biol*, **305**, 643-656.

Lill, R., Diekert, K., Kaut, A., Lange, H., Pelzer, W., Prohl, C. and Kispal, G. (1999) The essential role of mitochondria in the biogenesis of cellular iron-sulfur proteins. *Biol Chem*, **380**, 1157-1166.

Lill, R. and Kispal, G. (2000) Maturation of cellular Fe-S proteins: an essential function of mitochondria. *Trends Biochem. Sci.*, **25**, 352-356.

Lim, J.H., Martin, F., Guiard, B., Pfanner, N. and Voos, W. (2001) The mitochondrial Hsp70-dependent import system actively unfolds preproteins and shortens the lag phase of translocation. *EMBO J.*, **20**, 941-950.

Lithgow, T., Junne, T., Suda, K., Gratzer, S. and Schatz, G. (1994) The mitochondrial outer membrane protein Mas22p is essential for protein import and viability of yeast. *Proc. Natl. Acad. Sci. U.S.A.*, **91**, 11973-11977.

Liu, X., Kim, C.N., Yang, J., Jemmerson, R. and Wang, X. (1996) Induction of apoptotic program in cell-free extracts: requirement for dATP and cytochrome c. *Cell*, **86**, 147-157.

Lohret, T.A., Jensen, R.E. and Kinnally, K.W. (1997) Tim23, a protein import component of the mitochondrial inner membrane, is required for normal activity of the multiple conductance channel, MCC. *J. Cell Biol.*, **137**, 377-386.

Lorenzo, H.K., Susin, S.A., Penninger, J. and Kroemer, G. (1999) Apoptosis inducing factor (AIF): a phylogenetically old, caspase- independent effector of cell death. *Cell Death Differ*, **6**, 516-524.

Maarse, A.C., Bloom, J., Grivell, L.A. and Meijer, M. (1992) MPI1, an essential gene encoding a mitochondrial membrane protein, is possibly involved in protein import into yeast mitochondria. *EMBO J.*, **11**, 3619-3628.

Maarse, M., Keil, P., Rassow, J., Dekker, P., Blom, J., Meijer, M. and Pfanner, N. (1994) Identification of the essential yeast protein MIM17, an integral mitochondrial inner membrane protein involved in protein import. *FEBS Lett*, **349**, 215-221.

Macasev, D., Newbigin, E., Whelan, J. and Lithgow, T. (2000) How do plant mitochondria avoid importing chloroplast proteins? Components of the import apparatus Tom20 and Tom22 from Arabidopsis differ from their fungal counterparts. *Plant Phys.*, **123**, 811-816.

Maloney, P.C., Yan, R.T. and Abe, K. (1994) Bacterial anion exchange: reductionist and integrative approaches to membrane biology. *J Exp Biol*, **196**, 471-482.

Mannella, C.A., Buttle, K., Rath, B.K. and Marko, M. (1998) Electron microscopic tomography of rat-liver mitochondria and their interaction with the endoplasmic reticulum. *Biofactors*, **8**, 225-228.

Mannella, C.A., Marko, M., Penczek, P., Barnard, D. and Frank, J. (1994) The internal compartmentation of rat-liver mitochondria: tomographic study using the high-voltage transmission electron microscope. *Microsc Res Tech*, **27**, 278-283.

Mannella, C.A., Neuwald, A.F. and Lawrence, C.E. (1996) Detection of likely transmembrane beta strand regions in sequences of mitochondrial pore proteins using the Gibbs sampler. *J. Bioenerg. Biomembranes*, **28**, 163-169.

Margolin, B.S., Freitag, M. and Selker, E.U. (1997) Improved plasmids for gene targeting at the *his-3* locus of *Neurospora crassa* by electroporation. *Fungal Genet. Newsl.*, **44**, 34-36.

Margolin, B.S., Freitag, M. and Selker, E.U. (2000) Improved plasmids for gene targeting at the *his-3* locus of *Neurospora crassa* by electroporation: correction. *Fungal Genet. Newsl.*, **47**, 112.

Margulis, L. (1975) Symbiotic theory of the origin of eukaryotic organelles; criteria for proof. *Symposia of the Society for Experimental Biology*, 21-38.

Margulis, L. (1976) Genetic and evolutionary consequences of symbiosis. *Experimental Parasitology*, **39**, 277-349.

Margulis, L. and Tzertzinis, G. (1987) Symbiosis as a mechanism of evolution: status of cell symbiosis theory. *Annals of the New York Academy of Sciences*, **503**, 187-197.

Martin, J., Mahlke, K. and Pfanner, N. (1991) Role of an energized inner membrane in mitochondrial protein import. *J. Biol. Chem.*, **266**, 18051-18057.

Martin, W., Hoffmeister, M., Rotte, C. and Henze, K. (2001) An overview of endosymbiotic models for the origins of eukaryotes, their ATP-producing organelles (mitochondria and hydrogenosomes), and their heterotrophic lifestyle. *Biol Chem*, **382**, 1521-1539.

Martindale, J.L. and Holbrook, N.J. (2002) Cellular response to oxidative stress: signaling for suicide and survival. *J Cell Physiol*, **192**, 1-15.

Marzo, I., Brenner, C., Zamzami, N., Susin, S.A., Beutner, G., Brdiczka, D., Remy, R., Xie, Z.H., Reed, J.C. and Kroemer, G. (1998) The permeability transition pore complex: a target for apoptosis regulation by caspases and bcl-2-related proteins. *J Exp Med*, **187**, 1261-1271.

Matlack, K.E., Misselwitz, B., Plath, K. and Rapoport, T.A. (1999) BiP acts as a molecular ratchet during posttranslational transport of prepro-alpha factor across the ER membrane. *Cell*, **97**, 553-564.

Matouschek, A., Azem, A., Ratliff, K., Glick, B.S., Schmid, K. and Schatz, G. (1997) Active unfolding of precursor proteins during mitochondrial protein import. *EMBO J*, **16**, 6727-6736.

Matouschek, A., Pfanner, N. and Voos, W. (2000) Protein unfolding by mitochondria. The Hsp70 import motor. *EMBO Reports*, **1**, 404-410.

Mayer, A., Driessen, A., Neupert, W. and Lill, R. (1995a) Purified and protein-loaded mitochondrial outer membrane vesicles for functional analysis of preprotein transport. *Methods Enzymol.*, **260**, 252-263.

Mayer, A., Lill, R. and Neupert, W. (1993) Translocation and insertion of precursor proteins into isolated outer membranes of mitochondria. *J. Cell Biol.*, **121**, 1233-1243.

Mayer, A., Nargang, F.E., Neupert, W. and Lill, R. (1995b) MOM22 is a receptor for mitochondrial targeting sequences and cooperates with MOM19. *EMBO J.*, **14**, 4204-4211.

Mayer, A., Neupert, W. and Lill, R. (1995c) Mitochondrial protein import: Reversible binding of the presequence at the *trans* side of the outer membrane drives partial translocation and unfolding. *Cell*, **80**, 127-137.

McBride, H., Goping, I. and Shore, G. (1996) The human mitochondrial import receptor, hTom20p, prevents a cryptic matrix targeting sequence from gaining access to the protein translocation machinery. *J. Cell Biol.*, **134**, 307-313.

McBride, H.M., Millar, D.G., Li, J.M. and Shore, G.C. (1992) A signal-anchor sequence selective for the mitochondrial outer membrane. *J. Cell Biol.*, **119**, 1451-1457.

McEwen, B.F. and Frank, J. (2001) Electron tomographic and other approaches for imaging molecular machines. *Curr Opin Neurobiol*, **11**, 594-600.

McStay, G.P. and Halestrap, A.P. (2002) The permeability transition pore complex: another view. *J Biol Chem*, **277**, 34793-34799.

Meisinger, C., Ryan, M.T., Hill, K., Model, K., Lim, J.H., Sickmann, A., Müller, H., Meyer, H.E., Wagner, R. and Pfanner, N. (2001) Protein import channel of the outer mitochondrial membrane: a highly stable Tom40-Tom22 core structure differentially interacts with preproteins, small tom proteins, and import receptors. *Mol. Cell. Biol.*, **21**, 2337-2348.

Merlin, A., von Ahsen, O., Craig, E.A., Dietmeier, K. and Pfanner, N. (1997) A mutant form of mitochondrial GrpE suppresses the sorting defect caused by an alteration in the presequence of cytochrome b2. *J Mol Biol*, **273**, 1-6.

Metzenberg, R., Stevens, J., Selker, E. and Morzycka-Wroblewska, E. (1984) A method for finding the genetic map position of cloned DNA fragments. *Neurospora Newsl.*, **31**, 35-39.

Metzenberg, R., Stevens, J., Selker, E. and Morzycka-Wroblewska, E. (1985) Identification and chromosomal distribution of 5S rRNA genes in *Neurospora crassa*. *Proc. Natl. Acad. Sci. USA*, **82**, 2067-2071.

Metzenberg, R.L. and Grotelueschen, J.S. (1992) Disruption of essential genes in *Neurospora* by RIP. *Fungal Genet. Newsl.*, **39**, 37-49.

Milisav, I., Moro, F., Neupert, W. and Brunner, J. (2001) Modular structure of the TIM23 preprotein translocase of mitochondria. *J. Biol. Chem.*, **276**, 25856-25861.

Mitoma, J. and Ito, A. (1992) Mitochondrial targeting signal of rat liver monoamine oxidase B is located at its carboxy terminus. *J Biochem (Tokyo)*, **111**, 20-24.

Moczko, M., Bömer, U., Kübrich, M., Zufall, N., Hönlinger, A. and Pfanner, N. (1997) The intermembrane space domain of mitochondrial Tom22 functions as a trans binding site for preproteins with N-terminal targeting sequences. *Mol. Cell. Biol.*, **17**, 6574-6584.

Moczko, M., Dietmeier, K., Söllner, T., Segui, B., Steger, H.F., Neupert, W. and Pfanner, K. (1992) Identification of the mitochondrial receptor complex in *S. cerevisiae*. *FEBS Lett.*, **310**, 265-268.

Model, K., Meisinger, C., Prinz, T., Wiedemann, N., Truscott, K.N., Pfanner, N. and Ryan, M.T. (2001) Multistep assemblyof the protein import channel of the mitochondrial outer membrane. *Nat. Struct. Biol.*, **8**, 361-370.

Model, K., Prinz, T., Ruiz, T., Radermacher, M., Krimmer, T., Kühlbrandt, W., Pfanner, N. and Meisinger, C. (2002) Protein translocase of the outer mitochondrial membrane: Role of the import receptors in the structural organization of the TOM complex. *J. Mol. Biol.*, **316**, 657-666.

Mokranjac, D., Paschen, S.A., Kozany, C., Prokisch, H., Hoppins, S.C., Nargang, F.E., Neupert, W. and Hell, K. (2003) Tim50, a novel component of the TIM23 preprotein translocase of mitochondria. *EMBO J*, **22**, 816-825.

Moraes, C.T., DiMauro, S., Zeviani, M., Lombes, A., Shanske, S., Miranda, A.F., Nakase, H., Bonilla, E., Werneck, L.C., Servidei, S. and et al. (1989)

Mitochondrial DNA deletions in progressive external ophthalmoplegia and Kearns-Sayre syndrome. *N Engl J Med*, **320**, 1293-1299.

Morgan-Hughes, J.A. and Hanna, M.G. (1999) Mitochondrial encephalomyopathies: the enigma of genotype versus phenotype. *Biochim Biophys Acta*, **1410**, 125-145.

Moro, F., Okamoto, K., Donzeau, M., Neupert, W. and Brunner, M. (2002) Mitochondrial protein import: Molecular basis of the ATP-dependent interaction of mtHsp70 with Tim44.

Moro, F., Sirrenberg, C., Schneider, H.C., Neupert, W. and Brunner, M. (1999) The TIM17.23 preprotein translocase of mitochondria: composition and function in protein transport into the matrix. *EMBO J.*, **18**, 3667-3675.

Mozdy, A.D., McCaffery, J.M. and Shaw, J.M. (2000) Dnm1p GTPase-mediated mitochondrial fission is a multi-step process requiring the novel integral membrane component Fis1p. *J Cell Biol*, **151**, 367-380.

Mukhopadhyay, A., Avramova, L.V. and Weiner, H. (2002) Tom34 unlike Tom20 does not interact with the leader sequences of mitochondrial precursor proteins. *Arch Biochem Biophys*, **400**, 97-104.

Munnich, A. and Rustin, P. (2001) Clinical spectrum and diagnosis of mitochondrial disorders. *Am J Med Genet*, **106**, 4-17.

Murakami, H., Pain, D. and Blobel, G. (1988) 70K heat-shock related protein is one of at least two distinct cytosolic factors stimulating protein import into mitochondria. *J. Cell Biol.*, **107**, 2051-2057.

Murakami, K. and Mori, M. (1990) Purified presequence binding factor (PBF) forms an import-competent complex with a purified mitochondrial precursor protein. *EMBO J.*, **9**, 3201-3208.

Murakami, K., Tanase, S., Morino, Y. and Mori, M. (1992) Presequence binding factor-dependent and -independent import of proteins into mitochondria. *J Biol Chem*, **267**, 13119-13122.

Murcha, M.W., Lister, R., Ho, A.Y. and Whelan, J. (2003) Identification, expression, and import of components 17 and 23 of the inner mitochondrial membrane translocase from Arabidopsis. *Plant Physiol*, **131**, 1737-1747.

Muto, T., Obita, T., Abe, Y., Shodai, T., Endo, T. and Kohda, D. (2001) NMR identification of the Tom20 binding segment in mitochondrial presequences. *J. Mol. Biol.*, **306**, 137-143.

Nakai, M., Kinoshita, K. and Endo, T. (1995) Mitochondrial receptor complex protein. The intermembrane space domain of yeast Mas17 is not essential for its targeting or function. *J. Biol. Chem.*, **270**, 30571-30575.

Nakase, H., Moraes, C.T., Rizzuto, R., Lombes, A., DiMauro, S. and Schon, E.A. (1990) Transcription and translation of deleted mitochondrial genomes in Kearns-Sayre syndrome: implications for pathogenesis. *Am J Hum Genet*, **46**, 418-427.

Nargang, F.E., Drygas, M.E., Kwong, P.L., Nicholson, D.W. and Neupert, W. (1988) A mutant of *Neurospora crassa* deficient in cytochrome *c* heme lyase activity cannot import cytochrome *c* into mitochondria. *J. Biol. Chem.*, **263**, 9388-9394.

Nargang, F.E., Künkele, K.-P., Mayer, A., Ritzel, R.G., Neupert, W. and Lill, R. (1995) "Sheltered disruption" of *Neurospora crassa* MOM22, an essential component of the mitochondrial protein import complex. *EMBO J.*, **14**, 1099-1108.

Nargang, F.E., Rapaport, D., Ritzel, R.G., Neupert, W. and Lill, R. (1998) Role of the negative charges in the cytosolic domain of TOM22 in the import of precursor proteins into mitochondria. *Mol. Cell. Biol.*, **18**, 3173-3181.

Neupert, W. (1997) Protein import into mitochondria. *Annu. Rev. Biochem.*, **66**, 863-917.

Neupert, W. and Brunner, M. (2002) The protein import motor of mitochondria. *Nat. Rev. Mol. Cell Biol.*, **3**, 355-365.

Nguyen, M., Millar, D.G., Yong, V.W., Korsmeyer, S.J. and Shore, G.C. (1993) Targeting of Bcl-2 to the mitochondrial outer membrane by a carboxy-terminal signal anchor sequence. *J. Biol. Chem.*, **268**, 25265-25268.

Nunnari, J.M., Fox, T. and Walter, P. (1993) A mitochondrial protease with two catalytic subunits of nonoverlapping specificities. *Science*, **262**, 1997-2004.

Nuttall, S.D., Hanson, B.J., Mori, M. and Hoogenraad, N.J. (1997) hTom34: a novel translocase for the import of proteins into human mitochondria. *DNA Cell Biol*, **16**, 1067-1074.

Okamoto, K., Brinker, A., Paschen, S., Moarefi, I., Hayer-Hartl, M., Neupert, W. and Brunner, M. (2002) The protein import motor of mitochondria: a targeted molecular ratchet driving unfolding and translocation. *EMBO J.*, **21**, 3659-3671.

Ono, H. and Tuboi, S. (1988) The cytosolic factor required for import of precursors of mitochondrial precursor proteins into mitochondria. *J. Biol. Chem.*, **263**, 3188-3193.

Ono, H. and Tuboi, S. (1990) Purification and identification of a cytosolic factor required for import of precursors of mitochondrial proteins into mitochondria. *Arch. Biochem. Biophys.*, **280**, 299-304.

Ostermann, J., Horwich, A.L., Neupert, W. and Hartl, F.-U. (1989) Protein folding in mitochondria requires complex formation with hsp60 and ATP hydrolysis. *Nature*, **341**, 125-130.

Osteryoung, K.W. (2000) Organelle fission. Crossing the evolutionary divide. *Plant Physiol*, **123**, 1213-1216.

Osteryoung, K.W. (2001) Organelle fission in eukaryotes. *Curr Opin Microbiol*, **4**, 639-646.

Otsuga, D., Keegan, B.R., Brisch, E., Thatcher, J.W., Hermann, G.J., Bleazard, W. and Shaw, J.M. (1998) The dynamin-related GTPase, Dnm1p, controls mitochondrial morphology in yeast. *J Cell Biol*, **143**, 333-349.

Palade, G. (1952) The fine structure of mitochondria. *Anat. Rec*, **114**, 427-451.

Palmieri, F. (1994) Mitochondrial carrier proteins. *FEBS Lett.*, **346**, 48-54.

Paschen, S. and Neupert, W. (2001) Protein import into mitochondria. *Life*, **52**, 101-112.

Paschen, S., Rothbauer, U., Kaldi, K., Bauer, M., Neupert, W. and Brunner, M. (2000) The role of TIM8-13 complex in the import of Tim23 into mitochondria. *EMBO J.*, **19**, 6392-6400.

Perkins, G., Renken, C., Martone, M.E., Young, S.J., Ellisman, M. and Frey, T. (1997) Electron tomography of neuronal mitochondria: three-dimensional structure and organization of cristae and membrane contacts. *J Struct Biol*, **119**, 260-272.

Pfaller, R., Pfanner, N. and Neupert, W. (1989) Mitochondrial protein import: Bypass of proteinaceous surface receptors can occur with low specificity and efficiency. *J. Biol. Chem.*, **264**, 34-39.

Pfanner, N., Craig, E.A. and Honlinger, A. (1997) Mitochondrial preprotein translocase. *Ann. Rev. Cell Dev. Biol.*, **13**, 25-51.

Pfanner, N. and Geissler, A. (2001) Versatility of the mitochondrial import machinery. *Nat. Rev. Mol. Cell Biol.*, **2**, 339-349.

Pfanner, N., Hartl, F.-U. and Neupert, W. (1988) Import of proteins into mitochondria: a multi-step process. *Eur. J. Biochem.*, **175**, 205-212.

Pfanner, N. and Neupert, W. (1990) The mitochondrial protein import apparatus. *Annu. Rev. Biochem.*, **59**, 331-353.

Pfanner, N., Rassow, J., Guiard, B., Söllner, T., Hartl, F.-U. and Neupert, W. (1990) Energy requirements for unfolding and membrane translocation of precursor proteins during import into mitochondria. *J. Biol. Chem.*, **265**, 16324-16329.

Pfanner, N., Tropschug, M. and Neupert, W. (1987) Mitochondrial protein import: nucleoside triphosphates are involved in conferring import-competence to precursors. *Cell*, **49**, 815-823.

Pfanner, N. and Wiedemann, N. (2002) Mitochondrial protein import: two membranes, three translocases. *Curr. Opin. Cell Biol.*, **14**, 400-411.

Pilgrim, D. and Young, E.T. (1987) Primary structure requirements for correct sorting of the yeast mitochondrial protein ADH III to the yeast mitochondrial matrix space. *Mol Cell Biol*, **7**, 294-304.

Plattner, H.a.G.S. (1969) Protomitochondria of anaerobically grown yeast. III. Morphology. *Biochemistry*, **8**, 339-343.

Prokisch, H., Neupert, W. and Westermann, B. (2000) Role of MMM1 in maintaining mitochondrial morphology in Neurospora crassa. *Mol Biol Cell*, **11**, 2961-2971.

Rabilloud, T., Carpentier, G. and Tarroux, P. (1988) Improvement and simplification of low-background silver staining of proteins by using sodium dithionite. *Electrophoresis*, **9**, 288-291.

Race, H.L., Herrmann, R.G. and Martin, W. (1999) Why have organelles retained genomes? *Trends Genet*, **15**, 364-370.

Ramage, L., Junne, T., Hahne, K., Lithgow, T. and Schatz, G. (1993) Functional cooperation of mitochondrial protein import receptors in yeast. *EMBO J.*, **12**, 4115-4123.

Rapaport, D., Brunner, M., Neupert, W. and Westermann, B. (1998a) Fzo1p is a mitochondrial outer membrane protein essential for the biogenesis of functional mitochondria in Saccharomyces cerevisiae. *J Biol Chem*, **273**, 20150-20155.

Rapaport, D., Künkele, K.P., Dembowski, M., Ahting, U., Nargang, F.E., Neupert, W. and Lill, R. (1998b) Dynamics of the TOM complex of mitochondria during binding and translocation of preproteins. *Mol. Cell. Biol.*, 5256-5262.

Rapaport, D., Mayer, A., Neupert, W. and Lill, R. (1998c) Cis and trans sites of the TOM complex of mitochondria in unfolding and initial translocation of preproteins. *J. Biol. Chem.*, **273**, 8806-8813.

Rapaport, D. and Neupert, W. (1999) Biogenesis of Tom40, core component of the TOM complex of mitochondria. *J. Cell Biol.*, **146**, 321-331.

Rapaport, D., Neupert, W. and Lill, R. (1997) Mitochondrial protein import: Tom40 plays a major role in targeting and translocation of preproteins by forming a specific binding site for the presequence. *J. Biol. Chem.*, **272**, 18725-18731.

Rapaport, D., Taylor, R., Käser, M., Langer, T., Neupert, W. and Nargang, F.E. (2001) Structural requirements of Tom40 for assembly into preexisting TOM complexes of mitochondria. *Mol. Biol. Cell*, **12**, 1189-1198.

Rassow, J., Dekker, P.J.T., van Wilpe, S., Meijer, M. and Soll, J. (1999) The preprotein translocase of the mitochondrial inner membrane: function and evolution. *J Mol Biol*, **286**, 105-120.

Rassow, J., Guiard, B., Wienhues, U., Herzog, V., Hartl, F.-U. and Neupert, W. (1989) Translocation arrest by reversible folding of a precursor protein imported into mitochondria: a means to quantitate translocation contact sites. *J. Cell Biol.*, **109**, 1421-1428.

Rassow, J., Mohrs, K., Koidl, S., Barthelmess, I.B., Pfanner, N. and Tropschug, M. (1995) Cyclophilin 20 is involved in mitochondrial protein folding in cooperation with molecular chaperones Hsp70 and Hsp60. *Mol. Cell. Biol.*, **15**, 2654-2662.

Rehling, P., Wiedemann, N., Pfanner, N. and Truscott, K.N. (2001) The mitochondrial import machinery for preproteins. *Crit. Rev. Biochem. Mol. Biol.*, **36**, 291-336.

Reid, G.A., Yonetani, T. and Schatz, G. (1982) Import of proteins into mitochondria: import and maturation of intermembrane space enzymes cytochrome b_2 and cytochrome c peroxidase in intact yeast cells. *J. Biol. Chem.*, **257**, 13068-13074.

Rizzuto, R., Pinton, P., Carrington, W., Fay, F.S., Fogarty, K.E., Lifshitz, L.M., Tuft, R.A. and Pozzan, T. (1998) Close contacts with the endoplasmic reticulum as determinants of mitochondrial Ca2+ responses. *Science*, **280**, 1763-1766.

Robb-Gaspers, L.D., Burnett, P., Rutter, G.A., Denton, R.M., Rizzuto, R. and Thomas, A.P. (1998a) Integrating cytosolic calcium signals into mitochondrial metabolic responses. *EMBO J*, **17**, 4987-5000.

Robb-Gaspers, L.D., Rutter, G.A., Burnett, P., Hajnoczky, G., Denton, R.M. and Thomas, A.P. (1998b) Coupling between cytosolic and mitochondrial calcium oscillations: role in the regulation of hepatic metabolism. *Biochim Biophys Acta*, **1366**, 17-32.

Rodriguez-Cousino, N., Nargang, F.E., Baardman, R., Neupert, W., Lill, R. and Court, D.A. (1998) An import signal in the cytosolic domain of the Neurospora mitochondrial outer membrane protein TOM22. *J. Biol. Chem.*, **273**, 11527-11532.

Rojo, E.E., Buiard, B., Neupert, W. and Stuart, R.A. (1998) Sorting of D-lactate dehydrogenase to the inner membrane of mitochondria. *J. Biol. Chem.*, **273**, 8040-8047.

Rountree, M.R. and Selker, E.U. (1997) DNA methylation inhibits elongation but not initiation of transcription in Neurospora crassa. *Genes Dev*, **11**, 2383-2395.

Rowley, N., Prip-Buus, C., Westermann, B., Brown, C., Schwarz, E., Barrell, B. and Neupert, W. (1994) Mdj1p, a novel chaperone of the DnaJ family, is involved in mitochondrial biogenesis and protein folding. *Cell*, **77**, 249-259.

Rutter, G.A.a.R.R. (2000) Regulation of mitochondrial metabolism by ER Ca2+ release: an intimate connection. *TIBS*, **25**, 215-221.

Ryan, K.R. and Jensen, R.E. (1993) Mas6p can be crosslinked to an arrested precursor and interacts with other proteins during mitochondrial protein import. *J. Biol. Chem.*, **268**, 23743-23746.

Ryan, K.R., Menold, M.M., Garrett, S. and Jensen, R.E. (1994) SMS1, a high copy suppressor of the mas6 mutant, encodes an essential inner membrane protein required for mitochondrial protein import. *Mol. Cell. Biol.*, **5**, 529-538.

Ryan, M.T., Muller, H. and Pfanner, N. (1999) Functional staging of ADP/ATP carrier translocation across the outer mitochondrial membrane. *J Biol Chem*, **274**, 20619-20627.

Saeki, K., Suzuki, H., Tsuneoka, M., Maeda, M., Iwamoto, R., Hasuwa, H., Shida, S., Takahashi, T., Sakaguchi, M., Endo, T., Miura, Y., Mekada, E. and Mihara, K. (2000) Identification of mammalian Tom22 as a subunit of the preprotein translocase of the mitochondrial outer membrane. *J. Biol. Chem.*, **275**, 31996-32002.

Sagan, L. (1967) On the origin of mitosing cells. *J Theor Biol*, **14**, 255-274.

Sagan, L. (1993) On the origin of mitosing cells. 1967. *J NIH Res*, **5**, 65-72.

Sambrook, J. and Russell, D.W. (2001) *Molecular cloning. A laboratory manual.* Cold Spring Harbor Laoratory Press, Cold Spring Harbor, New York.

Saraste, M. (1999) Oxidative phosphorylation at the fin de siecle. *Science*, **283**, 1488-1493.

Schägger, H., Cramer, W.A. and von Jagow, G. (1994) Analysis of molecular masses and oligomeric states of protein complexes by blue native electrophoresis and isolation of membrane protein complexes by two-dimensional native electrophoresis. *Anal. Biochem.*, **217**, 220-230.

Schägger, H. and von Jagow, G. (1991) Blue native electrophoresis for isolation of membrane complexes in enzymatically active form. *Anal. Biochem.*, **199**, 223-231.

Schapira, A.H. (1999a) Mitochondrial disorders. *Biochim Biophys Acta*, **1410**, 99-102.

Schapira, A.H. (1999b) Mitochondrial involvement in Parkinson's disease, Huntington's disease, hereditary spastic paraplegia and Friedreich's ataxia. *Biochim Biophys Acta*, **1410**, 159-170.

Scherer, P.E., Krieg, U.C., Hwang, S.T., Vestweber, D. and Schatz, G. (1990) A precursor protein partly translocated into yeast mitochondria is bound to a 70kd mitochondrial stress protein. *EMBO J.*, **9**, 4315-4322.

Schimper, A.F.W. (1883) Ueber die entwickelung der chloropylkörner und farbkörper. *Bot. Ztg*, **41**, 105-114.

Schleiff, E. and Turnbull, J.L. (1998a) Characterization of the N-terminal targeting signal binding domain of the mitochondrial outer membrane receptor, Tom20. *Biochemistry*, **37**, 13052-13058.

Schleiff, E. and Turnbull, J.L. (1998b) Functional and structural properties of the mitochondrial outer membrane receptor Tom20. *Biochemistry*, **37**, 13043-13051.

Schleyer, M. and Neupert, W. (1982) Requirement of a membrane potential for the posttranslational transfer of proteins into mitochondria. *Eur. J. Biochem.*, **125**, 109-116.

Schleyer, M. and Neupert, W. (1985) Transport of proteins into mitochondria: translocation intermediates spanning contact sites between inner and outer membranes. *Cell*, **43**, 330-350.

Schlossmann, J., Lill, R., Neupert, W. and Court, D.A. (1996) Tom71, a novel homolog of the mitochondrial preprotein receptor Tom70. *J. Biol. Chem.*, **271**, 17890-17896.

Schneider, H.-C., Berthold, J., Bauer, M.F., Dietmeier, K., Guiard, B., Brunner, M. and Neupert, W. (1994) Mitochondrial Hsp70/MIM44 complex facilitates protein import. *Nature*, **371**, 768-774.

Schon, E.A., Kim, S.H., Ferreira, J.C., Magalhaes, P., Grace, M., Warburton, D. and Gross, S.J. (2000) Chromosomal non-disjunction in human oocytes: is there a mitochondrial connection? *Hum Reprod*, **15 Suppl 2**, 160-172.

Schwartz, M.P. and Matouschek, A. (1999) The dimensions of the protein import channels in the outer and inner mitochondrial membranes. *Proc. Natl. Acad. Sci. USA*, **96**, 13086-13090.

Schweizer, M., Case, M.E., Dykstra, C.C., Giles, N.H. and Kushner, S.R. (1981) Identification and characterization of recombinant plasmids carrying the complete *qa* gene cluster from *Neurospora crassa* including the *qa-1*$^{+}$ regulatory gene. *Proc. Natl. Acad. Sci. U.S.A.*, **78**, 5086-5090.

Segui-Real, B., Kispal, G., Lill, R. and Neupert, W. (1993) Functional independence of the protein translocation machineries in mitochondrial outer and inner

membranes: passage of preproteins through the intermembrane space. *EMBO J.*, **12**, 2211-2218.

Selker, E.U. (1990) Premeiotic instability of repeated sequences in *Neurospora crassa*. *Ann. Rev. Genet.*, **24**, 579-613.

Sesaki, H. and Jensen, R.E. (2001) UGO1 encodes an outer membrane protein required for mitochondrial fusion. *J Cell Biol*, **152**, 1123-1134.

Shanske, S., Moraes, C.T., Lombes, A., Miranda, A.F., Bonilla, E., Lewis, P., Whelan, M.A., Ellsworth, C.A. and DiMauro, S. (1990) Widespread tissue distribution of mitochondrial DNA deletions in Kearns- Sayre syndrome. *Neurology*, **40**, 24-28.

Shaw, J.M. and Nunnari, J. (2002) Mitochondrial dynamics and division in budding yeast. *Trends Cell Biol*, **12**, 178-184.

Sheffield, W.P., Shore, G.C. and Randall, S.K. (1990) Mitochondrial protein import; effects of 70-kd hsp70 on polypeptide folding, aggregation and import competence. *J. Biol. Chem.*, **265**, 11069-11076.

Shore, G.C., McBride, H.M., Millar, D.G., Steenaart, N.A.M. and Nguyen, M. (1995) Import and insertion of proteins into the mitochondrial outer membrane. *Eur. J. Biochem.*, **227**, 9-18.

Shoubridge, E.A. (2000) Mitochondrial DNA segregation in the developing embryo. *Hum Reprod*, **15 Suppl 2**, 229-234.

Shoubridge, E.A. (2001) Nuclear genetic defects of oxidative phosphorylation. *Hum Mol Genet*, **10**, 2277-2284.

Sirrenberg, C., Bauer, M., Guiard, B., Neupert, W. and Brunner, M. (1996) Import of carrier proteins into the mitochondrial inner membrane mediated by Tim22. *Nature*, **384**, 582-585.

Sirrenberg, C., Endres, M., Fölsch, H., Stuart, R.A., Neupert, W. and Brunner, M. (1998) Carrier protein import into mitochondria mediated by the intermembrane space proteins Tim10/Mrs11p and Tim12/Mrs10p. *Nature*, **391**, 912-915.

Sjöstrand, F.S. (1956) The ultrastructure of cells as revealed by the electron microscope. *Int. Rev. Cytol.*, **5**, 455-533.

Smagula, C.S. and Douglas, M.G. (1988) ADP/ATP carrier of S. cerevisiae contains a mitochondrial import signal between amino acids 72 and 111. *J. Cell. Biochem.*, **36**, 323-328.

Soll, J. (2002) Protein import into chloroplasts. *Curr Opin Plant Biol*, **5**, 529-535.

Söllner, T., Pfaller, R., Griffiths, G., Pfanner, N. and Neupert, W. (1990) A mitochondrial import receptor for the ADP/ATP carrier. *Cell*, **62**, 107-115.

Söllner, T., Rassow, J., Wiedmann, M., Schlossmann, J., Keil, P., Neupert, W. and Pfanner, N. (1992) Mapping of the protein import machinery in the mitochondrial outer membrane by crosslinking of translocation intermediates. *Nature*, **355**, 84-87.

Staben, C., Jensen, B., Singer, M., Pollock, J. and Schechtman, M. (1989) Use of bacterial hygromycin B resistance gene as a dominant selectable marker in *Neurospora crassa* transformation. *Fungal Genet. Newsl.*, **36**, 79-81.

Stan, T., Ahting, U., Dembowski, M., Künkele, K.-P., Nussberger, S., Neupert, W. and Rapaport, D. (2000) Recognition of preproteins by the isolated TOM complex of mitochondria. *EMBO J.*, **19**, 4895-4902.

Steger, H.F., Söllner, T., Kiebler, M., Dietmeier, K.A., Trülzsch, K.S., Tropschug, M., Neupert, W. and Pfanner, N. (1990) Import of ADP/ATP carrier into mitochondria: two receptors act in parallel. *J. Cell Biol.*, **111**, 2353-2363.

Stevens, B.J. (1977) Variation in number and volume of the mitochondria in yeast according to growth conditons. A study based on serial sectioning and computer graphics reconstruction. *Biol. Cell.*, **28**, 37-56.

Stuart, R. (2002) Insertion of proteins into the inner membrane of mitochondria: the role of the Oxa1 complex. *Biochim Biophys Acta*, **1592**, 79-87.

Suzuki, H., Okazawa, Y., Komiya, T., Saeki, K., Mekada, E., Kitada, S., Ito, F. and Mihara, K. (2000) Characterization of rat Tom40, a central component of the preprotein translocase of the mitochondrial outer membrane. *J. Biol. Chem.*, **275**, 37930-37936.

Tang, X.B., Fujinaga, J., Kopito, R. and Casey, J.R. (1998) Topology of the region surrounding Glu681 of human AE1 protein, the erythrocyte anion exchanger. *J Biol Chem*, **273**, 22545-22553.

Tatton, W.G. and Olanow, C.W. (1999) Apoptosis in neurodegenerative diseases: the role of mitochondria. *Biochim Biophys Acta*, **1410**, 195-213.

Taylor, A.B., Smith, B.S., Kitada, S., Kojima, D., Miyaura, H., Otwinowski, Z., Ito, A. and Deisenhofer, J. (2001) Crystal structures of mitochondrial processing peptidase reveal the mode for specific cleavage of imort signal sequences. *Structure*, **9**, 615-625.

Taylor, R.D., McHale, B.J. and Nargang, F.E. (2003) Characterization of Neurospora crassa Tom40-deficient mutants and effect of specific mutations on Tom40 assembly. *J Biol Chem*, **278**, 765-775.

Terada, K., Kanazawa, M., Yano, M., Hanson, B., Hoogenraad, N. and Mori, M. (1997) Participation of the import receptor Tom20 in protein import into mammalian mitochondria: analyses in vitro and in cultured cells. *FEBS Lett*, **403**, 309-312.

Tieu, Q. and Nunnari, J. (2000) Mdv1p is a WD repeat protein that interacts with the dynamin-related GTPase, Dnm1p, to trigger mitochondrial division. *J Cell Biol*, **151**, 353-366.

Tieu, Q., Okreglak, V., Naylor, K. and Nunnari, J. (2002) The WD repeat protein, Mdv1p, functions as a molecular adaptor by interacting with Dnm1p and Fis1p during mitochondrial fission. *J Cell Biol*, **158**, 445-452.

Tokatlidis, K. and Schatz, G. (1999) Biogenesis of mitochondrial inner membrane proteins. *J. Biol. Chem.*, **274**, 35285-35288.

Truscott, K.N., Kovermann, P., Geissler, A., Merlin, A., Meijer, M., Driessen, A.J., Rassow, J., Pfanner, N. and Wagner, R. (2001) A presequence- and voltage-sensitive channel of the mitochondrial preprotein translocase formed by Tim23. *Nat. Struct. Biol.*, **8**, 1074-1082.

Tsujimoto, Y. (2002) Bcl-2 family of proteins: life-or-death switch in mitochondria. *Bioscience Reports*, **22**, 47-58.

Turnbull, D.M., Lightowlers, R.N. and Taylor, R.W. (2001) Current perspectives in the treatment of mitochondrial DNA diseases. *Funct Neurol*, **16**, 89-96.

Ungermann, C., Neupert, W. and Cyr, D.M. (1994) The role of Hsp70 in conferring unidirectionality on protein translocation into mitochondria. *Science*, **266**, 1250-1253.

van der Bliek, A.M. (2000) A mitochondrial division apparatus takes shape. *J Cell Biol*, **151**, F1-4.

van Geest, M., and Lolkema, JS. (2000) Membrane topology and insertion of membrane proteins: search for topogenic signals. *Microbiol Mol Biol Rev*, **64**, 13-33.

van Wilpe, S., Ryan, M.T., Hill, K., Maarse, A.C., Meisinger, C., Brix, J., Dekker, P.J., Moczko, M., Wagner, R., Meijer, M., Guiard, B., Honlinger, A. and Pfanner, N. (1999) Tom22 is a multifunctional organizer of the mitochondrial preprotein translocase. *Nature*, **401**, 485-489.

Vaskova, M., Bentley, A.M., Marshall, S., Reid, P., Thummel, C.S. and Andres, A.J. (2000) Genetic analysis of the Drosophila 63F early puff. Characterization of mutations in E63-1 and maggie, a putative Tom22. *Genetics*, **156**, 229-244.

Vestweber, D., Brunner, K.P., Baker, A. and Schatz, G. (1989) A 42K outer membrane protein is a component of the yeast mitochondrial import site. *Nature*, **341**, 205-209.

Voet, D.a.V., J. (1990) *Biochemistry*. John Wiley and Sons, Inc.

Voisine, C., Craig, E.A., Zufall, N., von Ahsen, O., Pfanner, N. and Voos, W. (1999) The protein import motor of mitochondria: unfolding and trapping of preproteins are distinct and separable functions of matrix Hsp70. *Cell*, **97**, 565-574.

von Heijne, G. (1986) Mitochondrial targeting sequences may form amphiphilic helices. *EMBO J.*, **5**, 1335-1342.

Voos, W., Gambill, B.D., Guiard, B., Pfanner, N. and Craig, E.A. (1993) Presequence and mature part of preproteins strongly influence the dependence of mitochondrial protein import on heat shock protein 70 in the matrix. *J. Cell Biol.*, **123**, 119-126.

Voos, W., Gambill, B.D., Laloraya, S., Ang, D., Craig, E.A. and Pfanner, N. (1994) Mitochondrial GrpE is present in a complex with Hsp70 and preproteins in transit across membranes. *Mol. Cell. Biol.*, **14**, 6627-6634.

Voos, W., Martin, H., Krimmer, T. and Pfanner, N. (1999) Mechanisms of protein translocation into mitochondria. *Biochim. Biophys. Acta*, **1422**, 235-254.

Wachter, C., Schatz, G. and Glick, B.S. (1994) Protein import into mitochondria: The requirement for external ATP is precursor-specific, whereas intramitochondrial

ATP is universally needed for translocation into the matrix. *Mol. Biol. Cell*, **5**, 465-474.

Wallace, D.C. (1999) Mitochondrial diseases in man and mouse. *Science*, **283**, 1482-1488.

Wallace, D.C., Brown, M.D. and Lott, M.T. (1999) Mitochondrial DNA variation in human evolution and disease. *Gene*, **238**, 211-230.

Wallace, D.C. and Murdock, D.G. (1999) Mitochondria and dystonia: the movement disorder connection? [comment]. *Proc Natl Acad Sci U S A*, **96**, 1817-1819.

Wei, Y.H. and Lee, H.C. (2002) Oxidative stress, mitochondrial DNA mutation, and impairment of antioxidant enzymes in aging. *Exp Biol Med (Maywood)*, **227**, 671-682.

Wendland, J., Lengeler, K. and Kothe, E. (1996) An instant preparation method for nucleic acids of filamentous fungi. *Fungal Genet. Newslett.*, **43**, 54-55.

Werhahn, W., Niemeyer, A., Jansch, L., Kruft, V.V., Schmitz, U.K. and Braun, H.P. (2001) Purification and Characterization of the Preprotein Translocase of the Outer Mitochondrial Membrane from Arabidopsis. Identification of Multiple Forms of TOM20. *Plant Physiol*, **125**, 943-954.

Westermann, B., Prip-Buus, C., Neupert, W. and Schwarz, E. (1995) The role of the GrpE homolog, Mge1p, in mediating protein import and protein folding in mitochondria. *EMBO J.*, **14**, 3452-3460.

White, B. and Woodward, D. (1995) A simple method for making disposable race tubes. *Fungal Genetics Newslett.*, **42**, 79.

Wiedemann, N., V. Kozjak, A. Chacinska, B. Schonfisch, S. Rospert, M.T. Ryan, N. Pfanner, and C. Meisinger. (2003) Machinery for protein sorting and assembly in the mitochondrial outer membrane. *Nature*, **424**, 565-571.

Witte, C., Jensen, R.E., Yaffe, M.P. and Schatz, G. (1988) MAS1, a gene essential for yeast mitochondrial assembly, encodes a subunit of the mitochondrial processing peptidase. *EMBO J.*, **7**, 1439-1447.

Wong, E.D., Wagner, J.A., Gorsich, S.W., McCaffery, J.M., Shaw, J.M. and Nunnari, J. (2000) The dynamin-related GTPase, Mgm1p, is an intermembrane space protein

required for maintenance of fusion competent mitochondria. *J Cell Biol*, **151**, 341-352.

Yaffe, M.P. and Schatz, G. (1984) Two nuclear mutations that block mitochondrial protein import in yeast. *Proc. Natl. Acad. Sci U.S.A.*, **81**, 4819-4823.

Yamamoto, H., Esaki, M., Kanamori, T., Tamura, Y., Nishikawa, S. and Endo, T. (2002) Tim50 is a subunit of the TIM23 complex that links protein translocation across the outer and inner mitochondrial membranes. *Cell*, **111**, 519-528.

Yang, C.S. and Weiner, H. (2002) Yeast two-hybrid screening identifies binding partners of human Tom34 that have ATPase activity and form a complex with Tom34 in the cytosol. *Arch Biochem Biophys*, **400**, 105-110.

Yang, M., Jensen, E.R., Yaffe, M.P., Opplinger, W. and Schatz, G. (1988) Import of precursor proteins into yeast mitochondria: the purified matrix processing protein contains two subunits which are encoded by the nuclear MAS1 and MAS2 genes. *EMBO J.*, **7**, 3857-3862.

Yano, M., Hoogenraad, N., Terada, K. and Mori, M. (2000) Identification and functional analysis of human Tom22 for protein import into mitochondria. *Mol. Cell. Biol.*, **20**, 7205-7213.

Young, J.C., Hoogenraad, N.J. and Hartl, F.U. (2003) Molecular chaperones Hsp90 and Hsp70 deliver preproteins to the mitochondrial import receptor Tom70. *Cell*, **112**, 41-50.

Zhou, X.W., Pfahnl, A., Werner, R., Hudder, A., Llanes, A., Luebke, A. and Dahl, G. (1997) Identification of a pore lining segment in gap junction hemichannels. *Biophys J*, **72**, 1946-1953.